THE ISOTOPIC COMPOSITION OF NEODYMIUM IN THE MARINE ENVIRONMENT: INVESTIGATIONS OF THE SOURCES AND TRANSPORT OF RARE EARTH ELEMENTS IN THE OCEANS

Thesis by

Donald John Piepgras

In Partial Fulfillment of the Requirements

for the Degree of

Doctor of Philosophy

California Institute of Technology

Pasadena, California

1984

(Submitted March 30, 1984)

To my parents, for letting me choose my own path through life

"Thus ocean trace-element chemistry is now undergoing
a true revolution"

...1982, quoted from the National Science
Foundation Annual Report, referring in
part to some of Nd isotopic studies undertaken
in this thesis

"His papers on Nd oceanography are an embarrassment
to an outstanding scientist's reputation"

...1983, comment by an anonymous reviewer of
an NSF proposal to support the research
reported herein

Acknowledgements

I would like to express my sincerest gratitude to Professor G. J. Wasserburg for his ever enthusiastic support for this research. In the face of incredible opposition from many members of the scientific community, he has fought diligently for the survival of this program. Without his recognition of the importance of this research, the accomplishments achieved during the course of this work would never have been realized. I would also like to thank Professor E. J. Dasch at Oregon State University for providing me with the opportunity to come to Caltech to pursue this research while I was a graduate student there.

I have benefitted greatly from my interactions with colleagues in the Lunatic Asylum and other members of the department here. Dr. Dimitri Papanastassiou has not only shared with me his expertise on mass spectrometry and laboratory operations, he has also been of great help to me during times of academic hardship. Henry Shaw has been a tremendous help to me during my tenure here with his considerable knowledge of computers and many discussions on transport equations. Discussions with Dr. C. C. Patterson have contributed greatly to the understanding of some of the problems encountered during this work. Evelyn Brown provided a stability which was often needed in the midst of the generally excited state of the Lunatic Asylum.

Special thanks are owed to several others who have supported this work in many ways. Karl Turekian of Yale University had an enthusiasm for this work from the very beginning which helped to keep this project and my interest in it alive. Discussions with him and his reviews of two manuscripts have greatly benefitted this research and my understanding of some of the problems involved. John Edmond of the Massachusetts Institute

of Technology provided a major source of intellectual exchange on the problems of trace element chemistry in the oceans and hydrothermal systems during his year at Caltech as a Fairchild Scholar. He also made available the long sought for hydrothermal solutions from the East Pacific Rise. Kenneth Bruland of the University of California at Santa Cruz provided early support which was a major factor in the initial funding of this research. He also collected many of the seawater samples analyzed in this study.

Many close friends have given me much needed moral support throughout my stay here at Caltech. I would especially like to express my appreciation to Jim Conca, Mary Torregrossa, and Andy Astor. Mary also helped by sharing her artistic abilities in preparing one of the figures in this thesis. A special thanks to Mardi, without whom I would be an oil tycoon now. Finally, I would like to thank Steven (no T.) Fosseen for always being a friend.

This research was made possible through these grants from the following funding agencies: NASA: NGL-05-002-188, and NAG 9-43; NSF: PHY 76-02724, GX 28675, OCE 81-08595, OCE 83-08884, and OCE 83-20516.

Abstract

In this study, the isotopic composition of neodymium in the marine environment has been determined from analysis of marine ferromanganese precipitates and seawater. An initial survey of the isotopic composition of Nd in the marine environment was made utilizing the analyses of authigenic ferromanganese sediments. These included ferromanganese nodules, metalliferous sediments, and hydrothermal ferromanganese crust deposits. Large variations in $\varepsilon_{Nd}(0)$ values are observed which exhibit a clear separation of the ocean basin. Nd isotopic variations within an ocean basin fall within a relatively small, well defined range which is characteristic of the ocean basin sampled. Based on these results, the following average $^{143}Nd/^{144}Nd$ ratios for the ocean basins have been determined: Atlantic Ocean, $\varepsilon_{Nd}(0) \approx -12$; Indian Ocean, $\varepsilon_{Nd}(0) \approx -8$; Pacific Ocean, $\varepsilon_{Nd}(0) \approx -3$. These values are considerably lower than $\varepsilon_{Nd}(0)$ values associated sources having oceanic mantle affinities, indicating that the REE in the oceans are dominated by continental sources. Therefore, the variations must reflect primarily the age and $^{147}Sm/^{144}Nd$ ratio of the continental masses being sampled.

Direct measurements of the isotopic composition of Nd in seawater samples from the Atlantic and Pacific are in excellent agreement with the values determined from the ferromanganese sediments indicating that these sediments accurately reflect the isotopic composition of Nd dissolved in seawater. The results clearly demonstrate the existence of distinctive Nd isotopic differences in waters of the major ocean basins. These values correspond to a difference in the absolute abundance of ^{143}Nd between the Atlantic and the Pacific Oceans of $\sim 10^6$ atoms ^{143}Nd per gram of seawater. In addition to the isotopic differences observed between the ocean basins,

smaller but distinctive variations are observed in the water column of both the Pacific and the Atlantic, indicating different sources of REE at different levels in the water column. This suggests that it may be possible to distinguish the sources of water masses within an ocean basin on the basis of Nd isotopic composition.

The isotopic composition of Nd was determined in seawater samples from the Drake Passage in order to monitor the exchange of REE between the Pacific and Atlantic Oceans. The Antarctic Circumpolar Current, which flows eastward through this passage, represents the primary conduit through which the major ocean basins communicate with each other. The isotopic composition of Nd is found to be uniform with depth at all stations and corresponds to $\varepsilon_{Nd}(0) \simeq -9.0$. This value is intermediate between the values for the Atlantic and the Pacific and indicates that the Antarctic Circumpolar Current consists of about 70 percent Atlantic water. By using a box model to describe the exchange of water between the Southern Ocean and the ocean basins to the north together with the isotopic results, an upper limit of approximately 33 million cubic meters per second is calculated for the rate of exchange between the Pacific and the Southern Ocean.

The concentration of Nd exhibits a regular increase with depth at all locations studied. In contrast, Nd isotopic compositions can exhibit substantial variations in the water column which vary depending on the location. Where isotopic differences in the water column occur, substantial lateral transport of REE from different sources and at different levels in the water column is required to maintain these differences. It is shown that the concentration gradients are established without significantly affecting the isotopic distribution, and that the enrichment of Nd in the deep water cannot be a result of resolution of REE scavenged from surface waters.

The isotopic distributions are compared to water mass analyses based on temperature and salinity characteristics in the water column at the various sampling locations. It is shown that differences in isotopic compositions in the water column are well correlated with changes in the temperature and salinity characteristics. Thus, the isotopic distributions are fully consistent with the circulation of major water masses. This indicates that while Nd is nonconservative in concentration, the isotopic composition is conserved and can be used as a tracer for studying the origin and circulation of water masses.

The results of these studies have provided some important contributions to the understanding of trace element transport in the oceans. First, the Nd isotopic differences in the water column clearly indicate that transport of Nd from the surface to the deep ocean cannot account for the observed increase in concentration of Nd with depth. These isotopic differences must be maintained by lateral transport of the REE and indicates that the concentration gradients of the REE and possibly other trace elements must also be related in part to lateral transport processes. Second, the close correlation observed between changes in Nd isotopic compositions and temperature-salinity relationships in the water column indicates that the lateral transport of REE in the oceans is directly related to the origin and flow of water masses. Thus, the isotopic composition of Nd in seawater is shown to be a useful tracer for studying the sources of injection and transport of trace elements in the oceans.

In addition to the seawater studies, the concentrations and isotopic compositions of Nd and Sr were determined in hydrothermal solutions emanating from hot springs on the crest of the East Pacific Rise at 21°N and at Guaymas Basin, Gulf of California. This study represents the first

effort to measure the Nd isotopic compositions in hydrothermal solutions. Endmember samples (T=350°C) from 21°N exhibit a small range in ε_{Sr} values from -13.4 to -15.7. Correcting to C_{Mg}=0, the pure hydrothermal solutions are estimated to have $\varepsilon_{Sr} \simeq -18$. These results indicate that the fluids have undergone extensive but not complete exchange with Sr in the depleted oceanic crust ($\varepsilon_{Sr} \simeq -30$). C_{Sr} ranges from 5.8 to 8.7 ppm and is similar to seawater (7.6 ppm) indicating that there must be buffering. Hydrothermal solutions from Guaymas Basin (T=315°C) rise through several hundred meters of sediment before reaching the sea floor. One sample from here has ε_{Sr} = +5.8, indicating that the solutions have reacted first with oceanic crust and then sediments. The high Sr concentration in this sample (19.3 ppm) is consistent with late stage interaction between the ascending fluid and carbonate rich sediments.

Nd shows a wide range in concentration and isotopic compositions in solutions from 21°N. C_{Nd} ranges from 20 to 659 pg/g, indicating substantial enrichments of Nd over typical seawater concentrations of ~3 to 4pg/g. ε_{Nd} ranges from -10.8 to +7.9. The data clearly show substantial contributions of Nd from depleted oceanic crust to many of the samples analyzed. In spite of enrichments in Nd of up to about 100 times seawater, none of the samples have ε_{Nd} values equal to MORB ($\varepsilon_{Nd} \simeq +10$). One sample from Guaymas Basin has ε_{Nd} = -11.4 consistent with leaching of Nd from sediments derived from old, continental sources. There is some inconsistency in the Nd isotopic data indicating that there is a possibility of contamination during sampling and/or handling of the solutions.

TABLE OF CONTENTS

CHAPTER 1: Introduction

1.1 Objectives

There were two major objectives to this investigation. The first objective was to determine the isotopic composition of Nd in the marine environment and the extent to which it is variable. Transport of the REE into the oceans will produce isotopic compositions of Nd which directly reflect the type of materials from which they were derived. From the isotopic composition of authigenic marine sediments and seawater, it should be possible to identify these sources of the rare earth elements (REE) in the different oceans. Relative to the turnover rate for the oceans, the residence time of Nd in seawater (defined as the total mass of Nd in the oceanic reservoir divided by the rate of Nd input to the oceans) is believed to be short, possibly less than 300 years [Goldberg et al., 1963; Wildeman and Haskin, 1965]. The major consequence of a short residence time is that the REE will not be well mixed in the oceans. Thus, Nd isotopic variations would be expected in the world ocean which reflect isotopic variations in possible source reservoirs of REE supply to the oceans. It is believed, therefore, that the Nd isotopic composition may have the possibility of serving as a natural tracer of ocean currents and water masses for short time scales and as a monitor of mixing in and between the oceans.

The second objective of this study was to apply the measurement of the isotopic composition of Nd in ocean waters as a tracer for studying, specifically, the problem of rare earth element transport in the oceans. In addition, the isotopic composition of Nd in ocean waters is used as a water mass tracer for studying problems related to the general circulation of the

oceans. To this end, several areas have been studied where direct Nd isotopic measurements of seawater have been used to elucidate the origin and mixing of water masses and trace element transport in the oceans. Most of the data in this study are for samples from the Atlantic Ocean where a detailed effort has been made to determine the extent to which REE transport can be related to the general circulation of ocean basins. In addition, Nd isotopic and concentration determinations have been made in solutions emanating from submarine hydrothermal springs on actively spreading mid-ocean ridges in an effort to determine the hydrothermal fluxes of REE and their possible influence on the isotopic composition of Nd in the oceans. These data also have important implications for the impact on REE during the hydrothermal exchange of seawater with the oceanic crust.

The basic approach to the problems addressed in this thesis was to first establish the magnitude of Nd isotopic variations, if any, in the marine environment. This was accomplished by measuring the isotopic composition of Nd in authigenic ferromanganese sediments. There were two reasons for studying ferromanganese sediments. First, it was plausible that REE in these sediments were precipitated from seawater and that their Nd isotopic compositions should therefore closely represent seawater isotopic compositions. This hypothesis is related to the growth mechanisms of manganese nodules and was not self evident. Furthermore, ferromanganese sediments contain REE at levels which are 6 to 8 orders of magnitude higher in concentration than in seawater, and thus, only a small amount of sample ($<<$1g) is required for the Nd isotopic analysis. The results of these data are summarized in Chapter 3. Once the range of Nd isotopic compositions in the ocean basins was estimated from the sediment data, it was necessary to confirm the results by direct analysis of Nd dissolved in ocean waters.

This required the development of techniques for the separation and isotopic analysis of small quantities of Nd ($<2 \times 10^{-8}$g) from large volumes of seawater without introducing significant levels of contamination. The success of these techniques has led to the direct confirmation of the inter-ocean Nd isotopic variations established from the ferromanganese sediment data and demonstrated the promise of using Nd isotopic measurements of seawater as an oceanographic tracer.

1.2 Data representation

Representation of Sm, Nd and Sr data follows that given by DePaolo and Wasserburg [1976a; 1976b]. Measured $^{143}Nd/^{144}Nd$ ratios are presented as fractional deviations in parts in 10^4 (ε units) from $^{143}Nd/^{144}Nd$ in a chondritic uniform reservoir (CHUR) as measured today:

$$\varepsilon_{Nd}(0) = \left[\frac{(^{143}Nd/^{144}Nd)_M}{I_{CHUR}(0)} - 1 \right] \times 10^4 \qquad (1.1)$$

where M is the ratio measured in the sample today, and $I_{CHUR}(0) = 0.511847$ is the $^{143}Nd/^{144}Nd$ in the CHUR reference reservoir today [Jacobsen and Wasserburg, 1980). Similarly, an enrichment factor for $^{147}Sm/^{144}Nd$ in a sample relative to CHUR is given by:

$$f_{Sm/Nd} = \left[\frac{(^{147}Sm/^{144}Nd)_M}{(^{147}Sm/^{144}Nd)_{CHUR}} - 1 \right] \qquad (1.2)$$

where $(^{147}Sm/^{144}Nd)_{CHUR} = 0.1967$ [Jacobsen and Wasserburg, 1980].

Model ages, T^{Nd}_{CHUR}, are calculated for the samples as follows:

$$T^{Nd}_{CHUR} = \frac{1}{\lambda}\ln\left[\ 1 + \frac{\varepsilon_{Nd}(0) I_{CHUR}(0) \times 10^{-4}}{f_{Sm/Nd}\left(^{147}Sm/^{144}Nd\right)_{CHUR}}\ \right] \qquad (1.3)$$

The ^{147}Sm decay constant, $\lambda = 6.54 \times 10^{-12}\ yr^{-1}$. Sr isotopic data are presented in a manner analogous to that used for Sm-Nd data. Thus:

$$\varepsilon_{Sr}(0) = \left[\ \frac{\left(^{87}Sr/^{86}Sr\right)_M}{I_{UR}(0)} - 1\ \right] \times 10^4 \qquad (1.4)$$

where $I_{UR}(0) = 0.7045$ is the estimated $^{87}Sr/^{86}Sr$ value for the bulk earth as determined by DePaolo and Wasserburg [1976b] and O'Nions et al. [1977].

1.3 Neodymium isotopic systematics relevant to REE in the oceans

The isotopic abundance of ^{143}Nd changes through geologic time due to the decay of ^{147}Sm (half-life = 1.06×10^{11} years). Relative to the oceanic residence times of the REE, the half-life of ^{147}Sm is extremely long and consequently, there will be no measurable in situ decay effects on the isotopic composition of Nd in seawater and modern marine sediments. Observed $^{143}Nd/^{144}Nd$ ratios will reflect the age and $^{147}Sm/^{144}Nd$ ratio of the materials which are sampled. The average evolution of $^{143}Nd/^{144}Nd$ for the earth has been found to approximately follow a simple growth curve which corresponds to the $^{147}Sm/^{144}Nd$ ratio of chondritic meteorites [DePaolo and Wasserburg, 1976a]. However, terrestrial differentiation processes have segregated material into continental and oceanic crustal rocks with distinctive ages and Sm/Nd ratios. As a result, there is a clear difference in the $^{143}Nd/^{144}Nd$ ratios in the samples of different types of crustal rocks.

Rocks derived from an undifferentiated source (Sm/Nd = chondritic) will be characterized by initial isotopic compositions of Nd identical to that in a chondritic uniform reservoir (CHUR) and if they were segregated from this source today, they would have $\varepsilon_{Nd}(0) = 0$. The oceanic crust is derived from a mantle source with a light REE depleted abundance pattern relative to CHUR and, therefore, has Sm/Nd ratios which are greater than the Sm/Nd ratio of CHUR. Consequently, the growth of ^{143}Nd in the oceanic mantle over geologic time has proceeded at an accelerated rate relative to CHUR resulting in positive values of $\varepsilon_{Nd}(0)$ in rocks derived from this reservoir. Conversely, most continental crustal rocks have light REE enriched abundance patterns and, therefore, have Sm/Nd ratios which are less than CHUR. As a result, the growth of ^{143}Nd in light REE enriched continental rocks proceeds at a slower rate than in CHUR producing, over geologic time, negative values of $\varepsilon_{Nd}(0)$. Young continental flood basalts have isotopic compositions showing a spread of $\varepsilon_{Nd}(0)$ values averaging near zero but with substantial variations. DePaolo and Wasserburg [1979] hypothesized that the source of these basalts was from a CHUR reservoir although the average value of $\varepsilon_{Nd}(0) \approx 0$ could result from an "accidental" mixing of continental crust and oceanic mantle.

1.4 Some observations on rare earth elements and their sources in the oceans

There are several pathways by which REE can be supplied to the oceans. These are shown in a cartoon in Figure 1.1. The major pathways include 1) runoff from continental and oceanic island land masses, 2) submarine hydrothermal and volcanic activity at mid-ocean ridge crests, 3) atmospheric

Figure 1.1. A cartoon depicting the major pathways by which rare earth elements are supplied to the oceans. These include runoff from continental and oceanic island land masses, atmospheric injections resulting from precipitation and settling of wind blown dust over the oceans, diffusion of REE released from sediments during diagenesis, and submarine volcanic sources resulting from volcanic and/or hydrothermal activity.

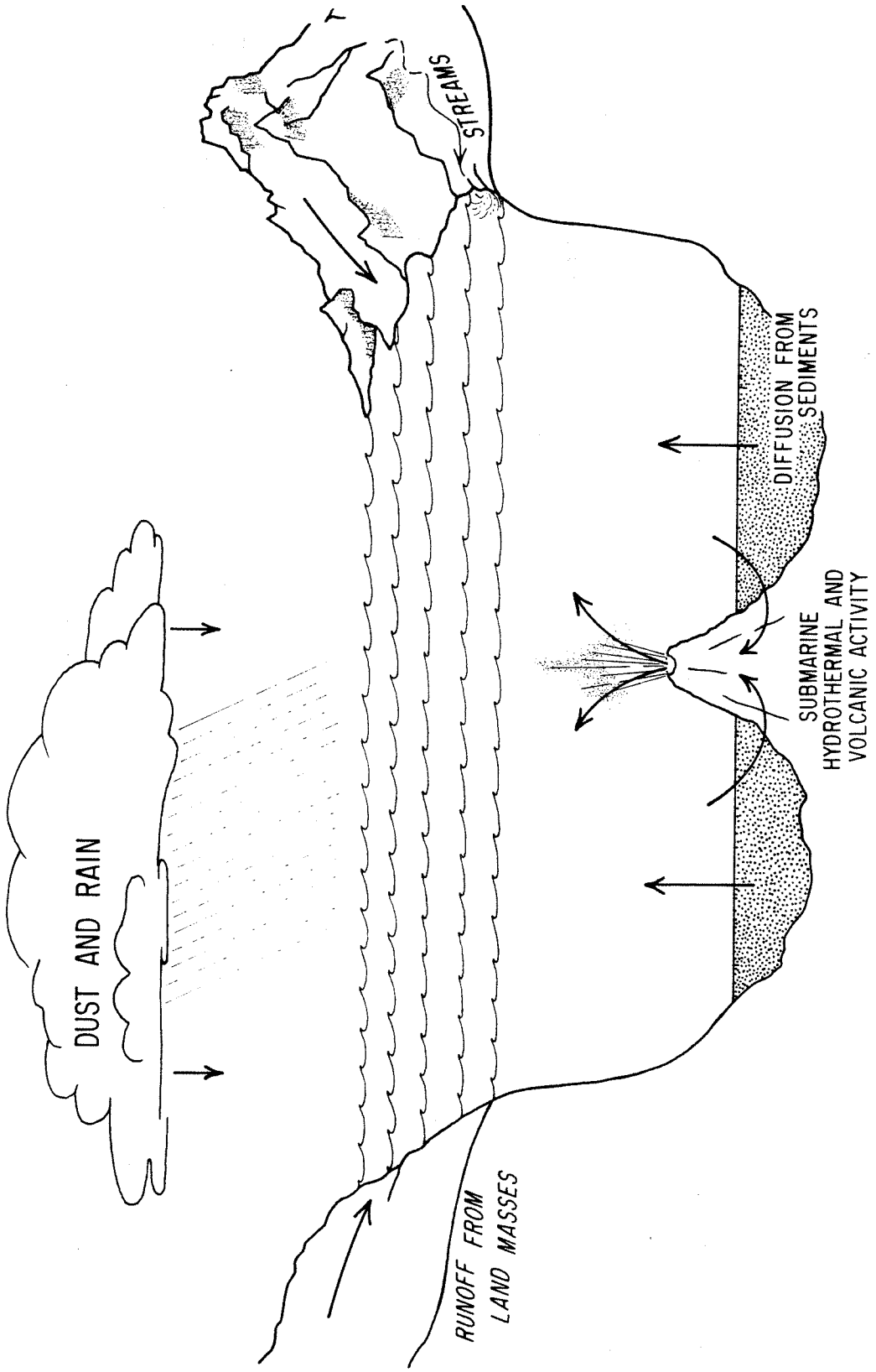
DUST AND RAIN
STREAMS
RUNOFF FROM
LAND MASSES
DIFFUSION FROM
SEDIMENTS
SUBMARINE
HYDROTHERMAL AND
VOLCANIC ACTIVITY

Figure 1.1.

dust fallout, and 4) remobilization of REE during diagenesis of marine sediments. Of these, the first three represent the primary input of new REE to the oceans. The fourth pathway may include both new inputs and the recycling of substantial amounts of the REE which were removed from the oceanic reservoir by adsorption onto particulate matter and incorporated into the sediment layer. It is difficult to assess the relative contribution that REE supply from each pathway makes to the total rare earth element budget of the oceans. This is due mainly to a lack of sufficient data relating to each of these pathways. Based on a very small data set for REE concentrations in rivers [Martin and Meybeck, 1979], the annual flux of dissolved Nd from continental runoff is estimated to be $\sim 10^9$ grams. By comparison, the annual submarine hydrothermal flux of Nd is estimated to be one to two orders of magnitude lower [Michard et al., 1983; this study (see Chap. 7)]. However, about 75% of the world's river drainage empties into the Atlantic and its adjacent seas, whereas most of the hydrothermal fluxes are supplied in the Pacific where the mid-ocean ridge spreading rates are fastest. Thus, continental fluxes would be expected to dominate in Atlantic waters, but hydrothermal fluxes could represent a significant proportion of the total REE flux to the Pacific Ocean. The actual fluxes of REE from rivers could be much different than estimated above. There is increasing evidence that most of the REE in rivers are associated with suspended matter [Stordal and Wasserburg, 1983]. The REE fluxes could be much lower or higher depending on whether there is significant desorption from the suspended material after entering the oceans. Estimates for the soluble REE fluxes from the atmosphere and diagenetic fluxes from marine sediments are not available at the present time.

Figure 1.2. Sm and Nd parameters in primary sources of rare earth elements in seawater. Continental sources are shown on the left and are dominately characterized by negative values of $\varepsilon_{Nd}(0)$. Oceanic sources are shown on the right side of the figure and are characterized by positive values of $\varepsilon_{Nd}(0)$. The oceans will be characterized by blends of REE from these different sources. Thus, the distinct separation of the Nd isotopic character observed for continental sources of REE from that of oceanic sources provides a fingerprint from which it will be possible to identify sources of REE in the oceans.

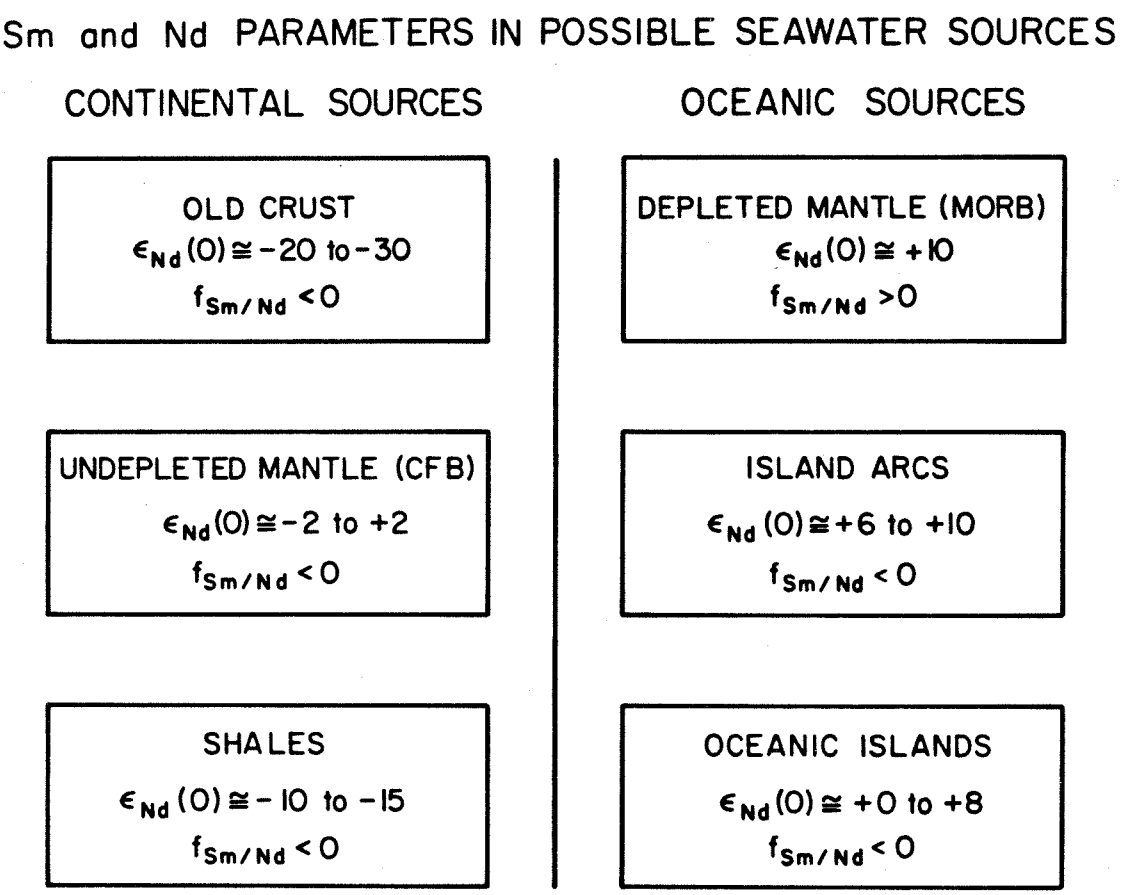
Sm and Nd PARAMETERS IN POSSIBLE SEAWATER SOURCES
CONTINENTAL SOURCES
OCEANIC SOURCES
OLD CRUST
$\epsilon_{Nd}(0) \cong -20$ to -30
$f_{Sm/Nd} < 0$
DEPLETED MANTLE (MORB)
$\epsilon_{Nd}(0) \cong +10$
$f_{Sm/Nd} > 0$
UNDEPLETED MANTLE (CFB)
$\epsilon_{Nd}(0) \cong -2$ to $+2$
$f_{Sm/Nd} < 0$
ISLAND ARCS
$\epsilon_{Nd}(0) \cong +6$ to $+10$
$f_{Sm/Nd} < 0$
SHALES
$\epsilon_{Nd}(0) \cong -10$ to -15
$f_{Sm/Nd} < 0$
OCEANIC ISLANDS
$\epsilon_{Nd}(0) \cong +0$ to $+8$
$f_{Sm/Nd} < 0$
$\epsilon_{Nd}(0) = Q\ f_{Sm/Nd}\ T$
$Q = \frac{\lambda\,(^{147}Sm/^{144}Nd)_{CHUR} \cdot 10^4}{I_{CHUR}(0)}$

Figure 1.2.

A sufficiently large body of data on the isotopic composition of Nd in oceanic and continental crustal reservoirs exists making it possible to estimate the average Nd isotopic character of the primary sources of REE supply to the oceans. It has been shown from early studies that there is a clear separation of the Nd isotopic characteristics of the continental and oceanic crust [DePaolo and Wasserburg, 1976a, 1976b, 1977; Richard et al., 1976; O'Nions et al., 1977]. Figure 1.2 summarizes the average Sm-Nd characteristics for major continental and oceanic crustal reservoirs. In general, continental sources of rare earth elements are found to be characterized by $\varepsilon_{Nd}(0) \leq 0$. Old continental crust, as typified by Precambrian shield terranes, are characterized by substantial light rare earth enrichments and typically have $\varepsilon_{Nd}(0)$ values ranging from -20 to -30. Young continental flood basalts on the average typically have $\varepsilon_{Nd}(0) \approx 0$. Sedimentary rocks on the continents, as represented by shales, have $\varepsilon_{Nd}(0)$ in the range from -10 to -15, reflecting a derivation primarily from old (but not ancient) preexisting continental crust [McCulloch and Wasserburg, 1978] and may represent the mean Nd isotopic composition of the continental crust. Oceanic crustal rocks as sources of REE in the oceans are generally characterized by derivation from an old light rare earth depleted mantle. Young mid-ocean ridge basalts (MORB) have $\varepsilon_{Nd}(0) \approx +10$. DePaolo and Wasserburg [1976b] have calculated that the mantle source region for MORB must have undergone a depletion event and been separated from CHUR for at least 10^9 years in order to account for its present day isotopic composition. Oceanic island basalts exhibit a range in $\varepsilon_{Nd}(0)$ from 0 to +8, and island arc volcanics are found to vary from +6 to +10. This very distinct difference between the Nd isotopic characteristics of oceanic and continental sources of REE will allow for a relatively straightforward evaluation

of the primary REE sources in the marine environment. The Nd isotopic character of sources due to diagenetic remobilization of REE in marine sediments will probably be similar to local seawater and thus may also reflect the isotopic character of these primary sources.

The chemical forms of the REE in seawater are not well known. However, all of the REE, with the exception of Ce, occur in the +3 oxidation state in seawater. Cerium may also occur in the +4 oxidation state which may account for its anomalous behavior in seawater. Turner et al. [1981] used an equilibrium speciation model to predict the speciation of the REE in seawater and fresh waters. The results of their calculations indicated that in seawater, the speciation of the REE should, in general, be dominated by carbonate complexes in solution. This is substantiated by the laboratory studies of Lundqvist [1982] which demonstrate that Eu carbonate complexes will dominate over hydrolysis products at the pH (~8) and CO_3^{2-} concentration ($\sim 10^{-4}$M) of seawater . The concentrations of the REE in seawater have been well known for about two decades now, since Goldberg et al. [1963] made the first reliable measurements. The upper limit of the absolute concentrations of the individual rare earths vary from about 1 to 50 picomolar with a maximum variation for any single rare earth being about a factor of three. These concentrations are about 6 to 8 orders of magnitude lower than the concentration limits allowed by the solubility of REE carbonates and hydroxides, indicating that there is substantial removal of the REE from the water column by scavenging processes, either organic or inorganic. Furthermore, Ce is more intensely scavenged from seawater than its neighboring REE, producing a negative Ce anomaly [Goldberg et al., 1963 and others] which is a characteristic feature of most ocean waters. Strong positive correlations between the REE and Fe in ferromanganese nodules give evidence that

precipitation of iron oxides and hydroxides may be controlling the removal process [Elderfield et al., 1981]. Slow growing nodules generally have the high REE concentrations (>50ppm Nd) and an abundance pattern which is a mirror image of seawater, including a positive Ce anomaly [Piper, 1974], further indicating that the growth of ferromanganese nodules on the ocean floor plays a major role in the removal of REE from seawater. A more detailed discussion of the general solution chemistry of the REE and processes affecting their distribution in natural waters is presented in Appendix XI.

1.5 The general circulation of the oceans and the major water mass characteristics of the Atlantic and Pacific Oceans

The purpose of this section is to provide a brief review of the general circulation of the oceans, and because most of the seawater samples analyzed in this study are from the Atlantic, a description of the major water mass characteristics of this ocean basin is included. This will provide the basis for putting the Nd isotopic data into an oceanographic framework. The discussion follows largely from the more detailed presentations from oceanography texts by Dietrich et al. [1980] and Pickard [1979]. As the origin and circulation of water masses are subjects of intense study in oceanography and theories are often changing, some of the review on water mass origins presented below may be subject to debate. New ideas from the results of the present study on Nd isotopes in the North Atlantic will hopefully add to the debate.

There are two main components to the general circulation of the oceans, the wind driven circulation and the thermohaline circulation. The wind

driven circulation is mainly horizontal, affecting primarily the upper 200 to 300 meters of the water column. Because of Coriolis forces, the wind induced currents, driven primarily by the trade winds in the respective hemispheres, form large gyres that rotate in a clockwise direction in the Northern Hemisphere and in a counter-clockwise direction in the Southern Hemisphere. The general surface circulation patterns that result are shown in Figure 1.3. The Atlantic and Pacific Oceans each have two gyres which are separated in part by an equatorial counter current which flows to the east. The Indian Ocean, which has very little surface area north of the equator has a permanent gyre south of the equator and a seasonably present circulation gyre north of the equator. In general, warm, saline waters are carried poleward in strong western boundary currents from the equator, and cool, less saline waters are transported toward the equator in weaker eastern boundary currents. The depth of penetration of the circulation in these gyres is generally limited by the depth of the warm water sphere. All of the major ocean basins are openly connected where they merge with the Southern Ocean. In this region, the West Wind Drift results in a strong eastward flowing current known as the Antarctic Circumpolar Current which extends to the ocean bottom (~4000 meters) and completely circles the Antarctic continent. The Antarctic Circumpolar Current has a volumetric flow rate averaging $130 \times 10^6 m^3 s^{-1}$ [Bryden and Pillsbury, 1977], making it one of the largest ocean currents in the world.

The deep water circulation of the oceans is thermohaline in nature. It is driven by density variations originating at or near the ocean surface owing to changes in temperature and salinity of the water. Cooling of surface waters at high latitudes results in an increase in the density, which if great enough, can cause the water to sink until it reaches a level

Figure 1.3. Map showing the general circulation at the surface of the oceans. In general, the Northern Hemisphere basins are characterized circulation gyres rotating in a clockwise direction, and the Soutern Hemisphere basins are characterized by circulation gyres rotating in a counter-clockwise direction.

Figure 1.3.

where it again achieves hydrostatic equilibrium. These currents are initiated as vertical flows, but when the new density level is reached they become horizontal, generally flowing in a meridional direction. Thus, the sinking of cold, dense waters in polar regions results in the southward flow of water masses generated in the north polar regions and a northward flow of water masses generated in the south polar regions. Only in the North Atlantic and in the Southern Ocean are winter cooling conditions sufficient to result in bottom water formation. The Pacific and Indian oceans have no northerly sources of bottom waters, and as a consequence, the deep waters of these basins are not as well circulated as the deep Atlantic. Deep waters can be formed when density levels of warm waters are raised due to excess evaporation. While waters of this type, such as formed in the Red and Mediterranean Seas, are important, they are quantitatively small in amount and do not significantly influence the deep circulation of the oceans.

Figure 1.4 summarizes the major water masses of the Atlantic Ocean and shows the general flow of each mass. Descriptions of the characteristics of these water masses follows. The deep and intermediate water masses of the Atlantic originate in the polar seas at the northern and southern extremes of this basin where winter cooling is sufficient to raise the density of near surface waters which then sink until their new density level is reached. Antarctic Bottom Water (AABW) is formed primarily in the Weddell Sea and to a lesser extent in the Ross Sea. It is a mixture of Shelf Water and Antarctic Circumpolar Water [Pickard, 1979]. In its purest form, AABW from the Weddell Sea has a temperature of -0.9°C and a salinity of 34.65°/oo [Dietrich et al. 1980]. This water mass flows north along the bottom into the South Atlantic as well as eastward into the Indian and Pacific sectors of the Southern Ocean. The northward flow of AABW is impeded on the eastern

Figure 1.4. Longitudinal section through the western Atlantic showing the characteristic water masses of the Atlantic Ocean (after Dietrich et al. [1980]). The general flow patterns of these water masses are indicated by the arrows. The salinity maximum (S_{max}) associated with southward flowing North Atlantic Deep Water and the salinity minimum (S_{min}) associated with northward flowing Antarctic Intermediate Water are indicated by the dashed lines.

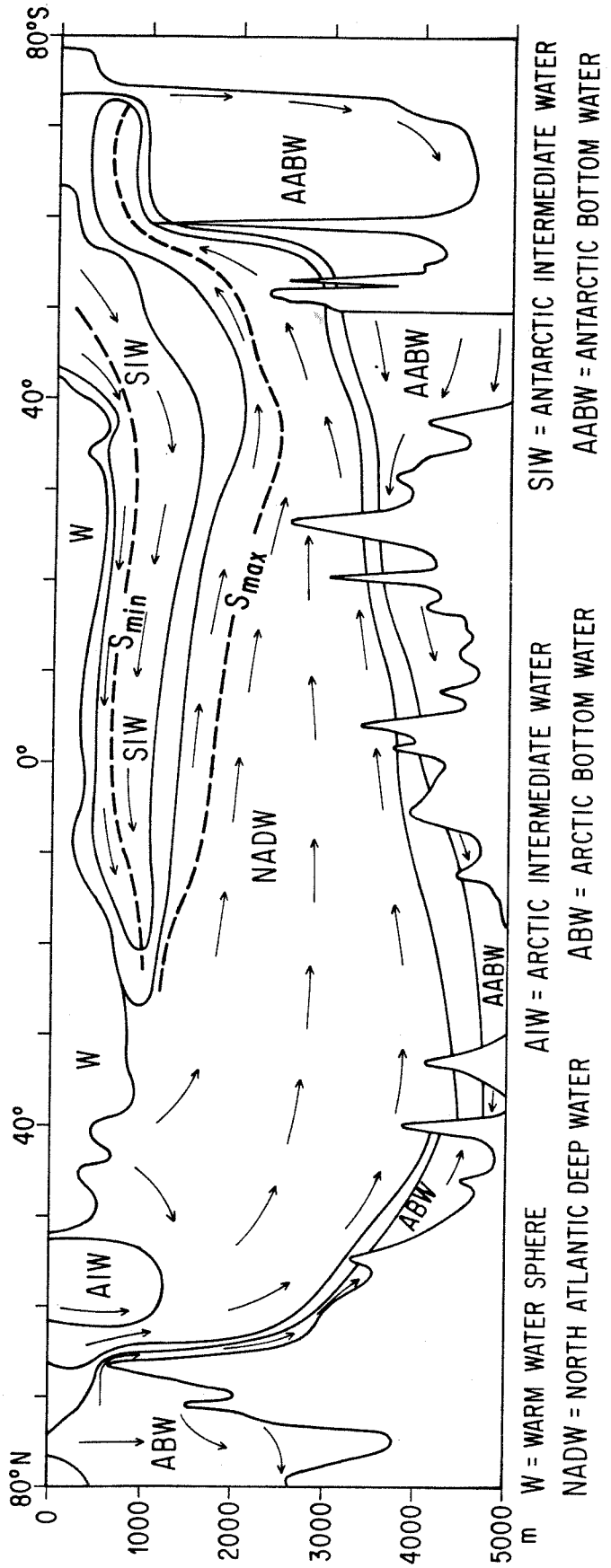
80°S
40°
0°
40°
80°N
0
1000
2000
3000
4000
5000
m
W
W
AIW
ABW
SIW
SIW
S_{min}
S_{max}
NADW
AABW
AABW
AABW
ABW
W = WARM WATER SPHERE
NADW = NORTH ATLANTIC DEEP WATER
AIW = ARCTIC INTERMEDIATE WATER
ABW = ARCTIC BOTTOM WATER
SIW = ANTARCTIC INTERMEDIATE WATER
AABW = ANTARCTIC BOTTOM WATER

Figure 1.4.

side of the Mid-Atlantic Ridge by the Walvis Ridge. As a result, the northward flow occurs on the western side of the Atlantic. AABW finally enters the eastern basin near the equator where it flows through the Romanche Fracture zone. From here, AABW can spread both north and south in the eastern basin. Although greatly mixed, evidence of AABW can be traced from its high silica content [Broecker, 1979] as far north as 45° in the Atlantic. Total production of AABW in the Weddell and Ross Seas appears to be sufficient to support northward fluxes of about 20 x $10^6 m^3 sec^{-1}$ at mid latitudes [Gill, 1973]. In the Atlantic, this should be in approximate balance with southward flowing deep waters.

Another major water mass of Antarctic origin found in the Atlantic Ocean is Sub-Antarctic Intermediate Water (SIW). This water mass is generated in regions just poleward of the oceanic polar front, a zone of convergence of wind-generated surface currents stretch all around Antarctica. It is a region where precipitation greatly exceeds evaporation, thus salinities tend to be low (~ 33.8°/oo). This water sinks to a depth of about 900 meters and flows northward. It can be identified in the Atlantic Ocean up to a latitude of about 25°N [Dietrich et al. 1980] as an intermediate depth salinity minimum in the water column. From the results of the Drake Passage Study discussed in Chapter 3, it is estimated that the isotopic composition of Nd in AABW and SIW should correspond to $\varepsilon_{Nd}(0) \cong -9$ at the point of origin of these water masses. As these water masses flow northward, the temperature and salinities are modified due to diffusive and advective mixing with southward flowing water masses. This mixing would presumably affect the Nd isotopic compositions as well, a point which will be addressed later in this thesis.

In the North Atlantic, only small areas at the sea surface are available for bottom water production. The most favorable locations for the formation of Arctic Bottom Water (ABW) are in the Arctic Ocean and Norwegian Sea. Bottom waters produced here have $T \sim -1.2°C$ and $S \sim 34.92^{o}/oo$ [Dietrich et al. 1980]. The high salt content of this water mass gives it the highest density of any water mass in the world. Most of the ABW produced is restricted to the area of its formation because submarine ridges separate the Arctic and Norwegian basins from the deep Atlantic. Overflow of ABW occurs intermittently over these ridges through the Faeroe Channel, Iceland-Faeroe Ridge and Denmark Strait where the sill depths are deepest though still quite shallow (< 1000 meters). Lee and Ellett [1965] have traced ABW as far south as 43°N in the Atlantic.

The dominant water mass in the Atlantic is North Atlantic Deep Water (NADW). The major components of this water mass are believed to be generated in regions north of the polar front in the Norwegian, Greenland and Labrador Seas. According to Wüst [1936, as referenced in Dietrich et al. 1980] this water mass has three levels, upper, middle and lower. The upper NADW receives injections of warm, high salinity Mediterranean Sea water having low oxygen content. Middle and lower NADW have higher oxygen content owing to being derived from waters recently at the surface in the north polar seas. The middle layer of NADW contains admixtures of intermediate water formed in the Labrador and Irminger Seas, while the lower NADW contains admixtures of ABW. NADW spreads southward and eventually ascends above northward spreading AABW. Upon reaching the Southern Ocean, NADW is entrained into the Antarctic Circumpolar Current and spread into other ocean basins. Reid and Lynn [1971] have identified the spreading of NADW, though highly diluted, into the North Indian and North Pacific Oceans on the basis

of observational data of temperature and salinity. In general, NADW is characterized by temperatures less than 6°C and salinities below 35°/oo.

The Mediterranean outflow, though not generally considered as a separate water mass in the Atlantic, is important in that it has a profound influence on the overall temperature and salinity characteristics of the Atlantic Ocean. The high evaporation rate in the Mediterranean Sea produces water masses with salinities greater than 38°/oo. Some of this dense, saline water spills into the Atlantic over the Gibraltar sill at a rate of about 1.04 X $10^6 m^3 sec^{-1}$ [Tchernia, 1980]. This outflow is replaced by an inflow of less saline Atlantic surface water at a rate of about 1.11 X $10^6 m^3 sec^{-1}$, which balances the outflow and net evaporation losses of water in the Mediterranean. The dense Mediterranean outflow water moves downward along the continental slope, mixing with Atlantic water as it sinks to a depth of about 1000 meters, where it reaches water of the same density. At this level it spreads out across the Atlantic mixing with the upper layer of NADW. This results in an intermediate-depth salinity maximum which is considered to be a characteristic feature of upper NADW. As such, the tongue of water which flows out from the Mediterranean is considered to be a source of one component of upper NADW rather than a separate water mass in the Atlantic. Of major consequence, though, is that the relatively high, overall salinity of the Atlantic is directly attributable to the Mediterranean outflow. In addition, the Mediterranean outflow results in the Atlantic having a warmer median temperature relative to the Pacific or Indian Oceans [Knauss, 1978]. The isotopic composition of Nd in this outflow and its implication for REE distributions in the Atlantic will be a major subject of this chapter.

Intermediate water is only formed in limited areas along the polar front in the North Atlantic, primarily in the Labrador and Irminger Seas. The salinities are much higher than in intermediate waters of Antarctic origin averaging about $34.8^{o}/oo$. This high salinity makes Arctic Intermediate Water (AIW) less conspicuous from other water masses in the region and it descends to greater depth than its southern counterpart due to its higher density. As a result, AIW mixes with NADW and spreads southward as a component of NADW.

Lying above the deep water masses is the warm water sphere. The thermohaline characteristics of the warm water sphere are strongly influenced by several factors including latitude, climate and the wind driven circulation of surface waters. In the tropics, a strong thermocline and pycnocline is developed year round. At the higher latitudes of the subtropics these features become seasonal as winter cooling tends to cause convection and mixing of the thermocline region with cooler water below. At high latitudes where the weather is cooler year round, strong stratification does not develop in summer months. The high latitude boundaries of the warm water sphere correspond to the locations of the polar fronts. The lower boundary is denoted by an oxygen minimum and is deepest (~ 800 m) in the regions of subtropical convergences and is shallowest (~ 250 m) in the vicinity of the equatorial divergences.

The major water masses of the Pacific are depicted in Figure 1.5. Below the warm water sphere there are four major water masses, two intermediate water masses, deep water, and Antarctic Bottom Water. One of the intermediate water masses is sub-Antarctic Intermediate Water (SIW) which forms in the same manner as in the Atlantic. This water mass spreads

Figure 1.5. Longitudinal section through the Pacific Ocean at 160°W showing the characteristic water masses (after Dietrich et al. [1980]). The general flow patterns of these water masses are indicated by the arrows. The salinity minimums (S_{min}) associated with northward flowing Antarctic Intermediate Water and southward flowing Arctic Intermediate Water are indicated by the dashed lines.

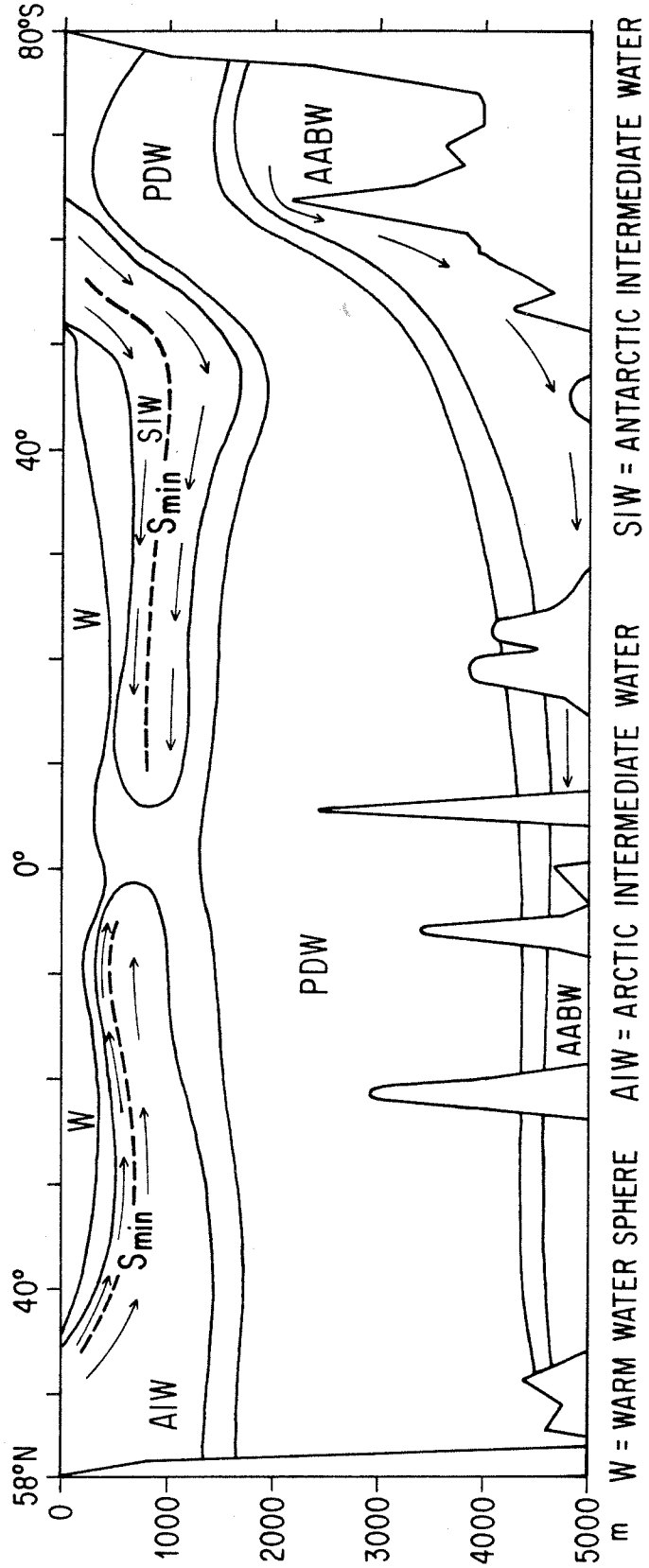
58°N
40°
0°
40°
80°S
0
1000
2000
3000
4000
5000
m
W
W
W
AIW
PDW
PDW
AABW
AABW
SIW
Smin
Smin
W = WARM WATER SPHERE
AIW = ARCTIC INTERMEDIATE WATER
SIW = ANTARCTIC INTERMEDIATE WATER
PDW = PACIFIC DEEP WATER
AABW = ANTARCTIC BOTTOM WATER

Figure 1.5.

northward to about the equator and is identified as a salinity minimum (S = ~34.3°/oo). The other intermediate water mass in the Pacific is of sub-Arctic origin and is referred to here as Arctic Intermediate water (AIW). This water mass, also identified by a salinity minimum, flows southward in the North Pacific to the equator where it encounters SIW. Underlying the intermediate water masses is Pacific Deep Water (PDW). As there is no production of deep water within the Pacific as in the Atlantic, it is generally assumed that the Pacific deep water complex comes from other oceans. This water mass has fairly uniform temperature (T = 1.1 to 2.2°C) and salinity (S = 34.65 to 34.75°/oo). Below the deep water lies Antarctic Bottom Water (AABW) which, according to Dietrich et al. [1980], can be traced as far north as 50°N latitude.

Chapter 2. Samples: expeditions and descriptions, collection methods, and chemical analysis

2.1 Descriptions of ferromanganese sediment samples

Samarium and neodymium concentrations and Nd isotopic compositions were measured in a variety of authigenic ferromanganese sediments from the major ocean basins and one freshwater body. Marine ferromanganese sediments were used in this study because they (1) occur in relative abundance over a wide geographic range allowing for a broad sampling of the ocean basins, (2) form in a variety of depositional environments, (3) apparently form primarily by authigenesis, so that REE incorporated in these sediments may be derived from seawater, and (4) have high REE concentrations, thus requiring only a few milligrams of sample for analysis. Samples were selected from major ocean basins and mid-ocean ridge spreading centers. Locations are shown on a map in Figure 2.1 and include locations of samples for which Nd isotopic data is available from other studies. Exact locations of samples analyzed as part of this study can be found in Table A1 in the appendix section.

There are several types of ferromanganese sediments which are classified according to their depositional environment as summarized by Bonatti et al. [1972]. Hydrogenous deposits result from the slow precipitation of Fe and Mn from seawater in oxidized environments generally in areas of low sedimentation such as abyssal plains. Deposits of this type include manganese nodules and ferromanganese pavements, the latter generally forming in areas with strong bottom currents. Hydrogenous precipitates are characterized by Mn/FE $\approx$ 1. Hydrothermal deposits result from the fairly rapid precipitation of Fe and Mn from hydrothermal solutions injected into

Figure 2.1. Locations of ferromanganese sediment and seawater samples analyzed in this study. Also included are manganese nodule and metalliferous sediment sites from O'Nions et al. [1978], Goldstein and O'Nions [1981], and Elderfield et al. [1981]. Symbols identifying sample types are as follows: (squares) manganese nodules; (diamonds) hydrothermal crusts; (triangles) metalliferous sediments; (circles) seawater samples.

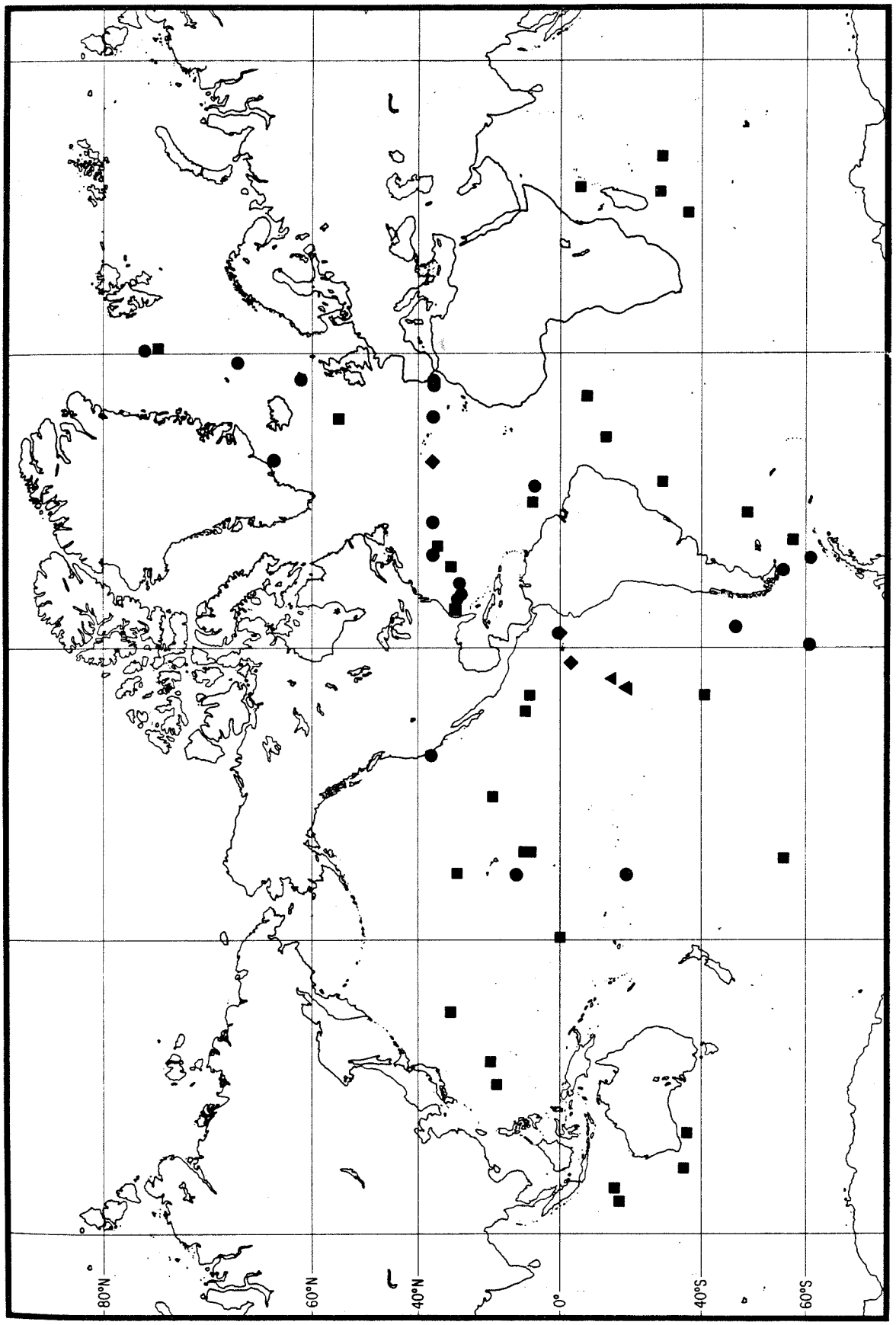

Figure 2.1

seawater in areas of submarine volcanism occurring primarily along mid-ocean ridge crests. These deposits include metalliferous sediments on the flanks of active mid-ocean ridges and as coatings (crusts) on basalts at mid-ocean ridges. Because of differences in the kinetics of oxidation of dissolved Fe and Mn, hydrothermal deposits are characterized by extremes of Fe and Mn fractionation. Halmyrolytic deposits are formed in limited areas such as seamounts where Fe and Mn are supplied by the submarine weathering of basaltic debris. Much of the Fe and Mn in these deposits are probably derived from precipitation out of seawater. Diagenetic deposits result from the precipitation of Mn which has been diagenetically remobilized from the sediment column. These types of deposits may be most important in hemipelagic areas of the oceans where sediments often have a high enough organic content to establish reducing conditions. In general, diagenetic ferromanganese deposits are characterized by Mn/Fe $\gg$ 1, reflecting lower mobility of iron in deep sea sediments.

It is probable that a combination of precipitation mechanisms are active during the formation of ferromanganese sediments and may preclude classification by the simple scheme of Bonatti et al. [1972]. A single manganese nodule on the ocean floor may form by both hydrogenous precipitation and precipitation of diagenetically remobilized Mn. A key to the origin of the Mn may be in the mineralogy. There are three major manganese minerals recognized in the marine environment which are distinguished primarily by their x-ray diffraction patterns. These are birnessite: (Na, Ca, K)(Mg, Mn)$Mn_6O_{14}\cdot 5H_2O$, todorokite: (Ca, Na, K)(Mg, Mn) $Mn_5O_{12}\cdot xH_2O$, and δ-MnO_2: $MnO_2\cdot nH_2O\cdot m(R_2O, RO, R_2O_3)$ (R = Na, Ca, Co, FeMn) [Burns and Burns, 1979]. Birnessite and todorokite are virtually Fe free, whereas δ-MnO_2 contains abundant Fe in its structure which is presumed to be due to the association

of this phase with colloidal Fe oxyhydroxides in seawater. Birnessite is most commonly associated with hydrothermal deposits. Todorokite is found in both hydrothermal sediments and in manganese nodules. δ-MnO_2 is primarily associated with manganese nodules. Usui [1979] has suggested that todorokite in manganese nodules is associated with diagenetic sources of Mn from underlying sediments and that it precipitates primarily on the bottom sides of nodules. δ-MnO_2, on the other hand, is formed by precipitation out of seawater and is deposited on the top sides of nodules. Thus, it appears that mineralogical variations within a nodule could be used to separate out fractions with different sources of Mn. Whether the source of Mn in a particular mineral phase has any bearing on the source of the REE within the same phase is unclear. Arguments on the sources of REE in ferromanganese sediments are presented below. In this study, no chemical or mineralogical analyses were made, As a consequences, it was not possible to compare the Nd data to chemical and mineralogical parameters.

In this study, manganese nodules, hydrothermal crusts, and metalliferous sediments were analyzed. Manganese nodules comprise the bulk of hydrogenous ferromanganese sediments. The primary reason for selecting manganese nodules for this study was the assumption that their REE were precipitated directly out of seawater, and therefore, their Nd isotopic composition should represent that of the seawater from which they were derived. Support for the hypothesis of seawater derivation for REE in manganese nodules comes from many authors who have observed consistent relationships between patterns of REE in seawater and in manganese nodules, the most significant of which is the opposite behavior of Ce in these two reservoirs [Goldberg et al., 1963; Bonatti et al., 1972; Piper, 1974; Glasby, 1972; Glasby, 1972-73]. Ehrlich [1968] and Bender [1972], however,

preferred a mechanism of diagenetic remobilization of REE from underlying sediments as a source for these elements. The Nd isotopic data presented in this work are critical to this debate. Elderfield et al. [1981] argued in favor of diagenetic processes for the incorporation of REE in manganese nodules, but concluded that the REE were ultimately derived from seawater based on Nd isotopic considerations which will be discussed in Chapter 3. Many nodules are also characterized by the presence of clay and other particles dispersed throughout their structures [Sorem and Fewkes, 1977]. These latter features, if detrital, could have a significant effect on elemental composition, possibly including Nd. In addition to Nd dissolved in seawater, other possible sources which could affect the Nd isotopic composition in the samples include continental detritus, oceanic basalts and sediments, and juvenile material.

Manganese nodule samples were chosen to achieve two main objectives: (1) to establish differences or similarities in Nd isotopic composition between various water bodies, and (2) to determine if variations exist within a body of water, which may be related to differences in provenance. To meet these objectives, broad geographic sampling of nodules within the Atlantic, Pacific, and Indian Oceans was made (Fig. 2.1). Samples from the Scotia Sea and Antarctic Ocean were chosen as representing locations where mixing between two different water masses may be taking place. A manganese nodule and an associated red clay from the Indian Ocean (RC-1 and MN-15) were analyzed to compare the Nd isotopic composition between manganese nodules and the underlying sediment substrate in the same area. In addition, one lacustrine nodule from Lake Oneida, New York, was analyzed. This latter sample was chosen on the assumption that all of its REE were continentally derived.

Two types of hydrothermal samples have also been sampled, hydrothermal crusts and metalliferous sediments. These samples were chosen to determine if there were effects due to hydrothermal activity on the Nd isotopic composition. The direct association of these deposits with hydrothermal activity and their relatively rapid rate of deposition [Bender et al., 1971; Scott et al., 1974; Moore and Vogt, 1976] make them genetically distinct from manganese nodules. These deposits are now known to form by direct precipitation of Fe and Mn out of hydrothermal solutions upon injection into oxygenated seawater [Edmond et al., 1979b]. Crust samples form as coatings on exposed basalts along ridge crests, whereas metalliferous sediments contain Fe and Mn which has been more widely dispersed along the flanks of ridge crests. Metalliferous sediments are most abundant on the flanks of the East Pacific Rise reflecting the active hydrothermal system associated with this ridge. Crust deposits have been discovered in relative abundance from Pacific and Atlantic ridge systems. While iron and manganese have been shown to have a source related to hydrothermal alteration of basalts, this has not been clearly established for the rare earth elements. Corliss [1971] studied altered oceanic basalts and concluded that REE in marine sediments could be accounted for by derivation from the basalts. However, REE patterns for hydrothermal deposits are similar to seawater REE patterns and not basalt, leading many authors to conclude their REE were derived from seawater [Bender et al., 1971; Corliss et al., 1978; Toth, 1977]. The isotopic composition of Nd was determined for metalliferous sediments from the East Pacific Rise and for hydrothermal crusts from the Galapagos hydrothermal mounds and the FAMOUS site on the Mid-Atlantic Ridge in an attempt to clarify their origin.

2.2 Seawater sampling

Seawater samples have been collected from several locations in the Atlantic and Pacific Oceans and in the Drake Passage to achieve a variety of objectives. For many of the sampling sites, vertical profiles of the water column were collected. Locations of all seawater samples analyzed during this study are shown in Figure 2.1 along with the ferromanganese sediment sample locations. Exact locations and cruise identifications for the seawater samples are listed in Table A2 in the appendix. A listing of all the cruises from which samples were collected for this research is given in Table 2.1 along with the collection methods which will be described later in this chapter. Unless otherwise stated, all samples were collected by myself.

The initial objective for the seawater sampling was to compare the isotopic composition of Nd dissolved in seawater to that determined for ferromanganese sediments from the respective basins. To meet this objective, samples were collected for our use by K. Bruland from the Northeast Pacific during the CEROP II expedition of the R/V Wecoma in July 1978. One other sample was collected from the Galapagos Rise by L. Gordon during the University of Miami Galapagos expedition (R/V Gillis 7901-139) to explore hydrothermal springs in March, 1979. Samples from the Atlantic were collected from four closely spaced stations in May 1979 during Cruise 63 of the R/V Oceanus in the Sargasso Sea south of Bermuda. In addition to allowing a direct comparison between seawater and ferromanganese sediment results for this basin, the Atlantic samples were collected from several depths to determine the depth dependency of the concentration and isotopic composition of Nd.

Table 2.1. Seawater sampling expeditions and collection methods.

Ship	Cruise and date	Sampling area	Sampling method
R/V Wecoma	CEROP-II July, 1978	Northeast Pacific	Niskin
R/V Gillis	7901-139 March, 1979	Galapagos Rise	Niskin
R/V Oceanus	OCE 63 May, 1979	Sargasso Sea	Niskin
R/V Atlantis II	A-II 107-11 Sept.-Oct., 1980	Drake Passage and S.E. Pacific	GO-FLO
R/V T. Thompson	Marine Chem. 80 Sept.-Oct. 1980	Central Pacific	GO-FLO
R/V Atlantis II	A-II 109-1 June-July, 1981	N. Atlantic (36°N)	GO-FLO and Niskin
R/V Knorr	TTO/NAS Leg 5 July, 1981	Norwegian-Greenland and Irminger Seas	Niskin
R/V Knorr	TTO/TAS Leg 2 January, 1983	Equatorial Atlantic	GO-FLO

Subsequent seawater sampling was oriented towards specific problems related to the distribution and transport of rare earth elements in the oceans. In an effort to study the exchange of rare earths between the Pacific and Atlantic Oceans, samples from vertical profiles of the water column at several locations in the Drake Passage and the Southeast Pacific were collected during Cruise 107-11 of the R/V Atlantis II in September and October, 1980. The importance of this area is that it is the major conduit through which the waters of these two oceans communicate. The flow rate between the Pacific and the Atlantic through the Drake Passage is about $130 \times 10^6 m^3 s^{-1}$ [Bryden and Pillsbury, 1977], about 100 times greater than through the Arctic Ocean. During this same period of time, samples from two profiles in the central Pacific were collected by K. Bruland during an expedition of the R/V T. Thompson. These samples represented the first vertical profiles of the Pacific for Nd isotopic analysis and included bottom water samples of Antarctic origin which would allow for a comparison with isotopic results for waters from the Drake Passage area close to the sources of Antarctic Bottom Water.

The remaining seawater sampling has been limited to the Atlantic Ocean where efforts to determine the detailed distribution characteristics of Nd isotopes have been made. The major objectives of this sampling have been to determine the sources and transport mechanisms of REE in the Atlantic by collecting samples in a vertical profile through the thermocline to the bottom at selected sites. Furthermore, the data afford a comparison to be made between the distribution of Nd isotopes and the circulation and water mass characteristics of this ocean basin. In addition to the initial sampling from OCE 63, samples have been collected during three other expeditions. In June and July, 1981 samples were collected from several

stations on a transect across the North Atlantic at 36°N during cruise 109-1 of the R/V Atlantis II. This sampling included a second detailed profile of the western basin of the North Atlantic to compare with results from the 1979 sampling, and the first detailed profile of the eastern basin of the North Atlantic including the Mediterranean outflow. During the same time period, samples were collected from major overflows from the Arctic seas by T. Takahashi during the Transient Tracers in the Oceans North Atlantic Study (TTO/NAS). These samples, which did not include vertical profiles, are presumed to represent the major components of North Atlantic Deep Water and were collected for comparison to Nd isotopic values of NADW at other locations farther south in the Atlantic. The last expedition made in the Atlantic was during the TTO Tropical Atlantic Study in January, 1983 in the equatorial North Atlantic. These samples were collected to study the possible southward transport of REE in NADW and to determine if REE in northward spreading AABW can be identified this far north in the Atlantic.

2.3 Seawater collection and storage methods

Much of the success of this work has depended on the ability to collect seawater samples and to extract the REE from these samples without introducing significant levels of contamination. Great care has been taken in this regard to keep blanks at a minimum. During the course of this work, two types of water sampling devices have been used, Niskin bottles and GO-FLO bottles, both of which are manufactured by General Oceanics Inc. In both cases, the water samplers are attached to a stainless steel cable and lowered over the side of the ship to the desired sampling depth by means of a winch. Niskin bottles are constructed of PVC tubing of various diameters

depending on the capacity of the bottle. When closed, the bottles are sealed at each end by means of beveled caps which are connected to each other by a Teflon coated spring running through the inside of the bottle. In the open position, the ends are pulled back and held in place by a spring loaded pin mounted on the side of the bottle. This pin is released by a sliding weight, or messenger, delivered down the wire after the desired sampling depth has been reached. GO-FLO bottles are also constructed of PVC tubing, but the ends are sealed by rotating balls which are operated by external rubber elastics, thus eliminating exposure of the sample to an internal spring. In addition, the interior surfaces of the GO-FLO bottles have been coated with Teflon to provide non-stick surfaces in an effort to reduce the possibility of contamination between samples. Closing of the GO-FLO bottles at the desired depth is done by the same method as with Niskin bottles. The bottles are designed to be lowered through the water column in an open position to avoid collapse of the bottles resulting from the hydrostatic pressures encountered in the deep ocean. The GO-FLO bottles, however, are designed to go through the upper ten meters of the water column in a closed position. At about ten meters depth, a pressure switch opens the bottle to the flushing position. The purpose of this is so that the inside surfaces of the samplers are not exposed to possible contaminants in the surface layer of the ocean such as those derived from the research vessel. Any number of sampling bottles desired can be mounted to the wire making it possible to collect a profile of the entire water column in a single cast. The samplers can also be mounted in a rosette and closed at the desired depth by means of an electronic release mechanism actuated from the vessel. Both methods have been employed during the course of this work. No determinations of sampling blanks have been made, but

compatible results for samples collected by the different methods and the general consistency of the overall data sets indicate that contamination during sampling is not a serious problem.

Immediately after collection, water samples which are to be returned to the laboratory are transferred to acid cleaned 10-liter polyethylene containers for storage. Each sample is acidified with sufficient ultrapure HCl to bring the pH of the sample down to ~2. The purpose of this is to prevent any rare earths from plating out onto the walls of the containers during storage. The sample bottles are then put into plastic bags and stored in wooden crates until their return to the laboratory. With the exception of the Pacific samples collected by K. Bruland, the seawater samples used in this study have not been filtered to remove particles. As discussed in Appendix III, it is apparent that only minor amounts of REE (< 20%) reside on particles greater than 0.4μm in diameter. As a result, filtering should have a negligible effect on the measured REE concentrations and Nd isotopic compositions. The possibility of contamination during filtering at sea was also a consideration in choosing not to filter the samples.

2.4 Extraction of REE from seawater

Two techniques have been employed for the extraction of the REE from seawater samples. For most of the samples analyzed in this study, the REE were extracted by coprecipitation on to iron hydroxides. This method has been widely used for the extraction of REE from seawater since first employed for this purpose by Goldberg et al. [1963]. It is a fairly simple technique to perform, the overall chemical yields are quite high (generally greater than 95%), and can be carried out under clean lab conditions with

very low blanks ($<25 \times 10^{-12}$ grams per sample). A complete description of this technique is presented in the papers in Appendices I and II.

There are two major drawbacks to the coprecipitation method. First, it requires the need for transport and storage of large volumes of water. Second, it requires a lengthy period of time (usually two to three days) to perform the bulk extraction. Because of the need for clean lab conditions due to the necessary exposure of the sample to the air at various times during the extraction and the need for a still environment to allow the precipitates to settle out, it is not practical to perform this type of separation at sea. In an effort to get around these problems, a ship board extraction technique was developed which could be carried out with virtually no exposure of the sample to the local atmosphere. The method involves the extraction of the REE in the sample onto a chelating resin. Immediately after collection the samples are transferred to acid cleaned plastic aspirator bottles and spiked with preweighed ^{147}Sm and ^{150}Nd spikes. The samples are connected to 1.5 cm x 15 cm columns containing the chelating resin and the water is pumped through the resin by means of a peristaltic pump positioned downstream from the column. The REE are extracted onto the resin and the water is discarded. After the extraction procedure the columns are sealed in plastic until their return to the land based laboratory. The columns, being light weight, are easily hand carried back to the laboratory. The REE are stripped from the resin using ~25 ml 4N HNO_3. The REE yields for this extraction are ~ 100% with typical blank levels of 25 x 10^{-12} grams per sample. A detailed description of this procedure is presented in Appendix X where a comparison to the $Fe(OH)_3$ coprecipitation method is made.

2.5 Chemical separation and mass spectrometry of Sm and Nd

For sediment samples and REE concentrates from seawater samples, Sm and Nd are separated and purified from other rare earths using standard ion exchange procedures which are described in Appendices I and II. Overall chemical yields for Sm and Nd are better than 85% and total Nd blank levels are typically $< 50 \times 10^{-12}$ grams. Mass spectrometric analyses are generally performed with 5 to 15 ng Nd for seawater samples. For sediment samples which generally have high concentrations of Nd, 100 to 200 ng are used. Duplicate Nd isotopic analyses of many samples generally agree within ± 0.5 ε units, well within the 2σ errors of the measurements, indicating the reproducibility of the methods. The details of the mass spectrometry including descriptions of the ion beam characteristics are presented in Appendix I and II.

In this laboratory, Nd is oxidized and analyzed in the NdO^+ form in the mass spectrometer. The measured ratios are then corrected for the isotopic composition of oxygen. During the course of this work, two different oxygen corrections were used. Originally, the isotopic composition of oxygen as determined by Nier [1950] was used for these corrections. A new determination of the isotopic composition of oxygen was made from Nd isotopic measurements [Wasserburg et al., 1981] and is now being used for the oxygen corrections. The new corrections yield $^{143}Nd/^{144}Nd$ ratios which differ slightly from values determined from the old corrections, however, the $\varepsilon_{Nd}(0)$ for the two different corrections are identical. As an internal check of the consistency of the two methods, the nonradiogenic isotopes of Nd were monitored and found to yield consistent results with both methods. All of the data presented in this thesis have been corrected for the new oxygen isotopic composition

CHAPTER 3: The Isotopic Composition of Neodymium in Ferromanganese Sediments and Seawater

3.1 Introduction

It is the objective of this chapter to establish the nature of the isotopic composition of Nd in the marine environment in order to identify the sources of the REE in the oceans and to determine the extent to which the isotopic composition of Nd in seawater may be useful as a tracer in oceanography. A preliminary attempt to estimate the isotopic composition of Nd in seawater was made by DePaolo and Wasserburg [1977] using fossilized fish debris and was presumed to be representative of Nd in the Pacific Ocean. A more extensive study was presented by O'Nions et al. [1978] who measured Nd in manganese nodules and metalliferous sediments. While substantial variations were found, O'Nions et al. inferred that seawater had a uniform $^{143}Nd/^{144}Nd$ ratio and that variations were dominantly due to the inclusion of detrital components. In this chapter, it will be shown that there is a wide spread in $^{143}Nd/^{144}Nd$ in authigenic ferromanganese sediments in agreement with the more limited data base of O'Nions et al. [1978], but that there is a distinct clustering of the isotopic data within a given ocean basin which is manifested as a clear separation in the Nd isotopic character of the ocean basins It will be further demonstrated from the direct analysis of Nd in seawater samples from the Atlantic and Pacific Oceans that the variations reported for ferromanganese sediments are due largely to isotopic differences of Nd dissolved in seawater which reflect the ages and $^{147}Sm/^{144}Nd$ ratios of the continental mass supplying Nd to a given seawater mass and not to addition of detrital components as suggested by O'Nions et al. [1978].

3.2 Results of ferromanganese sediment measurements

Results of Sm and Nd concentration measurements and Nd isotopic analyses for ferromanganese sediment samples are given in the appendix in Table A1. The Nd isotopic results are also shown on the middle level of the histogram in Figure 3.1 along with data from O'Nions et al. [1978], Goldstein and O'Nions [1981], and Elderfield et al. [1981]. For reference, the ranges in $\varepsilon_{Nd}(0)$ for possible REE sources in the oceans are shown at the bottom of the histogram in Figure 3.1. All samples measured have $\varepsilon_{Nd}(0)$ less than 0 and range as low as -14. Figure 3.1 clearly shows that these samples lie well below typical values observed for oceanic igneous rocks such as mid-ocean ridge, oceanic island, and island arc basalts. It is noted, however, that the data lie between (and overlap to some extent) typical values for average crustal rocks and many continental flood basalts. Clearly, these data show that the dominant contribution to the REE in these samples is from the continents and not from rocks with oceanic crust or mantle affinities. Furthermore, it is observed from Figure 3.1 that there is a distinct clustering of isotopic data from the Pacific, Indian, and Atlantic Oceans. Samples associated with each water mass occupy an isotopically distinct range, with the Atlantic Ocean data having the most negative values of $\varepsilon_{Nd}(0)$, the Pacific Ocean the least negative, and the Indian Ocean having intermediate values. There is only a slight overlap of values for ferromanganese sediments between the Atlantic and Indian Oceans, and there are no overlapping data with Pacific values. This regular pattern is found to be independent of the nature of the material analyzed. The Nd isotopic results for all ferromanganese sediment data from this study and the literature are summarized below.

Figure 3.1. Histograms of $\varepsilon_{Nd}(0)$ values of seawater (top) and ferromanganese sediments (middle). Possible sources of rare earth elements in seawater and their typical $\varepsilon_{Nd}(0)$ values are indicated at the bottom of the histogram. The stippled portion of the oceanic island range represents the relatively rare occurrence of $\varepsilon_{Nd}(0)$ values in these rock types which are below zero. There are three important observations to note in this figure. First, all of the data have isotopic compositions which lie in the direction of continental sources. Second, there is a clear separation in the isotopic compositions observed for ferromanganese sediments for each of the major ocean basins. Third, there is a close correspondence between the values of $\varepsilon_{Nd}(0)$ in ferromanganese sediments and seawater from the respective oceans, indicating that ferromanganese sediment data accurately reflect the isotopic composition of Nd in the dissolved load of an ocean basin. Data for ferromanganese sediments are from O'Nions et al. [1978], Piepgras et al. [1979], Goldstein and O'Nions [1981], and Elderfield et al. [1981]. Seawater data are all from this study. The ranges in isotopic compositions of crustal rocks were adapted from DePaolo and Wasserburg [1977] and White and Hoffman [1982].

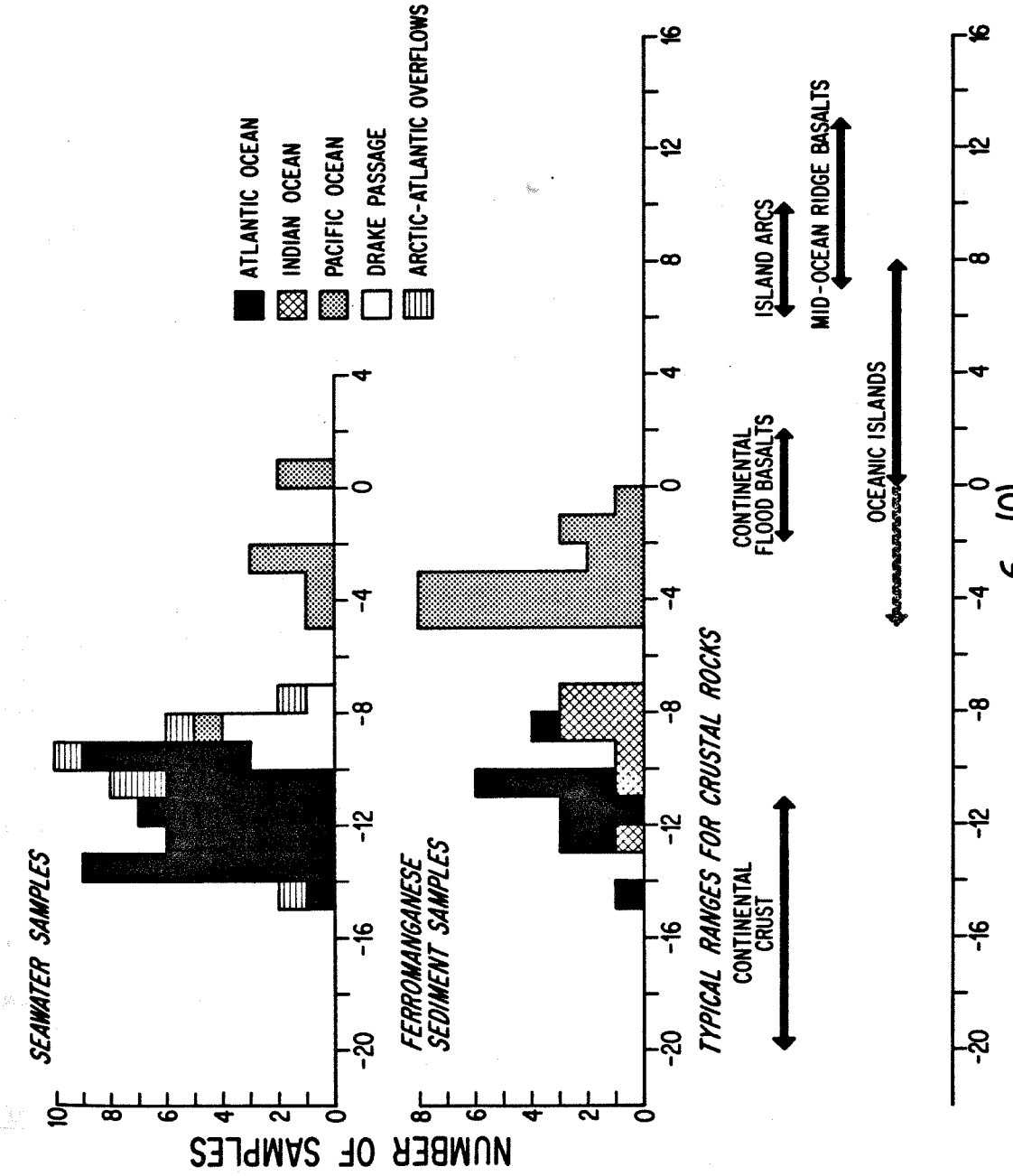
SEAWATER SAMPLES
FERROMANGANESE SEDIMENT SAMPLES
NUMBER OF SAMPLES
ATLANTIC OCEAN
INDIAN OCEAN
PACIFIC OCEAN
DRAKE PASSAGE
ARCTIC-ATLANTIC OVERFLOWS
TYPICAL RANGES FOR CRUSTAL ROCKS
CONTINENTAL CRUST
CONTINENTAL FLOOD BASALTS
ISLAND ARCS
MID-OCEAN RIDGE BASALTS
OCEANIC ISLANDS
$\epsilon_{Nd}(0)$

Figure 3.1.

Pacific Ocean. Samples analyzed from the Pacific Ocean occupy a narrow range of $\varepsilon_{Nd}(0)$ from -0.2 to -4.6. Manganese nodules range from -2.9 to -4.6, including data from other studies mentioned above. Top and bottom material from an apparently unturned manganese nodule (MD1-1-1, Table A1) have identical Nd isotopic compositions, although the topmost sample has about a factor of 2 higher concentration of both Sm and Nd. It is noted that two metalliferous sediment samples from the East Pacific Rise (OC73-3-12P, Table A1, and V-19-53(40), O'Nions et al. [1978]) and the Galapagos hydrothermal crust (52DR5, Table A1) exhibit the least negative values observed and are distinctly separated from the bulk of Pacific samples. All other hydrothermal ferromanganese sediment data lie entirely within the range exhibited by the manganese nodules.

Atlantic Ocean. $\varepsilon_{Nd}(0)$ values for Atlantic samples are distinctly different from Pacific samples. Values range from -8.4 to -14.0, with the bulk of the samples lying between -10.0 and -12.1. The most radiogenic value of $\varepsilon_{Nd}(0)$ determined for Atlantic ferromanganese samples in this study was -10.0. One sample (CYP74-12) is a manganese rich hydrothermal crust from the project FAMOUS site in the North Atlantic. It has $\varepsilon_{Nd}(0) = -11.5$ and it is indistinguishable from most other Atlantic samples which consist of manganese nodules.

Indian Ocean. The total range in $\varepsilon_{Nd}(0)$ for Indian Ocean samples is from -7.3 to -12.5. Most of the ferromanganese sediments analyzed from this ocean basin have values between -7.3 and -8.5, approximately midway between Pacific and Atlantic sample values. Samples which fall outside this narrow range all have $\varepsilon_{Nd}(0)$ values more typical of Atlantic samples. A deep-sea

clay (bulk sample) from the Indian Ocean (DODO 62D Sed.) is also more negative than the bulk of the reported data for this ocean ($\varepsilon_{Nd}(0) = -9.5$).

Other samples. Two nodules from southern oceans, the Scotia Sea (E28-5) and the Antarctic Ocean (BT-14-3), have $\varepsilon_{Nd}(0)$ values which lie between those observed for the Pacific and Indian Oceans. One lucustrine manganese nodule from Lake Oneida, New York was analyzed. Because of the isolation of this lake from the oceans, all of the REE in this nodule must be derived from the weathering of continental materials, eliminating the ambiguities which exist regarding possible sources of REE in seawater. The value of $\varepsilon_{Nd}(0) = -10.9$ for this sample indicates that the REE were indeed derived from an old (but not ancient) light rare earth enriched continental source region.

3.3 Results of Nd isotopic measurements of seawater samples

Results of Nd isotopic measurements made on seawater samples are presented in Table A2 in the appendix. These data are also plotted on the top level of the histogram in Figure 3.1. It is seen that the Atlantic and Pacific seawater samples lie in two distinct groups, the Atlantic samples having the most negative $\varepsilon_{Nd}(0)$ values. The Pacific seawater samples exhibit a total range in $\varepsilon_{Nd}(0)$ values from +0.3 to -8.1, a substantially greater spread than observed for ferromanganese sediments from this Ocean, although the majority of samples do lie within the range exhibited by Pacific ferromanganese samples. Atlantic samples exhibit a range in $\varepsilon_{Nd}(0)$ values from -9.4 to -14.1. All of the Atlantic seawater samples lie within the range of Nd isotopic values determined for Atlantic ferromanganese sediment samples. Samples from the Drake Passage area have $\varepsilon_{Nd}(0)$ values

which lie in a restricted range from -7.9 to -9.2. These values are intermediate between the bulk of Atlantic and Pacific seawater data and are similar to the Indian Ocean ferromanganese sediments. Samples from Arctic overflows exhibit a wide range in $\varepsilon_{Nd}(0)$ from -7.7 to -14.1. These values generally are close to or within typical Atlantic values. As shown for ferromanganese sediment samples, the $\varepsilon_{Nd}(0)$ values for seawater samples lie well below sources of REE having an oceanic mantle affinity but within the range exhibited by continental sources.

Within an ocean basin there are substantial variations in the isotopic compositions of Nd in seawater samples. These variations are observed to occur both as a function of water depth and geographic location indicating stratification of the REE in the oceans. The significance of these variations will be discussed in later chapters of this thesis.

Concentrations of Sm and Nd have also been determined for seawater samples. Where measured, Sm exhibits a total range from 0.347 to 0.800 X 10^{-12}g/g and Nd ranges from 1.14 to 9.01 X 10^{-12}g/g. In general, the concentrations are found to increase with depth. The values reported here are of the same order of magnitude as reported by Goldberg et al. [1963] and Høgdahl et al. [1968], but the large spread observed here is a result of the broader sampling done during this study. Concentration data will also be discussed in more detail in later chapters.

3.4 Results of strontium isotopic measurements

Six ferromanganese sediment samples, two Atlantic, one Indian, and three Pacific were analyzed for $^{87}Sr/^{86}Sr$. In addition, two seawater samples, one Atlantic and one Pacific, were analyzed for $^{87}Sr/^{86}Sr$. Results

of the sediment sample measurements are given in Table A1. The seawater results are listed in Appendix 2 (Table 1). The Sr data are also plotted as a function of their Nd isotopic composition in Figure 3.2. As shown in this figure, all samples have $\varepsilon_{Sr}(0)$ values which are very close to or indistinguishable from seawater ($\varepsilon_{Sr}(0) \approx +65.0$) in spite of geographic separation of the samples and in sharp contrast to the wide range of Nd isotopic compositions in these samples . OC73-3-12P (Table A1) has a slightly lower $\varepsilon_{Sr}(0)$ value of +63.5, but is clearly dominated by a seawater source of Sr.

3.5 Discussion

Neodymium isotopic data for ferromanganese nodules, hydrothermal crusts, and metalliferous sediments exhibit distinctive and tightly clustered $\varepsilon_{Nd}(0)$ values within each of the major oceans analyzed. This is in sharp contrast with the $^{87}Sr/^{86}Sr$ isotopic composition of these sediments which is uniform in all samples studied and is identical to that of dissolved Sr in modern seawater. The $\varepsilon_{Nd}(0)$ values of all the ferromanganese sediment samples analyzed are less than 0. The Atlantic Ocean has the most negative values (average $\varepsilon_{Nd}(0) \cong -12$), the Indian Ocean has intermediate values (average $\varepsilon_{Nd}(0) \cong -8$), and the Pacific Ocean has the least negative values (average $\varepsilon_{Nd}(0) \cong -3$). Data for samples from each ocean show relatively small dispersion about the respective average $\varepsilon_{Nd}(0)$ values regardless of the sediment type (ie. hydrogenous and hydrothermal sediments) and other factors such as growth rate and rare earth concentrations. The maximum spread in each ocean is about ± 2 ε units. The Nd isotopic data for ferromanganese sediment samples from all oceans clearly

Figure 3.2. $\varepsilon_{Sr}(0)$ versus $\varepsilon_{Nd}(0)$ for a variety of ferromanganese sediments and seawater from the Atlantic, Indian, and Pacific Oceans. Note the uniform $\varepsilon_{Sr}(0)$ values in all samples in spite of a wide variation in $\varepsilon_{Nd}(0)$ values. The uniform values of $\varepsilon_{Sr}(0)$ reflect the homogenization of the oceans with respect to $^{87}Sr/^{86}Sr$ as a result of a long residence time for Sr relative to the mixing rate of the oceans. Conversely, the wide variation of $\varepsilon_{Nd}(0)$ reflects a very short residence time for Nd relative to the mixing time for the oceans.

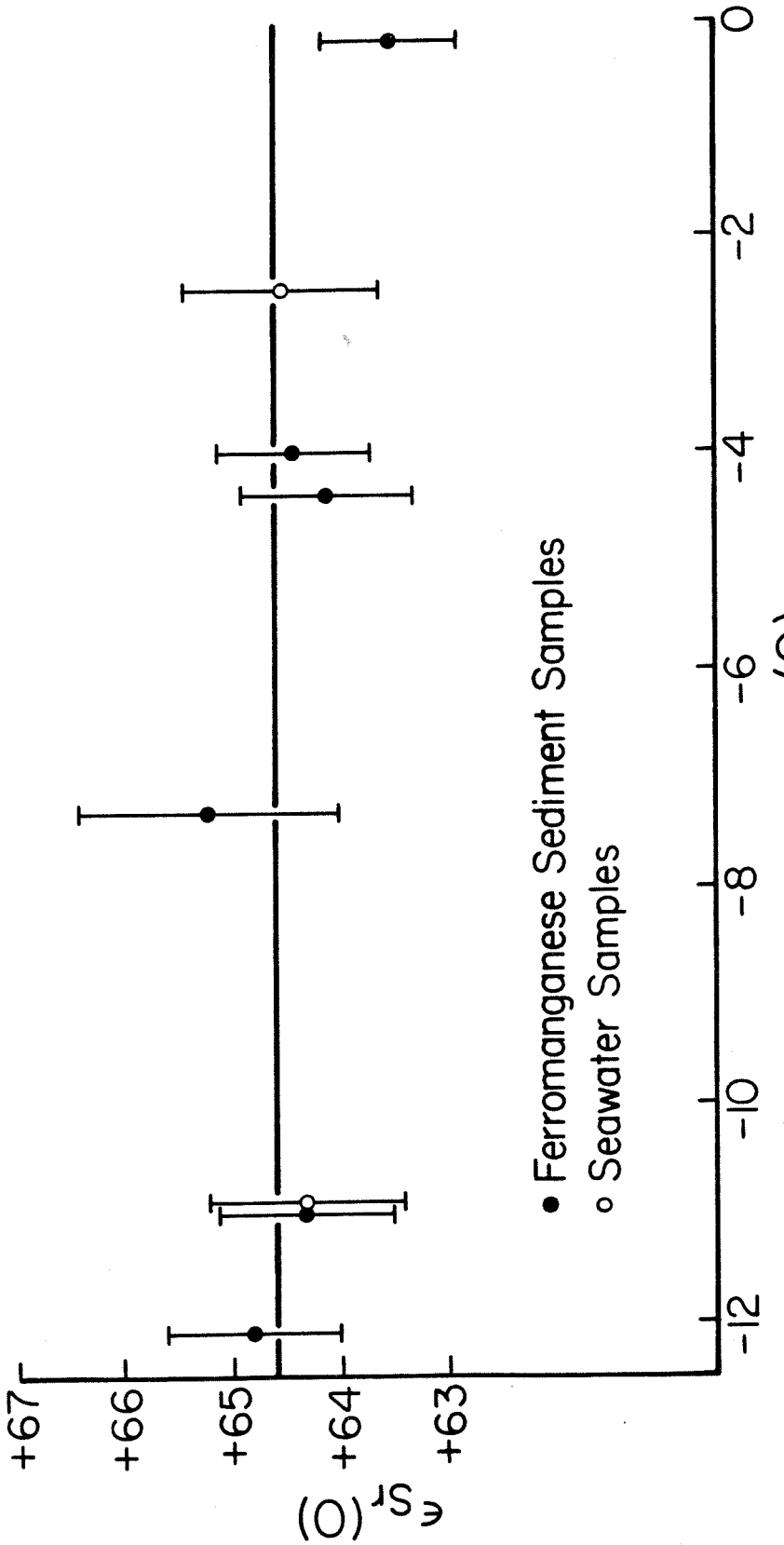
+67
+66
+65
+64
+63
$\epsilon_{Sr}(0)$
-12
-10
-8
-6
-4
-2
0
$\epsilon_{Nd}(0)$
• Ferromanganese Sediment Samples
○ Seawater Samples

Figure 3.2.

indicate that these sediments are dominated by continental sources of rare earth elements ($\varepsilon_{Nd}(0) \leq 0$) and not oceanic sources ($\varepsilon_{Nd}(0) \approx +10$) as shown in Figure 3.1. This is true in spite of the fact that some of the samples were formed by precipitation of Fe and Mn in a hydrothermal environment on mid-ocean ridges. Only small shifts toward more radiogenic $^{143}Nd/^{144}Nd$ values from average Pacific values are observed in some of the hydrothermal sediments from this basin. The most radiogenic sample (OC73-3-12P) may have as much as a 35% contribution from MORB relative to other Pacific samples. The mechanisms for the incorporation of the REE in ferromanganese sediments could include the precipitation of REE dissolved in seawater and the trapping detrital materials. A small variation in the proportions of these individual components between samples may be responsible for the limited Nd isotopic variations in ferromanganese sediments within an ocean. However, the observed Nd uniformities in each ocean indicate that contributions to this element from different sources are relatively well mixed within an ocean basin but distinctly different for each major water mass.

It was originally suggested by O'Nions et al. [1978] that Nd isotopic variations in manganese nodules analyzed by them were possibly due to a detrital component in the nodules. To assess the effects of detrital contributions, consider mixtures (m) of two components A and B. The Nd composition is given by:

$$\varepsilon^{m}_{Nd}(0) = \frac{[X_A][C^{A}_{Nd}][\varepsilon^{A}_{Nd}(0)] + [1 - X_A][C^{B}_{Nd}][\varepsilon^{B}_{Nd}(0)]}{(X_A)(C^{A}_{Nd}) + (1 - X_A)(C^{B}_{Nd})} \qquad (3.1)$$

where X_A is the weight fraction of component A and C^{A}_{Nd} and C^{B}_{Nd} are the concentrations of Nd (in ppm) in components A and B. Taking the shift between Atlantic and Pacific samples to represent a detrital component (B)

added to seawater component (A) with $\varepsilon^{A}_{Nd}(0) \cong -3$, one can calculate the value of $\varepsilon^{B}_{Nd}(0)$ in the detrital component. Using $(1 - X_A) = 0.2$ as a reasonable limit on the weight fraction of detrital material in a manganese nodule (based on world averages for Al and Si abundances in nodules [Cronan, 1977]) and a low value of C^{A}_{Nd} = 100 ppm Nd in the uncontaminated nodule, this yields:

$$[\varepsilon^{B}_{Nd}(0) - \varepsilon^{m}_{Nd}(0)]\ C^{B}_{Nd} = \frac{X_A C^{A}_{Nd}}{(1 - X_A)}\ [\varepsilon^{m}_{Nd}(0) - \varepsilon^{A}_{Nd}(0)] \qquad (3.2)$$

$$\cong 3.6 \times 10^{3} \text{ (units of ppm)}$$

for the Atlantic Ocean where $\varepsilon^{m}_{Nd}(0) \cong -12$. For $C^{B}_{Nd} \cong 35$ ppm, a high value for most crustal rocks, this yields $\varepsilon^{B}_{Nd}(0) \cong -115$ which is close to the total growth of Nd over the history of the earth. The lowest observed $\varepsilon_{Nd}(0)$ is about -30 and yields $C^{B}_{Nd} \cong 200$ ppm which is an excessively high value for possible detrital sources. It follows that the presence of detrital material in the manganese nodules cannot reasonably explain the observed differences between Pacific and Atlantic samples. If 20% by weight of a nodule is derived from an oceanic basalt with $\varepsilon_{Nd}(0) \cong +10$ and $C_{Nd} \cong 10$ ppm, a shift of 0.36ε units is obtained. Some contributions from oceanic basalts and detrital material must obviously take place, but the above considerations show that the magnitude of their effects is likely to be less than an ε unit for manganese nodules. On the basis of these considerations, it is most reasonable that the variations between the ocean basins reflect the dissolved content of Nd in different waters draining off of the various continental masses which are not completely mixed over the time scale for Nd deposition, and only a small contribution comes from oceanic magma

sources. Variations within an ocean basin may also be due dominantly to variations in the dissolved load of Nd within the given ocean basin, but the detrital components of ferromanganese sediments may also be important contributors to these smaller variations.

The results of direct analyses of Nd in seawater shown at the top of Figure 3.1 further demonstrate that there are distinctive Nd isotopic variations between the oceans. The isotopic compositions of Nd in Pacific and Atlantic waters are found to be clearly separated and lie in the same general ranges as observed for ferromanganese sediments from these basins. From this it is concluded that the isotopic composition of Nd in ferromanganese sediments does indeed closely reflect the isotopic composition of Nd dissolved in seawater, and it confirms the distinctive Nd isotopic separation of the major ocean basins determined from ferromanganese sediments. It is reasonable to assume, therefore, that the average isotopic composition of Nd in Indian Ocean waters, though not measured directly, can be accurately inferred from the ferromanganese sediment data for this ocean basin. The isotopic variations can best be explained by a relatively short residence time for Nd in the oceans relative to the rates of exchange between the oceans coupled with the necessity for an older ($\geq$1.5 AE) continental source for the Nd in the Atlantic samples relative to Pacific samples. The fact that ocean waters and ferromanganese sediments in each ocean appear to lie in a rather restricted range suggests a rather thorough mixing of Nd within each ocean basin and indicates that the residence time of Nd is comparable to the mixing rate within isolated ocean basins.

The bottom of Figure 3.1 indicates typical $\varepsilon_{Nd}(0)$ values of possible sources of REE in the oceans. Comparison of seawater and ferromanganese sediment data in Figure 3.1 with possible sources clearly shows that

substantial contributions from continental sources are necessary to produce the observed $\varepsilon_{Nd}(0)$ values in the marine environment. Assuming North American Shale ($\varepsilon_{Nd}(0) = -14.1$ [DePaolo and Wasserburg, 1976b]) to represent average continental crust, then it is determined that contributions from continental sources account for at least 80% of the Nd in the Atlantic Ocean and a minimum of 50% in the Pacific Ocean. Differences in the $\varepsilon_{Nd}(0)$ values between the Pacific and Atlantic Oceans may be due to differences in the $\varepsilon_{Nd}(0)$ values of the continental sources directly supplying REE to each of these oceans and without significant transport of REE between the oceans. Another possibility is that the $\varepsilon_{Nd}(0)$ values in the continental sources are the same for both oceans, with the Pacific Ocean having much larger contributions (as much as 50%) from oceanic mantle sources with $\varepsilon_{Nd}(0) \cong +10$. Continental drainage patterns indicate a far greater drainage for fresh water into the Atlantic Ocean relative to the Pacific Ocean [Budyko, 1974], whereas mid-ocean ridge inputs in the Pacific may be much greater than in the Atlantic due to the much faster ridge spreading rates in the Pacific [Rona, 1984]. Consideration of these observations suggest that the observed $\varepsilon_{Nd}(0)$ values for Pacific water may reflect a large contribution of oceanic mantle sources ($\varepsilon_{Nd}(0) \cong +10$) mixed with Atlantic waters ($\varepsilon_{Nd}(0) \cong -12$) with only small, direct contributions into the Pacific basin from older continental sources. However, no marine sediments or seawater have been analyzed as yet which have $\varepsilon_{Nd}(0)$ values significantly greater than zero. The best place to look for positive $\varepsilon_{Nd}(0)$ values in the marine environment may be in waters emanating from deep-sea hydrothermal springs associated with mid-ocean ridge spreading centers such as those observed at the Galapagos Rift [Corliss et al., 1979] and 21°N on the East Pacific Rise [Rise Project Group, 1980]. Submarine hydrothermal fluids have been investigated and

found to have positive $\varepsilon_{Nd}(0)$ values. These data are discussed in detail in Chapter 7. However, the fact that positive values of $\varepsilon_{Nd}(0)$ have not been observed for sediments and seawater surrounding ridge crest areas indicates that submarine volcanic sources (or hydrothermal systems) cannot play a dominant role as a source of rare earth elements. Some contributions from oceanic mantle sources with positive $\varepsilon_{Nd}(0)$ values are likely, however, to account for the Nd isotopic differences between the Atlantic and Pacific Oceans. The data suggest that Nd is derived dominantly from continental sources draining into each ocean basin to produce the negative $\varepsilon_{Nd}(0)$ values but that this component is diluted with with Nd having $\varepsilon_{Nd}(0) > 0$ from oceanic mantle sources primarily in the Pacific to produce the large isotopic difference between the Atlantic and Pacific.

In an attempt to determine paleo-isotopic variations of Nd in seawater over short time scales (<30 m.y.), surface and central layers of a Pacific manganese nodule (MN139) have been analyzed. The growth rate of this nodule has been determined by ^{10}Be and uranium series methods to be 1 to 2 mm/10^6 years [Ku et al., 1979]. From this information, the time span represented by this nodule is estimated to be at least 19 m.y. Results of Nd isotopic analyses are given in Table 3.1. The $\varepsilon_{Nd}(0)$ values for the 0 to1 mm and 36 to 37 mm layers are not significantly different to indicate changes in the REE sources in the Pacific Ocean during this time interval.

Neodymium isotopic variations over longer time scales would be expected, however. Sr isotopic variations in seawater during Phanerozoic time have been documented [Peterman et al., 1970; Dasch and Biscaye, 1971] and a similar approach as used for Sr paleo-isotopic research could be applied to Nd isotopic studies. If one considers the hypothetical Pangean super-continent, the surrounding Panthalassa Ocean should have had a fairly

TABLE 3.1. Results of Nd isotopic measurements in two layers of a Pacific Ocean manganese nodule (MN139) recovered from a depth of 3916 m at 20°01'N,136°36'W. This nodule has been dated by radiometric methods [Ku et al., 1979] and found to have a growth rate of 1.3 to 1.9 mm/10^6yr.

Depth of layer(mm)	Age (m.y.)	$^{143}Nd/^{144}Nd$	$\varepsilon_{Nd}(0)$
0 - 1	0 - 0.8	0.511662 ± 20	-3.6 ± 0.4
36 - 37	19 - 28	0.511608 ± 24	-4.6 ± 0.5

uniform Nd isotopic composition as there would have been no isolation of water masses by continental barriers which would prevent mixing. Authigenic and pelagic sediments deposited in this ocean should reflect this, and the isotopic compositions may be preserved in the sedimentary record. Isolation of water masses by the formation of interior seas and new oceans (i.e., the Tethys Sea and the Atlantic Ocean) as a result of continental drift and seafloor spreading rearranging the configuration of the continental land masses would produce drainage patterns which are unique for each body of water into which they flow. These isolated seas would have Nd isotopic compositions characteristic of the waters issued from the adjacent continental drainage systems and would not be mixed with the larger oceans. The isotopic composition of individual seas would most likely be different from one water mass to another as observed in today's oceans as well as being different from Panthalassa. The Nd isotopic composition of paleo-seas, if preserved in the sedimentary record, should provide a crude reconstruction of surface drainage patterns and the degree of isolation of ocean basins at times in the geologic past corresponding to changes in the configuration of the continents.

There do appear to be small differences between Nd isotopic data from seawater and values determined for ferromanganese sediments within the same ocean basin. For example, one sample from the Scotia Sea (E28-5) has $\varepsilon_{Nd}(0) = -5.3$, whereas seawater in the nearby Drake Passage has $\varepsilon_{Nd}(0) \approx -9$. This and similar discrepancies are hard to explain in view of the more general similarity between seawater and ferromanganese sediment isotopic results and suggests that ferromanganese sediments may derive part of their REE from sources other than the direct precipitation from seawater. Elderfield et al. [1981] made detailed comparisons between REE in manganese nodules and

underlying sediment substrates. Based on correlations between REE concentrations manganese nodules and associated sediments, they concluded that the REE in nodules were derived at least in part by diagenesis of the underlying sediments. However, they pointed to an original seawater source for the REE in both the nodules and the sediments based on Nd isotopic arguments resulting primarily from the findings of this study. The available data base for Nd in deep sea sediments is small. While there is often a close similarity between Nd isotopic results for deep sea sediments and seawater or ferromanganese sediments from a given ocean basin, data from Goldstein and O'Nions [1981] indicate that pelagic sediments can have very different isotopic compositions from overlying seawater. For example, they report one Atlantic deep sea sediment sample as having $\varepsilon_{Nd}(0) \approx -3$. Their results indicate that diagenesis of deep sea sediments could supply Nd of diverse isotopic composition to manganese nodules and other authigenic sediments growing on sediment substrates.

3.6 Conclusions

Authigenic ferromanganese sediments indicate sharp and clear Nd isotopic compositional differences between the Atlantic, Pacific, and Indian Oceans. The composition of Nd measured in Atlantic and Pacific Ocean waters is very close to that of ferromanganese sediments in these respective ocean basins indicating that the isotopic composition of Nd in authigenic ferromanganese sediments accurately reflects seawater values in the basin sampled. The data firmly establish that there are distinct Nd isotopic variations in seawater and that the isotopic composition of Nd in ocean water is characteristic of the individual ocean basins. These differences

are directly reflected in the ferromanganese sediments. The clear distinction between the ocean basins should permit the application of the Nd isotopic composition of ocean water and chemical precipitates as a general tracer in oceanography. This characteristic difference between the Atlantic and Pacific Oceans corresponds to a difference in the relative abundance of ^{143}Nd between these water masses of only 10^6 atoms/g seawater.

The Nd isotopic composition of modern ambient seawater appears to be rather accurately reflected in ferromanganese sediments. It is possible that this may prove to be more generally true for a wider variety of chemical sediments including carbonates. If the isotopic composition of ambient "local" seawater is preserved in ancient chemical sediments, it may be possible to use the ^{143}Nd isotopic abundance in paleo-oceanographic studies and in testing models of the geometrical configurations resulting from continental drift.

Besides serving as a tracer for studying rare earth element transport in the oceans, several aspects to the observations made here lead to the conclusion that the isotopic composition of Nd in seawater may serve broadly as a tracer for studying a variety of oceanographic problems unrelated to the rare earth elements. The large difference in $\varepsilon_{Nd}(0)$ between the Atlantic and Pacific Oceans indicate that the isotopic composition of Nd may be useful as a tracer to monitor the exchange of water between these two oceans through the Drake Passage. Isotopic differences observed between surface waters and deep waters in the Atlantic and Pacific Oceans suggest that the Nd isotopic composition may also be useful for distinguishing the origin and mixing of water masses in an ocean basin. These aspects to the isotopic measurements presented here are a major focus of remaining chapters in this thesis.

CHAPTER 4: Isotopic Composition of Neodymium in Waters from the Drake Passage and Central Pacific

4.1 Introduction

Because of the difference in $\varepsilon_{Nd}(0)$ between the Atlantic and Pacific Oceans, it should be possible to use the Nd isotopic composition to monitor the exchange and mixing of water between these oceans. The Drake Passage is the only region where significant transport of water can take place between the Atlantic and Pacific basins, and it is presumed that some Pacific water is entrained into the Atlantic after entry through the Drake Passage, where there is a net eastward flow of water at ~ 130 sverdrups (1 Sv = 10^6 cubic meters per second) [Bryden and Pillsbury, 1977; Nowlin et al., 1977]. The isotopic composition of Nd in water flowing through the Drake Passage has been determined and is compared with the results for the Atlantic and Pacific Oceans discussed in Chapter 3. Because of the eastward transport through the Drake Passage, it was expected that there would be Pacific signatures in the Nd isotopic composition of water flowing through this region. In this chapter some ideas will be put forward that are derived from limited data on Nd isotopic variations which appear to be pertinent to the problems of large-scale transport and mixing of the oceans. This represents an initial exploration of these problems with a new isotopic tracer. The data presented are a small supplement to the extensive and diverse observations made by oceanographers for many decades and can only be interpreted within the larger framework of oceanographic studies.

4.2 Sampling

Samples were collected during leg 11 of cruise 107 of the R/V Atlantis II from vertical profiles of the water column at several stations in the Drake Passage and southeast Pacific. Locations of the sampling sites are shown in Figure 4.1. Exact sampling locations and depths of individual samples are listed in Table A2 in the appendix. Stations 292 and 315 are south of the Antarctic polar front, which was located at about 58°S in the Drake Passage during this cruise [McCartney, in preparation]. Stations 261 and 327 are both to the north of the polar front. The Antarctic polar front results from convergence of cold, northward flowing Antarctic surface waters with warmer, southward flowing subantarctic surface waters and is characterized by a relatively large meridional surface temperature gradient of 3° to 5°C. This polar frontal zone is sometimes considered to represent the northern boundary of the Southern Ocean, although a more northerly boundary defined by the subtropical convergence (located at approximately 50°S) is also used as this includes the subantarctic zone of surface water. The deep waters of the subantarctic zone include components derived outside of the Antarctic, whereas waters south of the Antarctic polar front are entirely of Antarctic origin [Gordon, 1967].

Samples from two central Pacific locations (Marine Chem. 80, Stations 17 and 31) including one vertical profile (Station 31) are also presented here. The locations of these samples are listed in Table A2 and are shown in Figure 2.1 of Chapter 2. The bottom water sample from Station 31 of this expedition was collected with the intent of obtaining northward spreading Antarctic Bottom Water and will be compared with the results for the Drake Passage area samples.

Figure 4.1. Map showing locations of water sampling sites in the Drake Passage and southeast Pacific for Nd analysis. Stations for which Nd data were obtained in this study are labeled with station numbers.

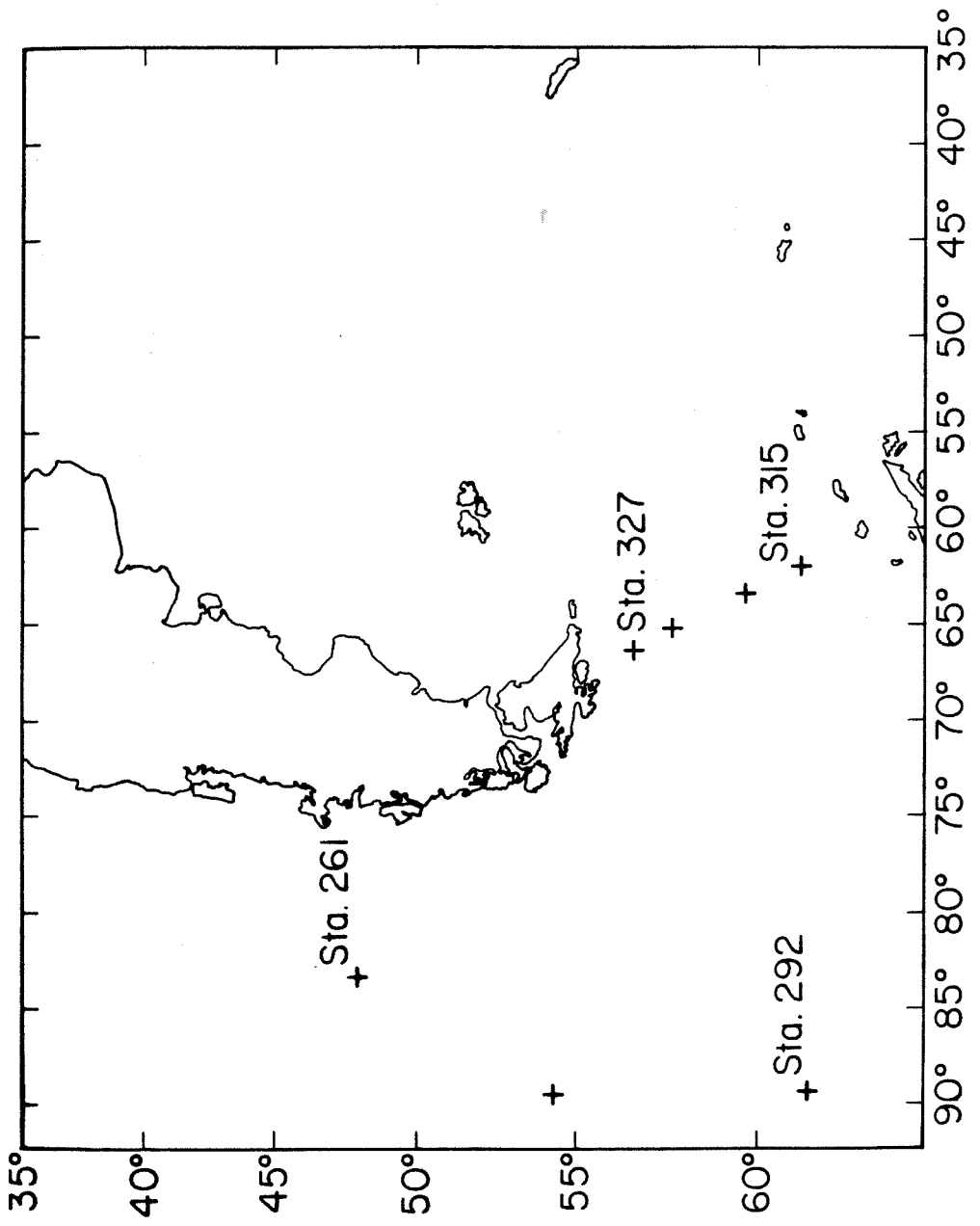
Sta. 261
Sta. 327
Sta. 315
Sta. 292
35°
40°
45°
50°
55°
60°
90°
85°
80°
75°
70°
65°
60°
55°
50°
45°
40°
35°

Figure 4.1.

4.3 Results

Results of the Nd isotopic measurements on seawater samples from the Drake Passage and the Central Pacific are listed in Table A2 and are shown in the histogram in Figure 3.1. The isotopic data are also shown in Figure 4.2 where they are plotted as a function of water depth. In addition to isotopic measurements, Sm and Nd concentrations were measured, and these results are shown in Table A2 and Figure 4.3.

The results for samples from the Drake Passage show $\varepsilon_{Nd}(0)$ values which are fairly uniform at all depths, ranging from -8.2 to - 9.2 (Fig. 4.2A). The Antarctic polar front, which divides the transect along which the samples were taken, has no observable effect on the distribution of isotopic compositions of Nd in the Drake Passage. Two bottom water samples from stations in the general vicinity of the Drake Passage in the Southeast Pacific were also analyzed (Fig. 4.2A). Station 261 is about 700 kilometers west of the coast of Chile in the Humboldt Plain and far north of the Drake Passage, and the sample has $\varepsilon_{Nd}(0) = -7.9$. Station 292 is west of the Drake Passage in the Bellingshausen Plain within the Antarctic Circumpolar Current, and has $\varepsilon_{Nd}(0) = -8.2$. These deep waters are indistinguishable in terms of Nd isotopic composition from the waters in the Drake Passage.

At station 31 in the South Central Pacific, $\varepsilon_{Nd}(0)$ decreases with depth from 0.3 at 30 m to -8.1 at 4500 m (Figure 4.2C). A single sample from 2000 m at station 17 in the North Central Pacific has $\varepsilon_{Nd}(0) = 0.0$, compared to a value of -4.5 for a sample at 2800 m at station 31. Unlike the Drake Passage samples which exhibit uniform $\varepsilon_{Nd}(0)$ values with depth, the central Pacific samples exhibit substantial depth variations. Comparison of $\varepsilon_{Nd}(0)$ for the Central Pacific sample from 4500 m at station 31 ($\varepsilon_{Nd}(0) = -8.1$)

Figure 4.2. Value of $\varepsilon_{Nd}(0)$ as a function of water depth in (A) the Drake Passage, (B) OCE 63 in the North Atlantic, and (C) the south central Pacific (Station 31). The isotopic data for the Drake Passage and nearby Pacific stations have very uniform $\varepsilon_{Nd}(0)$ values with both depth and location indicating that the waters in this region are very well mixed with respect to Nd isotopic composition. In contrast, both the Pacific and Atlantic profiles shown here have distinct variations in $\varepsilon_{Nd}(0)$ with depth indicating the lateral transport of Nd from different and isotopically distinct sources. In the case of the Pacific profile, the bottom water value is interpreted to represent northward spreading AABW. Symbols in (A): (square) Station 315; (circle) Station 327; (diamond) Station 261; (triangle) Station 292.

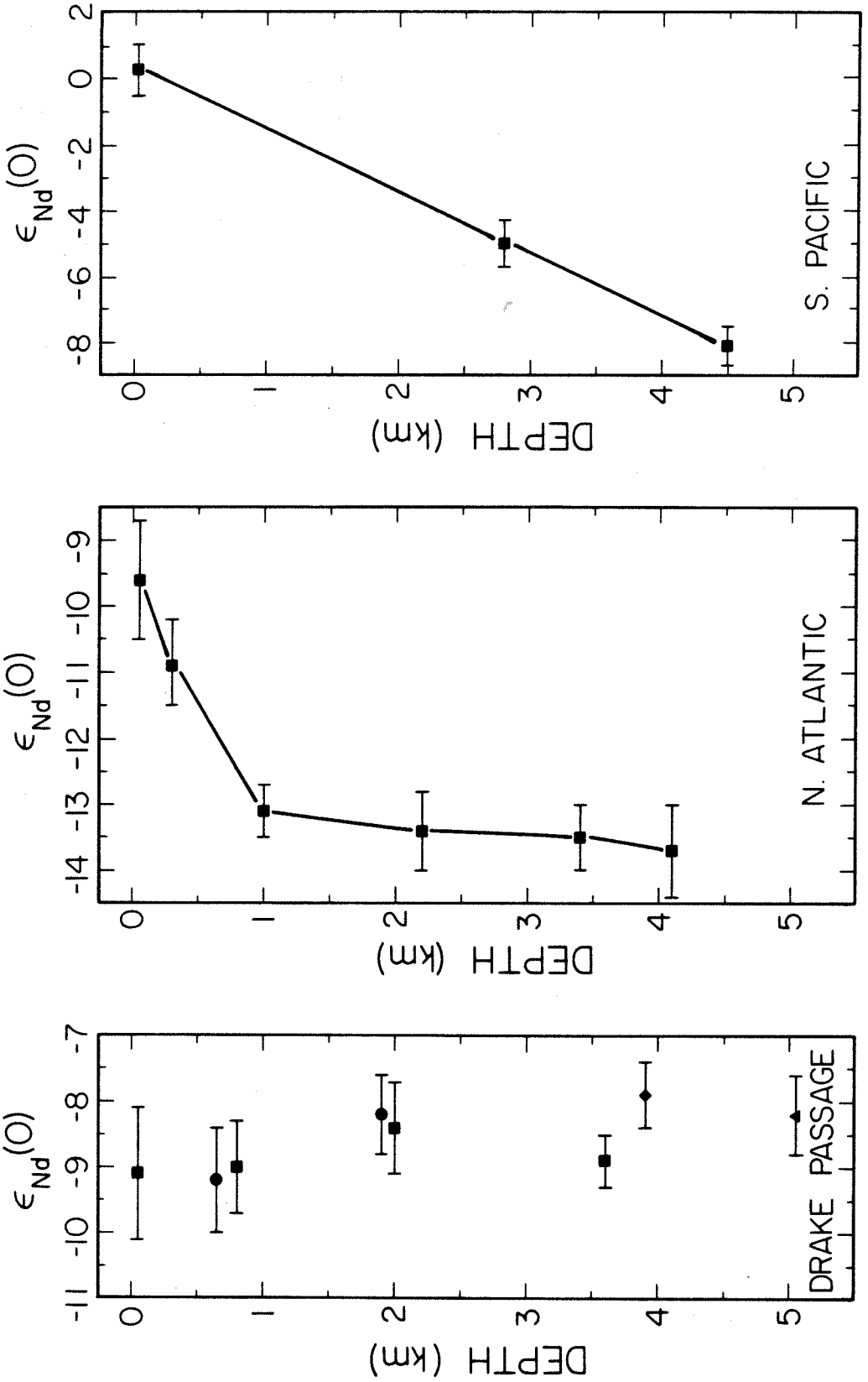

Figure 4.2.

Figure 4.3. Neodymium concentration as a function of depth in (A) the Drake Passage (Stations 315 and 327), (B) OCE 63 in the North Atlantic, and (C) Station 31 in the south central Pacific. In contrast to the isotopic data, the Drake Passage samples show distinct increases in Nd concentration with depth indicating that while these waters are isotopically well mixed, they are chemically stratified. The similarity of the Drake Passage profiles to the Atlantic and Pacific profiles indicate that the transport mechanisms which generate Nd concentration gradients are similar everywhere in the oceans. Errors on the data points are negligible compared to the size of the symbols.

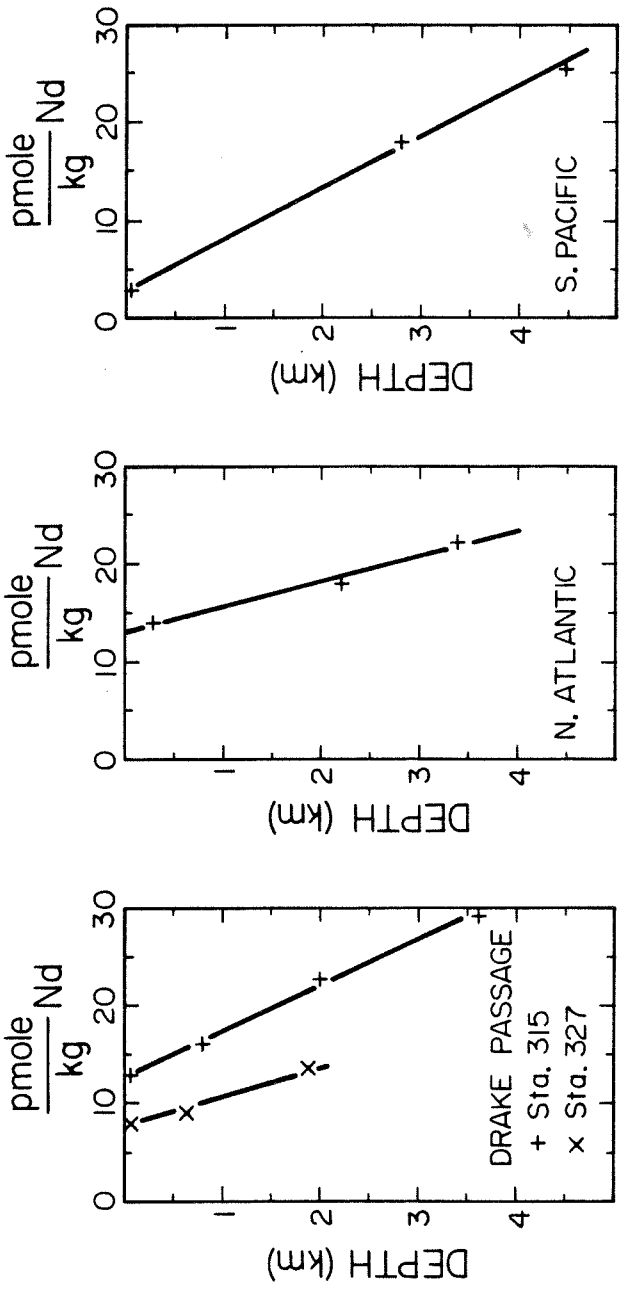
pmole/kg Nd
DEPTH (km)
DRAKE PASSAGE
+ Sta. 315
× Sta. 327
A
N. ATLANTIC
B
S. PACIFIC
C
PIEPGRAS AND WASSERBURG, 1982

Figure 4.3.

with values from the Drake Passage (Fig. 4.2A) shows them to be indistinguishable and indicates that this sample represents Antarctic Bottom Water underlying middle and deep Pacific water.

Where measured, both Sm and Nd concentrations are found to increase with depth at all locations. The Nd concentration profiles for several stations including one from the North Atlantic are shown in Figure 4.3 All stations show an approximately linear increase in Nd concentration with depth. The sample from 30 m at Station 31 has the lowest Nd concentration yet measured in seawater.

4.4 Discussion

The $\varepsilon_{Nd}(0)$ values for the Drake Passage shown in Figure 3.1 (Chapter 3) and Figure 4.2A are close to -9. These values lie in the direction of more ancient continental sources than the Pacific and are far removed from young oceanic mantle-type sources, for which $\varepsilon_{Nd}(0) \cong +10$. They are intermediate between North Atlantic and mid-depth Pacific values and closer to the Atlantic values, and they are similar to and possibly slightly lower than the values inferred for the Indian Ocean. From these data it is concluded that the water flowing out of the Pacific sector of the Southern Ocean and into the Atlantic sector has Nd which is dominantly of Atlantic or Indian Ocean origin rather than dominantly of Pacific Origin.

Bottom waters of the Bellingshausen Plain to the west of the Drake Passage and the Humboldt Plain west of central Chile far north of the Antarctic Convergence have the same $\varepsilon_{Nd}(0)$ as the Drake Passage. These data show a coherence in Nd isotopic composition for the Southern Ocean and support its identification as a distinctive water body. In addition, a

sample of cold bottom water from the Central Pacific has the same value of $\varepsilon_{Nd}(0)$ as the Drake Passage, which identifies this bottom water with a northward spreading part of the Southern Ocean. These results are in agreement with observations by Reid and Lynn [1971] and Reid [1981], who showed that waters having physical oceanographic properties with Atlantic characteristics are preserved in the bottom waters of the Pacific Ocean. More generally, the results presented here support extensive observations of physical oceanographic properties which identify the Southern Ocean as a distinct water mass that is preserved in the bottom waters over extensive regions of the world ocean (see color plates in Dietrich et al. [1980]).

It should be noted here that only the bottom water samples from stations 261 and 292 were analyzed. It is not known from the present data base whether or not the water column at these two stations is uniform with respect to $\varepsilon_{Nd}(0)$ values as in the Drake Passage. Station 292 is located south of the Antarctic polar front, and for this reason it may be expected that the water column will be isotopically uniform. Station 261, on the other hand, is considerably north of the polar front and the surface waters are much warmer and saltier than in the Drake Passage. This condition might also be reflected in the Nd isotopic composition. Until further work is done on these waters, conclusions regarding the origin and transport of Nd in the waters of this region of the Southeast Pacific must be limited to bottom water transport.

If it is assumed that the water in the Drake Passage consists only of mixtures of Atlantic and Pacific seawater (ignoring fresh water) and that the Nd concentrations in these waters are equal, estimates of the relative amounts of water contributed by these sources which would yield $\varepsilon_{Nd}(0) \cong -9$ can be determined. Using the estimates of $\varepsilon_{Nd}(0)$ for the two oceans given

in Chapter 3, it is calculated that about 70 percent of the water flowing through the Drake Passage into the Atlantic Ocean is of Atlantic origin. Allowing for errors in the estimates of $\varepsilon_{Nd}(0)$ for the Atlantic and Pacific oceans, a lower limit of at least 50 percent Atlantic water is required to balance the Nd isotopic data for the Drake Passage. The Pacific contribution to the Nd budget appears to be smaller than or equal to that of the Atlantic.

This balance, however, is in disagreement with some views based on physical oceanographic observations which indicate that the Pacific should dominate the water properties of this region. The salinity maximum in the Drake Passage has been reported to be 34.725 °/oo [Georgi, 1981; Bainbridge, 1980], which is confirmed at our stations (see Fig. 4.4A). Using this salinity maximum for the Drake Passage and Montgomery's [1958] values for the mean salinities of the Atlantic (≈ 34.9 °/oo) and the Pacific (≈ 34.6 °/oo mil), then at least 60 percent of the water in the Drake Passage should be of Pacific origin if only Pacific and Atlantic mixtures are considered. As there is a substantial contribution of fresh water to the Southern Ocean, it is not clear that Drake Passage water may be considered as a mixture of components having the mean salinity characteristics of the Atlantic and Pacific. Heat budget calculations by Hastenrath [1980] indicate that there must be a net heat transfer from the Pacific to the Atlantic. Stommel [1980], using data from Hastenrath [1980], indicates that the South Pacific Ocean supplies heat dominantly by mass flow in the South Atlantic and that the transfer takes place through the Drake Passage (see figure 1 in [Stommel, 1980]). However, the available heat budget data are subject to large uncertainties and may not be a reliable indicator of the mass flow and hence the relative sources of water in the Drake Passage. The

possibility that the Nd isotopic compositions in the Southern Ocean are controlled by contributions of dissolved Nd from Antarctica has also been considered. Using an estimate for the runoff from Antarctica of 0.075 Sv [Kozoun et al., 1974] and an upper limit of 40 nanograms per liter for the Nd concentration in fresh water [Martin and Maybeck, 1979], the transport of dissolved Nd to the Southern Ocean from Antarctica is estimated to be 3 grams per second. Gordon [1971] estimates a rate of exchange of ~ 20 Sv between the Atlantic and Southern oceans. If deep water has an average Nd concentration of 3 ng/liter, the transport of dissolved Nd from the Atlantic to the Southern Ocean is ~ 63 g/sec. The value calculated for the Nd flux from Antarctica is only 5 percent of this, indicating that runoff from Antarctica is not an important source of Nd in the Southern Ocean. It is concluded that, unless there is another source of rare earths in the Southern Ocean (possibly atmospheric dust), less than 50 percent of the water flowing through the Drake Passage is from the Pacific and the salt and heat budgets of the region should be reconsidered.

Potential temperature versus salinity for stations 315 and 327 from the Drake Passage and station 31 in the Pacific are shown in Figure 4.4. The diagrams for stations 315 and 327 indicate that four components of water having distinctive temperature and salinity characteristics are involved in mixing. In spite of samples representing these different components, the uniform Nd isotopic values for the Drake Passage indicate only one component of Nd in the water column. The T-S diagram for station 31 also indicates four components of water involved in mixing, but only two components are indicated for Nd from the isotopic data. In general, these T-S relations indicate that lateral and vertical transport must play a role in mixing. These observations indicate that the distribution and transport of Nd in

Figure 4.4. Potential temperature versus salinity diagrams for (A) two stations from the Drake Passage (stations 315 and 327) and (B) station 31 in the central South Pacific. (A) Drake Passage. The T-S characteristics in the water column at station 315 are observed to lie along the curve represented by the points A (surface), B (~1900m), and C (~3600m). Squares labeled 1 to 4 correspond to the Nd samples analyzed from this station (see Figure 4.2a and 4.3a) at 50, 800, 2000, and 3600 m, respectively. The temperature and salinity characteristics of the water column at station 327 are observed to lie along the curve between points D (surface) and B (~1900m). Circles labeled 5 and 6 correspond to Nd samples (see Figures 4.2a and 4.3a) at 650 and 1900 m, respectively. The T-S data are for 50 m intervals from CTD casts.
(B) Central South Pacific, station 31. Points 1 to 3 correspond to Nd samples (see Figures 4.2c and 4.3c) at 30, 2800, and 4500 m, respectively. The shape of this curve is inferred from eight T-S measurements made at this station.

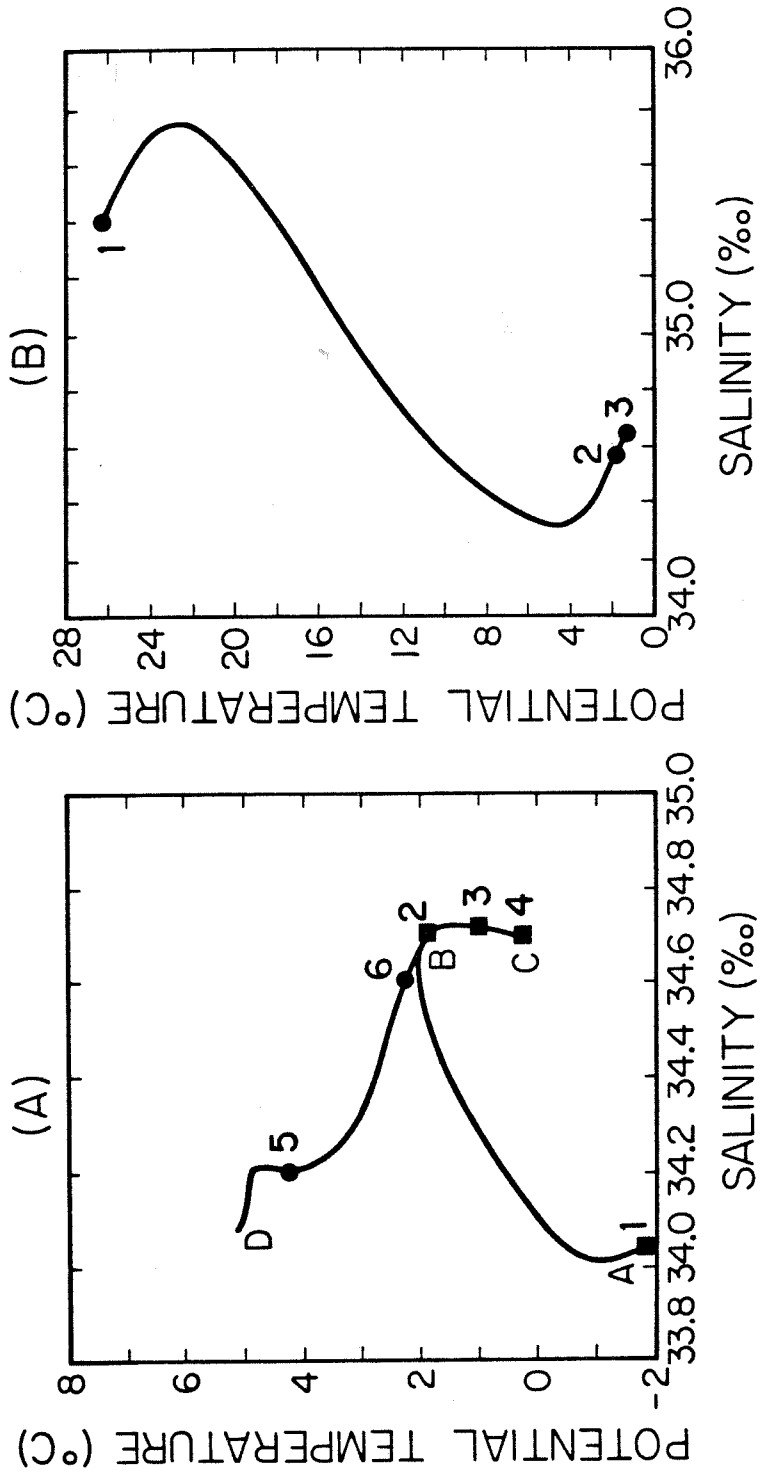
(A)
POTENTIAL TEMPERATURE (°C)
SALINITY (‰)
8
6
4
2
0
-2
33.8 34.0 34.2 34.4 34.6 34.8 35.0
A
B
C
D
1
2
3
4
5
6
(B)
POTENTIAL TEMPERATURE (°C)
SALINITY (‰)
28
24
20
16
12
8
4
0
34.0 35.0 36.0
1
2
3

Figure 4.4.

seawater may not be dependent on factors that directly influence local temperature and salinity variations.

The uniform values of $\varepsilon_{Nd}(0)$ in the Drake Passage (Fig. 4.2A) also contrast with the vertical distribution of $\varepsilon_{Nd}(0)$ observed elsewhere, such as seen for a typical North Atlantic profile (Fig. 4.2B, from OCE 63 data) and the south central Pacific profile (Fig. 4.2C). The changes in Nd isotopic composition with depth in the profiles from the North Atlantic and south central Pacific indicate that the profiles consist of water layers with different sources and that the vertical mixing rates must be slow relative to the horizontal transport. This suggests that the addition of Nd to Southern Ocean waters form other source regions (Pacific, Indian, and Atlantic oceans) must be slow relative to the vertical mixing rates of Nd in the Southern Ocean. The more rapid vertical mixing of Nd in the Drake Passage must be related to the weak density stratification in this region resulting from convective overturn in the water column by cold, dense surface waters.

In contrast to differences in $\varepsilon_{Nd}(0)$ in the water column at different locations, Nd concentration profiles all exhibit approximately linear increases with depth as shown in Figure 4.3. A similar distribution is observed for Sm, indicating that the same processes control the vertical transport of these two elements in the water column. The data indicate that while Nd is isotopically well mixed in the Drake Passage, it is not chemically well mixed. The concentration data require some sort of vertical transport to explain the observations. This presumably involves sequestering by particles to deplete the surface layers and allow for an enrichment in the deep waters. This problem will be dealt with in greater detail in a later chapter.

4.5 Box Model

A six-box model is constructed in order to characterize the mixing of the Southern, Atlantic, Indian, and Pacific oceans. Figure 4.5 depicts the model and the exchange paths. The Southern Ocean is divided into three boxes, 1,2,and 3, adjacent to the Atlantic, Indian, and Pacific oceans, represented by boxes 1', 2', and 3', respectively. This subdivision is to account for interactions with the other oceans. (Georgi [1981] presented data for a series of transects of the Southern Ocean including the Drake Passage and regions south of Africa and New Zealand, which have boundaries between the Southern Ocean and Major Ocean basins to the north. He showed that salinity in the Southern Ocean decreases from a maximum south of Africa to a minimum in the Drake Passage and interpreted this as resulting from successive interactions with the Atlantic, Indian, and Pacific oceans.) Flow between the Southern Ocean boxes is constrained to be unidirectional and toward the east by the Antarctic Circumpolar Current. Flow between the Southern Ocean and the major oceans to the north is two-directional and constrained to be between adjacent primed and unprimed boxes only, as shown in Figure 4.5. If it is assumed that there are no sources of Nd within the Southern Ocean, then for box 1 at steady state the relation is

$$0 = \varepsilon_3 C_3 \dot{W}_{31} - \varepsilon_1 C_1 \dot{W}_{12} + \varepsilon_{1'} C_{1'} \dot{W}_{1'1} - \varepsilon_1 C_1 \dot{W}_{11'} \qquad (4.1)$$

where the ε's are the Nd isotopic compositions, the C's are Nd concentrations, and the $\dot{W}_{ij}$ are rates of volume transport of water from box i to box j. Taking the flow of the Antarctic Circumpolar Current to be

Figure 4.5. Box model for mixing in the Southern Ocean. The Southern Ocean is divided into three boxes (1, 2, and 3) adjacent to the Atlantic (1'), Indian (2'), and Pacific (3') Oceans, respectively. The equations at steady state governing the exchange of Nd between each box are given in the text. Note that the flow between adjacent Southern Ocean boxes is constrained to be in one direction only. From this model and the Nd isotopic data, an upper limit for the exchange of water between the Pacific and the Southern ocean has been calculated to be 33×10^6 $m^3 s^{-1}$.

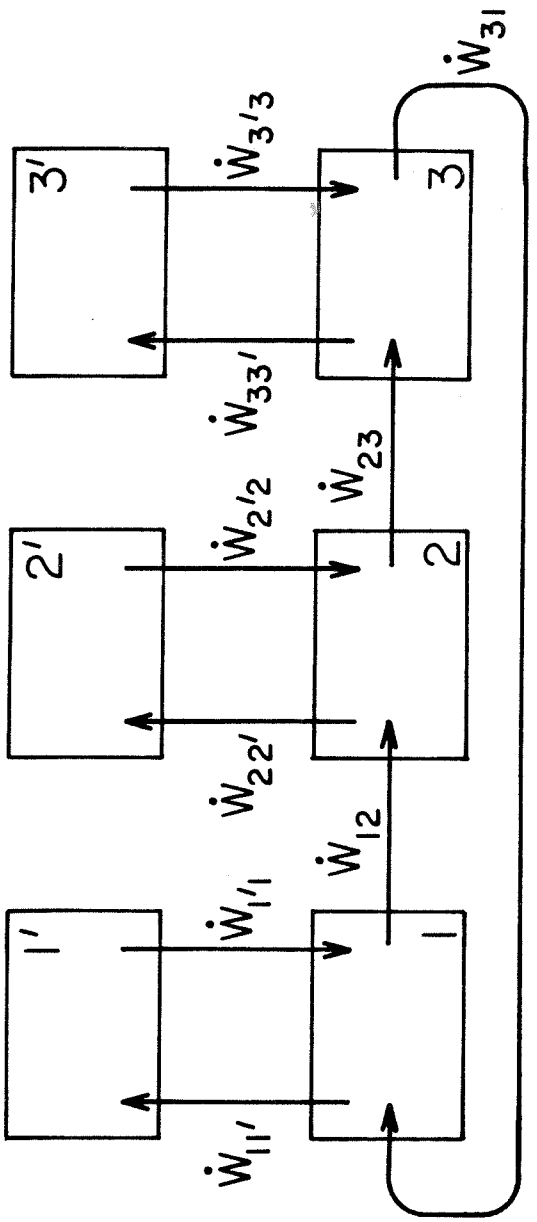
1'
2'
3'
1
2
3
$\dot{W}_{11'}$
$\dot{W}_{1'1}$
$\dot{W}_{22'}$
$\dot{W}_{2'2}$
$\dot{W}_{33'}$
$\dot{W}_{3'3}$
$\dot{W}_{12}$
$\dot{W}_{23}$
$\dot{W}_{31}$

Figure 4.5.

uniform, yields $\dot{W}_{12} = \dot{W}_{23} = \dot{W}_{31}$. Letting $\dot{W}_{11'} = \dot{W}_{1'1}$ and taking the C's to be approximately equal, Eq. 4.1 reduces to

$$0 \approx (\varepsilon_3 - \varepsilon_1)\dot{W}_{12} - (\varepsilon_1 - \varepsilon_{1'})\dot{W}_{11'} \tag{4.2}$$

Similarly, for boxes 2 and 3, respectively

$$0 \approx (\varepsilon_1 - \varepsilon_2)\dot{W}_{12} - (\varepsilon_2 - \varepsilon_{2'})\dot{W}_{22'} \tag{4.3}$$

$$0 \approx (\varepsilon_2 - \varepsilon_3)\dot{W}_{12} - (\varepsilon_3 - \varepsilon_{3'})\dot{W}_{33'} \tag{4.4}$$

With the available data base this box model is underdetermined, but $\varepsilon_{Nd}(0)$ was estimated for the undetermined Southern Ocean boxes in order to calculate an upper limit for the rate of exchange between the Southern Ocean and the Pacific ($\dot{W}_{33'}$). Bounds may be obtained on the unknown ε values by assuming that $0 \leq \dot{W}_{11'}/\dot{W}_{12} \leq 1$. This yields equations of the form $0 \leq (\varepsilon_i - \varepsilon_j)/(\varepsilon_j - \varepsilon_{j'}) \leq 1$. Taking $\varepsilon_3 = -9$, $\varepsilon_{3'} = -3$, and $\varepsilon_{2'} = -8$, yields $-9.25 \geq \varepsilon_2 \geq -10.5$. Using this result in Eq. 3.4 and taking $\dot{W}_{12} = 130$ Sv, an upper limit of $\dot{W}_{33'} \approx 33$ Sv is calculated for the flow rate between the Pacific and Southern oceans. From this a lower limit of ~ 800 years is obtained for the mean time for exchange between the Atlantic and Pacific. The most sensitive parameters are the values of $\varepsilon_{Nd}(0)$ associated with the different segments of the Southern Ocean. If the difference between these values goes to zero, then mixing, as constrained by these approximations, cannot occur, and it would be necessary to consider concentration differences as well. Actual estimates for the rate of

exchange of water between the Southern Ocean and the Atlantic is on the order of 20Sv. At this rate of exchange, the calculated values for each of the Southern Ocean boxes would be nearly identical and could not be distinguished at the present levels of resolution for Nd isotopic measurements. The analysis of water samples from other Southern Ocean locations for Nd isotopic composition will be necessary to verify the approach used in this model.

4.6 Conclusions

Water flowing through the Drake Passage has an average Nd isotopic composition corresponding to $\varepsilon_{Nd}(0) \cong -9$. The $\varepsilon_{Nd}(0)$ values reported here indicate that about two-thirds of the Nd in these waters is of Atlantic origin. Considering the uncertainties, at most one-half can be of Pacific origin. These sources of the water mass do not agree with those based on the estimated salt budget for the Drake Passage or on heat transport considerations. From the Nd data reported here, the Antarctic Circumpolar Current is dominated by Atlantic water, which it spreads to other ocean basins and recirculates back into the Atlantic. These observations are in qualitative agreement with those of Reid and Lynn [1971] and Reid [1981], who inferred the presence of Atlantic water in the Indian and Pacific oceans from physical properties of the water and concluded that the Antarctic Circumpolar Current spreads the Atlantic water to other ocean basins, but made no quantitative estimates of the amount of Atlantic water in the Circumpolar Current.

Concentrations of Sm and Nd in the water column show an approximately linear increase with depth in the Drake Passage and at other locations. In

contrast to Nd isotopic data for the Drake Passage which is relatively uniform at all depths, the concentration data suggest that the Drake Passage, while isotopically well mixed, is not chemically well mixed. The concentration gradient requires some means of transport and replenishment of these elements in the water column on a short time scale. This transport may be governed by settling and resolution of particles. If replenishment of Nd in the bottom waters is due to resolution of the underlying sediments, the Nd isotopic composition must reflect materials previously deposited rather than recent continental drainage.

An upper limit of 33 Sv for the rate of exchange between the Pacific and Southern oceans has been calculated on the basis of a box model describing Nd transfer between the oceans. At present, the model is underdetermined, but with more data for the Nd isotopic composition of Southern Ocean waters, it may be possible to put further constraints on the rates of exchange between the Southern Ocean and ocean basins to the north.

Insofar as the differences observed in $\varepsilon_{Nd}(0)$ between the Atlantic and the Pacific reflect the rate of water exchange between these oceans, then this must be controlled by the flow through the Drake Passage. It may be assumed that as the passage was opened in late Oligocene time [Kennett, 1977], the degree of isotopic difference decreased. If the Nd isotopic composition of seawater is preserved in sediments over geologic time, it may be possible to study the degree of isolation of earlier oceans under different arrangements of the continents. This has considerable interest in terms of determining the disposition of earlier ocean basins and may possibly be used to trace the flow of major paleo-ocean currents. In the case of the Southern Ocean, it is believed that the dominant source must be North Atlantic deep water. The changes of such flow over the past few million years may be of use in understanding climate change.

CHAPTER 5: The Concentration and Isotopic Composition of Nd in Oceanic Profiles: Constraints on the Transport of Rare Earth Elements in the Oceans

5.1. Introduction

The determination of trace element distributions in the water column of the oceans has been an area of considerable interest to oceanographers over the past decade. The primary thrust of these studies has been to determine the processes controlling the distribution of trace elements and how they relate to the known biological, physical, and geochemical processes in the oceans. In a recent review of this field, Bruland [1983] has summarized several distinct types of trace element concentration profiles. These are: (1) Conservative Those elements for which the concentrations exhibit a linear covariation with salinity are considered to be conservative. (2) Nutrient-type Elements in this category exhibit a linear covariation with either PO_4^{3-} and NO_3^-, or SiO_2. These elements are involved in the biogeochemical cycles of the oceans, and their vertical profiles are characterized by surface depletions and various types of deep water enrichments resulting from regeneration at depth due to dissolution of settling particles. Dissolved PO_4^{3-} and NO_3^- are consumed by organisms in surface waters and are excreted with organic fecal material. They are then dissolved back into the water column during the oxidation of the settling organic material. These nutrients reach a concentration maximum within the oxygen minimum zone (generally above 1000 meters) and remain fairly constant below this depth to the bottom. That PO_4^{3-} and NO_3^- are involved in the same cycles is indicated by the linear correlation between the concentrations of these two species.

This is illustrated in Figure 5.1a where PO_4^{3-} is plotted as a function of NO_3^- for two North Atlantic profiles. Thus, elements whose distributions are controlled by the same biological cycles will have profiles similar to PO_4^{3-} and NO_3^-. Silica is consumed in surface waters by organisms which secrete silica tests. When these organisms die, silica dissolves as the tests settle, but unlike PO_4^{3-} and NO_3^-, silica dissolution is not connected to oxidative processes, so it may continue to dissolve below the oxygen minimum. As a result, elemental distributions controlled by the silicate cycle generally have deeper concentration maxima than those correlated with phosphate and nitrate. This difference between silicate and either phosphate or nitrate is illustrated in Figure 5.1b where PO_4^{3-} is plotted as a function of SiO_2. The curvature in this plot results from the continued release of biogenic silica into the water column below the phosphate maximum. (3) Surface enrichment and depletion at depth Those elements which are injected primarily at the ocean surface and scavenged throughout the water column exhibit this sort of concentration profile. This pattern is observed for Pb which is known to be injected from the atmosphere, and for Mn and ^{228}Ra which are remobilized from coastal sediments and transported seaward by horizontal advection in surface waters. (4) Surface or mid-depth minima, bottom water maxima These elements generally show a nearly linear increase in concentration with depth. A surface maximum sometimes results if there is a high input at the surface. The mechanism generally appealed to for explaining the this type of distribution is a process involving scavenging of the element at all levels in the water column, coupled with the need for a source at the bottom to maintain the high deep water concentrations. (5) Mid-depth maxima This refers to maxima resulting from mid-depth injections such as from hydrothermal activity on

Figure 5.1. The concentration of dissolved phosphate vs. (a) dissolved nitrate and (b) dissolved silicate in two North Atlantic profiles. The linear correlation between phosphate and nitrate indicate similar transport and regeneration cycles in the water column for these two species. The lack of a linear correlation between phosphate and silicate indicates that these two species have very different transport and regeneration cycles in the water column.

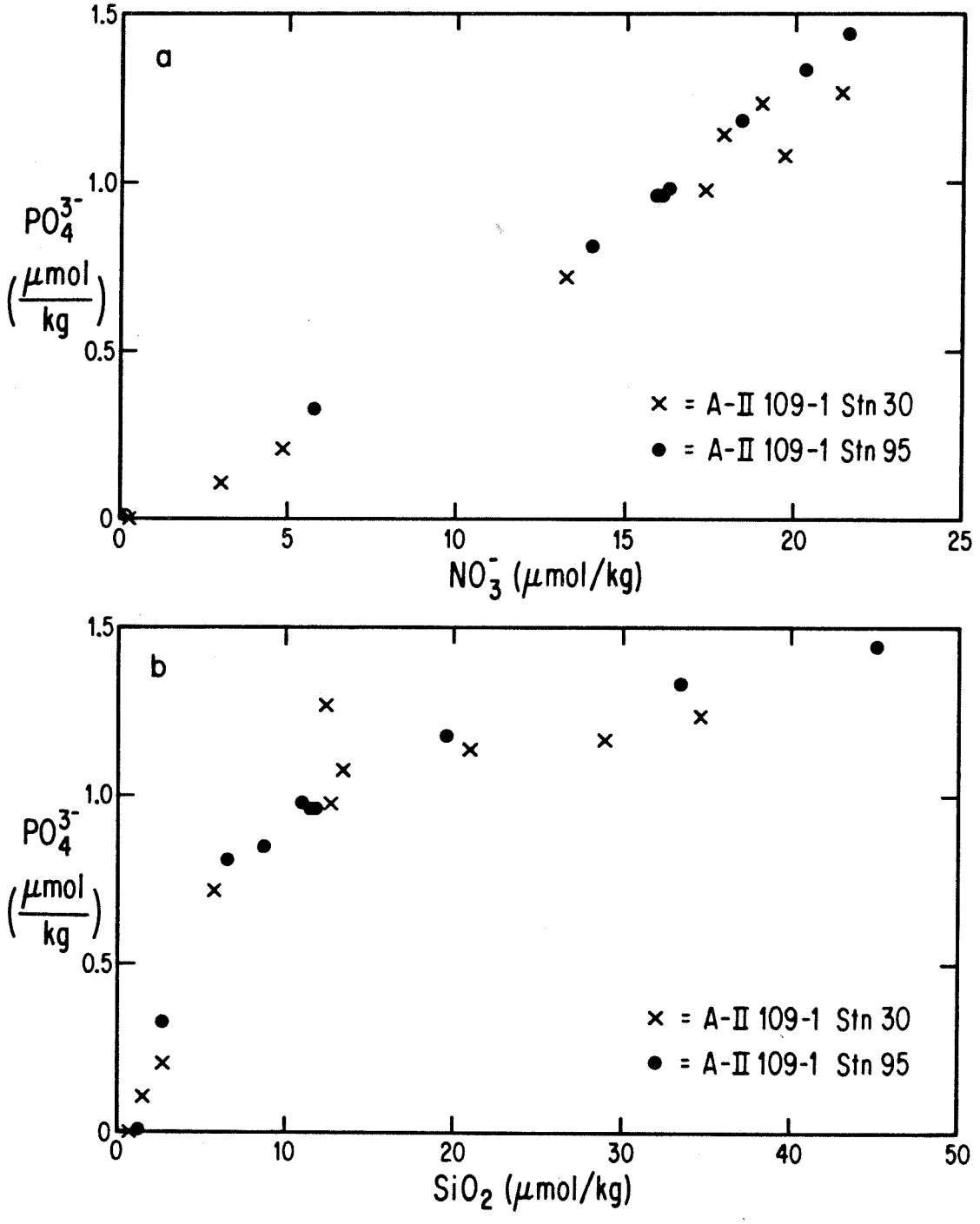
a
1.5
1.0
0.5
0
PO_4^{3-} ($\frac{\mu mol}{kg}$)
0
5
10
15
20
25
NO_3^- (μmol/kg)
× = A-II 109-1 Stn 30
● = A-II 109-1 Stn 95
b
1.5
1.0
0.5
0
PO_4^{3-} ($\frac{\mu mol}{kg}$)
0
10
20
30
40
50
SiO_2 (μmol/kg)
× = A-II 109-1 Stn 30
● = A-II 109-1 Stn 95

Figure 5.1.

mid-ocean ridges. Examples include Mn and ^{3}He. (6) Mid-depth maxima or minima in sub-oxic and anoxic waters Elements which commonly occur in more than one oxidation state can exhibit local maxima or minima in waters of very low oxygen content. Maxima result if the reduced form is more soluble such as for Mn(II) and Fe(II). Minima result if the reduced form is less soluble such as for Cr(III).

A key to some of the transport processes that may occur in the marine environment has come from study of abundances of the decay products of uranium and thorium. These decay series are important because some of the nuclides are at extremely low concentration due to their removal from solution. For example, from the near absence of ^{232}Th in seawater and the presence of the daughter ^{228}Th ($\tau_{1/2}$ = 1.9 years) it is inferred that the more soluble intermediate daughter ^{228}Ra ($\tau_{1/2}$ = 5.7 years) is transported from coastal waters into the surface ocean waters to provide the source of ^{228}Th with a lateral transport time scale of ~ 20 years [Moore, 1969]. Dissolved U has a relatively high and uniform concentration in seawater (~ 3μg/kg) [Rona et al., 1956; Turekian and Chan, 1971; Amin et al., 1976], but one of its daughters, ^{230}Th ($\tau_{1/2}$ = 7.7 X 10^{4} years), has a very low concentration, well below secular equilibrium (~ 10^{-3}) [Moore and Sackett, 1964]. Recent experiments [Nozaki et al., 1981] showed the dissolved ^{230}Th to increase regularly with depth in an approximately linear manner. These data can be explained by constant production of ^{230}Th throughout the water column from ^{238}U decay (^{238}U [$\tau_{1/2}$ = 4.5 X 10^{9} years] → ^{234}Th [$\tau_{1/2}$ = 24 days] → ^{234}U [$\tau_{1/2}$ = 2.4 X 10^{5} years] → ^{230}Th [$\tau_{1/2}$ = 7.7 X 10^{4} years] → ^{226}Ra [$\tau_{1/2}$ = 1.6 X 10^{3} years]) with subsequent adsorption of ^{230}Th on particulate matter, which settles to the bottom [Moore and Sackett, 1964; and others]. For some nuclides from this decay series such as ^{210}Pb there

are direct observations of the proportions associated with particles (about 10%) and in solution (about 90%) [Somayajulu and Craig, 1976]. In addition to scavenging from solution and particle settling, there is evidence for element transport from the sediments into the water column over at least a few hundred meters from the bottom. This is demonstrated by the presence of excess ^{222}Rn ($\tau_{1/2}$ = 3.8 days) [Key et al., 1979; Sarmiento et al., 1976] as well as ^{228}Ra and ^{228}Th (from the decay of dissolved ^{228}Ra) [Moore, 1969; Cochran, 1980] in the lower levels of the deep sea. There is in general no direct connection between the processes controlling these short-lived nuclides and the more abundant stable elements; however, Chan et al. [1976] showed an excellent correlation between Ra (about 6 X 10^{-14} grams per kilogram) and Ba (about 10^{-5} grams per kilogram) in regions above a bottom layer for basins in widely different areas.

Theoretical analyses of trace element distribution in ocean water are primarily based on one dimensional transport models that involve diffusion (with eddy diffusion parameter $\kappa \sim 1$ square centimeter per second and upward advective velocity $\omega \sim 10^{-5}$ cm/sec.). These phenomenological transport models are based on the view that there is an upward component of velocity in the ocean from the cold deep waters that balances the downward diffusion of heat from the warm surface layers [Stommel, 1958]. This approach has led to a set of abyssal recipes [Munk, 1966]. Craig [1969] has discussed this class of models as well as the problem of scavenging for the case of Cu [Craig, 1974]. A review of the vertical advection-diffusion model of Craig [1969] including a modification to the general equation to explicitly account for the role of particulate scavenging is presented in Appendix III.

Any explanation for the observed distribution of the REE in the water column must be considered in the context of these numerous studies of other

trace and radioactive element distributions in the oceans. The observations presented above indicate that the concentration of the REE may depend on scavenging by particles, re-solution from particles, re-solution from sediments at the sea bottom, and advective and upward transport from deep waters. A distinct advantage can be realized for studies of rare earth element distributions in the oceans if the concentration data are complemented with Nd isotopic measurements. The isotopic composition of Nd provides crucial information regarding the sources of rare earth elements in the water column. Thus, any model for the transport of REE in the water column must satisfy both the concentration and isotopic distributions. From the data presented in the previous two chapters, it is clear that the isotopic composition of Nd exhibits substantial variations in the water column at many locations indicating transport from different sources at different levels in the water column. Unequivocal information regarding sources in the water column is generally lacking for most other trace elements. In this chapter, Nd isotopic profiles are compared to corresponding Nd and Sm concentration profiles. These observations will be used to put constraints on transport models for REE and other trace elements in the oceans. Detailed discussions of the isotopic profiles in relation to other oceanographic observations will be deferred to Chapter 6.

5.2. Nd concentration and isotopic profiles

Concentration profiles. During the course of this work, Nd and Sm concentration profiles were determined for a total of seven sampling locations, including four in the Atlantic Ocean, two in the Drake Passage, and one in the Pacific. These data are reported in Table A2 in the appendix.

Four of these profiles for Nd were shown in Figure 4.3. Although these profiles covered the entire water column, only three or four depths were analyzed at each location. Two more detailed profiles from the Atlantic are shown in Figures 5.2 and 5.3. All profiles exhibit the same general trend of increasing Nd concentration with depth, and this is also found to be true for Sm as shown for an eastern North Atlantic profile in Figure 5.3. The detailed profiles shown in Figures 5.2 and 5.3 indicate, however, that the concentration gradients can be much more complex and diverse than indicated from profiles shown in Figure 4.3. This general trend of increasing concentration of Nd and Sm with depth has been extended to all of the rare earths in seawater regardless of the sampling location [Elderfield and Greaves, 1982; DeBaar et al., 1983; Klinkhammer et al., 1983]. Surface samples generally yield the lowest REE concentrations at a given location. Only one example of a profile showing substantial surface enrichments for REE has been reported [Elderfield and Greaves, 1982].

The regular change of REE concentrations with depth is found to be similar to Cu [Boyle et al., 1977; Bruland, 1980], Pd [Lee, 1983], Ag [Martin et al., 1983], Al [Moore, 1981; Stoffyn and MacKenzie, 1982], and ^{230}Th [Nozaki et al., 1981] and indicates that they fit best in group (4) of Bruland's [1983] classification scheme. The usual explanation for copper-like profiles is that there is scavenging of the element at all levels in the water column coupled with the necessity for a strong source at the bottom to maintain the deep water concentrations. It is generally assumed that diffusion from deep sea sediments provides the primary source at the bottom. Craig [1974] suggested that Cu transported in Antarctic Bottom Water might also provide the deep water source.

It can be shown that the rare earth distributions in the water column

Figure 5.2. Nd concentration as a function of depth at A-II 109-1, Station 30 in the western North Atlantic. The data show a general increase in concentration with depth with a substantial increase in concentration near the bottom. The high bottom water concentration may possibly include Nd stripped from particles resulting from acidification of the samples after collection. An expanded scale plot of the concentration in the upper 3km of the water column is also shown. A sharp increase in concentration is observed between 800 and 1100 meters depth which is coincident with the base of the thermocline at this station. The errors on the measurements are smaller than the size of the dots used to denote the samples in both figures.

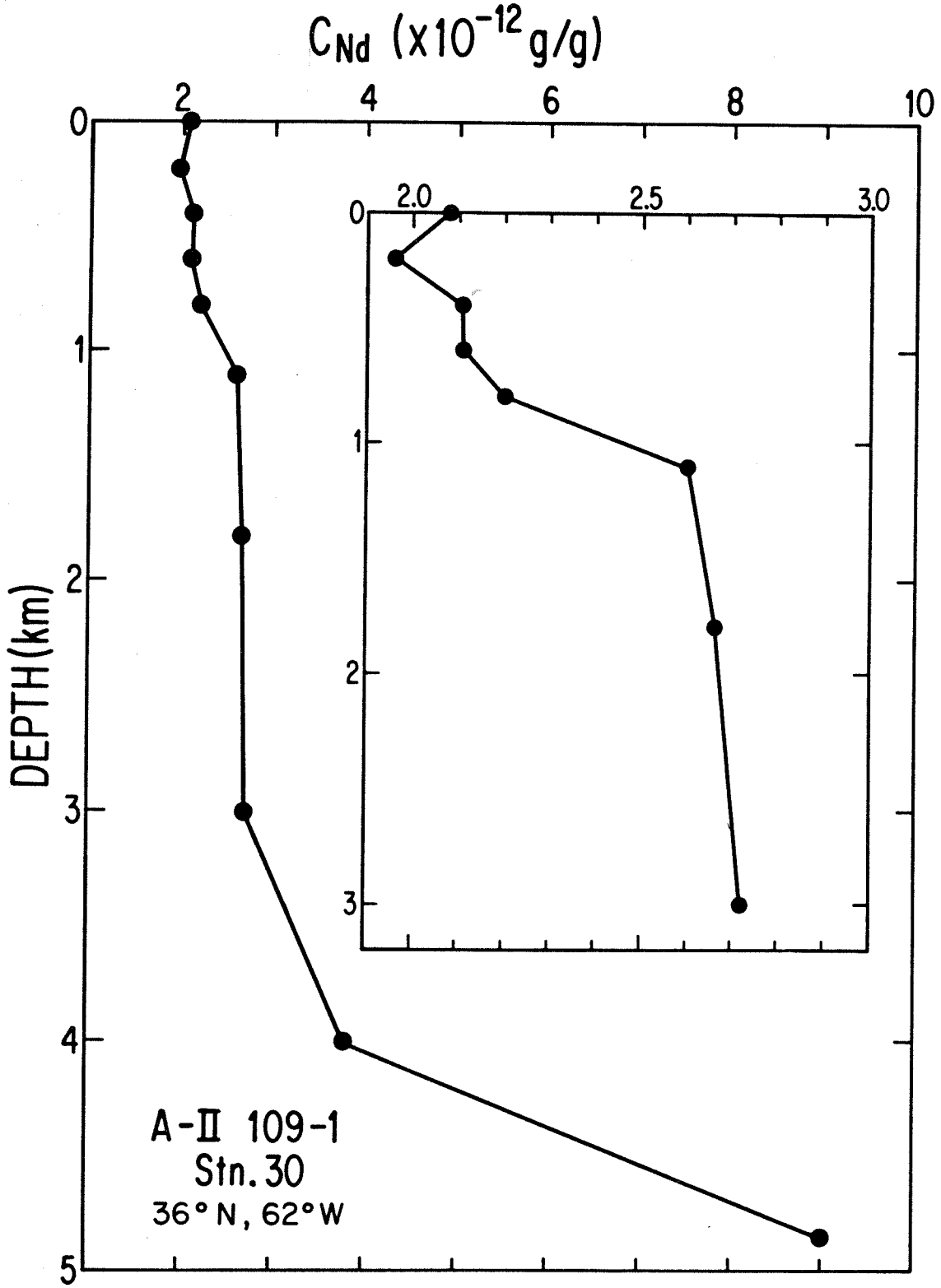
C_{Nd} (x10^{-12} g/g)
2
4
6
8
10
0
1
2
3
4
5
DEPTH(km)
2.0
2.5
3.0
A-II 109-1
Stn. 30
36° N, 62° W

Figure 5.2.

Figure 5.3. Concentration of Sm (open circles) and Nd (solid circles) as a function of depth at A-II 109-1, Station 95 in the eastern North Atlantic in the vicinity of the Mediterranean outflow. Both Sm and Nd show a regular increase in concentration with depth. These data illustrate the very similar nature of the distribution of Sm and Nd. Note that both elements exhibit perturbations in their concentration gradients at depths corresponding to the level of the Mediterranean outflow.

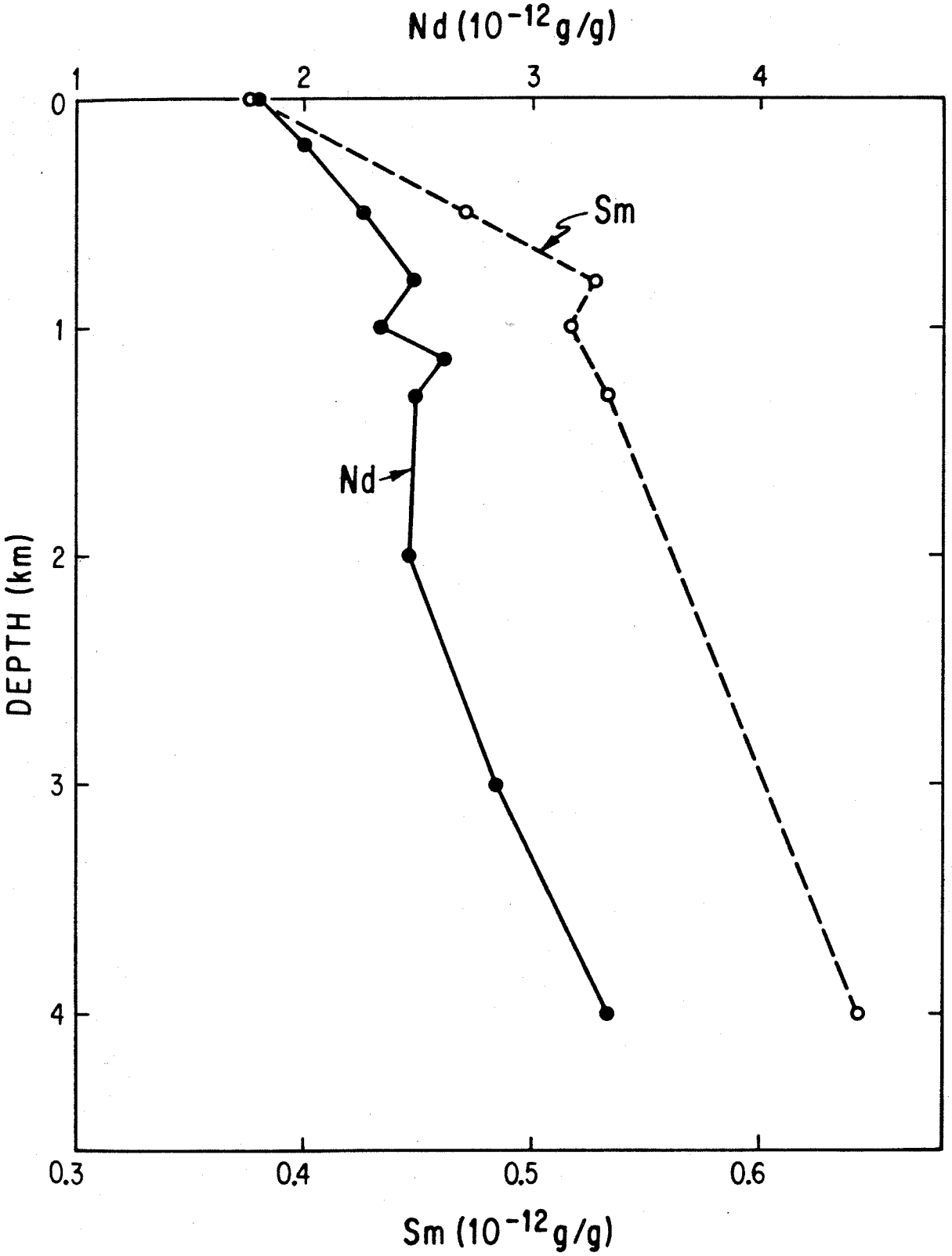

Figure 5.3.

are not associated with the regenerative cycles of the nutrients. If the REE distributions in the oceans are related to the nutrient transport in the water column, then a linear correlation between Nd and one or more of the nutrients would be expected such as that shown for phosphate and nitrate in Figure 5.3. Figures 5.4 and 5.5 show the Nd concentrations from the two Atlantic profiles shown in Figures 5.2 and 5.3 as a function of the nutrient concentrations in these water samples. If Nd distributions were controlled by the biogeochemical cycles, then a correlation should be observed for the data points in these diagrams. Instead, each of the curves exhibit a sharp bend which corresponds to depths near the base of the thermocline. The continued rapid increase of Nd below the bends indicates that Nd is not correlated with the nutrients. These considerations indicate that there is another source of Nd in the deep water.

Nd isotopic profiles. In contrast to the fairly regular distribution of Nd and other REE in the water column, Nd isotopic distributions in the water column can exhibit very diverse patterns depending on the location. Three types of distribution profiles for $\varepsilon_{Nd}(0)$ were shown in Chapter 4 in Figure 4.2. A western North Atlantic profile (OCE 63, Fig. 4.2B) has $\varepsilon_{Nd}(0) = -9.6$ in the near surface waters and decreases to -13.1 at 1000 m. Below 1000 m, the isotopic composition remains fairly constant. This distribution pattern has been observed in a second western North Atlantic station (about 800 km north of OCE 63) corresponding to the concentration profile in Figure 5.1 (A-II 109-1 Stn. 30) and indicates that there is an abrupt shift of 2 to 3 ε-units in the interval from 800 to 1000 m (see Figure 6.2). Two stations in the Drake Passage (Fig. 4.2A) exhibited uniform isotopic compositions at all levels in the water column. One Pacific station exhibited a linear decrease in $\varepsilon_{Nd}(0)$ from 0.0 at the

Figure 5.4. Nd concentrations vs. (A) PO_4^{3-}, (B) NO_3^-, and (C) SiO_2 for A-II 109-1, Station 30 in the western North Atlantic (see Fig. 5.2). In all cases, it is seen that there is a relatively abrupt change in the slope of the nutrient vs Nd concentrations which occurs at or near the mid-depth nutrient maximum (see Table A3). This nutrient maximum is found to be coincident with the base of the thermocline

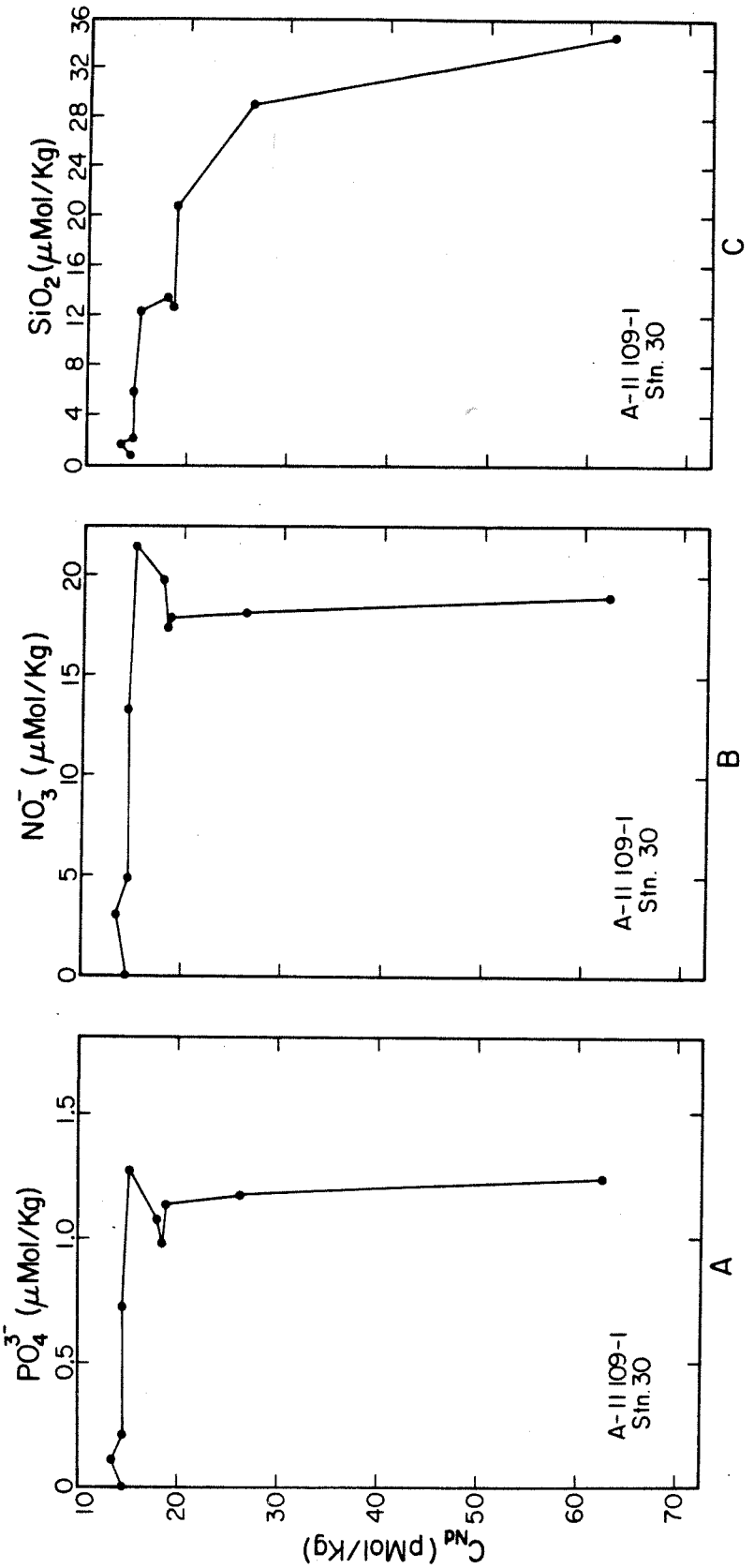
C_{Nd} (pMol/Kg)
10
20
30
40
50
60
70
PO_4^{3-} (μMol/Kg)
0
0.5
1.0
1.5
A-11 109-1
Stn. 30
A
NO_3^- (μMol/Kg)
0
5
10
15
20
A-11 109-1
Stn. 30
B
SiO_2 (μMol/Kg)
0
4
8
12
16
20
24
28
32
36
A-11 109-1
Stn. 30
C

Figure 5.4.

Figure 5.5. Nd concentrations vs. (A) PO_4^{3-}, (B) NO_3^-, and (C) SiO_2 for A-II 109-1, Station 95 in the eastern North Atlantic (see Fig. 5.3). For reference, the points labeled a, b, and c correspond to the depths 200, 1000, and 4000 m, respectively. Although this figure is plotted with different axes than in Figure 5.4, the features of this profile are essentially the same as for the Station 30 profile in the western basin. In this figure, the change in slope of the Nd vs. nutrient correlation occurs below the Mediterranean outflow. All of these plots exhibit irregular behavior in the region of the outflow, the core of which is near the point b on each of the figures.

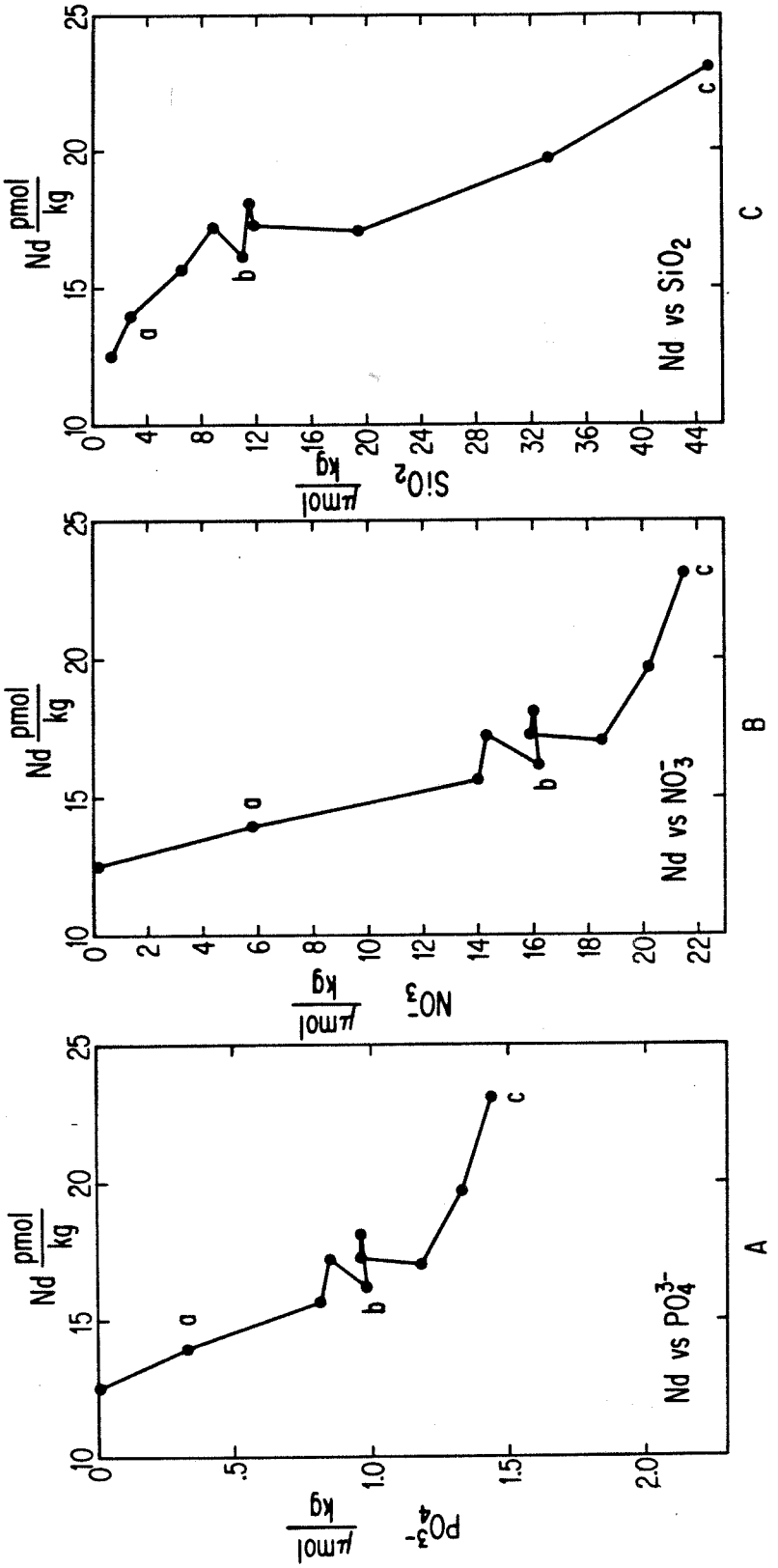
Nd vs PO_4^{3-}
A
PO_4^{3-} $\frac{\mu mol}{kg}$
Nd $\frac{pmol}{kg}$
Nd vs NO_3^-
B
NO_3^- $\frac{\mu mol}{kg}$
Nd vs SiO_2
C
SiO_2 $\frac{\mu mol}{kg}$
a
b
c

Figure 5.5.

surface to -8.1 at 4500 m. Two additional distribution patterns from the Atlantic have been observed. The eastern North Atlantic isotopic profile which corresponds to the concentration data in Figure 5.2 is shown in Figure 6.7 of the next chapter and has $\varepsilon_{Nd}(0) \approx -12$ at all depths except for a shift toward more radiogenic values between 800 and 1000 meters. $\varepsilon_{Nd}(0)$ reaches a maximum of -9.8 at 1000 m.

The final example of an Atlantic Nd isotopic profile is for TTO/TAS Station 63 shown in Figure 6.6 in the next chapter. In this profile, $\varepsilon_{Nd}(0)$ exhibits a gradient in the deep waters, increasing with depth from a minimum at 2000 m of $\varepsilon_{Nd}(0) = -13.3$ to -11.9 at 4850 m. In waters above the $\varepsilon_{Nd}(0)$ minimum at 2000 m, $\varepsilon_{Nd}(0)$ is also observed to increase to a more radiogenic value. One sample has been analyzed (from 790 m) and found to have $\varepsilon_{Nd}(0) = -11.8$. Although not shown, the concentration gradient for this station is similar to that observed at other locations.

5.3 Nd isotopic constraints on the vertical transport of the REE

The Nd concentration data all exhibit a regular pattern of increasing concentration with depth. This phenomenon requires a vertical transport mechanism which will deplete the surface concentrations and allow for the relatively constant rate of increase in concentration with depth to the ocean bottom. It is likely that sequestering of REE by particles will play a major role in producing the observed distributions in the oceanic environment and would be entirely consistent with the studies of U series decay products discussed above. By contrast, the Nd isotopic distributions in the water column exhibit no regularity. The vertical isotopic variations observed at many locations indicate that the water column is layered with

respect to $\varepsilon_{Nd}(0)$ values, indicating that different layers have different sources of Nd. This must require substantial lateral transport of the rare earth elements from more than one source region, and further, it indicates that replenishment of the REE at a given level in the water column by horizontal transport must occur at a rate which is significantly greater than for the time scales of removal and/or vertical mixing in order to preserve the water column isotopic differences. Thus, two competing processes are occurring, a lateral advective transport process which supplies REE from different sources to different levels in the water column, and a vertical transport or removal process which will establish a concentration gradient. The concentration gradient must be established without significantly disturbing the isotopic distribution. Furthermore, the very regular nature of the concentration profiles at all locations strongly indicates that the transport processes which establish these gradients are the same everywhere regardless of the isotopic distribution.

The Nd isotopic data put two fundamental constraints on the vertical transport of the rare earth elements in the oceans. First, deep water REE concentration levels cannot be maintained by simple resolution of REE scavenged from the surface waters onto settling particles. This follows from the indisputable observation that isotopic differences are preserved in the water column for most locations studied. The regular behavior of the Nd concentration suggests continuous mixing or exchange between the surface and bottom waters on a short time scale, but such a process would be expected to produce changes in the isotopic composition of Nd with depth which lie on a smooth, well defined mixing curve. If deep water concentrations were supported by significant contributions from redissolved surface Nd, then abrupt isotopic shifts such as observed in the western basin of the North Atlantic should not occur.

Conversely, the second constraint prohibits the upward advective and diffusive transport from being the REE source in surface waters. As discussed above, upward transport of trace elements which have diffused from bottom sediments is generally considered an important source to maintain the concentration gradients for elements such as Cu which have depth profiles similar to Nd. It is not even clear that upward advection or diffusion could transport REE more than a few hundred meters from the bottom in the Atlantic. For diffusion, the transport distance x is approximated by the expression $x^2 = Dt$, where D is the diffusion coefficient and t is time. In the oceans, $D \approx 1$ cm^2/s. For advection, $x = vt$, where v is the upward advective velocity which is estimated to be 10^{-5} cm/s in the oceans. When the advective transport equals the diffusive transport, $x^2/Dt = x/vt$. Using the values for D and v above, the distance, x = 1000 meters, and the time scale for transport across this distance is ~300 years. For distances less than 1000 meters, diffusion will dominate the transport, and for longer distances advection will dominate. Thus the time required to transport Nd across 4000 meters from abyssal sediments to the base of the thermocline in the Atlantic is about 1200 years. This is considerably longer than the estimated residence time of the deep water in the Atlantic of only 250 years [Worthington, 1976], suggesting that there must be other sources of REE besides that supplied by diffusion from sediments. Horizontal transport in the deep waters may provide an effective source. There is strong evidence for this from the isotopic profiles which will be discussed in more detail in the next chapter.

The processes by which vertical concentration gradients such as observed for the REE are not yet understood in terms of the isotopic constraints which must also be satisfied. In Chapter 6 it will be shown

that changes in the isotopic composition are well correlated with changes in temperature and salinity characteristics. For the concentrations though, there are no obvious changes across these boundaries indicating that the gradients are formed without regard to water mass transport boundaries. If a scavenging process is responsible for the concentration gradients, then there can be no significant resolution in deeper waters. If the REE were not in true solution, but rather associated with particles which are small enough to undergo brownian motion, then a concentration gradient similar to that observed could be produced. The distribution of such particles in a column of water under the influence of gravity is given by $C_h/C_0 = \exp(-mgh/\kappa T)$ where C_0 is the concentration of particles at the base of the water column, C_h is the concentration at height h above the base level, m the mass of the particles, κ is Boltzman's constant, and T is the absolute temperature. This relation shows that to a first order the concentration of particles in the column of water will increases with depth in a linear fashion. It is not clear that this is the proper approach to take, since it is restricted by the isotopic data to regions in the water column with uniform $\varepsilon_{Nd}(0)$. Any layered model using this approach would have to account for the regular increase in the concentration across the boundaries of adjacent layers which are characterized by significant isotopic shifts.

5.4 Conclusions

The vertical distributions of Nd and other rare earths exhibit a regular trend of increasing concentration with increasing water depth. This trend is similar for all oceanic profiles studied, regardless of location, and indicates that the mechanisms responsible for establishing these

gradients are the same at all locations. Some form of scavenging and transport on particulate matter may be necessary to maintain these concentration gradients. In contrast, Nd isotopic distributions in the water column vary from one location to another, and the vertical changes indicate horizontal transport at different levels in the water column from different sources. The horizontal components of transport must also be more rapid than than vertical mixing rates in order to maintain these isotopic differences.

One conclusion of major significance regarding the vertical transport of the REE in the water column can be drawn from the Nd isotopic data. The variations of $\varepsilon_{Nd}(0)$ clearly indicate that the deep water concentration enrichments cannot be supported by the downward transport and resolution of REE scavenged from the surface waters into the deep waters. Thus, any scavenging processes in the water column which result in the surface depletions must be essentially irreversible. these processes are not well understood in view of the isotopic constraints and will require detailed study of REE interactions with particulate matter in the oceans for further elucidation. The similarity of REE profiles to Cu, Al and several other trace elements indicates that the processes controlling the distribution of these elements are similar. Thus, the Nd isotopic constraints on the rare earth element transport should apply to these other elements as well.

The strong evidence presented here for the lateral transport of the rare earth elements indicates the Nd isotopic signatures of water masses might be preserved over large distances. In the next chapter, a detailed comparison of the isotopic data will be made to the general water mass characteristics of the oceans, with particular emphasis on the Atlantic distributions.

Chapter 6: The Transport of Rare Earth Elements in the Atlantic Inferred from Nd Isotopic Observations

6.1 Introduction

In previous chapters it has been shown that not only are there substantial Nd isotopic differences in seawater between the ocean basins, but that significant variations exist within ocean basins as well. In addition to the geographic variations that are observed within an ocean basin it was shown that very pronounced changes in the isotopic composition of Nd could also occur as a function of depth in the water column at a single location. It was further demonstrated that there was a regular increase in the concentration of Nd with depth regardless of the nature of the isotopic distribution. It was concluded that in order to maintain isotopic variations in the water column at a given location, significant lateral transport of REE from more than one isotopically distinct source region is required. In this chapter, I will attempt to demonstrate that the general distribution of ^{143}Nd within an ocean basin is consistent with rare earth transport within the framework of the general circulation of major water masses, and that isotopic compositions associated with a flowing water mass can be preserved during the transport of the water mass over long distances. Much of the discussion will focus on the transport in the western basin of the North Atlantic. Three water column profiles collected between 7°N and 36°N have been studied and will be compared to the water mass circulation in this region. In addition to providing valuable information on the transport of rare earth elements in the oceans, the Nd isotopic data presented here will

demonstrate that the isotopic composition of Nd can serve as a general tracer for water masses in the oceans.

6.2 Results

The results of Nd isotopic measurements for all seawater samples is given in Table A2 in the appendix along with the sampling locations for each station. Seawater sampling sites were also shown on Figure 2.1. A general presentation of the isotopic results was given in the histogram in Figure 3.1. Hydrographic measurements of salinity, dissolved oxygen, and nutrients are given in Table A3 for those samples for which determinations were made. Brief descriptions of the temperature, salinity, and Nd isotopic characteristics of the water column at three western basin locations in the North Atlantic (A-II 109-1 Stn. 30, OCE 63, and TTO/TAS Stn. 63) are presented below.

6.2.1 A-II 109-1, Station 30

The θ-S ($\theta \equiv$ potential temperature) diagram generated from CTD measurements for Station 30 is plotted in Figure 6.1. The portion of the θ-S curve between points A and B represents a thin surface layer about 5 meters deep which is characterized by constant temperature (~22°C) and a rapid increase in salinity from ~35.8 to 36.2°/oo. Between points B and C (C = 250 m), salinity is observed to increase with decreasing potential temperature until a salinity maximum of ~ 36.5°/oo is reached which occurs between 50 and 200 meters in the water column. Below the salinity maximum at point C, both θ and S decrease to the bottom. A slight bend in the θ-S curve occurs at point D (= 1000 m) and coincides with the base of the

Figure 6.1. Potential temperature vs. salinity for A-II 109-1 Station 30 in the western North Atlantic. The labeled points represent depths in the water column as follows: A = surface, B = 5 m, C = 200 m, D = 1000 m, E = 4900 m. The segment of this curve between points C and D represents the temperature and salinity characteristics in the main thermocline in this region of the Atlantic. Temperatures and salinities between points D and E are representative of North Atlantic Deep Water.

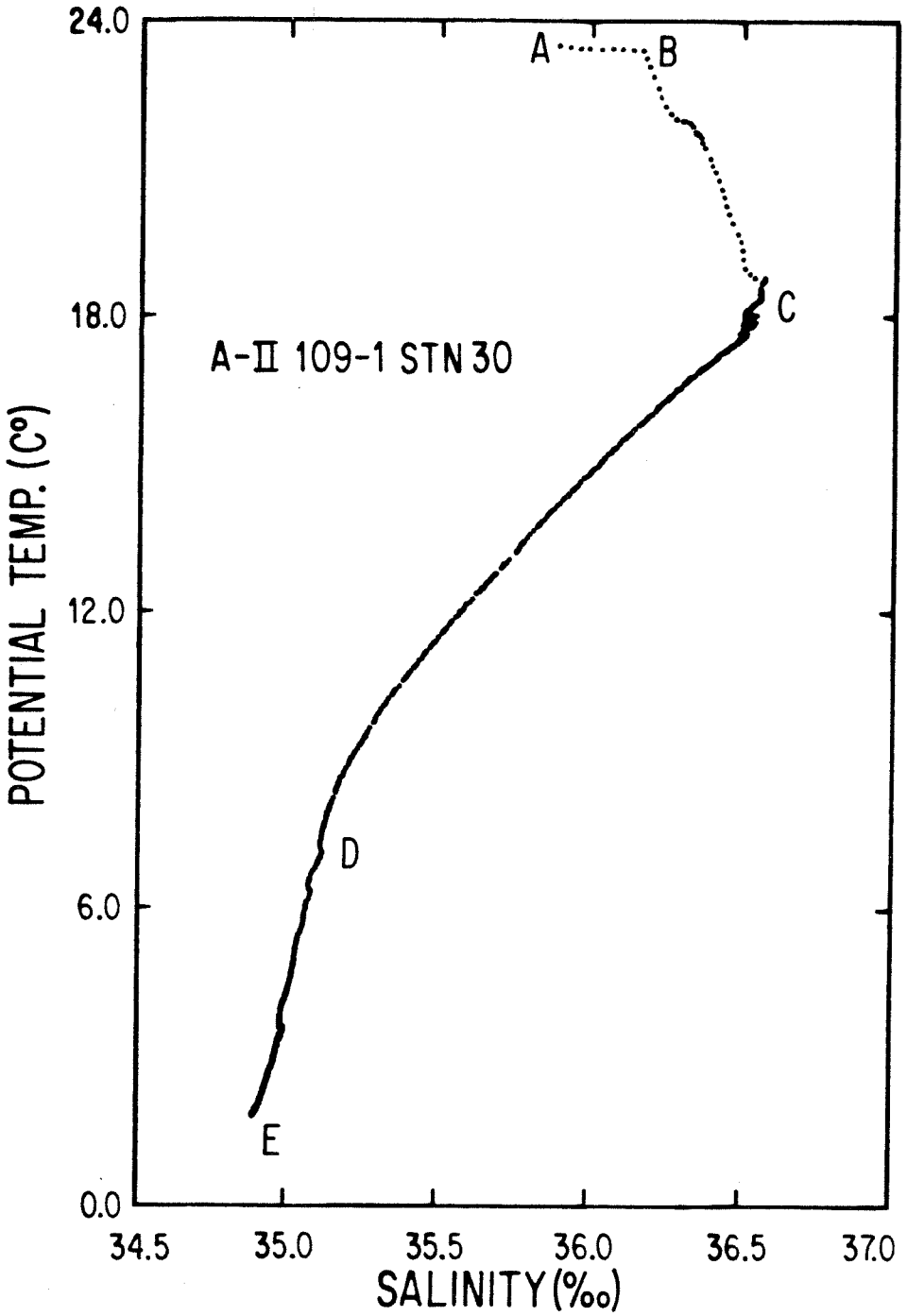
24.0
18.0
12.0
6.0
0.0
POTENTIAL TEMP. (C°)
A-II 109-1 STN 30
A
B
C
D
E
34.5
35.0
35.5
36.0
36.5
37.0
SALINITY (‰)

Figure 6.1.

thermocline. The linear T-S segment between points C and D is representative of upper waters as classified in Chapter 1 and lie within the main thermocline. The linear T-S segment between points D and E (= 4950 m) represents waters below 1000 meters has T-S characteristics which identify this mass as NADW according to the classification discussed in Chapter 1. The shape of this T-S diagram indicates that at least five components are involved in mixing at this location. If Mediterranean outflow water were present one would expect to see a salinity maximum at a temperature of about 6 to 10°C and corresponding to a depth of ~ 1000 to 1200 meters. However, this is not observed, and it is concluded that there is no identifiable Mediterranean component at this westerly station.

The Nd isotopic data are plotted as a function of depth in Figure 6.2. For comparison, the points labeled B through E on this diagram correspond to the depths labeled on the θ-S diagram in figure 6.1. Samples were not collected from the thin surface layer corresponding to component A. $e_{Nd}(0)$ is observed to have a uniform maximum of $\varepsilon_{Nd}(0) \approx -9.5$ from 5 meters (B) to 200 meters (C). Between 200 and 800 meters $e_{Nd}(0)$ exhibits a small range from -10.3 to -10.9 (between C and D). This is followed by a sharp decrease of 3.1 ε-units to $\varepsilon_{Nd}(0) = -14.0$ at 1100 meters. Below 1100 meters (between D and E), $\varepsilon_{Nd}(0)$ remains fairly uniform to the ocean bottom, although there is some hint of a mid-depth maximum at 3000 meters of $\varepsilon_{Nd}(0) = -13.0$. The samples in this depth range are all associated with NADW. Inspection of Figure 6.1 shows that shifts in the isotopic compositions occur at similar levels in the water column as do changes in the θ-S curve. Nd concentrations at this station were shown in Figure 5.1 and found to increase regularly with depth. There do not appear to be major shifts in the concentration in this profile at the depths observed for the isotopic shifts.

Figure 6.2. $\varepsilon_{Nd}(0)$ as a function of depth at A-II 109-1 Station 30 in the western North Atlantic. The depths which are labeled (A, B, C, D, and E) correspond to the depths labeled on the T-S curve in Figure 6.1 where distinct changes in the temperature and salinity characteristics are observed. (The depth interval between points A and B is not resolvable at the scale of this figure, so they are shown on the same line at the surface). It can be seen from comparison of this figure with Figure 6.1 that there are distinct shifts in the isotopic composition of Nd at depths corresponding to bends in the T-S curve. (The surface sample corresponds to the depth represented by point A, but no sample was analyzed from a depth corresponding to point B). The close correlation of the Nd isotopic shifts to changes in the T-S relationships indicates that the isotopic shifts reflect changes in the water mass characteristics and, therefore, the sources of the REE. This observation also provides a clear indication that the REE undergo substantial horizontal transport from more than one source region the Atlantic. It is evident that the Nd below 1000m is not derived from the material above this depth. The Nd concentrations for the samples shown in this figure were shown in Figure 5.2. The error bars represent the 2σ errors on the isotopic measurements.

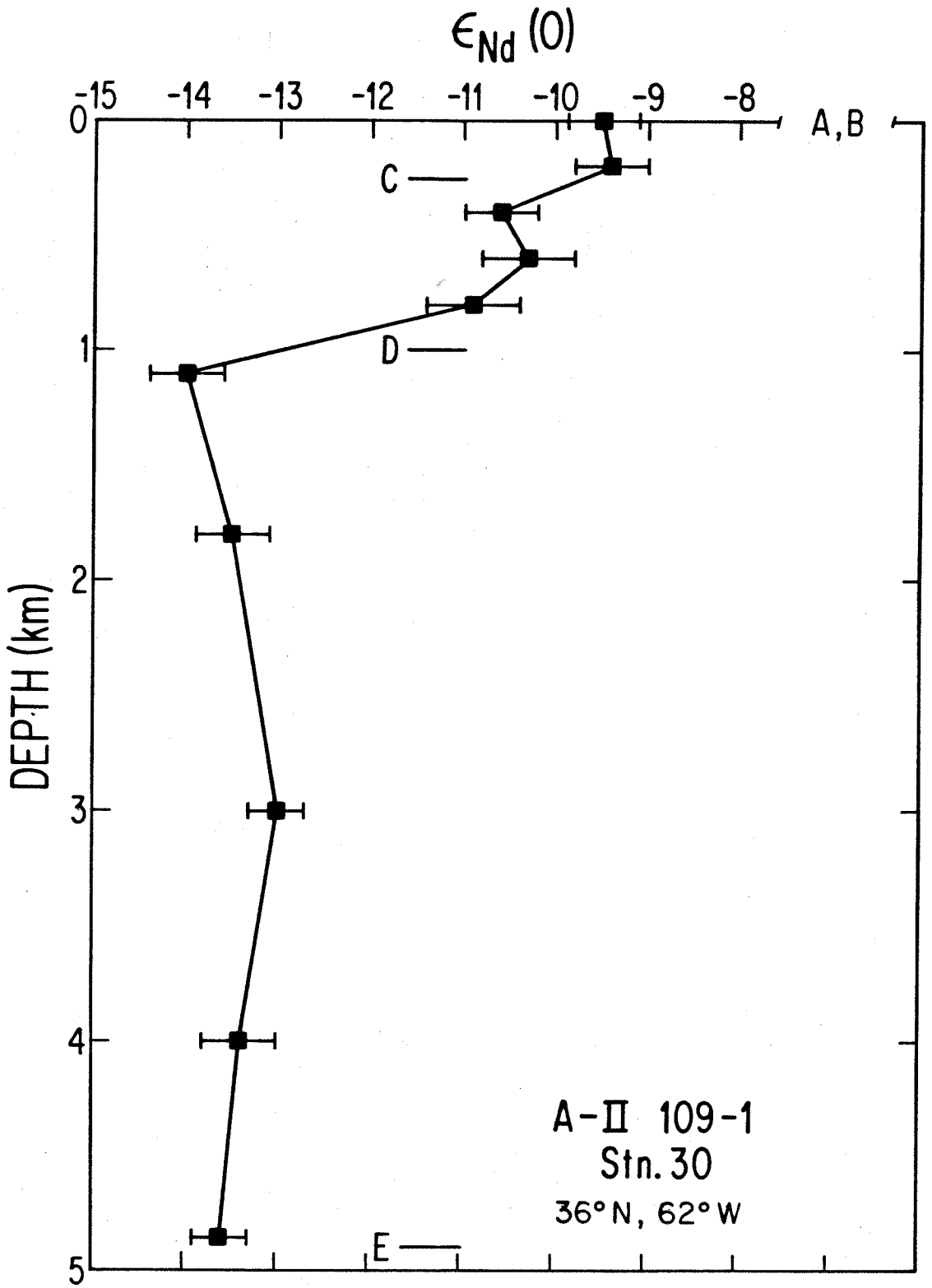
ϵ_{Nd} (0)
-15
-14
-13
-12
-11
-10
-9
-8
0
1
2
3
4
5
DEPTH (km)
A,B
C
D
E
A-II 109-1
Stn. 30
36°N, 62°W

Figure 6.2.

6.2.2 OCE 63

No temperature, salinity, oxygen, or nutrient measurements were made for water samples collected during this expedition. Figure 6.3 is a temperature vs. salinity for Crawford 17, Stn 316 [Fuglister, 1960] located at approximately 28°N, 66°W and should closely represent the T-S conditions at the sampling locations of the OCE 63 samples. There are two nearly linear segments of the T-S diagram, one between points labeled A (100 m) and B (1000 m) and the other between points C (1400 m) and D (4500 m). The first segment (A to B) corresponds to temperatures in the main thermocline between ~ 20°C and 6°C and salinities between ~ 36.5°/oo and 35.0°/oo and is representative of upper water. The point B is located at the base of the main thermocline at 1000 meters. The second linear segment (C to D) lies between temperatures of ~5°C to 2°C and salinities of ~ 35.1°/oo to 34.9°/oo. On the basis of general water mass classifications for the Atlantic as discussed in Chapter 1, this segment of the T-S diagram is interpreted to be representative of NADW. The slight bend below the second T-S segment from D to E indicates the intrusion of a cooler, less saline water mass at the bottom, and may be a diluted form of AABW. Between the points B and C there is a slight rise in the salinity which reaches a maximum at about 1400 meters depth. This maximum corresponds to the core of upper NADW and, as discussed in Chapter 1, is a direct result of the Mediterranean outflow. The upper 100 meters of the water column is isothermal and indicates the presence of a surface mixed layer. With the exceptions of the small Mediterranean influence and the small sill of cooler water at the sea bottom, this T-S diagram is nearly identical to that for A-II 109-1 Station 30 shown in Figure 6.1 and it is concluded that the major water mass characteristics of these two sampling localities are similar.

Figure 6.3. A temperature versus salinity diagram for Crawford Station 317 in the Sargasso Sea. This diagram is taken to represent the approximate conditions of temperature and salinity in the water column at the OCE 63 sampling locations. Data are from Fuglister [1960]. The points labeled represent depths in the water column as follows: A = 100m, B = 1000m, C = 1400m, D = 4500m, and E = 5100m. The segment between A and B represents T-S conditions the main thermocline. The salinity maximum at point C is interpreted as resulting from westward spreading of a diluted component of the Mediterranean outflow and is considered to be a characteristic feature of upper NADW (see discussion in Chapter 1). The segment of the T-S curve between points D and E is characterized by a shift towards lower temperatures and salinities than is typical of NADW and may indicate the presence of a diluted component of AABW underneath the North Atlantic Deep Water complex.

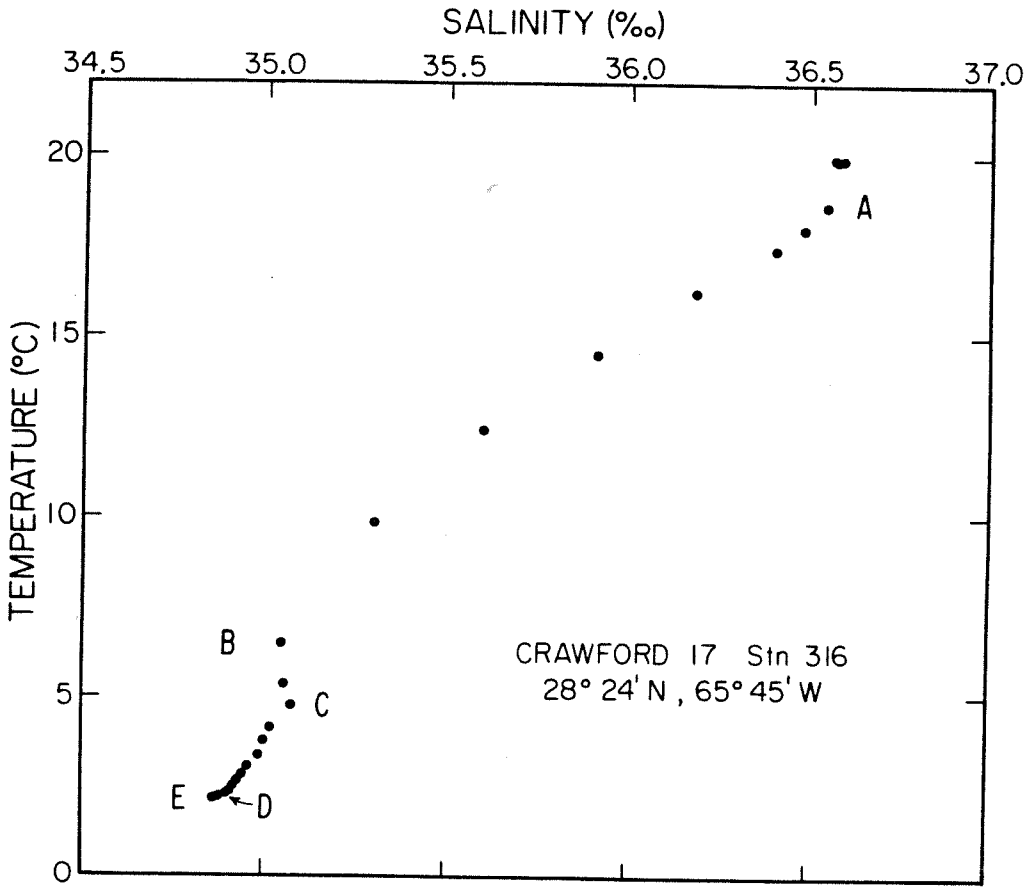
SALINITY (‰)
34.5
35.0
35.5
36.0
36.5
37.0
TEMPERATURE (°C)
0
5
10
15
20
A
B
C
D
E
CRAWFORD 17 Stn 316
28° 24' N, 65° 45' W

Figure 6.3.

Figure 6.4. $\varepsilon_{Nd}(0)$ as a function of depth for OCE 63 samples in the Sargasso Sea in the western North Atlantic. These data represent a composite of samples from several closely spaced stations. Depths labeled A, B, C, and D correspond to the points labeled on the T-S curve in Figure 6.3. This isotopic profile is very similar to that shown in Figure 6.2 for A-II, 109-1 Station 30. Once again, note the close correspondence between shifts in the isotopic composition in the water column with changes in the T-S characteristics. If Nd of Mediterranean origin were present at the depths associated with the salinty maximum at point C, then a shift toward more radiogenic values of $\varepsilon_{Nd}(0)$ would be expected (see Figure 6.7 for $\varepsilon_{Nd}(0)$ in the Mediterranean outflow). Since there is no isotopic shift in the vicinity of point C, it is concluded that there is either no Mediterranean component of Nd at this westerly location or it has become very diluted as indicated by the temperature and salinity in Figure 6.3. The error bars represent the 2σ errors on the isotopic measurements.

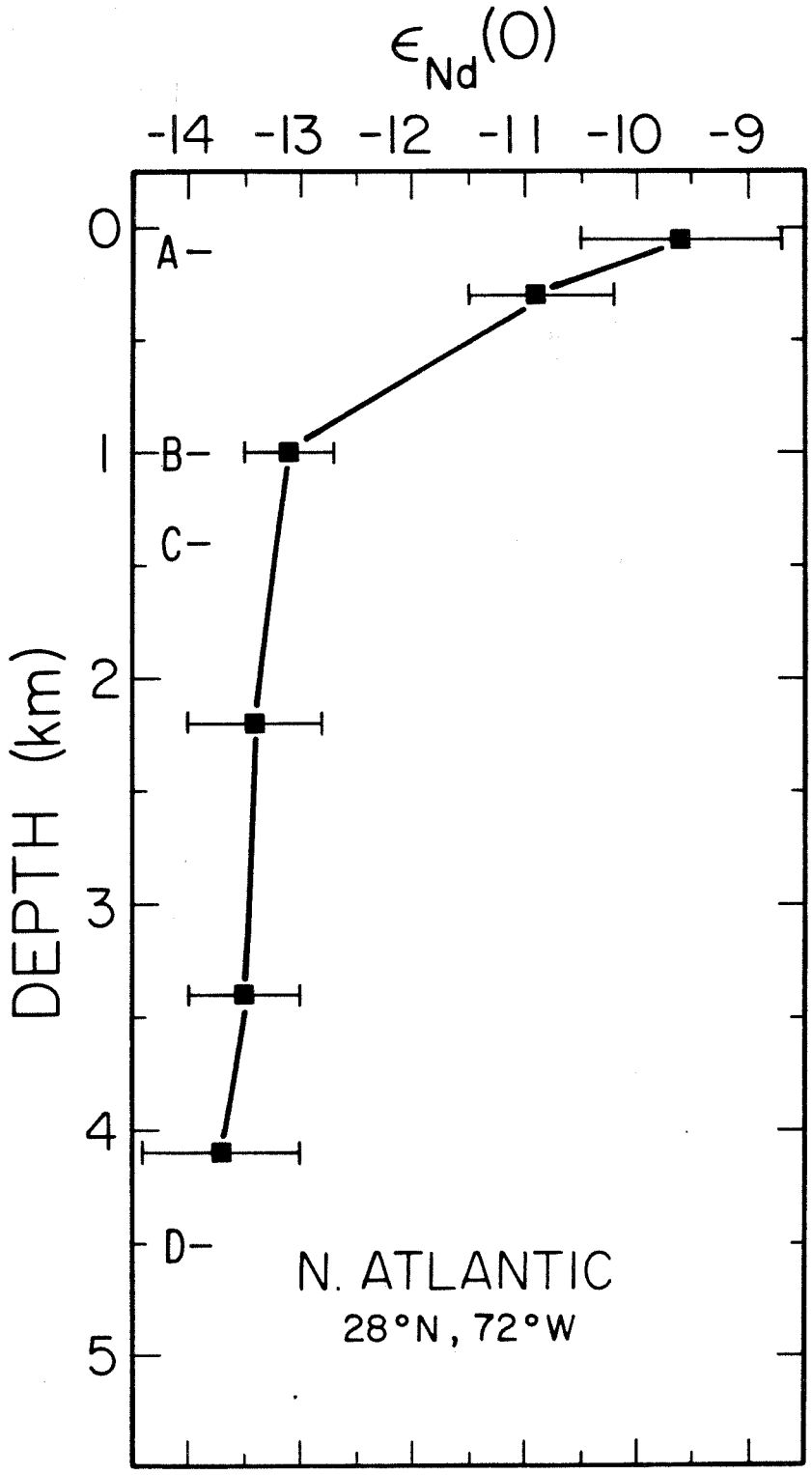
$\epsilon_{Nd}(0)$
-14
-13
-12
-11
-10
-9
0
1
2
3
4
5
A
B
C
D
DEPTH (km)
N. ATLANTIC
28°N, 72°W

Figure 6.4.

The $\varepsilon_{Nd}(0)$ values for these samples are plotted in Figure 6.4 as a function of water depth. For reference, the depths corresponding to the points A through D in the T-S diagram in Figure 6.3 are also shown in this figure. Deep water samples ($\geq$ 1000 meters) have very uniform Nd isotopic compositions corresponding to $\varepsilon_{Nd}(0) \cong -13.5$. Three of these samples lie between points C and D and within NADW. The fourth sample lies at point B at the base of the thermocline. At depths less than 1000 meters $\varepsilon_{Nd}(0)$ values are found to become increasingly more radiogenic toward the surface. One sample lies between points A and B at 300 meters and has $\varepsilon_{Nd}(0) = -10.9$. The other lies above point A at 50 meters and has $\varepsilon_{Nd}(0) = -9.6$. For the depths analyzed, this profile is nearly identical to that at A-II 109-1 Stn. 30 shown in Figure 6.2 and is consistent with the similarity of the T-S characteristics of these two localities. The concentration of Nd at this station exhibits a regular increase with depth as reported earlier. These data are shown in Figure 4.3B.

6.2.3 TTO/TAS Station 63

The θ-S diagram generated from CTD measurements for this station is shown in Figure 6.5. The surface salinity is about 36.0°/oo and temperature about 27°C and are represented by point A on the diagram. These values remain constant to 65 meters. Between A and B, the θ-S diagram shifts toward higher salinity but lower temperature reaching a salinity maximum of about 36.5°/oo at a depth of about 80. The interval between B and C encompasses the salinity maximum region to 120 meters. Below point C, the θ-S segment is linear with both salinity and temperature decreasing to a salinity minimum (~34.6°/oo) at a depth of about 800 meters denoted by the point D. On the basis of conventional water mass classifications, this

Figure 6.5. Potential temperature vs. salinity at TTO/TAS Station 63 in the equatorial western North Atlantic. These are preliminary results from CTD measurements and have not been calibrated for instrumental drift. These corrections would not be sufficient to alter the major θ-S features shown in this diagram. The depths at the labeled points are as follows: A = 65 m, B = 80 m, C = 120 m, D = 800 m, E = 1500 m, F = 3100 m, and G = 4810 m. The salinity minimum at point D is interpreted to represent the core of northward flowing Antarctic Intermediate Water. Point E represents the salinity maximum associated with the upper layer of NADW. Below point F, a diluted component of Antarctic Bottom Water flowing northward underneath NADW is indicated by the low temperatures and salinities. below point F.

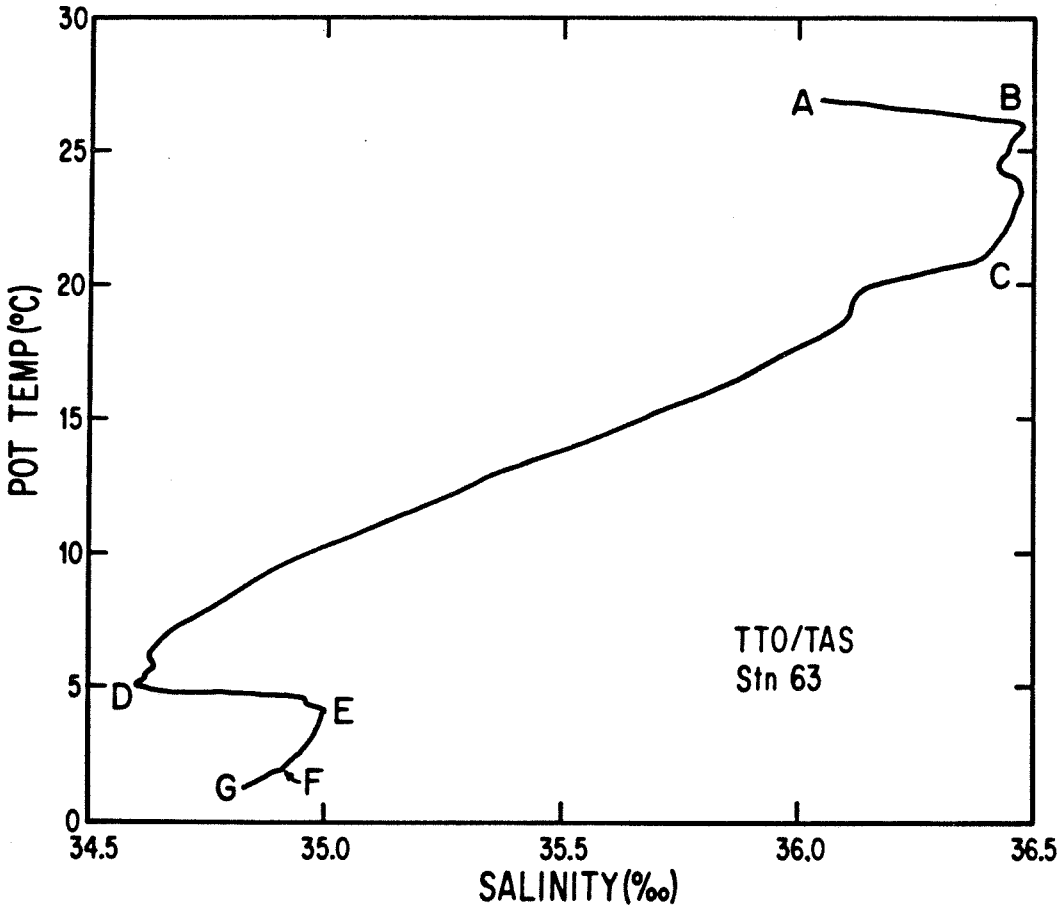
30
25
20
15
10
5
0
POT TEMP(°C)
34.5
35.0
35.5
36.0
36.5
SALINITY(‰)
A
B
C
D
E
F
G
TTO/TAS
Stn 63

Figure 6.5.

salinity minimum corresponds to the core of northward spreading Sub-Antarctic Intermediate Water (SIW) as shown in Figure 1.4. Below the salinity minimum another linear segment of the θ-S diagram continues along a trend of decreasing θ and increasing S. A mid-depth salinity maximum is reached at a depth of about 1500 meters (S ≈ 35.0°/oo) denoted by the point E. This salinity maximum corresponds to the upper layer of NADW shown in Figure 1.4. Below point E, both θ and S decrease to the bottom. A slight bend in the lower portion of this θ-S segment at point F (= 3100 m) is observed. This is interpreted to be due to the intrusion of a thin layer of northward spreading Antarctic Bottom Water (AABW) at this level. The temperature (θ = 1.23°C) and salinity (34.82°/oo) at the sea bottom (G = 4810 m) are significantly lower than would be expected if only NADW (θ ≈ 2°C and S ≈ 34.9°/oo) was present in the deep water.

Results of Nd isotopic measurements for this station are shown in Figure 6.6. For reference, the depths corresponding to the points labeled C through G in Figure 6.5 are shown on this figure. $\varepsilon_{Nd}(0) = -11.9$ at 790 meters which is at the core of SIW as defined by the salinity minimum at point D in Figure 6.5. The next lower depth analyzed is 1990 meters and this has $\varepsilon_{Nd}(0) = -13.3$ which is similar to other western basin isotopic compositions at this depth. Below this depth, $\varepsilon_{Nd}(0)$ is observed to increase with depth to a bottom water value of $\varepsilon_{Nd}(0) = -11.8$. As shown in Figure 6.6, this increase is approximately linear and the difference between the 1990 meter sample and bottom sample is clearly resolvable. As with other locations, there is a regular increase in concentration observed with depth for these samples.

Figure 6.6. $\varepsilon_{Nd}(0)$ as a function of depth at TTO/TAS Station 63. The depths which are labeled (C, D, E, F, and G) correspond to the depths labeled on the T-S curve in Figure 6.5. This profile is interpreted to result from the northward flow of Nd in water masses of Antarctic origin at depths above and below NADW. The sample at 2000m has $\varepsilon_{Nd}(0)$ which is inferred for undiluted NADW (see Figures 6.2 and 6.4). The shifts toward more radiogenic values of $\varepsilon_{Nd}(0)$ at depths both shallower and deeper than the 2000m sample are in the direction inferred for the isotopic composition of Nd in waters of Antarctic origin ($\varepsilon_{Nd}(0) \approx -9$, see Figure 4.2). This interpretation is entirely consistent with the analysis of the T-S diagram in Figure 6.5 and further demonstrates the close correlation between Nd isotopic shifts in the water column and changes in the T-S characteristics. The concentration data for these samples have not benn plotted but show a fairly regular increase in concentration with depth. The error bars represent the 2σ errors on the isotopic measurements.

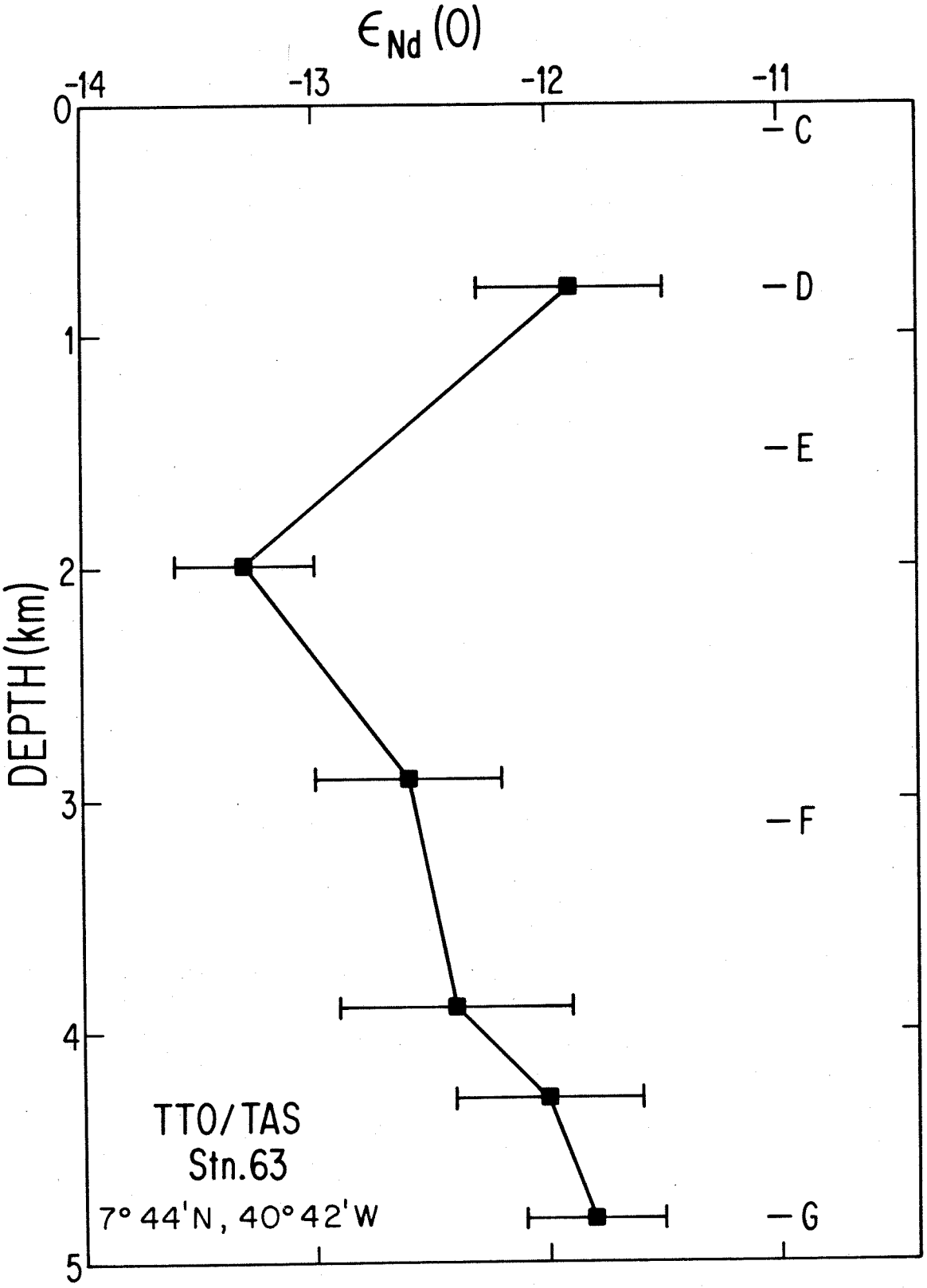
ϵ_{Nd} (0)
-14
-13
-12
-11
0
1
2
3
4
5
DEPTH (km)
C
D
E
F
G
TTO/TAS
Stn.63
7° 44'N, 40° 42'W

Figure 6.6.

6.3. Discussion

6.3.1 REE Transport in the Western Basin

Nd isotopic data for three profiles of the water column in the western basin of the North Atlantic indicate that there are both vertical and horizontal variations within this region of the Atlantic. The $\varepsilon_{Nd}(0)$ versus depth profiles for the OCE 63 sites (Figure 6.4) and A-II 109-1 Station 30 (Figure 6.2) are nearly identical, indicating that these two locations are seeing the same distribution of REE sources in the water column. The similarities between the T-S properties of these two stations indicate that it would be justifiable to combine the isotopic data for these two profiles and consider them as representing a single profile. In the analysis below, the combined data set is considered for sake of brevity.

The profiles exhibit nearly uniform deep water (1000 m to the bottom) isotopic compositions corresponding to $\varepsilon_{Nd}(0) \approx -13.5$. There is a relatively large and abrupt shift in $\varepsilon_{Nd}(0)$ of 2 to 3 ε-units observed for the depth interval between 800 and 1000 meters. Samples analyzed from depths of less than 1000 meters at these locations are distinctly more radiogenic than the underlying deep waters, having $\varepsilon_{Nd}(0) = -10.9$ to -9.4. There is indication of another, but smaller, shift in $\varepsilon_{Nd}(0)$ of about 1 ε-unit between 200 and 300 meters as shown in Figure 6.2. Samples from these two stations at depths between 300 and 800 meters have $\varepsilon_{Nd}(0)$ in a limited range from -10.3 to -10.9. Between 0 and 200 meters the range is from -9.4 to -9.6. These differences clearly indicate that there are at least two sources of REE in the water column having distinctly different Nd isotopic compositions, and possibly a third source, being supplied by horizontal transport. The sharp difference in $\varepsilon_{Nd}(0)$ between 800 and 1000 meters depth

indicates that there may be only limited exchange of Nd across this 200 meter interval of the water column, and indicates that the water masses above and below this interval must be decoupled from each other as a result of the horizontal flow between them. If there were significant exchange of Nd across this boundary then a smooth change in isotopic composition between the surface and deep waters should occur instead of the abrupt shift observed. The data for the interval between 800 meters and the surface do not appear to lie on a smooth curve either. The smaller isotopic shift between 200 and 300 meters may also be indicative of a transport boundary between two sources. It appears from these observations that intervals in the water column characterized by distinctive Nd isotopic compositions may be reflecting Nd isotopic signatures corresponding to a specific water mass. If this is the case, then the isotopic data should be consistent with identification of water masses based on temperature (T) and salinity (S) relationships in the water column. Three water masses can be identified in the water column from the T-S diagrams for the OCE 63 and A-II 109-1 sites shown in Figures 6.1 and 6.3 (a water mass is defined by a linear segment of the T-S diagram). These were identified above on the basis of general classifications of Atlantic water masses discussed in Chapter 1. A deep water mass in waters below 1000 m is identified as NADW. (AABW may be present below 4500 m at OCE 63 but no samples were analyzed from these depths at this location). A second water mass is observed within the main thermocline between 1000 m and about 200 m and is loosely referred to as "upper water". Though the T-S segment corresponding to the upper 200 meters of the water column is not linear, a third water mass (or surface mixed layer) may be indicated by the departure of the T-S characteristics of this surface layer from the more regular T-S character of "upper water." The

thickness of this surface layer depends on both the latitude and season and may account for the difference in the T-S character in this depth region at these two locations.

The Nd isotopic data for this region are clearly consistent with the water mass analysis based on the T-S properties discussed above. The isotopic shift between 800 and 1000 meters also marks the boundary between two linear segments of the T-S diagrams, and indicates that the very uniform deep water Nd isotopic composition at these locations is representative of North Atlantic Deep Water. It is not clear from the data whether the REE in NADW are derived from a single source or from several sources which have been well homogenized. This point will be considered a bit later, however. The upper waters may have two sources of REE as indicated by the small isotopic shift between 200 and 300 meters. The location of this shift in the water column coincides with the boundary between the T-S segments representing the upper water and surface water at these stations and is therefore consistent with there being a third source of rare earths being transported in waters flowing under the surface layer. Rare earths in such a source may be associated with transport by the Gulf Stream. Although no samples have been analyzed from the Gulf Stream, data from Stordal and Wasserburg [1983] for a sample from the loop current in the Gulf of Mexico which feeds into the Gulf Stream has $\varepsilon_{Nd}(0) = -10$ and is consistent with these observations. The lower $\varepsilon_{Nd}(0)$ values below 200 meters could simply be the result of exchange with Nd in the deep waters. One source of REE in the upper waters clearly must result from injections at the surface having $\varepsilon_{Nd}(0) \approx -9.5$. These REE are most likely supplied by river runoff from North and South America.

Data for a third western basin location indicate that there are also horizontal variations in the isotopic composition of Nd in this basin which can be related to lateral transport phenomena. The $\varepsilon_{Nd}(0)$ versus depth profile for TTO/TAS Station 63 (Figure 6.6) in the western equatorial Atlantic differs from other western basin profiles discussed above in that there is a gradient in the isotopic composition of Nd in the deep waters instead of a uniform composition. The $^{143}Nd/^{144}Nd$ ratio increases from a minimum of $\varepsilon_{Nd}(0) = -13.3$ at ~ 2000 meters to a bottom water maximum of $\varepsilon_{Nd}(0) = -11.8$ at ~ 4800 meters. From T-S considerations, the 2000 meter sample is clearly representative of NADW as described above, and its Nd isotopic composition is identical to that inferred for this water mass. The gradual increase in $\varepsilon_{Nd}(0)$ with depth below this minimum must be due to the injection of REE from another source region with a more radiogenic source of Nd. The relatively high SiO_2 content (Table A3) and relatively low temperature and salinity of the bottom waters at this location indicate the presence of a diluted component of AABW. These observations indicate that the gradual increase in $\varepsilon_{Nd}(0)$ below 2000 meters is consistent with the mixing of southward spreading NADW with northward spreading Antarctic Bottom Water (AABW). In its purest form, AABW has $\varepsilon_{ND}(0) \approx -9$ (see Chapters 3 and 4), but at this location it has presumably been diluted with Nd in NADW. Above the deep water $\varepsilon_{Nd}(0)$ minimum, only one other sample from this profile has been analyzed. This sample is from the core of Sub-Antarctic Intermediate Water (SIW) which is defined by the salinity minimum (Fig. 6.5) and nutrient maxima (Table A3) at ~ 800 meters. This sample has $\varepsilon_{Nd}(0) = -11.9$ and is significantly different from the underlying sample at ~2000 meters. It is also very different from $\varepsilon_{Nd}(0)$ values for a similar depth at the more northerly western basins discussed above indicating it represents a

different source of REE. The Nd isotopic composition of this sample lies in the direction of values which would be expected for waters of Antarctic origin.

The Nd isotopic data for the western basin clearly establish that there is significant lateral transport of the REE in this part of the Atlantic. The results are compatible with a conventional water mass analysis for the western basin of the North Atlantic in which NADW is spreading southward from northern polar regions passing below northward spreading upper waters which are being transported in the Gulf Stream system. Further south, NADW begins to encounter and flow between northward spreading AABW and SIW. The more gradual shifts in Nd isotopic composition between NADW and AABW at the TTO/TAS sampling site indicates that the boundaries separating these water masses are more diffuse than observed between NADW and upper waters at the locations farther north. This may be related to differences in the relative velocities at which water masses are flowing past one another, suggesting that relative water mass flow rates in the equatorial region are slower and thus allow for more extensive vertical exchange between water masses.

Nd isotopic data contrast sharply with the concentration data. The concentration data exhibit the same approximate distribution pattern everywhere. The concentration gradient implies removal from the water column and points to a nonconservative behavior for the REE. The isotopic distribution, which appears to correlate reasonably well with the T-S relationships, exhibits a conservative behavior. This clearly indicates that the removal process does not significantly affect the isotopic distribution, but as indicated in Chapter 5, the mechanism for this is not understood.

6.3.2 REE Transport in Other Areas

The relationship between Nd isotopic distributions in the water column and corresponding water mass characteristics demonstrated above for the western basin of the North Atlantic can also be demonstrated for other areas. One such area that has been studied is a region in the eastern North Atlantic in the vicinity of the Mediterranean outflow. As discussed in Chapter 1, the outflow from the Mediterranean has a profound influence on the temperature and salinity characteristics of the Atlantic Ocean. The most pronounced feature is a salinity maximum near 1000 meters which in the eastern basin reaches salinities as high as 36.5°/oo, about 1.5°/oo higher than corresponding depths in the western basin. The isotopic composition of Nd was determined in this outflow in the eastern North Atlantic (A-II 109-1 Station 95) to determine the influence it may have on the isotopic composition of Nd in Atlantic waters it flows into.

The results of Nd isotopic measurements made for this station are shown as a function of water depth in Figure 6.7. As can be seen from this figure, there is a clear shift in the isotopic composition of about 2 ε-units at 1000 meters towards more radiogenic values of $\varepsilon_{Nd}(0)$ relative to waters above and below this level. This shift occurs within the salinity maximum corresponding to the core of this outflow indicating that Nd was transported from the Mediterranean Sea. Though Mediterranean water was not analyzed, it is estimated that the $\varepsilon_{Nd}(0)$ value of undiluted Mediterranean water is about -6. This is somewhat surprising in view of the fact that 99% of the Mediterranean water budget is derived from inflowing Atlantic water. This finding indicates that there are substantial sources of REE in the Mediterranean Sea which dominate the REE budget of this basin. These problems, as well as a comparison between the isotopic composition of Nd in eastern and western basin waters, are discussed in detail in Appendix 4.

Figure 6.7. $\varepsilon_{Nd}(0)$ as a function of depth at A-II 109-1, Station 95 in the eastern North Atlantic near the Mediterranean outflow. Notice the maximum in $\varepsilon_{Nd}(0)$ at 1000 m. This is interpreted as resulting from the injection at this depth of Mediterranean water having $\varepsilon_{Nd}(0) \approx -6$. As shown for western North Atlantic sampling locations, the Nd isotopic distribution observed here is consistent with water mass observations made from T-S characteristics. The Sm and Nd concentrations corresponding to these samples were shown in Figure 5.3. The error bars represent the 2σ errors on the isotopic measurements.

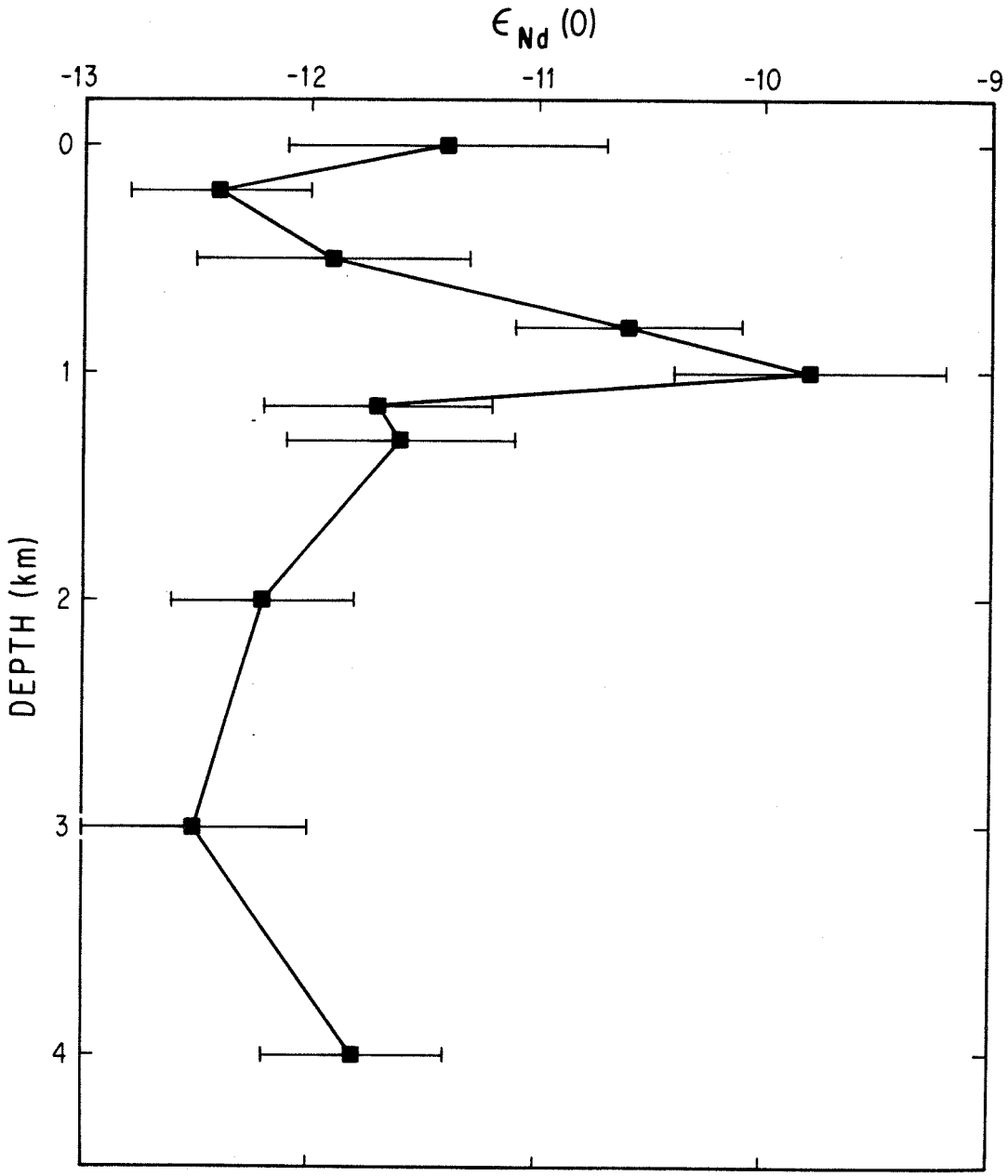

Figure 6.7.

Detailed water column profiles of $\varepsilon_{Nd}(0)$ have not been made in the Pacific. Only one profile consisting of samples from three depths has been measured. These results were discussed in Chapter 4 along with the Drake Passage results. It was concluded that the the isotopic composition of Nd in the bottom water from this location was representative of northward spreading Antarctic Bottom Water. The other two samples from this profile are associated with two separate water masses from the bottom water (upper water and Pacific Deep Water). All three samples have distinctly different isotopic compositions, but the lack of adequate vertical sampling density prohibits a strict interpretation of these results in the framework of well known water mass characteristics of this region. The data would appear to be consistent, however, with transport processes similar to those demonstrated for the Atlantic.

6.3.3 The Source of Nd in NADW.

The source of relatively non-radiogenic Nd in the deep waters of the North Atlantic remains to be determined. The data discussed above indicates that the REE are transported over large distances within the NADW mass while still maintaining the isotopic characteristics of the source suppling the REE to this water mass. It seems likely, therefore, that isotopic characteristics of the REE should be imparted at the source of this water mass. As discussed in Chapter 1, the major sources of the North Atlantic deep water complex are from overflows from Arctic seas. These seas receive extensive fresh water drainage from Precambrian terranes of North America and Asia. Based on data for composite samples from the Canadian Shield [McCulloch and Wasserburg, 1978], runoff from Archean terranes would be expected to have $\varepsilon_{Nd}(0) \lesssim -25$. If fresh water injections from North America

and Asia into the Arctic are characterized by such low values of $\varepsilon_{Nd}(0)$, then this component should be easily identified in Arctic Ocean waters.

In order to test the possibility of a northerly source of REE in NADW, samples were collected from water masses in the Irminger, Greenland and Norwegian Seas which are believed to represent the major components of NADW. The results of Nd isotopic analyses made on these waters are given in Table A2 and on Figure 3.1. The data exhibit a wide range in $\varepsilon_{Nd}(0)$ from -7.7 to -14.1. Most of these samples yielded $\varepsilon_{Nd}(0)$ values which are clearly too radiogenic ($\varepsilon_{Nd}(0) > -11$) to be the source of the Nd in NADW. The present data base is limited, however, and as a result the data are not easily understood. Of all these samples, only one representative of Labrador Sea water ($\varepsilon_{Nd}(0) = -14.1$) appears to have an isotopic composition similar to NADW. Labrador Sea water is estimated to account for a maximum of only 30% of the budget for NADW (J.W. Swift, personal communication). From mass balance considerations, a more negative $\varepsilon_{Nd}(0)$ value than -14.1 is clearly necessary for the undiluted Labrador Sea component if it is a major source of the non-radiogenic Nd in NADW. A recent expedition to the Labrador Sea and Baffin Bay was made to collect more water samples to study this possibility further. Results from this expedition are forthcoming and should provide further insight to this problem.

6.4. Conclusions

Nd isotopic measurements for vertical profiles of the water column at several localities in the North Atlantic demonstrate that the REE are undergoing extensive lateral transport from several different sources. In contrast to the nonconservative behavior of Nd, $\varepsilon_{Nd}(0)$ appears to be conserved

within a water mass, correlating well with temperature and salinity distributions in the water column. In the western basin, the distribution of Nd isotopes in the water column is shown to be consistent with the general circulation of water masses in the Atlantic. One source of rare earth elements is associated with NADW and is found to have an average $\varepsilon_{Nd}(0) \cong -13.5$. Deep water with this isotopic signature is found at all western basin locations sampled. However, in the equatorial North Atlantic, water of this composition is underlain by waters having a more radiogenic source of REE. The bottom water at this equatorial region is concluded to be diluted AABW based on temperature, salinity, and nutrient data. The observed $\varepsilon_{Nd}(0) = -11.8$ is fully consistent with this bottom water being a mixture of southward flowing NADW and northward flowing AABW ($\varepsilon_{AABW} \cong -9$) and provides the first direct evidence of lateral transport of rare earths in the deep ocean below 1000 meters. Waters in the upper 1000 meters of the water column in the western North Atlantic have a third source of REE which are presumably being transported northward within the Gulf Stream system and which may reflect major injections of REE in runoff from the Mississippi and Amazon drainage systems.

Nd isotopic results presented here from the eastern basin of the North Atlantic have established that the outflow of Mediterranean water into the Atlantic is characterized by a shift in isotopic composition relative to inflowing Atlantic waters corresponding to $\varepsilon_{Nd}(0) \geq -9.8$ for Mediterranean waters. This outflow is seen as a shift toward more radiogenic values of $^{143}Nd/^{144}Nd$ in the water column of the eastern North Atlantic at a water depth of 1000 m relative to overlying and underlying waters which have $\varepsilon_{Nd}(0) \approx -12$. This shift of two ε units coincides with the core of the Mediterranean outflow as identified from salinity measurements. The

isotopic composition of Mediterranean water is estimated to be $\varepsilon_{Nd}(0) \approx -6$. The source of Nd with this isotopic composition may be runoff from a relatively young continental terrane or injection of Nd from deep-sea sediments having significant young volcanogenic components. The total flux of Nd from this outflow to the Atlantic is about 10% of that estimated for rivers and may in part account for differences in the isotopic compositions of the deep waters of the eastern and western basins.

The bulk of waters in the North Atlantic are characterized by lower values of $\varepsilon_{Nd}(0)$ (-11.5 to -14.0) indicating that there must be a major source of REE injections which has not been identified. It is expected that the isotopic signatures associated with deep waters should be imparted at the sources of the deep water masses. An attempt was made to investigate the role of overflows from the Norwegian, Greenland, and Labrador Seas in providing the source of REE in the deep waters of the North Atlantic. It is into these northern seas that most of the fresh water runoff from Precambrian shields of Asia and North America drain. The data indicate that only the overflow from the Labrador Sea has an isotopic composition which is compatible as a source of REE in NADW. The sampling of these overflows appears to be inadequate, however, to draw any firm conclusions from the data set at the present time.

Chapter 7: A Strontium and Neodymium Isotopic Study of Hot Springs on the East Pacific Rise at 21° North and Guaymas Basin, Gulf of California

7.1. Introduction

The presence of metal rich sediments on the flanks of the East Pacific Rise led to the suggestion that submarine hydrothermal activity could be the principle source of metals in these deposits [Bostrom and Peterson, 1966; Bonatti and Joensuu, 1966]. Hydrothermal input of manganese was suggested to account for the high accumulation of manganese in surficial sediments [Lyle, 1976]. The hydrothermal flux of Mn was estimated to be about three times higher than the continental flux. The discovery of submarine thermal springs on the Galápagos Rift [Corliss et al., 1979] and later on the East Pacific Rise [Rise Project Group, 1980] led to the direct confirmation of these theories [Edmond et al., 1979a]. Ridge-crest hydrothermal systems have since been shown to be the major sink for magnesium and sulphate and a major source for lithium, rubidium and manganese in the oceans [Edmond et al., 1982] as well as a substantial source of other elements.

It was shown in Chapter 3 that the oceanic budget of the rare earth elements (REE) is dominated by continental sources having $\varepsilon_{Nd}(0) < 0$, but they suggested that the Nd isotopic differences between the Atlantic and Pacific Oceans may be due in part to a submarine hydrothermal source of REE (REE) having radiogenic Nd. The Pacific Ocean has an average Nd isotopic composition corresponding to $\varepsilon_{Nd}(0) \approx -3$ compared to an Atlantic value of $\varepsilon_{Nd}(0) \approx -12$. A study of Nd in the suspended loads of rivers [Goldstein and O'Nions, 1982] suggests that continental drainage to the Pacific may be

characterized by similar Nd isotopic compositions as supplied to the Atlantic from continental sources. Mid-ocean ridge basalts (MORB), however, are characterized by positive values of $\varepsilon_{Nd}(0)$ (~ +10 to +13 [Richard et al., 1976; DePaolo and Wasserburg, 1976a; O'Nions et al., 1977]. The presence of active hydrothermal systems along mid-ocean ridge crests in the Pacific may, therefore, be a major source of the more radiogenic Nd observed in Pacific waters.

In this study, solutions collected from hot springs from the East Pacific Rise at 21°N and from Guaymas Basin, Gulf of California have been analyzed for Nd and Sr isotopic composition and Sm, Nd, and Sr concentrations. The samples from the East Pacific Rise represent fluids emanating at the crest of a sediment starved ridge, whereas the samples from Guaymas Basin have ascended through several hundred meters of sediment before emanating on the sea floor. The data have important implications for the geochemical cycles of Sr and the REE in ridge crest hydrothermal systems. These analyses represent the first measurements of Nd isotopes in submarine hydrothermal solutions.

7.2. Sampling and analytical methods

Hydrothermal solutions from 21°N on the East Pacific Rise and Guaymas Basin, Gulf of California were collected from the DSRV Alvin by J. Edmond using specially designed titanium samplers. The inlet port of the sampler was positioned in clear water inside the top of the vents as the samples were being drawn. Samples of various dilution resulted from the entrainment of ambient seawater during the sampling procedure. The fluids were acidified to pH ~ 2 with 6N HCl immediately after recovery and filtered

through 0.45μm filters in the laboratory at the Massacheusetts Institute of Technology (MIT). Sr, Nd and Sm were determined by techniques described in Appendix 1. Mg concentrations were determined by flameless atomic absorption at MIT by K. Von Damm and B. Grant.

In addition, one sample of a fresh basaltic glass was collected from an outcrop of pillow basalts at 21°N using the mechanical arm of the Alvin. This sample was analyzed under the assumption that its Sr and Nd isotopic compositions would be representative of the bulk composition of the oceanic crust at this location. The sample was hand picked under a microscope in an effort to obtain clean, unaltered fragments of the glass which were then crushed to a fine powder using a polished stainless steel mortar and pestle. The sample was dissolved and the Sr, Sm, and Nd were separated using procedures described by DePaolo and Wasserburg [1976a]

7.3. Results

7.3.1 21° North

Mg, Sr, Nd and Sm results from the hydrothermal solutions and one basalt glass sample from 21°N are listed in Table 7.1. The Mg content of the purest hydrothermal end-member samples is quite uniform, averaging about 2μmol/g. The index of "hydrothermal purity" is based on the Mg content of the solutions. The Mg present in the samples is due to the addition of "fresh" seawater, generally as a result of sampling artifacts. A pure hydrothermal solution has C_{Mg} = 0μmol/g compared with pure seawater which has C_{Mg} = 52.7μmol/g [Edmond et al., 1982]. The percent hydrothermal given in Table 7.1 for the solutions analyzed in this study assumes an ideal

linear mixing relationship for Mg (no Mg removal) between seawater and pure hydrothermal end-members upon injection of the hydrothermal plume into the overlying water column. From this, it is observed that the purest solutions analyzed in this study contain about four percent seawater.

The Nd content in the hydrothermal end-member samples is found to be quite variable, ranging from 20 to 659 pg/g. These are significantly higher than deep ocean water concentrations of 3 to 4 pg/g [Piepgras and Wasserburg, 1980, 1982, 1983; Elderfield and Greaves, 1982; DeBaar et al., 1983; Klinkhammer et al., 1983]. The Nd concentration data are plotted versus Mg content in Figure 7.1. With the exception of #1155-18, samples collected from the hydrothermal vent at the NGS site have Nd concentrations which exhibit a fairly linear array between the hydrothermal end-member and local ambient seawater when plotted against the magnesium concentration. The Sm content, where measured, is also variable and $f_{Sm/Nd}$ values are negative (-0.393 to -0.477), indicating that the solutions are light rare earth enriched. The sample of basalt glass has a positive $f_{Sm/Nd}$ value (+0.170) typical of light rare earth depleted mid-ocean ridge basalts.

The Nd isotopic compositions of the hydrothermal solutions are also variable. These data are shown in Figure 7.2 as a function of Mg concentration. In the purest hydrothermal end-member samples, $\varepsilon_{Nd}(0)$ is found to range from -10.8 to +7.9. Two of these end-member samples, 1155-14 ($\varepsilon_{Nd}(0)$ = +2.6; C_{Nd} = 336pg/g) and 1155-18 ($\varepsilon_{Nd}(0)$ = -10.8; C_{Nd} = 659pg/g), are from the same vent at the NGS site but were collected in different sampling devices. The large disparity in isotopic composition and Sm and Nd concentrations between 1155-18 and other samples from the same vent indicates that it may have been contaminated during collection and/or subsequent handling. Two other samples, 1151-14 and 1154-6, were collected

Figure 7.1. Nd concentrations as a function of Mg concentrations in hydrothermal solutions from 21°N, East Pacific Rise and Guaymas Basin, Gulf of California. The concentration of Nd for hydrothermal solutions is observed to be variable and enriched over seawater concentrations by factors of 5 to 300. The solid line represents a linear regression of the concentration data for NGS (excluding 1155-18). The good fit to a straight mixing line of hydrothermal water from this vent with ambient seawater (as represented by 1159-9) indicates that mixtures of these solutions with seawater follow the mixing model described by Equation 7.1. The high concentration observed for 1155-18 is believed to be related to contamination of this sample as discussed in the text. The large differences between vents may be related to subsurface precipitation of the REE or to differences in the plumbing of individual vents.

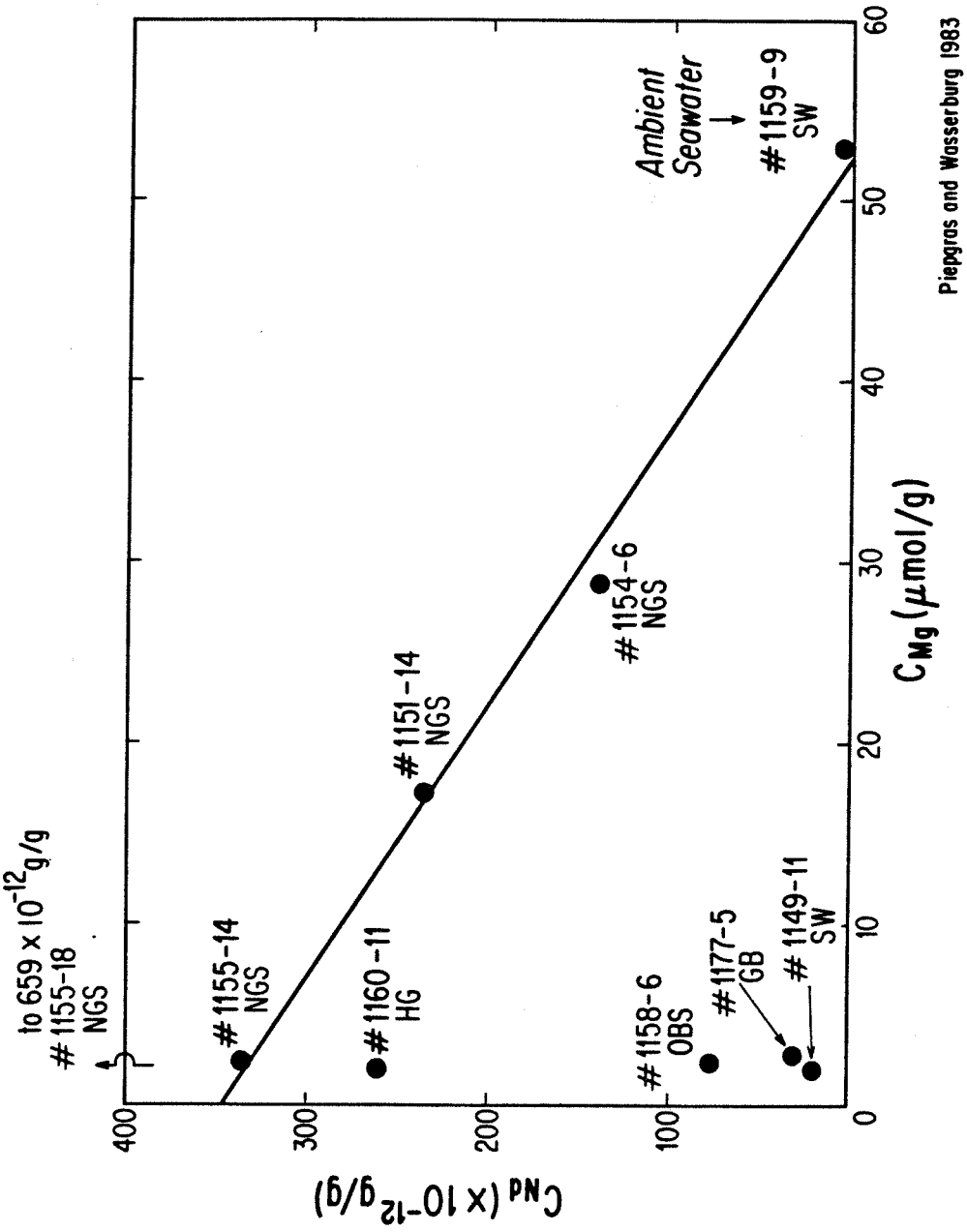
to 659 x 10⁻¹² g/g
#1155-18
NGS
#1155-14
NGS
#1160-11
HG
#1151-14
NGS
#1158-6
OBS
#1177-5
GB
#1149-11
SW
#1154-6
NGS
Ambient
Seawater
#1159-9
SW
C_Na (x 10⁻¹² g/g)
C_Mg (μmol/g)
0
10
20
30
40
50
60
100
200
300
400
Piepgras and Wasserburg 1983

Figure 7.1.

Figure 7.2. $\varepsilon_{Nd}(0)$ as a function of Mg concentration in hydrothermal solutions from 21°N and Guaymas Basin. This figure illustrates the wide spread in $\varepsilon_{Nd}(0)$ for the purest hydrothermal solutions at 21° N. $\varepsilon_{Nd}(0)$ for mid-ocean ridge basalt is also shown. It is observed that all of the solutions have isotopic compositions which are significantly less radiogenic than MORB in spite of Nd concentrations of up to 100 times seawater as shown in Figure 7.1. Some of this spread may be due to contamination as indicated by the large difference in $\varepsilon_{Nd}(0)$ (14 ε-units) for two samples from NGS (1155-14 and 1155-18) having similar Mg content and the generally poor fit to an ideal mixing curve for NGS samples with ambient seawater (calculated to fit through 1151-14 using Equations 7.1 and 7.2 as described in the text). 1155-18 appears to have been substantially contaminated with continental-like Nd. As discussed in the text, however, not all of the spread in $\varepsilon_{Nd}(0)$ is believed to result from contamination. The low value of $\varepsilon_{Nd}(0)$ observed for the Guaymas Basin sample is consistent with the fluid exchanging Nd with an old continental component in the sediments through which the solutions rise.

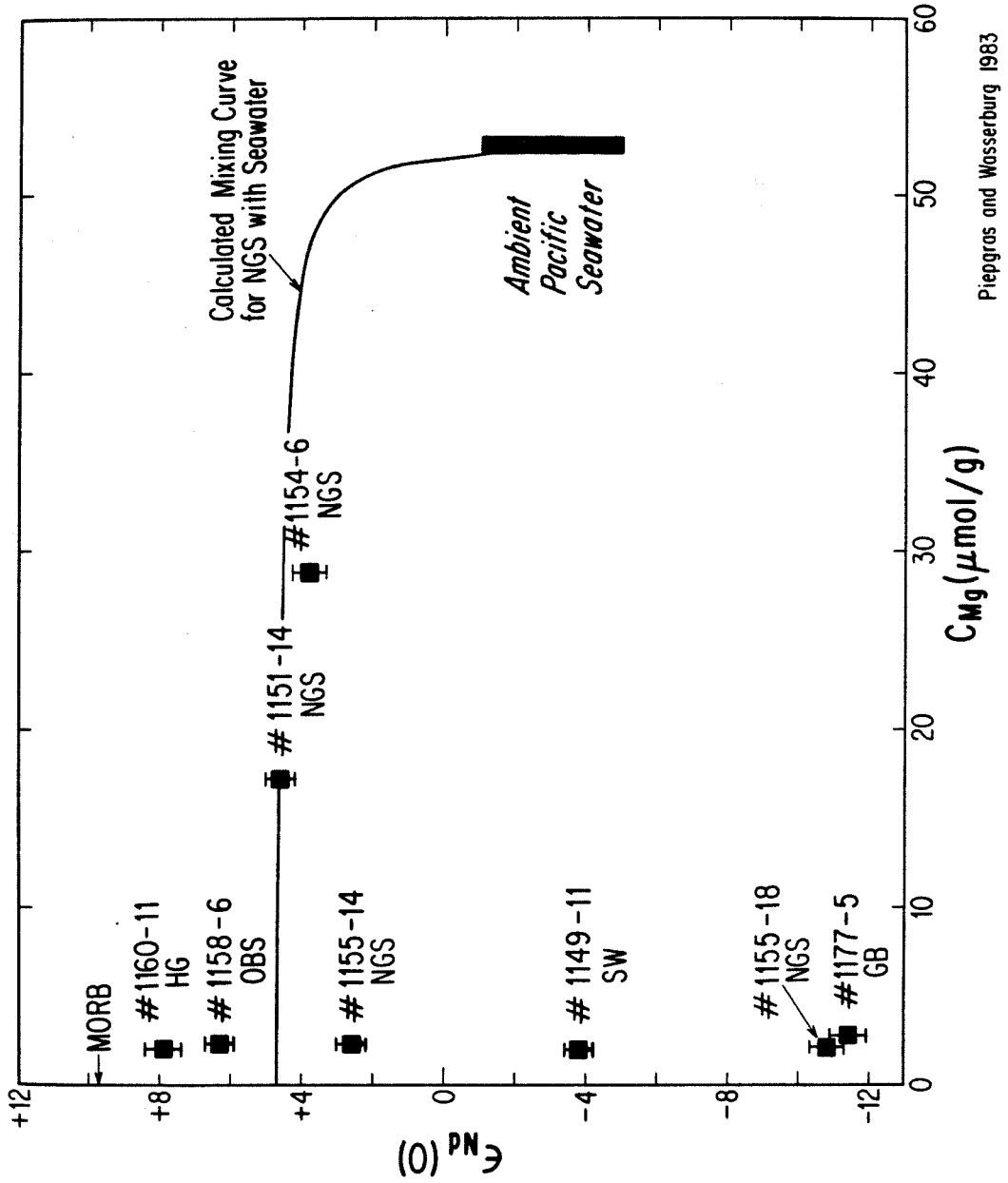
MORB
#1160-11
HG
#1158-6
OBS
#1151-14
NGS
#1155-14
NGS
#1149-11
SW
#1155-18
NGS
#1177-5
GB
#1154-6
NGS
Calculated Mixing Curve
for NGS with Seawater
Ambient
Pacific
Seawater
+12
+8
+4
0
-4
-8
-12
0
10
20
30
40
50
60
$\epsilon_{Nd}(0)$
$C_{Mg}(\mu mol/g)$
Piepgras and Wasserburg 1983

Figure 7.2.

from the vent at the NGS site but at much greater dilution. Though these samples lie on a dilution line for concentration, they deviate significantly from an ideal mixing curve between the seawater and hydrothermal end-members as shown in Figure 7.2. A discussion of the mixing equations for chemical and isotopic species used here is presented in section 7.3.3. One hydrothermal end-member sample from the southwest (SW) site (1149-11) has $\varepsilon_{Nd}(0) = -3.6$ which is similar to the average Pacific seawater value of about -3. The sample of basalt glass from 21°N has $e_{Nd}(0) = +9.7$, which is at the low end of the range of $\varepsilon_{Nd}(0)$ values for mid-ocean ridge basalts [O'Nions et al., 1977].

Sr concentrations in the hydrothermal solutions from 21°N vary only slightly from 5.8 ppm to to 8.7 ppm and are close to ambient seawater concentrations which average about 7.6 ppm [Brass and Turekian, 1972]. Figure 7.3 is a plot of Sr versus Mg concentration data for these samples. Concentration data from the NGS and OBS sites for several samples at different dilutions are observed to lie closely along dilution lines for seawater and the respective hydrothermal end-members (Some precipitation may be indicated for the NGS samples, because the sample of intermediate Mg content, 1154-6, has a lower C_{Sr} than would be predicted by the endmember concentrations). The $^{87}Sr/^{86}Sr$ ratios in the purest hydrothermal end-members are fairly constant at $\varepsilon_{Sr} = -13.4$ to -17.7 and are shown on an ε_{Sr} vs. C_{Mg} diagram in Figure 7.4. Samples from the same vent at NGS, but at different dilutions, lie fairly close to a calculated dilution curve fit through 1155-14 and ambient seawater. The mixing curve through these points shows that the pure hydrothermal end-member ($C_{Mg} = 0$) at the NGS site has $\varepsilon_{Sr} \approx -18$. This is in close agreement with previous observations by Albarede et al. [1981] for

Figure 7.3. The concentration of Sr as a function of Mg concentration in hydrothermal solutions from 21°N and Guaymas Basin. For solutions from 21°N, the concentrations are all very close to the ambient seawater concentration represented by 1159-9. Samples for NGS and OBS fit fairly close to straight mixing lines between the seawater and hydrothermal end-members, but some precipitation may be indicated for the intermediate Mg content sample from NGS (1154-6) which has a lower C_{Sr} than would be predicted from the mixing model of Eq. 7.1. The Guaymas Basin sample has C_{Sr} about a factor of 2 higher than seawater which may be due to the dissolution of $CaCO_3$ or other sources of Sr in the sediments through which this solution ascended.

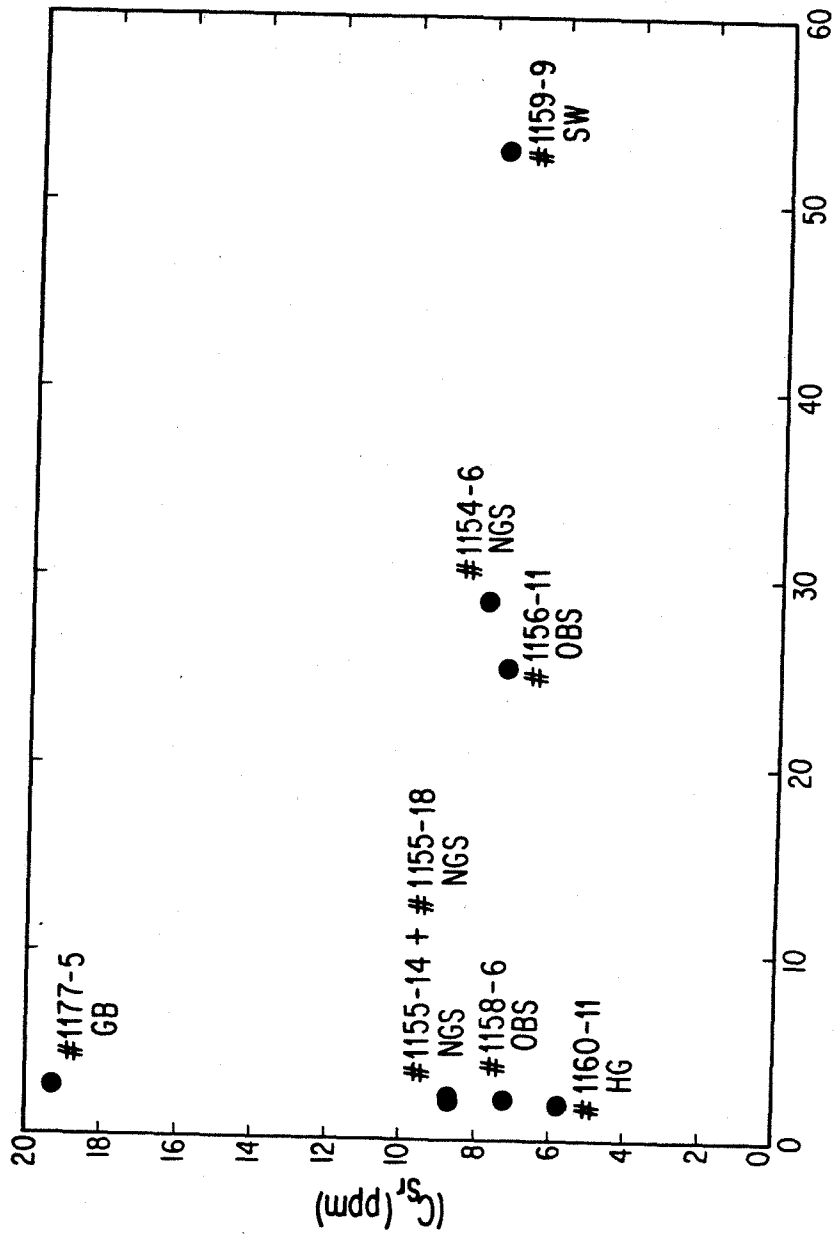
#1177-5
GB
#1155-14 + #1155-18
NGS
#1158-6
OBS
#1160-11
HG
#1154-6
NGS
#1156-11
OBS
#1159-9
SW
C_{Sr} (ppm)
C_{Mg} (μmol/g)
Piepgras and Wasserburg 1983

Figure 7.3.

Figure 7.4. $\varepsilon_{Sr}(0)$ as a function of Mg concentration in hydrothermal solutions from 21°N and Guaymas Basin. Note the tight clustering near $\varepsilon_{Sr}(0) \approx -16$ for samples from 21°N having $C_{Mg} \approx 2\mu mol/g$. The data for NGS are observed to fit very well to the calculated mixing curve shown (calculated to fit through 1155-14 and 1155-9 according to the same procedure as indicated in Figure 7.2) and indicate that the pure hydrothermal end-member has $\varepsilon_{Sr}(0) \approx -18$. The data indicate that the fluids at 21°N are fairly homogeneous with respect to Sr isotopic composition, but the pure hydrothermal end-members of all of these solutions have Sr which is significantly more radiogenic than the value of MORB shown in the lower left corner of this figure. This may be due to the presence of a small amount of seawater Sr retained by the solution during circulation through the oceanic crust. The single sample from Guaymas Basin has a considerably more radiogenic value of $\varepsilon_{Sr}(0)$ than 21°N samples in spite of having a similar Mg concentration. This result is consistent with the solution from Guaymas Basin reacting with sediments having $\varepsilon_{Sr}(0)$ which is more radiogenic than the oceanic crust.

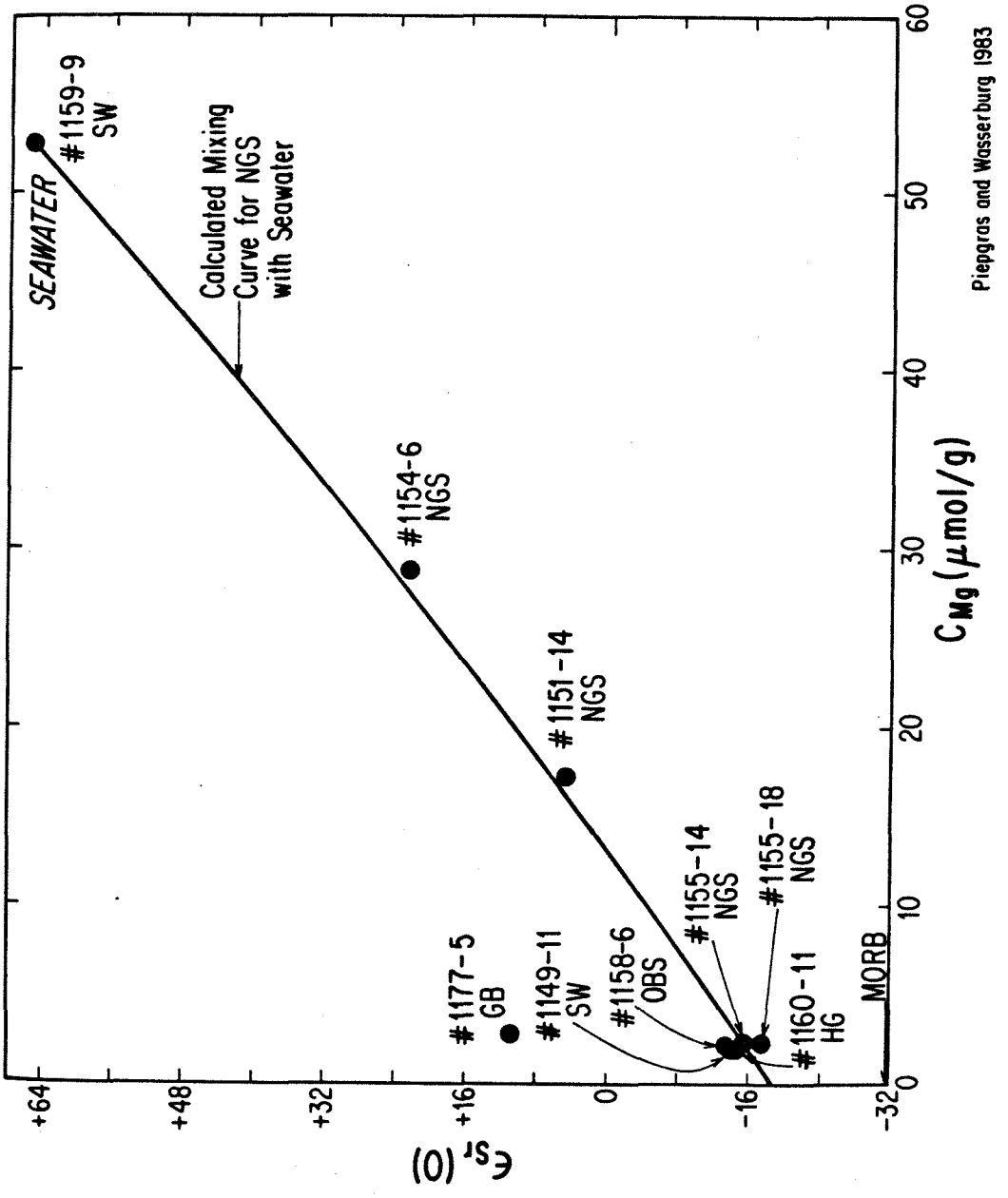
SEAWATER
#1159-9
SW
Calculated Mixing
Curve for NGS
with Seawater
#1154-6
NGS
#1151-14
NGS
#1155-14
NGS
#1155-18
NGS
#1160-11
HG
#1158-6
OBS
#1149-11
SW
#1177-5
GB
MORB
$\varepsilon_{Sr}(0)$
C_{Mg} (μmol/g)
+64
+48
+32
+16
0
-16
-32
0
10
20
30
40
50
60
Piepgras and Wasserburg 1983

Figure 7.4.

21°N solutions. Although there is a significant difference in the ε_{Sr} values for 1155-14 and 1155-18, the discrepancy is small as compared to the difference in $\varepsilon_{Nd}(0)$ and C_{Nd} values for these two samples. The basalt glass sample has $\varepsilon_{Sr}(0) = -31.8$ and $C_{Sr} = 99$ppm, typical values for mid-ocean ridge basalts.

7.3.2. Guaymas Basin

Results of Mg, Sr, Nd and Sm measurements of a single sample from Guaymas Basin (1177-5) are listed in Table 7.1. The Mg concentration is 2.82μmol/g, similar to values from the 21°N vent fields. The Nd concentration in this sample is 30.1 pg/g, about 10 times seawater. This value is at the low end of the range observed at 21°N. The isotopic composition of Nd in this sample corresponds to $\varepsilon_{Nd}(0) = -11.4$, and is considerably lower than most $\varepsilon_{Nd}(0)$ values observed at 21°N.

The Sr concentration in 1177-5 is 19.3 ppm, which is more than twice the ambient seawater Sr concentration and concentrations observed in 21°N hydrothermal solutions. $\varepsilon_{Sr}(0) = +11$ in this sample and is much more radiogenic than samples of similar Mg concentration from 21°N.

7.3.3 Composition of seawater and hydrothermal end-members

Due to sampling artifacts, there is always some seawater present in the purest hydrothermal solutions collected. It is desirable to correct for the small addition of seawater to determine the composition of the pure hydrothermal end-member. The equation governing the concentration, C, of any species, i, in a mixture, M, of seawater, S, and hydrothermal water, H,

is given by:

$$C_{Mi} = X\ C_{Hi} + (1 - X)\ C_{Si} \qquad (7.1)$$

where X represents the weight fraction of the hydrothermal end-member in the mixture. This equation is linear for all chemical species if they are conserved during mixing (ie. no removal due to precipitation). Thus, the concentration of any species in the pure hydrothermal solution can be determined from its concentration in the diluted solutions and ambient seawater by a linear regression analysis of the concentration of the selected species versus Mg content extrapolated to C_{Mg} = 0μmol/g.

The general equation for the isotopic composition of either Sr or Nd in such a mixture is non-linear and has the form:

$$\varepsilon_{Mi} = \frac{XC_{Hi}\ \varepsilon_{Hi} + (1 - X)\ C_{Si}\ \varepsilon_{Si}}{X\ C_{Hi} + (1 - X)\ C_{Si}} \qquad (7.2)$$

If $C_{Hi} \approx C_{Si}$ then ε_{Mi} reduces to a linear function of ε_{Hi} and ε_{Si}. In calculating hydrothermal end-member compositions from the diluted samples from 21°N, it will be assumed that ambient Pacific seawater from this location has ε_{Nd} = -3, C_{Nd} = 3pg/g, ε_{Sr} = +65, and C_{Sr} = 7.6 ppm.

7.4 Discussion

7.4.1 Strontium data

21°N, EPR. There are several aspects to the Sr data for 21°N hydrothermal solutions which have important implications for the chemical cycle

of Sr in mid-ocean ridge hydrothermal systems. When the measured $^{87}Sr/^{86}Sr$ ratios are corrected for the small amount of seawater addition during sampling using the relationships presented above, the average $^{87}Sr/^{86}Sr$ ratio in the pure hydrothermal fluids corresponds to $\varepsilon_{Sr}(0) \approx -18 \pm 2$ which is very close to the value of $\varepsilon_{Sr}(0) \approx -20$ determined previously by Albarede et al., [1981] for 21°N solutions. This is an important result because it shows that the Sr isotopic values determined for the pure hydrothermal fluids at 21°N are significantly more radiogenic than Sr in the local oceanic crustal reservoir ($\varepsilon_{Sr}(0) = -31.8$) as represented by the Sr in the glassy rim of a pillow basalt from the vent area. This difference must be due to the contribution of seawater Sr in the hydrothermal fluids. It is unlikely that late stage addition of "fresh" seawater could account for the elevated $\varepsilon_{Sr}(0)$ values observed. The lack of Mg in the solutions indicates that they have extensively reacted with the oceanic crust before being sampled. The high exit temperatures (~350°C) at 21°N are consistent with theoretical calculations for the adiabatic ascent of fluids above a magma chamber [Bischoff, 1980] which suggests that there could be very little cooling of the ascending fluid due to entrainment of waters which are at lower temperatures. This would indicate that a memory of the original seawater Sr is preserved in the fluids during the passage of seawater through the oceanic crust.

The concentration of Sr in the hydrothermal solutions is very close to that of seawater. As a result, the net flux of Sr into or out of the oceanic crustal reservoir affected by the hydrothermal circulation system must be small. From consideration of the isotopic data, about 85% of the Sr in the vent waters must be of oceanic crust origin which requires extensive exchange of Sr between the fluid and oceanic crust. This exchange most

likely results in the substantial leaching of strontium from oceanic crustal rocks into the circulating fluids. If there were substantial leaching of Sr in the hydrothermal reservoir, large Sr excesses would be expected in the solutions emanating from the rise crest relative to seawater. However, results from studies of experimental [Menzies and Seyfried, 1979a] and natural [Humphris and Thompson, 1978a,b] systems indicate that while Sr is extensively leached from silicate fractions during hydrothermal metamorphism of oceanic basalts, this leached Sr ends up in calcium bearing alteration products such as anhydrite and epidote. The observed similarity in Sr concentration between the hydrothermal solutions and seawater indicate that there is probably extensive subsurface removal of Sr. Anhydrite is a commonly observed mineral in the chimneys associated with the hydrothermal vents [Rise Project Group, 1980; Haymon and Kastner, 1981], and while sulfur isotopic data indicate that the sulphate precipitated from seawater [Styrt et al., 1981], Sr isotopic data show substantial contributions of mantle derived Sr in this mineral [Albarede et al., 1981]. However, anhydrite occurrence within dredged oceanic basalts is unknown [Menzies and Seyfried, 1979a]. Epidote has been suggested as the dominant Sr bearing phase in altered basalts [Humphris and Thompson, 1978a,b]. Epidote has also been reported to be an abundant constituent in sediments from a hydrothermally altered unit of DSDP Hole 477 in the Guaymas Basin. The observed similarity in the Sr concentrations between seawater and hydrothermal solutions may only be coincidental. Michard et al. [1982] reported Sr enrichments of a factor of two over seawater concentrations for solutions collected from vent fields at 13°N on the East Pacific Rise, indicating that the extent of subsurface removal is indeed variable and may be tied to the formation of alteration products.

It is also important to note that the Sr isotopic compositions determined for the hydrothermal end-member solutions are relatively uniform. It would appear from this that the 21°N vent field is sampling a relatively homogeneous fluid with respect to Sr isotopic composition. This strongly suggests that the chemical interactions affecting the exchange of Sr between seawater and oceanic crust locally reach an effective equilibrium. It does not appear that the same equilibrium is achieved at all locations along a ridge crest. The $^{87}Sr/^{86}Sr$ ratios in the hydrothermal end-member solutions at 13°N on the East Pacific Rise correspond to $\varepsilon_{Sr}(0) \approx -5$ [Michard et al., 1982]. The more radiogenic $^{87}Sr/^{86}Sr$ values at 13°N were interpreted by these authors to infer higher water/rock ratios at this site (W/R = 5) relative to 21°N samples (W/R = 1.5), although the possibility of mixing of the hydrothermal end-member with "evolved" ground water was suggested as well.

Water/rock ratios for the hydrothermal solutions are determined from mass balance considerations for the water-rock system. For the mixing of Sr or Nd between seawater and oceanic crust, the equation for mass balance between the initial (i) and final (f) products is given by:

$$w\varepsilon^{i}_{water} + r\varepsilon^{i}_{rock} = w\varepsilon^{f}_{water} + r\varepsilon^{f}_{rock} \quad . \qquad (7.3)$$

Here, w and r are the atomic proportions of Sr or Nd in the water and rock systems respectively, and the ε's refer to the isotopic compositions of Sr and Nd in the initial and final water-rock systems. For equilibrium exchange, $\varepsilon^{f}_{water} = \varepsilon^{f}_{rock}$, where ε^{f}_{rock} is the average ε value of the oceanic crust seen by the fluid. Substituting this expression into Eq. (7.3), the

water/rock mass ratio for the fluid phase is given by:

$$\frac{W}{R} = \frac{C_{rock}\left(\varepsilon^{f}_{water} - \varepsilon^{i}_{rock}\right)}{\left(C^{i}_{water}\varepsilon^{i}_{water} - C^{f}_{water}\varepsilon^{f}_{water}\right)} \qquad (7.4)$$

where the C's refer to the concentration of either Sr or Nd in the water and rock. In this expression, it is assumed that the initial and final concentrations of Sr or Nd in the oceanic crust are identical and that the mass of water, W, and oceanic crust, R, are not significantly altered during the hydrothermal event. From the Sr data in Table 7.1, and assuming that the initial fluid has a seawater isotopic composition ($\varepsilon_{Sr}(0) = +65$), the water/rock ratios determined for solutions from 21°N are about 1.5 to 2 as was determined previously by Albarede et al. [1981]. If equilibrium exchange between the circulating fluid and the oceanic crust does not occur, then $\varepsilon^{f}_{water} \neq \varepsilon^{f}_{rock}$ and the actual water/rock ratio will be less than the equilibrium water/rock ratio. Thus, the water/rock ratios determined for hydrothermal solutions may only represent upper limits. Nonequilibrium exchange processes could, in principal, account for the more radiogenic $^{87}Sr/^{86}Sr$ ratios observed by Michard et al. [1982] in the 13°N solutions relative to those from 21°N and, consequently, the higher water/rock ratios determined from their Sr data for 13°N.

Guaymas Basin. The isotopic composition of Sr in one hydrothermal solution analyzed from Guaymas Basin is markedly different from solutions at 21°N. The istopic composition of Sr in sample 1177-5 from this area corresponds to ε_{Sr} (0) = +11. Corrected to C_{Mg} = 0μmol/g, the isotopic composition of Sr in the pure hydrothermal solution corresponds to $\varepsilon_{Sr}(0) = +10$. The low Mg content of the sample analyzed precludes the

addition of fresh seawater to the ascending solution to account for its relatively high $^{87}Sr/^{86}Sr$ ratio. More likely, the ascending solutions have leached Sr from the carbonate and possibly other fractions of the sedimentary pile the solutions must rise through. This would be consistent with the high Sr concentration in the sample (19.3 ppm) and the high partial pressure of CO_2 in the solutions of about 20 atmospheres [J. Edmond, personal communication]. Calcareous nanofossils constitute up to 25% of the sediment in Guaymas Basin [Curray et al., 1982] which is sufficient to be a major source of Sr in the solutions. It could also account for the high CO_2, but no correlation is observed between the Ca and CO_2 contents of the sediment pore fluids leading Curray et al. [1982] to suggest that the CO_2 may be a result of biogenic respiration. The high $^{87}Sr/^{86}Sr$ ratios may also reflect, in part, the reaction of the hydrothermal fluid with an old continental component in the sediment layer.

It is not possible to determine the isotopic composition of Sr in the solution prior to its injection into the sedimentary column from the oceanic crust. The solution would appear to have interacted with the oceanic crust as evidenced by the high exit temperatures of the solutions (~300) and relatively low $^{87}Sr/^{86}Sr$ ratio as compared to seawater. It may be reasonable to assume that the ascending solution originally had a Sr isotopic composition similar to solutions emanating from vents along the East Pacific Rise and was subsequently modified during its rise through the sediment column. Furthermore, it is not clear what the initial composition of the fluid was before entering the hydrothermal system. If the initial fluid was derived from seawater in the Gulf of California, its composition could easily have been altered significantly by exchange with Sr in the sedimentary cover through which it would have to descend before reaching the

oceanic crust. Because of the uncertainties concerning the origin of the fluid and its history before circulating through the oceanic crust, it is impossible to determine the extent of exchange between the fluid and the sediments through which it rose from the Sr isotopic data reported here.

7.4.2 Neodymium data

21°N, EPR. In contrast to the relatively uniform distribution of Sr in the hydrothermal effluents at 21°N, both the isotopic composition and concentration of Nd in the same solutions exhibit substantial variations from one vent to another indicating a remarkably different chemical cycle for the REE in submarine hydrothermal systems from that of Sr. The Nd isotopic data for many of the samples clearly show substantial contributions of Nd from depleted oceanic crust as indicated by their positive $\varepsilon_{Nd}(0)$ values. However, none of the samples analyzed have isotopic compositions which are equal to MORB ($\varepsilon_{Nd}(0) = +9.7$ at this location) in spite of enrichments in Nd concentrations in the solutions of up to 100 times seawater concentrations. If it is assumed that the original source of the hydrothermal fluid is seawater and that any enrichment in the observed REE concentrations over their seawater values comes from the leaching of the oceanic crust, then all of the samples analyzed in this study should have Nd isotopic compositions which are close to or identical to MORB. The fact that all samples have $\varepsilon_{Nd}(0)$ values which are significantly less than MORB for their corresponding Nd concentration levels strongly indicates that the fluids have seen a reservoir of Nd in addition to the oceanic crust which has enriched the solution with Nd having $\varepsilon_{Nd}(0) <$ MORB. Evidence for this comes from one sample (1149-11) which has a Nd concentration about six times

seawater and $\varepsilon_{Nd}(0)$ within the range of average Pacific seawater indicating that the fluid may not have exchanged any Nd with the oceanic crust. The elevated Nd concentration of 1149-11 must have resulted, at least in part, from seawater exchanging with Nd in a reservoir other than the oceanic crust with $\varepsilon_{Nd}(0) \leq$ Pacific seawater. There is no direct evidence to identify this reservoir, but a likely candidate is deep-sea sediments from the flanks of the East Pacific Rise. Nd isotopic analyses of metalliferous sediments from the East Pacific Rise indicate that these sediments have $\varepsilon_{Nd}(0) \approx -2$ to -4 [O'Nions et al., 1978; Piepgras et al., 1979] which is in the range of Pacific seawater and compatible with the result for 1149-11. There are some irregularities in the Nd isotopic data which suggest that the isotopic variations may in part be the result of contamination either during the collection or subsequent handling of the samples. Evidence for contamination is indicated from the results of samples from the NGS site. A total of four samples from this site were analyzed for Nd and Sr isotopic composition (see Table 7.1). Two samples (1155-14 and 1155-18) represent the hydrothermal end-member while the other two (1151-14 and 1154-6) have been diluted with up to 55% ambient seawater during collection. Initially, three of the samples (1155-14, 1151-14, and 1154-6) were found to lie on a dilution line for concentration with local ambient seawater as shown in Figure 7.1, but they did not lie on a mixing curve for their Nd isotopic composition (Fig. 7.2). At the exit concentrations of Nd inferred for this vent from these three samples (~350pg/g), the the isotopic composition of Nd resulting from mixing with ambient seawater should not exhibit an appreciable shift from the exit composition until dilutions of greater than 95% are reached. While the two diluted samples have $\varepsilon_{Nd}(0)$ within 2σ of each other, the hydrothermal end-member (1155-14) is significantly less

radiogenic than these samples at greater dilution, suggesting that one or more of the samples have been contaminated at some point during or subsequent to sampling. In an effort to investigate this problem more thoroughly, another hydrothermal end-member sample (1155-18) was analyzed which was collected in a different sampling device from the one used to collect 1155-14. This sample was found to have C_{Nd} = 659pg/g and $\varepsilon_{Nd}(0)$ = -10.8 which are so radically different from concentrations and isotopic compositions in other samples from this vent that they must clearly be a result of contamination. Furthermore, the contaminant appears to have continental-like Nd as indicated by the shift towards a low $\varepsilon_{Nd}(0)$ value. The the isotopic composition of Nd in 1155-14 would be consistent with the introduction of a small amount of a similar contaminant. Replicate analyses of separate aliquots of three samples were made during this study (1155-14, 1155-18, and 1158-6) and gave reproducible results within analytical uncertainties, indicating the source of the suspected contamination was not from this laboratory. The only samples exhibiting evidence of contamination are the hydrothermal end-members suggesting the contamination may result during the sampling of the high temperature (~350°C) fluids. Except for a very small difference between $\varepsilon_{Sr}(0)$ in 1155-14 and 1155-18, none of the samples analyzed exhibited irregularities for Sr or Mg. It is important to note that the small difference observed for Sr between these two samples cannot be explained by addition of continental-like Sr to 1155-18 as in the case of Nd. Lead isotope data for these samples also show no irregularity [Chen et al., 1983] indicating that the contamination problem is restricted to the REE.

While some of the Nd isotopic variation in the 21°N hydrothermal vents can be explained in terms of contamination, it does not appear that it can

explain all of the variations. If contamination was responsible for the observed Nd concentration and isotopic variation, a correlation between concentration and isotopic composition might be expected. The concentration of Nd is plotted as a function of the isotopic composition in Figure 7.5. Inspection of this figure reveals no apparent correlation between the two quantities. Low concentration samples show both high and low isotopic compositions as do high concentration samples. Furthermore, the generally good fit of the NGS Nd concentration data (excluding 1155-18) to a straight mixing line with seawater cannot be reasonably explained by contamination. If it is assumed that the excess Nd in 1155-18 over that in 1155-14 is due to contamination and that $\varepsilon_{Nd}(0)$ in the hydrothermal end-member is ~ +4, then it can be shown that the contaminant must have $\varepsilon_{Nd}(0) \approx -25$. It would only require about 3% of this contaminant in the total of Nd in 1155-14 to lower its isotopic composition by one ε-unit to +3. Subtraction of three percent of the Nd from 1155-14 has a negligible impact on the fit of the concentration data to a straight line. On the basis of this analysis, it is concluded that most of the observed variations reflect geochemical processes related to the hydrothermal circulation system.

The Sm and Nd concentrations determined for hydrothermal end-member solutions from 21°N are a factor of 3 to 50 lower than values reported by Michard et al. [1983] for samples from vents at two locations near 13°N. Two vents at their northern site had similar Nd concentration values of ~1100pg/g. Samples from their southern site were diluted with about 50% seawater but still had concentrations which varied from about 570 to 1000pg/g. They did not report any Nd isotopic data for these samples so it cannot be determine whether their high concentrations are related to chemical differences in the hydrothermal system or if they may in part be a

Figure 7.5. $\varepsilon_{Nd}(0)$ as a function of Nd concentration in hydrothermal solutions from 21°N and Guaymas Basin. If the isotopic variations were the result of contamination with a continental component of Nd, a correlation between C_{Nd} and $\varepsilon_{Nd}(0)$ might be expected. No such correlation is observed for these samples, indicating that at least to some extent the isotopic variations are related to geochemical processes in the hydrothermal systems which affect the REE distributions.

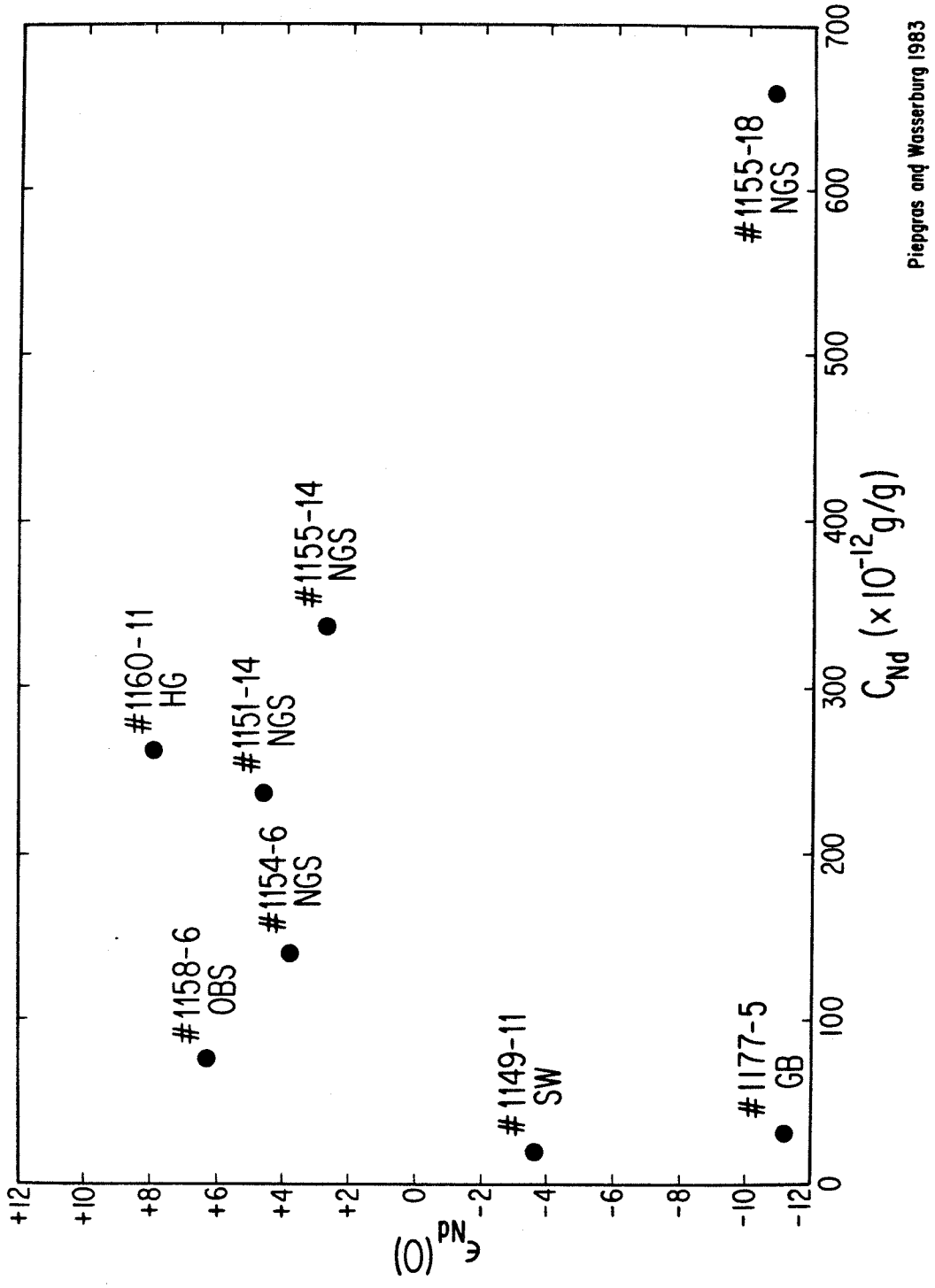
#1160-11
HG
#1151-14
NGS
#1155-14
NGS
#1154-6
NGS
#1158-6
OBS
#1149-11
SW
#1177-5
GB
#1155-18
NGS
Piepgras and Wasserburg 1983
$\varepsilon_{Nd}(0)$
C_{Nd} ($\times 10^{-12}$ g/g)
+12
+10
+8
+6
+4
+2
0
-2
-4
-6
-8
-10
-12
0
100
200
300
400
500
600
700

Figure 7.5.

result of contamination as suspected for some of the 21°N samples analyzed in this study. The reasons for the extreme variability in exit concentrations from on vent to another are not known may be related to the subsurface precipitation of alteration assemblages.

Although the concentrations measured by Michard et al. are much higher for Sm and Nd than reported here, both systems (21°N and 13°N) show a pronounced light rare earth enrichment indicating higher mobility for the light rare earths during hydrothermal alteration. Overall however, Sm and Nd and other REE in the oceanic crust do not appear to be very mobile. If essentially all of the REE in the hydrothermal solutions were leached from the oceanic crust at a water-rock ratio of about 2 as indicated from the Sr data, then even the highest concentration of Nd in any of the 21°N solutions analyzed in this study (336pg/g, excluding 1155-18) is still about 10^4 lower in two grams of water than observed in one gram of the basalt glass indicating that the maximum amount of Nd leached from the oceanic crust is negligible compared to the total available reservoir. The lack of significant mobility of the REE during the hydrothermal event is in agreement with laboratory studies on REE mobility in basalt glasses during high temperature interaction with seawater [Menzies and Seyfried, 1979b]. The results of ten different experiments by these workers at various temperatures (150-350°C) and water/rock ratios (10-125) and at a pressure of 500 bars showed no evidence of REE mobility in spite of the formation of alteration assemblages.

Guaymas Basin. One hydrothermal end-member sample from Guaymas basin has been analyzed for Nd isotopic composition, and like Sr it is distinctly different from its 21°N counterparts. The Nd concentration of 30pg/g in this sample lies at the low end of the range observed in samples from 21°N. Its Nd isotopic composition corresponds to $\varepsilon_{Nd}(0) = -11.4$ which is

considerably less radiogenic than samples from 21°N (with the exception of 1155-18 for which substantial contamination is suspected). This composition is consistent with the hydrothermal fluid exchanging Nd with an old continental component in the sedimentary column through which the solutions rise and shows no indication of exchange with the oceanic crust through which the fluids circulated. Descriptions of nearby Deep Sea Drilling Project cores (Holes 477, 478, and 481 [Curray et al., 1982]) indicate that the Yaqui delta is the major source of sediment in Guaymas Basin. The Yaqui River primarily drains a felsic Cenozoic volcanic terrane, although there is some Precambrian basement and Paleozoic sediment within the drainage basin [L. T. Silver, personal communication]. There are no Nd isotopic data available for materials from this basin or for sediments within Guaymas Basin to compare with the results of the hydrothermal fluid analysis. Contamination may be a problem as in sample 1155-18 which has a similar composition, but no other Nd isotopic data for Guaymas Basin are available for comparison to determine if the sample may be contaminated, but the Sr data above and Pb isotopic data of Chen et al. [1983] both demonstrate that the fluid composition has been modified by interaction with sediments having relatively radiogenic Pb and Sr which is consistent with the presence of an older continental component in the sediments.

At the present time there is no way of determining whether or not Nd, Pb, and Sr are leached from the same fractions of the sediment. Sr appears to have been leached primarily from the carbonate fraction as discussed above. Presumably the carbonate fraction could also supply the Nd. If it is assumed that the Sr concentration of the solution at the basalt-sediment interface is the same as in springs at 21°N and that the carbonate fraction of the sediments has ~1000ppm Sr then dissolution of about 1% of the

carbonate fraction could produce a Sr balance in reasonable agreement with the observations in the fluid. Assuming a Nd concentration of 1ppb or greater in the carbonate fraction [Shaw, 1983], this source could supply all of the Nd as well. Since the Nd in carbonate is probably derived from seawater as indicated by the work of Shaw [1983], an implication of this result is that Nd in seawater in the Gulf of California may be characterized by old continental sources of REE distinctly different from the adjacent Pacific. This could be easily verified by the direct analysis of Nd in Gulf of California seawater.

7.4.3 General discussion of Nd and Sr data

The hydrothermal fluxes of Nd and Sr to the oceans can be estimated from the concentration data reported here. It has been estimated, based on heat transport considerations, that the entire volume of the oceans is cycled through the oceanic crust every ten million years [Edmond et al., 1982]. This would correspond to an annual hydrothermal fluid discharge of $\sim 1.4 \times 10^{17}$g (Michard et al. [1983] have estimated the hydrothermal fluid discharge to be $\sim 10^{16}$g/y). Assuming an average Nd concentration of $\sim 3 \times 10^{-10}$g/g and Sr concentration of 7.6ppm in the hydrothermal fluid this would correspond to hydrothermal fluxes of $\sim 4 \times 10^{7}$gNd/y and $\sim 1 \times 10^{12}$gSr/y respectively. By comparison, the estimated fluxes from rivers for these elements based on an annual discharge of 4.6×10^{19}g/y having an Nd concentration of $\sim 4 \times 10^{-11}$g/g [Martin and Maybeck, 1979] and an Sr concentration of 0.15ppm [Stordal and Wasserburg, 1983] is about 1.8×10^{9}gNd/y and 6.9×10^{12}gSr/y respectively. If it is assumed that all of the Nd and Sr in

the river and hydrothermal discharges enters the ocean in solution, then it can be seen from these estimates that the hydrothermal flux of Nd to the oceans is small relative to the river flux (about 1/50th), whereas the hydrothermal flux of Sr is about 15% of the river flux. However, most of the hydrothermal flux probably enters the Pacific Ocean where mid-ocean ridge spreading rates are highest, whereas most of the fresh water drainage is into the Atlantic. Consequently, the hydrothermal flux of Nd in the Pacific may be as high as 20% of the river flux and the Sr flux could approach or possibly exceed the river Sr flux. This could account in part for the more radiogenic Nd isotopic values observed in the Pacific relative to other ocean basins, but additional inputs of radiogenic Nd would be required for the Pacific if the hydrothermal flux estimates here are correct. If the estimates for hydrothermal discharge of Michard et al. [1983] were used then the Nd and Sr flux estimates would be about one order of magnitude lower, further decreasing the significance of hydrothermal inputs of these elements relative to that from continental drainages.

There is no apparent Nd isotopic anomaly in Pacific waters collected from the crest of the Galapagos hydrothermal area [Piepgras et al., 1979], but Klinkhammer et al. [1983] found evidence that the REE are scavenged more intensely in bottom waters in the vicinity of hydrothermal vents suggesting that hydrothermal REE are extensively removed from solution after injection of the hydrothermal fluids into seawater. Some limits on the dispersal of the hydrothermal Nd can be estimated from observational data. Velocities of several meters per second (no numerical estimates were given) from vents up to 30cm in diameter were reported by the Rise Project Group [1979]. Using a value of 5m/s for the discharge, the annual flux of Nd from a single vent is of the order of ~140g/y. Metalliferous sediments on the East Pacific Rise

have ~15-20ppm Nd [Bender et al., 1971; Piepgras et al., 1979]. Assuming a ridge crest sedimentation rate of ~1.5cm/1000y and a bulk dry sediment density of ~0.7g/cc [Bender et al., 1971], then all of the hydrothermal Nd could be deposited in an area of $6.7 \times 10^5 m^2$ corresponding to a radius of about 460 meters from the vent. Nd isotopic analyses for these sediments show the REE to be derived primarily from seawater [O'Nions et al., 1978; Piepgras et al., 1979]. If only 10% of the Nd in metalliferous sediments is of hydrothermal origin, then the dispersal radius increases to about 1.5km.

7.5 Conclusions

The isotopic composition and concentration of Nd and Sr have been determined in a suite of samples at various dilutions for hydrothermal solutions emanating from the crest of the East Pacific Rise at 21°N and from for one sample from Guaymas Basin. At the 21°N site, the hydrothermal fluids show substantial Nd concentration and isotopic variation between the various vents which were sampled indicating that the fluids circulating in the oceanic crust are very heterogeneous with respect to their REE content and Nd isotopic composition. Nd concentrations range from 20 to 336 pg/g and $\varepsilon_{Nd}(0)$ from -3.6 to +7.9 in the hydrothermal end-member solutions (one sample has an anomalously high concentration of 659 pg/g and low $\varepsilon_{Nd}(0)$ = -10.8 relative to other samples from the same vent and may be contaminated). In spite of Nd enrichments of up to ~100 times seawater, none of the samples at 21°N have isotopic compositions identical to mid-ocean ridge basalt. This observation seems to require that the fluids have exchanged with another reservoir besides the oceanic crust which has enriched them to

varying degrees with continental-like REE. It is concluded that the most likely source of this component is deep-sea sediments on the flanks of the mid-ocean ridge. Sm and Nd concentration data indicate the the solutions are light rare earth enriched in agreement with previous observations [Michard et al., 1983] indicating that the light REE are more mobile than heavy REE during the hydrothermal alteration of oceanic crust. Overall however, the mobility of the REE is concluded to be very low.

In contrast to the variations in Nd at 21°N, Sr is found to have relatively uniform $\varepsilon_{Sr}(0) \approx -18$ in the hydrothermal end-members in agreement with previously published results for fluids from this site [Albarede et al., 1981], and the concentrations vary only slightly from 5.82 to 8.70 ppm which is close to seawater Sr concentrations. Like Nd, the $^{87}Sr/^{86}Sr$ values in these fluids are not the same as MORB, but if it is assumed that the Sr in the fluid is in equilibrium with the oceanic crust, then the water/rock mass ratio must be less than two as reported previously by Albarede et al., [1981]. Because of the extensive modification to the isotopic composition of the fluids (presumed to have originally been characterized by seawater compositions) by interaction with the oceanic crust, the similarity in the Sr concentrations of the hydrothermal fluids at 21°N to seawater indicates that the Sr concentration in the hydrothermal reservoir is being buffered by subsurface precipitation into alteration assemblages.

At the Guaymas Basin site the solutions rise through several hundred meters of sediment before reaching the seawater interface. Both the Nd and Sr properties of the fluid show evidence of being dominated by the interaction between the hydrothermal fluid and the sediment. The isotopic composition of Nd is very low ($\varepsilon_{Nd}(0) = -11.4$) indicating a substantial contribution from old continentally derived REE in the sediment. The Sr

isotopic composition ($\varepsilon_{Sr}(0) = +11.0$) and concentration (19.3ppm) are much higher than at 21°N and suggest that the hot fluids have exchanged Sr with the carbonate fraction of the sediments during the ascent of the fluids through the sediment column.

There is some evidence that the REE in these fluids have been affected by contamination which may account for some of the variations observed. The major indication of this comes from the failure of NGS samples at different dilutions to fall on a mixing curve with ambient seawater. With the exception of one sample (1155-18), however, the deviations from the mixing curve for NGS samples is small and would not account for the lack of equilibration with basalt Nd isotopic values. Thus the major conclusions regarding the Nd isotopic variations between vents are not changed. Furthermore, Sr in these solutions does not appear to have been affected by the contamination as Nd has. The Sr data fit very well to the mixing curve, including the sample which shows the highest apparent contamination for Nd (1155-18). This is probably due to differences in the concentration levels of these two elements in the hydrothermal solutions.

The hydrothermal fluxes of Nd and Sr have been estimated. For Nd, it is concluded that the global hydrothermal flux of this element must be very small compared to the estimated flux from rivers (about two orders of magnitude lower). However, in the Pacific it is estimated that the hydrothermal flux could be about 20% of the river flux to this basin. This could in part account for the more radiogenic Nd isotopic compositions observed in Pacific waters, but it is concluded that another source of radiogenic Nd may also be necessary. For Sr, the global hydrothermal flux is estimated to be about 10% of the river flux, and in the Pacific the hydrothermal flux could exceed the river flux.

Table 7.1. Sm, Nd and Sr results for hydrothermal solutions from 21°N. East Pacific Rise and Guaymas Basin.

Sample #	Sample wt(g)	Mg[a] (μMol/g)	% hydrothermal[b]	C_{Sm}[c] (pg/g)	C_{Nd}[c] (pg/g)	$\frac{^{147}Sm}{^{144}Nd}$	$f_{Sm/Nd}$	$\frac{^{143}Nd}{^{144}Nd}$[d]	$\varepsilon_{Nd}(0)$	C_{Sr}[c] (ppm)	$\frac{^{87}Sr}{^{86}Sr}$[e]	$\varepsilon_{Sr}(0)$
#1158-6 OBS	98.8	2.31	96	15.1	76.2	0.119	-0.393	0.512167 ±21	+6.3 ±0.4	7.22	0.703556 ±33	-13.4 ±0.4
#1158-6 OBS	99.9	2.31	96	-	77.9	-	-	0.512148 ±16	+5.9 ±0.3	-	-	-
#1156-11 OBS	-	25.2	52	-	-	-	-	-	-	7.37	0.706115 ±33	+22.9 ±0.5
#1160-11 HG	70.5	2.00	96	60.8	261	0.141	-0.284	0.512250 ±26	+7.9 ±0.5	5.82	0.703460 ±34	-14.8 ±0.5
#1155-14a NGS	65.4	2.27	96	57.3	336	0.103	-0.477	0.511986 ±18	+2.7 ±0.4	8.70	0.703397 ±17	-15.7 ±0.2
#1155-14b NGS	65.4	2.27	96	-	336	-	-	0.512001 ±20	+3.0 ±0.4	-	-	-
#1155-18a NGS	50.3	2.13	96	-	659	-	-	0.511294 ±23	-10.8 ±0.5	8.69	0.703252 ±24	-17.7 ±0.3
#1155-18b NGS	30.6	2.13	96	-	659	-	-	0.511296 ±23	-10.8 ±0.5	-	-	-
#1151-14 NGS	65.3	17.2	67	-	236	-	-	0.512083 ±19	+4.6 ±0.4	-	0.704912 ±26	+5.8 ±0.4
#1154-6 NGS	100.5	28.8	45	-	140		-	0.512042 ±23	+3.8 ±0.5	7.90	0.706088 ±25	+22.5 ±0.4

Table 7.1 (continued)

Sample #	Sample wt(g)	Mg[a] (μMol/g)	% hydrothermal[b]	C_{Sm}[c] (pg/g)	C_{Nd}[c] (pg/g)	$\frac{^{147}Sm}{^{144}Nd}$	$f_{Sm/Nd}$	$\frac{^{143}Nd}{^{144}Nd}$[d]	$\varepsilon_{Nd}(0)$	C_{Sr}[c] (ppm)	$\frac{^{87}Sr}{^{86}Sr}$[e]	$\varepsilon_{Sr}(0)$
#1149-11 SW	152.8	2.01	96	-	20.0	-	-	0.511663 ±23	-3.6 ±0.4	7.41	0.703504 ±43	-14.1 ±0.6
#1159-9 SW	131.4	52.8	0	0.813	5.46	0.090	-0.555	-	-	7.64	0.709109 ±32	+65.4 ±0.4
21°N EPR Basalt Glass	100.36mg	-	-	2.70[f] (ppm)	7.09[f] (ppm)	0.230	0.170	0.512342 ±25	+9.7 ±0.5	99	0.702260 ±32	-31.8 ±0.5
#1177-5 Guaymas Basin	168.3	2.82	95	-	30.1	-	-	0.511265 ±26	-11.4 ±0.5	19.3	0.705277 ±61	+11.0 ±0.9

[a] Mg determined at MIT by K. von Damm and B. Grant.
[b] Determined from Mg concentration.
[c] 2σ errors for Sm, Nd and Sr concentrations are ~ 0.1%.
[d] Spiked with ^{150}Nd and normalized to $^{144}Nd/^{142}Nd = 0.878499$. Reported errors are two standard deviations from the mean.
[e] Spiked with ^{84}Sr and normalized to $^{86}Sr/^{88}Sr = 0.1194$.
[f] Concentrations for basalt glass are in units of ppm.

REFERENCES

Albarede, F., A. Michard, J. F. Minster, and G. Michard, $^{87}Sr/^{86}Sr$ ratios in hydrothermal waters and deposits from the East Pacific Rise at 21°N, Earth Planet. Sci. Lett. 55, 229-236, 1981.

Amin, B. S., S. Krishnaswami, and B. L. K. Somayajulu, $^{234}Th/^{238}U$ activity ratios in Pacific Ocean bottom waters, Earth Planet. Sci. Lett. 21, 342-344, 1974.

Bainbridge, A. E. Ed., GEOSECS Atlantic Expedition, Vol. 2, Sections and Profiles, (National Science Foundation, Washington, D.C.) 1980.

Bender, M. L., Mechanisms of trace metal removal from the oceans, in: Ferromanganese Deposits on the Ocean Floor, D. R. Horn, ed., IDOE Publ. NSF, 1972.

Bender, M., W. Broeker, V. Gornitz, U. Middel, R. Kay, S.S. Sun and P. Biscaye, Geochemistry of three cores from the East Pacific Rise, Earth Planet. Sci. Lett. 12, 425-433, 1971.

Bischoff, J. L., Geothermal system at 21°N, East Pacific Rise: physical limits on geothermal fluid and role of adiabatic expansion, Science 207, 1465-1469, 1980.

Bonatti, E. and O. Joensuu, Deep sea iron deposits from the South Pacific, Science 154, 643-645, 1966.

Bonatti, E., T. Kraemer and H. Rydell, Classification and genesis of submarine iron-manganese deposits, in: Ferromanganese Deposits on the Ocean Floor, D. R. Horn, ed., IDOE Pub. NSF, 1972.

Boyle, E. A., F. Sclater, and J. M. Edmond, The distribution of dissolved copper in the Pacific, Earth Planet. Sci. Lett. 37, 38-54, 1977.

Bostrom, K. and M. N. A. Peterson, Precipitates from hydrothermal exhalations on the East Pacific Rise, Econ. Geol. 61, 1258-1265, 1966.

Brass, G. W. and K. K. Turekian, Strontium distributions in sea water profiles from the GEOSECS I (Pacific) and GEOSECS II (Atlantic) test stations, Earth Planet. Sci. Lett. 16, 117-121, 1972.

Broecker, W. S., A revised estimate for the radiocarbon age of North Atlantic Deep Water, J. Geophys. Res. 84, 3218-3226, 1979.

Bruland, K. W., Oceanographic distributions of cadmium, zinc, nickel, and copper in the North Pacific, Earth Planet. Sci. Lett. 47, 176-198, 1980.

Bruland, K. W., Trace elements in seawater, Chemical Oceanography vol. 8, J.P. Riley and R. Chester, eds., (Academic Press, London), 157-220, 1983.

Bryden, H. L., and R.D. Pillsbury, Variability of deep flow in the Drake Passage from year-long current measurements, J. Phys. Oceanogr. 7, 803-810, 1977.

Budyko, M. I., Climate and Life, Academic Press, New York, N.Y., 1974.

Burns, R. G. and V. M. Burns, Manganese oxides, in Marine Minerals, Minerol. Soc. Am. Short Course Notes, vol. 6, 1979.

Chan, L. H., J. M. Edmond, R. F. Stallard, W. S. Broecker, Y. C. Chung, R. E. Weiss, T. L. Ku, Radium and barium at GEOSECS stations in the Atlantic and Pacific, Earth Planet. Sci. Lett. 32, 258-267, 1976.

Chen, J. H., G. J. Wasserburg, K. L. von Damm, and J. M. Edmond, Pb, U and Th in hot springs on the East Pacific Rise at 21°N and Guaymas Basin, Gulf of California, EOS 64, 724, 1983.

Cochran, J. K., The flux of ^{226}Ra from deep-sea sediments, Earth Planet. Sci. Lett. 49, 381-392, 1980.

Corliss, J. B., The origin of metal-bearing submarine hydrothermal solutions, J. Geophys. Res. 76, 8128-8138, 1971.

Corliss, J. B., J. Dymond, L. I. Gordon, M. M. Edmond, R. P. von Herzon, R. D. Ballard, K. Green, D. Williams, A. Bainbridge, K. Crane and T. H. van Andel, Submarine thermal springs on the Galapagos Rift, Science 203, 1073-1083, 1979.

Corliss, J. B., M. Lyle, J. Dymond and K. Crane, The chemistry of hydrothermal mounds near the Galapagos Rift, Earth Planet. Sci. Lett. 40, 12-24, 1978.

Craig, H., Abyssal carbon and radiocarbon in the Pacific, J. Geophys. Res. 74, 5491-5506, 1969.

Craig, H., A scavenging model for trace elements in the deep sea, Earth Planet. Sci. Lett. 23, 149-159, 1974.

Cronan, D. S., Deep-sea nodules: distribution and geochemistry, in: Marine Manganese Deposits, G. P. Glasby, ed., Elsevier, Amsterdam, 1977.

Curray, J. R. et al., 4. Guaymas Basin: Sites 477, 478 and 481, in Init. Repts. DSDP 64, 211-287, 1982.

Dasch, E. J. and P. E. Biscaye, Isotopic composition of strontium in Cretaceous-to-Recent, pelagic foraminifera, Earth Planet. Sci. Lett. 11, 201-204, 1971.

DeBaar, H. J. W., M. P. Bacon, and P. G. Brewer, Rare-earth distributions with a positive Ce anomaly in the western North Atlantic Ocean, Nature 301, 324-327, 1983.

Dietrich, G., K. Kalle, W. Krauss and G. Sielder, General Oceanography: An Introduction, 2nd edition (J. Wiley and Sons, New York, 1980).

DePaolo, D. J. and G. J. Wasserburg, Nd isotopic variations and petrogenetic models, Geophys. Res. Lett. 3, 249-252, 1976a.

DePaolo, D. J. and G. J. Wasserburg, Inferences about magma sources and mantle structure from variations of $^{143}Nd/^{144}Nd$, Geophys. Res. Lett. 3, 743-746, 1976b.

DePaolo, D. J. and G. J. Wasserburg, The soures of island arcs as indicated by Nd and Sr isotopic studies, Geohys. Res. Lett. 4, 465-468, 1977.

DePaolo, D. J. and G. J. Wasserburg, Neodymium isotopes in flood basalts from the Siberian Platform and inferences about their mantle sources, Proc. Natl. Acad. Sci. USA 76, 3056-3060, 1979.

Edmond, J. M., C. Measures, R. E. McDuff, L. H. Chan, R. Collier, B. Grant, L. I. Gordon, and J. B. Corliss, Ridge crest hydrothermal activity and the balances of the major and minor elements in the ocean: the Galapagos data, Earth Planet. Sci. Lett. 46, 1-18, 1979a

Edmond, J. M., C. Measures, B. Mangum, B. Grant, F. R. Sclater, R. Collier A. Hudson, L. I. Gordon, and J. B. Corliss, On the formation of metal-rich deposits at ridge crests, Earth Planet. Sci. Lett. 46, 19-30, 1979b.

Edmond, J. M., K. L. Von Damm, R. E. McDuff, and C. I. Measures, Chemistry of hot springs on the East Pacific Rise and their effluent dispersal, Nature 297, 187-191, 1982.

Ehrlich, A. M., Rare earth abundances in manganese nodules, Ph.D. Thesis, Massachusetts Institute of Technology, Cambridge, Mass. 1968.

Elderfield, H. and M. J. Greaves, The rare earth elements in seawater, Nature 296, 214-219, 1982.

Elderfield, H., C. J. Hawkesworth, M. J. Greaves, and S. E. Calvert, Rare earth element geochemistry of oceanic ferromanganese nodules and associated sediments, Geochim. Cosmochim. Acta 45, 513-528, 1981.

Fuglister, F. C., Atlantic Ocean Atlas, Woods Hole Oceanographic Institution, 1960.

Georgi, D. T., On the relationship between the large-scale property variations and fine structure in the Circumpolar Deep Water, " J. Geophys. Res., 86, 6556-6566, 1981.

Gill, A. E., Circulation and bottom water production in the Weddell Sea, Deep Sea Res. 20, 111-140, 1973.

Glasby, G. P., The geochemistry of manganese nodules from the Northwest Indian Ocean, in: Ferromanganese Deposits on the Ocean Floor, D. R. Horn, ed., IDOE Publ. NSF, 1972.

Glasby, G. P., Mechanisms of enrichment of the rarer elements in marine manganese nodules, Mar. Chem. 1, 105-125, 1972-73.

Goldberg, E. D., M. Koide, R. A. Schmitt and R. H. Smith, Rare earth distributions in the marine environment, J. Geophys. Res. 68, 4209-4217, 1963.

Goldstein, S. L. and R. K. O'Nions, Nd and Sr isotopic relationships in pelagic clays and ferromaganese deposits, Nature 292, 324-327, 1981.

Goldstein, S. L and R. K. O'Nions, Nd isotopic study of river particulates, atmospheric dusts, and pelagic sediments, (abstract) Trans., Amer. Geophys. Union 63, 352-353, 1982.

Gordon, A. L., Oceanography of Antarctic waters, Antarct. Oceanol. I 15, 169-203, 1971.

Hastenrath, S., Heat budget of tropical ocean and atmosphere, J. Phys. Oceanogr. 10, 159-170, 1980.

Haymon, R. M. and M. Kastner, Hot spring deposits on the East Pacific Rise at 21°N: preliminary description of mineralogy and genesis, Earth Planet. Sci. Lett. 53, 363-381, 1981.

Høgdahl, S. Melson and V. T. Bowen, Neutron activation analysis of Lanthanide elements in seawater, Adv. Chem. Ser. 73, 308-325, 1968.

Humphris, S. E. and G. Thompson, Hydrothermal alteration of oceanic basalts by seawater, Geochim. Cosmochim. Acta 42, 107-125, 1978a.

Humphris, S. E. and G. Thompson, Trace element mobility during hydrothermal alteration of oceanic basalts, Geochim. Cosmochim. Acta 42, 127-136, 1978b.

Jacobsen, S. B. and Wasserburg, G. J., Sm-Nd isotopic evolution of chondrites, Earth Planet. Sci. Lett. 50, 139-155, 1980.

Kennett, J. P., Cenozoic evolution of Antarctic glaciation, the Circum-Antarctic Ocean, and their impact on global oceanography, J. Geophys. Res. 82, 3843-3860, 1977.

Key, R. M., N. L. Guinasso, Jr., and S. R. Schink, Emanation of Radon-222 from marine sediments, Mar. Chem. 7, 221-250, 1979.

Klinkhammer, G., H. Elderfield, and A. Hudson, Rare earth elements in seawater near hydrothermal vents, Nature 305, 185-188, 1983.

Knauss, J. A., Introduction to Physical Oceanography, Prentice-Hall, Englewood Cliffs, New Jersey, 1978.

Kozoun, V. I. et al., World Water Balance and Water Resources of the Earth (U.S.S.R. National Committee for the International Hydrological Decade, Leningrad) 1974.

Ku, T. L., A. Omura and P. S. Chem, ^{10}Be and U-series isotopes in manganese nodules from the central NorthPacific, in: Marine Geology and Oceanography of the Pacific Manganese Nodule Province, J. L. Bischoff and D. Z. Piper, eds., Plenum Press, New York, N.Y., pp. 791-814, 1979.

Lee, A. and D. Ellett, On the contribution of overflow from the Norwegian Sea to the hydrographic structure of the North Atlantic Ocean, Deep-Sea Res. 12, 129-142, 1965.

Lee, D. S., Palladium and nickel in north-east Pacific waters, Nature 305, 47-48, 1983.

Lundqvist, R., Hydrophilic complexes of the actinides. I. Carbonates of trivalent americium and europium, Acta Chem. Scand. A36, 741-750, 1982.

Lyle, M., Estimation of hydrothermal manganese input to the oceans, Geology 4, 733-736, 1976.

Martin, J. H., G. A. Knauer, and R. M. Gordon, Silver distributions and fluxes in northeast Pacific waters, Nature 305, 306-309, 1983.

Martin, J. -M. and M. Maybeck, Elemental mass-balance of material carried by major world rivers, Mar. Chem. 7, 173-206, 1979.

Masuda, A. and Y. Ikeuchi, Lanthanide tetrade effect observed in marine environment, Geochem. J. 13, 19-22, 1979.

McCartney, M. S., Observation of the convective formation of the Antarctic Intermediate Water of the South Pacific Ocean, (in preparation).

McCulloch, M. T. and G. J. Wasserburg, Sm-Nd and Rb-Sr chronology of continental crust formation, Science 200, 1003-1011, 1978.

Menzies, M. and W. E. Seyfried, Jr., Basalt-seawater interaction: trace element and strontium isotopic variations in experimentally altered glassy basalt, Earth Planet. Sci. Lett. 44, 463-472, 1979a.

Menzies, M. and W. Seyfried, Jr., Experimental evidence of rare earth element immobility in greenstones, Nature 282, 398-399, 1979b.

Michard, A., F. Albarede, G. Michard, J. F. Minster, and J. L. Charlou, Rare-earth elements and uranium in high-temperature solutions from East Pacific Rise hydrothermal vent field (13°N), Nature 303, 795-797, 1983.

Michard, G., A. Michard, F. Albarede, J. J. Minster and J. L. Charlou, The chemistry and $^{87}Sr/^{86}Sr$ ratios of the hydrothermal vent waters at 13°N (East Pacific Rise), EOS 63, 1014, 1982.

Montgomery, R. B., Water characteristics of Atlantic Ocean and of world ocean, Deep-Sea Res. 5, 134-148, 1958.

Moore, R. M., Oceanographic distributions of zinc, cadmium, copper and aluminum in waters of the central Arctic, Geochim. Cosmochim. Acta 45, 2475-2482, 1981.

Moore, W. S., Measurement of ^{228}Ra and ^{228}Th in seawater, J. Geophys. Res. 74, 694-704, 1969.

Moore, W. S. and W. M. Sackett, Uranium and thorium series inequilibrium in seawater, J. Geophys. Res. 69, 5401-5405, 1964.

Moore, W. S. and P. R. Vogt, Hydrothermal manganese crusts from two sites near the Galapagos spreading axis, Earth Planet. Sci. Lett. 29, 349-356 1976.

Munk, W. H., Abyssal recipes, Deep-Sea Res. 13, 707-730, 1966.

Nier, A. O., A redetermination of the relative abundances of the isotopes of carbon, nitrogen, oxygen, argon, and potassium, Phys. Rev. 77, 789-793, 1950.

Nowlin, W. D.,Jr., T. Whitworth III and R. D. Pillsbury, Structure and transport of the Antarctic Circumpolar Current at Drake Passage from short-term measurements, J. Phys. Oceanogr. 7, 788-802, 1977.

Nozaki, Y., Y. Horibe, H. Tsubota, The water column distributions of thorium isotopes in the western North Pacific, Earth Planet. Sci. Lett. 54, 203-216, 1981.

O'Nions, R. K., P. J. Hamilton and N. M. Evensen, Variations in $^{143}Nd/^{144}Nd$ and $^{87}Sr/^{86}Sr$ ratios in oceanic basalts, Earth Planet. Sci. Lett. 34, 13-22, 1977.

O'Nions, R. K., S. R. Carter, R. S. Cohen, N. M. Evensen and P. J. Hamilton, Pb, Nd and Sr isotopes in oceanic ferromanganese deposits and ocean floor basalts, Nature 273, 435-438, 1978.

Peterman, Z. E., C. E. Hedge and H. A. Tourtelot, Isotopic composition of strontium in seawater throughout Phanerozoic time, Geochim. Cosmochim. Acta 34, 105-120, 1970.

Pickard, G. L. Descriptive Physical Oceanography 3rd edition, (Pergamon Press, Oxford), 1979.

Piepgras, D. J. and G. J. Wasserburg, Neodymium isotopic variations in seawater, Earth Planet. Sci. Lett. 50, 128-138, 1980.

Piepgras, D. J. and G. J. Wasserburg, Isotopic composition of neodymium in waters from the Drake Passage, Science 217, 207-214, 1982.

Piepgras, D. J. and G. J. Wasserburg, Influence of the Mediterranean outflow on the isotopic composition of Neodymium in waters of the North Atlantic, J. Geophys. Res. 88, 5997-6006, 1983.

Piepgras, D. J., G. J. Wasserburg and E. J. Dasch, The isotopic composition of Nd in different ocean masses, Earth Planet. Sci. Lett. 45, 223-236, 1979.

Piper, D. Z., Rare earth elements in ferromanganese nodules and other marine phases, Geochim. Cosmochim. Acta 38, 1007-1022, 1974.

Reid, J. L. and R. L. Lynn, On the influence of the Norwegian-Greenland and Weddell seas upon the bottom waters of the Indian and Pacific oceans, Deep-Sea Res., 18, 1063-1088, 1971.

Reid, J. L., On the mid-depth circulation of the world ocean, in: Evolution of Physical Oceanography, B. A. Warren and C. Wunsch, eds., MIT Press, Cambridge, Mass., p. 70, 1981.

Richard, P., N. Shimizu and C. J. Allegre, $^{143}Nd/^{146}Nd$, a natural tracer: an application to oceanic basalts, Earth Planet. Sci. Let. 31 269-278, 1976.

Rise Project Group, East Pacific Rise: hot springs and geophysical experiments, Science 207, 1421-1433, 1980.

Rona, E., L. O. Gilpatric, L. M. Jeffrey, Uranium determination in sea water, Trans. Am. Geophys. Union, 37, 697-701, 1956.

Rona, P. A., Hydrothermal mineralization at seafloor spreading centers, Earth Sci. Rev. 20, 1-104, 1984.

Sarmiento, J. L., H. W. Freely, W. S. Moore, A. E. Bainbridge, W. S. Broecker, The relationship between vertical eddy diffusion and bouyancy gradient in the deep sea, Earth Planet. Sci. Lett. 32, 357-370, 1976.

Scott, M. R., R. B.Scott, P. A. Rona, L. W. Butler and A. J. Norwalk, Rapidly accumulating manganese deposit from the median valley of the Mid-Atlantic Ridge, Geophys. Res. Lett. 1, 355-358, 1974.

Shaw, H. F., Sm-Nd and Rb-Sr isotopic systematics of tektites and other impactites, Appalachian mafic rocks, and marine carbonates and phosphates, Ph.D. Thesis, California Institute of Technology, Pasadena, California, 1983.

Somayajulu, B. L. K. and H. Craig, Particulate and soluble ^{210}Pb activities in the deep sea, Earth Planet. Sci. Lett. 32, 268-276, 1976.

Sorem, R. K. and R. H. Fewkes, Internal characteristics, in: Marine Manganese Deposits, G. P. Glasby, ed., Elsevier, Amsterdam, 1977.

Stoffyn, M. and F. T. MacKenzie, Fate of dissolved aluminum in the oceans, Mar. Chem. 11, 105-127, 1982.

Stommel, H., Asymmetry of interoceanic fresh-water and heat fluxes, Proc. Nat'l. Acad. Sci. U.S.A. 77, 2377-2381, 1980.

Stommel, H., The abyssal circulation, Deep Sea Res. 5, 80-82, 1958.

Stordal, M. C. and G. J. Wasserburg, Sm-Nd and Rb-Sr measurements on river water, suspended load and sediment from the Mississippi delta, EOS 64, 1064, 1983.

Styrt, M. M., A. J. Blackman, H. D. Holland, B. C. Clarke, V. Pisutha-Arnond, C. S. Eldridge, and H. Ohmoto, The mineralogy and the isotopic composition of sulfur in hydrothermal sulfide/sulfate deposits on the East Pacific Rise at 21°N latitude, Earth Planet. Sci. Lett. 53, 382-390, 1981.

Tchernia, P., Descriptive Regional Oceanography (Pergamon Press, Oxford), 1980.

Toth, J. R., Deposition of submarine hydrothermal manganese and iron, and evidence for input of volatile elements to the ocean, M. S. Thesis, Oregon State University, Corvallis, Oregon 1977.

Turekian, K. K. and L. H. Chan, The marine geochemistry of the uranium isotopes, ^{230}Th, and ^{231}Pa, in: Activation Analysis in Geochemistry and Cosmochemistry, A. O. Brunfelt and E. Steinnes eds., (Universitetsforlaget, Oslo 1971) p. 311.

Usui, A., Minerals, metal contents, and mechanism of formation of manganese nodules from the central Pacific basin, in Marine Geology and Oceanography of the Pacafic Manganese Nodule Province, J.L. Bischoff and D.Z. Piper, eds., (Plenum Press, New York) 651-579, 1979.

Turner, D. R., M. Whitfield, and A. G. Dickson, The equilibrium speciation of dissolved components in freshwater and seawater at 25°C and 1 atm pressure, Geochim. Cosmochim. Acta 45, 855-881, 1981.

Wasserburg, G. J., S. B. Jacobsen, D. J. DePaolo, M. T. McCulloch, and T. Wen, Precise determination of Sm/Nd ratios, Sm and Nd isotopic abundances in standard solutions, Geochim. Cosmochim. Acta 45, 2311-2323, 1981.

White, W. M. and A. W. Hoffmann, Sr and Nd isotope geochemistry of oceanic basalts and mantle evolution, Nature 296, 821-825, 1982.

Wildeman, T. R., and L. Haskin, Rare-earth elements in ocean sediments, J. Geophys. Res. 70, 2905-2910, 1965.

Worthington, L. V., On the North Atlantic Circulation (Johns Hopkins University Press, Baltimore) 1976.

Wüst, G., Die vertikalschnitte der Temperatur, des salzgehaltes und der Dichte, Wiss. Ergebn. Dt. Atlant. Exped. "Meteor" 1925-27, Teil A des Atlas zu 6, Beilage II-XLVI. Berlin, 1936.

Earth and Planetary Science Letters, 45 (1979) 223–236

[2]

THE ISOTOPIC COMPOSITION OF Nd IN DIFFERENT OCEAN MASSES

D.J. PIEPGRAS, [1] G.J. WASSERBURG [1] and E.J. DASCH [2]

[1] *The Lunatic Asylum of the Charles Arms Laboratory, Division of Geological and Planetary Sciences, California Institute of Technology, Pasadena, CA 91125 (U.S.A.)*
[2] *Department of Geology, Oregon State University, Corvallis, OR 97331 (U.S.A.)*

Received May 15, 1979
Revised version received July 26, 1979

Sm-Nd data for authigenic ferromanganese sediments from the oceans indicate that the Atlantic, Pacific, and Indian Oceans each have a distinct range in Nd isotopic composition which are characteristic of each ocean basin and reflect the dissolved load of Nd in the water mass. Within each basin, Nd isotopic compositions show some variability but are relatively well defined. Isotopic compositions of Nd measured in these samples are all far less than the $^{143}Nd/^{144}Nd$ ratios of source rocks with oceanic affinities. Direct measurements of the Nd isotopic composition of seawater presented here support the view that REE in ferromanganese sediments are derived by the direct precipitation of these elements out of seawater. Nd isotopic variations in ferromanganese sediments cannot be explained by contributions from continental detritus. It is therefore believed that the Nd isotopic variations found for ferromanganese sediments represent true variations in the isotopic composition of Nd dissolved in seawater in various ocean masses. These variations reflect primarily the age and $^{147}Sm/^{144}Nd$ of the continental masses being sampled, which is believed to be the major source of REE in seawater. These variations indicate that the residence time of Nd in seawater must be very short relative to the mixing rates between ocean masses. Nd isotopic studies, both in seawater and sediments should, therefore, be useful as a monitor of ocean currents and interocean mixing over the past several million years.

1. Introduction

The purpose of this study was to determine the isotopic composition of Nd in the marine environment, and from the isotopic composition, to identify the sources of Nd in the different oceans. The Nd isotopic composition may have the possibility of serving as a natural tracer of ocean currents for short time scales and as a monitor of mixing in and between the oceans. The isotopic abundance of ^{143}Nd changes through geologic time due to the decay of ^{147}Sm ($\tau_{1/2} = 1.06 \times 10^{11}$ yrs). Observed $^{143}Nd/^{144}Nd$ ratios, therefore, reflect the age and $^{147}Sm/^{144}Nd$ ratio of the materials which are sampled. The average evolution of $^{143}Nd/^{144}Nd$ for the earth has been found to follow a simple growth curve which corresponds to the $^{147}Sm/^{144}Nd$ ratio of chondritic meteorites [1]. However, terrestrial differentiation processes have segregated material into continental and oceanic crustal rocks with distinctive ages and Sm/Nd ratios. As a result, there is a clear difference in the $^{143}Nd/^{144}Nd$ ratios in the samples of different types of crustal rocks. Transport of the rare earth elements (REE) into the oceans will thus produce isotopic compositions of Nd which directly reflect the type of materials from which they were derived. The isotopic composition of Nd in the marine environment should therefore prove to be of interest in understanding the sources, transport, and deposition of REE in the oceans.

Relative to the turnover rate for the oceans, the residence time of Nd in seawater is believed to be short, possibly less than 300 years [2,3]. Evidence for a short residence time can be demonstrated by comparing Na/Nd ratios for crustal rocks with that of seawater. Average crustal rocks have Na/Nd $\cong 10^3$ (Na $\cong$

[1] Division of Geological and Planetary Sciences; California Institute of Technology, Contribution No. 3254(307).

2.4%, Nd ≅ 28 ppm [4]), while seawater has Na/Nd ≅ 3.5×10^9, six orders of magnitude higher than crustal rocks. The concentration of Nd in seawater is only 3×10^{-6} ppm ([2,5], this study) compared with a Na concentration of 1.1% [6]. This difference between seawater and crustal Na/Nd is clear evidence for a short residence time for Nd in seawater.

In this study, $^{143}Nd/^{144}Nd$ and $^{147}Sm/^{144}Nd$ were measured in metal-rich authigenic sediments from the major oceans. Samples include manganese nodules, hydrothermal crusts, and metalliferous sediments. It is generally believed that the metals and REE in these sediments precipitate directly out of seawater [2, 7–12], although some nodules exhibit REE patterns that are quite fractionated relative to the observed average REE pattern in seawater [9,13,14]. This observation has been used as evidence against direct precipitation from seawater. However, variations of REE patterns may result entirely from fractionation during precipitation and not directly reflect the patterns of the source. In either case, the isotopic abundance of Nd would be unaffected by the precipitation process and, therefore, variations in the $^{143}Nd/^{144}Nd$ ratio will be a direct result of the isotopic abundance of Nd dissolved in seawater with possible contributions from marine rocks, sediments, and detrital materials. As the isotopic composition of Sr is rather uniform in seawater, we have tested for detrital contributions by measuring $^{87}Sr/^{86}Sr$ ratios in some of the same samples analyzed for Nd.

In addition to measurements on authigenic sediments, we also present direct measurement of the Nd isotopic composition for three seawater samples from the Pacific Ocean. These measurements give the present-day $^{143}Nd/^{144}Nd$ values in a given water mass, whereas data on deep ocean manganese nodules give values which can represent an average over several millions of years. The direct Nd isotopic measurements on seawater also afford greater confidence in interpretation of the sediment data and aids in answering questions regarding the derivation of REE in ferromanganese sediments.

Previous studies have shown that the isotopic composition of Nd in oceanic basalts is distinctly different from that in average continental rocks [1,15–17]. The Nd isotopic composition of seawater must be a result of mixing of Nd from these two sources. A preliminary attempt to estimate the isotopic composition of Nd in seawater was made by DePaolo and Wasserburg [18] using fish debris. A more extensive study was presented by O'Nions et al. [19] who measured Nd in manganese nodules and metalliferous sediments. While substantial variations were found, O'Nions et al. inferred that seawater had a uniform $^{143}Nd/^{144}Nd$ ratio and that variations were dominantly due to inclusion of detrital components. The present study will show that there is a wide spread in $^{143}Nd/^{144}Nd$ in authigenic sediments in support of previous observations but will attempt to show that this variation is due to isotopic differences in Nd dissolved in seawater as a result of the ages and $^{147}Sm/^{144}Nd$ ratios of the continental mass supplying Nd to a given seawater mass.

2. Samples

Marine ferromanganese sediments were used in this study because they (1) occur in relative abundance over a wide geographic range, (2) form in a variety of depositional environments, (3) apparently form primarily by authigenesis, commonly with minimal amount of included detritus, and (4) have high REE concentrations. There are several types of ferromanganese sediments which are classified according to their depositional environment as summarized by Bonatti et al. [8]. We have sampled two types of ferromanganese deposits, classified as hydrogenous and hydrothermal. Samples were selected from major ocean basins and mid-ocean ridge spreading centers. Locations are given in Table 1 and Fig. 1.

Manganese nodules comprise the bulk of hydrogenous ferromanganese sediments. The assumption leading to the selection of manganese nodules was that their REE precipitate directly out of seawater, and therefore their Nd isotopic composition would represent that of the seawater from which they were derived. Support for the hypothesis of seawater derivation for REE in manganese nodules comes from many authors [2,8,9,20,21]. Ehrlich [13] and Bender [14] prefer a mechanism of diagenetic remobilization of REE from underlying sediments as a source for these elements. This has been argued for other elements as well ([8,22–24], and others). Many nodules are also characterized by the presence of clay and other particles dispersed throughout their structures

TABLE 1

Sample locations and Sm and Nd results

Sample No.	Lab. No. [a]	Sample location	Nd (ppm)	Sm (ppm)	$^{147}Sm/^{144}Nd$	$^{143}Nd/^{144}Nd$ [b]
I. Pacific Ocean						
OC73-3-12P	MS-1	20°22'12"S, 112°19'12"W	20.7	5.01	0.146	0.511780 ± 20
duplicate	MS-1b		–	–	–	0.511828 ± 18
OC73-3-12MG3	MS-2a	20°43'12"S, 112°27'00"W	15.7	3.60	0.137	0.511633 ± 28
duplicate	MS-2b		16.5	3.56	0.130	0.511659 ± 25 [c]
52DR5	HC-1	00°36'N, 86°06'W	2.05	0.39	0.115	0.511768 ± 26
MD1-1-1 top	MN-1	31°N, 155°W	196	50.0	0.153	0.511618 ± 15
MD1-1-1 bottom	MN-2	31°N, 155°W	129	33.1	0.155	0.511620 ± 28
DWHD-47	MN-3	41°59'S, 102°01'W	175	42.5	0.146	0.511611 ± 22
Antp 58D	MN-4	18°57'N, 135°48'E	225	51.4	0.138	0.511565 ± 37
SCAN 35D	MN-5	20°55'N, 142°22'E	143	32.7	0.138	0.511656 ± 25
CEROP II 1000 m DISS	SW-1	36°47'N, 122°48'W	3.2×10^{-6}	0.63×10^{-6}	0.118	0.511641 ± 36 [c]
CEROP II 2400 m DISS	SW-2	36°50'N, 122°50'W	–	–	–	0.511712 ± 25
CEROP II 1000 m DISS	SW-3	36°47'N, 122°48'W	–	–	–	0.511718 ± 25
GS-7901-139	SW-4a	0°47'20"N, 86°07'21"W	2.2×10^{-6}	0.4×10^{-6}	0.112	0.511706 ± 34 [c]
duplicate	SW-4b		–	–	–	0.511731 ± 28 [c]
II. Atlantic Ocean						
CYP74-12	HC-2	36°56'N, 33°04'W	4.45	1.01	0.136	0.511245 ± 32
S-M	MN-6	33°57'N, 65°47'W	179	45.1	0.152	0.511223 ± 21
BP-2381	MN-7	31°04'12"N, 78°08'30"W	107	23.1	0.129	0.511273 ± 22
BP-2382	MN-8	31°01'36"N, 78°18'48"W	59.4	14.2	0.145	0.511312 ± 42
VEMA FRACTURE ZONE	MN-9	10°53'42"N, 45°17'48"W	155	38.5	0.149	0.511293 ± 18
CIRCE 244D	MN-10	08°22'S, 13°13'W	233	59.6	0.154	0.511216 ± 18
CHN115 Sta 146	MN-11a	30°12'48"S, 39°21'30"W	250	56.2	0.135	0.511118 ± 38
duplicate	MN-11b		–	–	–	0.511117 ± 22
KNR42-166	MN-20	35°36'18"N, 58°41'24"W	280	–	–	0.511256 ± 18
V27-58 195 m	MN-21	75°32'24"N, 02°39'47"E	117	30.0	0.155	0.511323 ± 22
III. Indian Ocean						
DODO 127D	MN-12	06°40'01"S, 51°54'00"E	199	44.0	0.133	0.511432 ± 26
Antp 109D	MN-13	29°58'23", 60°47'49"E	169	38.7	0.138	0.511404 ± 31
DODO 232D	MN-14	05°22'59"S, 97°28'59"E	262	68.6	0.158	0.511465 ± 29
DODO 62D	MN-15	16°18'00"S, 104°16'01',E	90.3	22.5	0.150	0.511461 ± 24
PCE 55-31	MN-16	36°27'07"S, 110°02'24"E	134	30.3	0.136	0.511281 ± 46
DODO 62D Sed	RC-1	16°18'00"S, 104°16'01"E	33.0	8.31	0.152	0.511350 ± 25
IV. Antarctic Ocean						
BT-14-3	MN-17	56°13'S, 164°20'W	67.2	17.4	0.156	0.511500 ± 30
V. Scotia Sea						
E28-5	MN-18	57°54'S, 57°00'W	63.0	14.2	0.136	0.511567 ± 28
VI. Lake Oneida, N.Y. – lacustrine						
Lake Oneida, N.Y.	MN-19	43°10'N, 75°45'W	34.0	9.19	0.163	0.511281 ± 29

[a] MN = manganese nodule, MS = metalliferous sediment, HC = hydrothermal crust, RC = red clay, SW = seawater.

[b] Data normalized to $^{150}Nd/^{142}Nd = 0.2096$. Reported errors are 2σ on the mean.

[c] Spiked with ^{150}Nd and normalized to $^{146}Nd/^{142}Nd = 0.636155$.

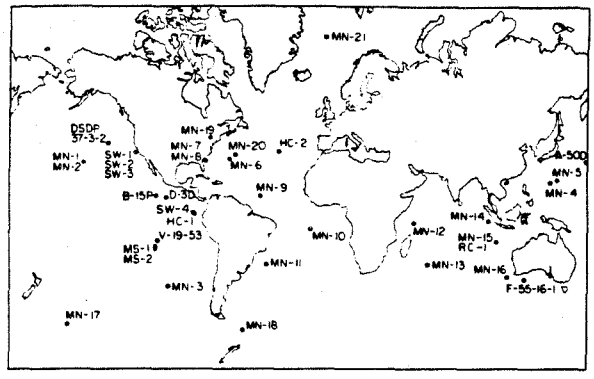

Fig. 1. Locations of samples analyzed in this study. Also included are manganese nodule and metalliferous sediment sites from O'Nions et al. [19] (A-50D, D-3D, B-15P, V-19-53, F-55-16-1) and a red clay (DSDP37-3-2) from McCulloch and Wasserburg [37].

[25]. These latter features, if detrital, could have a significant effect on elemental composition, possibly including Nd. In addition to Nd dissolved in seawater, other possible sources which could affect the Nd isotopic composition in the samples include continental detritus, oceanic basalts and sediments, and juvenile material.

Samples were chosen to achieve two main objectives: (1) to establish differences or similarities in Nd isotopic composition between various water bodies, and (2) to determine if variations exist within a body of water, which may be related to differences in provenance. To meet these objectives, broad geographic sampling of nodules within the Atlantic, Pacific, and Indian Oceans were made (Fig. 1). Samples from the Scotia Sea and Antarctic Ocean were chosen as representing locations where mixing between two different water masses may be taking place. A manganese nodule and an associated red clay from the Indian Ocean (RC-1 and MN-15) were analyzed to compare the Nd isotopic composition between manganese nodules and the underlying sediment substrate in the same area. In addition, one lacustrine-nodule from Lake Oneida, New York, was analyzed. This latter sample was chosen on the assumption that all of its REE were continentally derived.

Two types of hydrothermal samples have also been sampled. These are hydrothermal crusts and metalliferous sediments. Samples were chosen to determine if there were effects due to hydrothermal activity on the Nd isotopic composition. The direct association of these deposits with hydrothermal activity and their rapid rate of deposition [26–28] make them genetically distinct from manganese nodules. These deposits are believed to form by direct precipitation out of seawater ([7,8,11,12,26,29], and others). While iron and manganese have been shown by these authors to have a source related to hydrothermal alteration of basalts, this has not been clearly established for the rare earth elements. Corliss (12) studied altered oceanic basalts and concluded that REE in marine sediments could be accounted for by derivation from the basalts. However, REE patterns for hydrothermal deposits are similar to seawater REE patterns and not basalt, leading many authors to conclude their REE were derived from seawater [26,30,31]. Nd isotopic analyses were made on metalliferous sediments from the East Pacific Rise, and on hydrothermal crusts from the Galapagos hydrothermal mounds and the FAMOUS site on the Mid-Atlantic Ridge in an attempt to clarify their origin.

Finally, we have attempted to make a direct determination of the Nd isotopic composition of seawater at two Pacific sites. Three seawater samples were obtained which were collected from the Pacific Ocean by K. Bruland during the CEROP II expedition of the Oregon State University's R.V. "Wecoma". Samples were collected at approximately 1000 m (SW-1, SW-3) and 2400 m (SW-2) depths from a location offshore from Monterey, California (Fig. 1, Table 1). SW-1 and SW-3 are separate aliquots of the same water sample. In addition, one bottom water sample (~2500 m) from the Galapagos ridge crest (SW-4) was collected by L. Gordon during the Galapagos expedition of the University of Miami's R.V. "Gillis" in March 1979.

3. Analytical procedures and data representation

Ferromanganese sediment samples were treated with 4.0*N* HCl for the dissolution of the authigenic materials. A few samples were also treated with 1 ml 1 : 1 HF and $HClO_3$. The estimated mass of residue remaining after dissolution by these two methods were the same. Typical sample sizes were about 15–

20 mg. Samples were either aliquots of a powdered sample or, where available, intact nodules. Intact nodules were first stripped of surface layers down to a depth of about 2 mm, and the sample then was scraped from the clean surface below. Chemical separation and mass spectrometry of Sm and Nd have been described elsewhere [1,32]. Sm and Nd concentrations were determined by isotope dilution on small aliquots. Strontium was separated by our standard ion exchange techniques [33]. Typical blank levels for Sr and Nd were 100×10^{-12} g and 60×10^{-12} g respectively.

Seawater analyses were carried out on the REE fraction separated from 10- to 20-liter samples of seawater. Samples SW-1, 2, and 3 were filtered on board the R.V. "Wecoma" through acid-cleaned, 142-mm-diameter nucleopore filters with a pore size of 0.4 μm. SW-4 was analyzed without prior filtration. Our Sm-Nd separations and analyses were done on REE fractions prepared by Roberta Conard at Oregon State University following the procedure summarized below. Samples were acidified in the laboratory to pH $\cong$ 1.5 and set aside for one week. The REE were precipitated from the seawater using the method described by Goldberg et al. [2]. High-purity Fe_2O_3 powder dissolved in 6.0*N* HCl is added to the water samples. The iron was precipitated as $Fe(OH)_3$ by bubbling NH_3 gas through the water until a pH of 9.0 was attained; the REE were adsorbed onto these reactive surfaces. This procedure has typical REE yields of about 90% as determined from the activity of ^{170}Tm added to the samples prior to precipitation. Precipitates were then transferred to Caltech to separate Sm and Nd. The total chemistry blank for this separation of Nd was determined on a sample of reagents prepared in the same proportions as were used for the separation of REE from the seawater samples. The contribution from these reagents was found to be about 0.3×10^{-9} g of Nd, which comprises less than 1% of the total Nd yield.

The isotopic abundance of all the Nd isotopes were measured in every experiment and, with the exception of the three seawater samples were found to be in excellent agreement with values measured by DePaolo and Wasserburg [1]. An excess of ^{148}Nd, measured as ^{148}Nd/^{144}Nd, was found in each of the seawater samples ranging from approximately 15 to 47 ϵ units (Table 2) relative to the normal abundance

TABLE 2

ϵ_{Nd} values for non-radiogenic Nd isotopes in seawater samples [a]

Lab. No.	ϵ_{142}	ϵ_{145}	ϵ_{146}	ϵ_{148}
SW-1 [b]	−0.7 ± 0.5	−2.2 ± 1.4	–	+26.6 ± 1.4
SW-2 [c]	+0.7 ± 0.5	−0.5 ± 0.5	−0.6 ± 0.5	+18.9 ± 0.8
SW-3 [c]	+1.0 ± 0.5	−0.9 ± 1.0	−0.8 ± 0.8	+14.7 ± 1.7
SW-4a [b]	−0.3 ± 0.5	+0.9 ± 0.9	–	+47.0 ± 0.8
SW-4b [b]	−0.5 ± 0.9	−1.0 ± 0.9	–	+42.8 ± 2.1

[a] Normal isotopic abundances have $\epsilon_{Nd} = 0$.
[b] Spiked with ^{150}Nd and normalized to ^{146}Nd/^{142}Nd = 0.636155.
[c] Normalized to ^{150}Nd/^{142}Nd = 0.2096.

of this isotope as has been measured in the ferromanganese sediments. This excess of the ^{148}Nd/^{144}Nd occurs with or without the use of ^{170}Tm tracer (samples SW-1, SW-2) which was added to determine REE precipitation yields and ^{147}Sm and ^{150}Nd tracers added to determine Sm and Nd concentrations (SW-1, SW-4). A REE carrier solution is used routinely in the laboratory where the REE were precipitated from the seawater samples, for the purpose of determining chemistry yields on seawater REE samples measured by neutron activation analysis (see Goldberg et al. [2]). This REE carrier solution contains enriched ^{148}Nd as well as other REE, and it therefore seems plausible that the ^{148}Nd/^{144}Nd excess we observe may be due to cross contamination inadvertently introduced into our samples from this carrier. To verify this, SW-4 was precipitated at OSU using new reagents except Fe. The results, however, still showed the ^{148}Nd effect to be present. To be certain that the ^{148}Nd excess was not due to an interfering species from another element, a portion of SW-4 (SW-4b) was passed through the Nd separation procedure a second time. Because the ^{148}Nd excess was still observed during this run, data was taken at the end of the run with ion beam intensities increased by a factor of five. The results were identical. Had we not measured all of the Nd isotopes, the ^{148}Nd effect would have gone unnoticed. ^{148}Nd is not used for fractionation corrections, so we are confident that the ^{143}Nd isotopic abundance measured in the seawater samples is unaffected by contamination. All other isotopes of Nd have normal abundances.

Samples of Nd were analyzed on the Lunatic I

mass spectrometer [34] and NdO^+. Sample sizes for ferromanganese sediments were 200–300 × 10^{-9} g Nd. Typical ion beam intensities at mass 160 ($^{144}Nd^{16}O$) were 8.0 × 10^{-12} A. This beam intensity was maintained for 6–8 hours while approximately 200 ratios were measured for each sample. Seawater samples sizes were less than 50 × 10^{-9} g Nd. With the exception of SW-1, ion beam intensities were the same as those for ferromanganese samples just mentioned. SW-1 was analyzed at an ion beam intensity of 4.0 × 10^{-12} A. About 200 ratios were measured for each water sample.

Representation of Sm, Nd and Sr data follows that given by DePaolo and Wasserburg [1,18]. Measured $^{143}Nd/^{144}Nd$ ratios are presented as fractional deviations in parts in 10^4 (ϵ units) from $^{143}Nd/^{144}Nd$ in a chondritic uniform reservoir (CHUR) as measured today:

$$\epsilon_{Nd}(0) = \left[\frac{(^{143}Nd/^{144}Nd)_M}{I_{CHUR}(0)} - 1\right] \times 10^4$$

where M is the ratio measured in the sample today, and $I_{CHUR}(0) = 0.511836$ is the $^{143}Nd/^{144}Nd$ in the CHUR reference reservoir today. Similarly, an enrichment factor for $^{147}Sm/^{144}Nd$ in a sample relative to CHUR is given by:

$$f_{Sm/Nd} = \left[\frac{(^{147}Sm/^{144}Nd)_M}{(^{147}Sm/^{144}Nd)_{CHUR}} - 1\right]$$

where $(^{147}Sm/^{144}Nd)_{CHUR} = 0.1936$. Model ages, T^{Nd}_{CHUR}, are calculated for the samples as follows:

$$T^{Nd}_{CHUR} = \frac{1}{\lambda} \ln\left[1 + \frac{\epsilon_{Nd}(0)\, I_{CHUR}(0) \times 10^{-4}}{f_{Sm/Nd}(^{147}Sm/^{144}Nd)_{CHUR}}\right]$$

The ^{147}Sm decay constant, $\lambda = 6.54 \times 10^{-12}$ yr^{-1}. Errors reported for T^{Nd}_{CHUR} model ages are typically less than 10% and only include the errors in $\epsilon_{Nd}(0)$. Sr isotopic data is presented in a manner analogous to that used for Sm-Nd data. Thus:

$$\epsilon_{Sr}(0) = \left[\frac{(^{87}Sr/^{86}Sr)_M}{I_{UR}(0)} - 1\right] \times 10^4$$

where $I_{UR}(0) = 0.7045$ is the estimated $^{87}Sr/^{86}Sr$ value for the bulk earth as determined by DePaolo and Wasserburg [15] and O'Nions et al. [16].

4. Results

Results of Nd isotopic analyses are given in Tables 1 and 3 and Fig. 2. All samples measured have $\epsilon_{Nd}(0)$ less than 0 and range as low as –14. Fig. 2 clearly shows that these samples lie well below typical values observed for oceanic igneous rocks such as mid-ocean ridge, oceanic island, and island arc basalts. We note, however, that our data lie between (and overlap to some extent) typical values for continental flood basalts and average crustal rocks. Clearly, these data show that the dominant contribution to the REE in these samples is from the continents and not from rocks with oceanic crust or mantle affinities. Furthermore, we observe from Fig. 2 a distinct clustering of isotopic data from the Pacific, Indian, and Atlantic Oceans. Samples associated with each water mass occupy an isotopically distinct range, with the Atlantic Ocean data as the most negative, the Pacific Ocean the least negative, and the Indian Ocean having intermediate values. Only one sample, MN-16 from the Indian Ocean, overlaps the range defined by samples from another ocean. This regular pattern is independent of the nature of the material analyzed.

Pacific Ocean. Samples analyzed from the Pacific Ocean occupy a narrow range of $\epsilon_{Nd}(0)$ from –0.2 to –4.4. This is in excellent agreement with previous data from O'Nions et al. [19] for Pacific samples. Manganese nodules range from –2.6 to –4.4, including

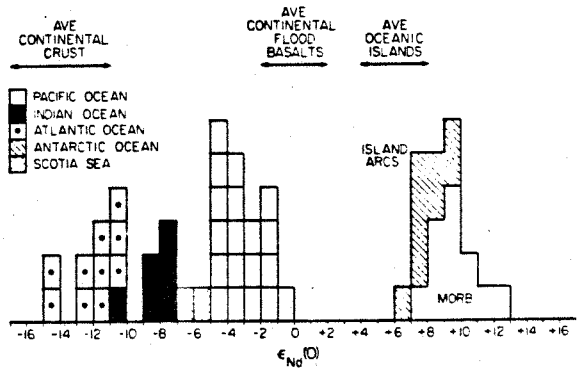

Fig. 2. Histogram of $\epsilon_{Nd}(0)$ of marine ferromanganese sediments and seawater measured in this study. Data from O'Nions et al. [19], renormalized to $^{150}Nd/^{142}Nd = 0.2096$, have been included. Data on continental and oceanic rocks have been adapted from DePaolo and Wasserburg [18].

TABLE 3

Nd evolutionary parameters

Lab. No.	$\epsilon_{Nd}(0)$	$f_{Sm/Nd}$	T^{Nd}_{CHUR} (AE)
I. Pacific Ocean			
MS-1a	−1.1 ± 0.4	−0.246	0.18
MS-1b	−0.2 ± 0.3	–	–
MS-2a	−4.0 ± 0.6	−0.292	0.55
MS-2b	−3.5 ± 0.5	−0.329	0.43
HC-1	−1.4 ± 0.5	−0.408	0.14
MN-1	−4.3 ± 0.3	−0.208	0.83
MN-2	−4.2 ± 0.5	−0.199	0.85
MN-3	−4.4 ± 0.4	−0.245	0.72
MN-4	−4.3 ± 0.7	−0.289	0.60
MN-5	−3.5 ± 0.5	−0.290	0.49
SW-1	−3.8 ± 0.7	−0.393	0.39
SW-2	−2.4 ± 0.5	–	–
SW-3	−2.3 ± 0.5	–	–
Sw-4a	−2.5 ± 0.7	−0.421	0.24
Sw-4b	−2.1 ± 0.5	–	–
II. Atlantic Ocean			
HC-2	−11.5 ± 0.6	−0.296	1.57
MN-6	−12.0 ± 0.4	−0.217	2.21
MN-7	−11.0 ± 0.4	−0.334	1.32
MN-8	−10.2 ± 0.8	−0.258	1.60
MN-9	−10.6 ± 0.4	−0.229	1.86
MN-10	−12.1 ± 0.4	−0.204	2.38
MN-11a	−14.0 ± 0.7	−0.301	1.87
MN-11b	−14.0 ± 0.4	−0.301	1.88
MN-20	−11.4 ± 0.3	–	–
MN-21	−10.0 ± 0.4	−0.200	2.01
III. Indian Ocean			
MN-12	−7.8 ± 0.5	−0.313	1.01
MN-13	−8.5 ± 0.6	−0.287	1.19
MN-14	−7.3 ± 0.6	−0.184	1.58
MN-15	−7.3 ± 0.5	−0.224	1.32
MN-16	−10.8 ± 0.9	−0.297	1.47
RC-1	−9.5 ± 0.5	−0.215	1.77
IV. Antarctic Ocean			
MN-17	−6.6 ± 0.6	−0.197	1.34
V. Scotia Sea			
MN-18	−5.3 ± 0.5	−0.298	0.72
VI. Lake Oneida, N.Y.			
MN-19	−10.9 ± 0.6	−0.159	273

data from O'Nions et al. Top and bottom material from an apparently unturned manganese nodule (MN-1, MN-2) have identical Nd isotopic compositions, although the topmost sample has about a factor of 2 higher concentration of both Sm and Nd. We note that two metalliferous sediment samples from the East Pacific Rise (MS-1, this study, and V-19-53(40), O'Nions et al. [19]) and the Galapagos hydrothermal crust (HC-1) exhibit the least negative values observed and are distinctly separated from the bulk of Pacific samples. MS-1a and b were separate aliquots of an unsplit powder. We also note that the average $\epsilon_{Nd}(0)$ value for four seawater samples is about −2.6 and lies in the range defined by the ferromanganese sediments.

Atlantic Ocean. $\epsilon_{Nd}(0)$ values for Atlantic samples are distinctly different from Pacific samples. Values range from −10.0 to −14.0, with the bulk of the samples lying between −10.0 and −12.1. One sample (HC-2) is a manganese-rich crust from the project FAMOUS site in the North Atlantic. It has $\epsilon_{Nd}(0)$ = −11.5 and it is indistinguishable from most other Atlantic samples which consist of manganese nodules. Samples MN-11a and b are duplicate analyses of a nodule from the South Atlantic. Their $\epsilon_{Nd}(0)$ values of −14.0 are the most negative reported.

Indian Ocean. Five manganese nodules have been analyzed. With the exception of MN-16, $\epsilon_{Nd}(0)$ values lie between −7.3 and −8.5, approximately midway between Pacific and Atlantic sample values. Previous data from O'Nions et al. [19] for an Indian Ocean nodule also lies in this range. MN-16 has $\epsilon_{Nd}(0)$ = −10.8 which is more typical of Atlantic samples. A deep-sea clay (bulk sample, untreated) from the Indian Ocean (RC-1) is also more negative than the bulk of the reported data for this ocean ($\epsilon_{Nd}(0)$ = −9.5).

Other samples. Two nodules from southern oceans, the Scotia Sea and the Antarctic Ocean, have $\epsilon_{Nd}(0)$ values which lie between those observed for the Pacific and Indian Oceans. MN-19 from Lake Oneida has $\epsilon_{Nd}(0) = -10.9$ which is within the range of data for Atlantic samples.

Four manganese nodules and two metalliferous sediment were also analyzed for $^{87}Sr/^{86}Sr$. Results of these measurements are given in Table 4. With the exception of MS-1, all samples have $\epsilon_{Sr}(0)$ indistinguishable from seawater ($\epsilon_{Sr}(0) = +65.0$) in spite of a wide range in $\epsilon_{Nd}(0)$ and geographic location. MS-1 has a slightly lower $\epsilon_{Sr}(0)$ value of +63.5.

TABLE 4

Nd and Sr evolutionary parameters for selected samples

Lab. No.	$^{143}Nd/^{144}Nd$	$^{87}Sr/^{86}Sr$ [a]	$\epsilon_{Nd}(0)$	$\epsilon_{Sr}(0)$
MS-1	0.511828 ± 18	0.708971 ± 30	−0.2 ± 0.3	+63.5 ± 0.6
MS-2	0.511633 ± 28	0.709040 ± 37	−4.0 ± 0.6	+64.4 ± 0.7
MN-7	0.511273 ± 22	0.709030 ± 40	−11.0 ± 0.4	+64.3 ± 0.8
MN-10	0.511216 ± 18	0.709068 ± 37	−12.1 ± 0.4	+64.8 ± 0.8
MN-15	0.511461 ± 24	0.709090 ± 60	−7.3 ± 0.5	+65.2 ± 1.2
MN-3	0.511611 ± 22	0.709015 ± 40	−4.4 ± 0.4	+64.1 ± 0.8
Seawater [b]		0.70909		+65.2

[a] Data normalized to $^{86}Sr/^{88}Sr = 0.1194$.
[b] Average of values measured on the Caltech Sr seawater standard [44].

5. Discussion

Neodymium isotopic data for ferromanganese nodules, hydrothermal crusts, and metalliferous sediments exhibit distinctive and tightly clustered $\epsilon_{Nd}(0)$ values within each of the major oceans analyzed. This is in sharp contrast with the $^{87}Sr/^{86}Sr$ isotopic composition of these sediments which is uniform in all samples studied and is identical to that of dissolved Sr in modern seawater. The Atlantic Ocean has the most negative values (average $\epsilon_{Nd}(0) \cong -12$), the Indian Ocean has intermediate values (average $\epsilon_{Nd}(0) \cong -8$), and the Pacific Ocean has the least negative values (average $\epsilon_{Nd}(0) \cong -3$). Data for samples from each ocean show relatively small dispersion about the respective average $\epsilon_{Nd}(0)$ values, with a maximum spread of only $\pm 2\epsilon$ units in each ocean. The possible sources for REE which could contribute to these sediments include: dissolved REE from continental sources, dissolved REE from marine sources, detrital debris from continental materials and debris from oceanic igneous rocks and sediments. Some of the oceanic sources (e.g., marine hydrothermal solutions) could in principle cause major changes in the local contribution of REE. Some mixture of REE from these sources determines the Nd isotopic composition of ferromanganese sediments in each ocean, and some small variation in the proportions of these individual components must be responsible for the small variations with an ocean. The observed Nd uniformities in each ocean indicate that contributions to this element are relatively well mixed and distinctly different for each major water mass.

Nd isotopic uniformity for ferromanganese sediments from each of the oceans is maintained despite many factors and genetic variables. Concentration of Nd shows no correlation with isotopic composition. Nd concentrations vary by more than two orders of magnitude in nodules and metalliferous sediments from the Pacific Ocean, and somewhat less in the Atlantic. In spite of this variation, all samples maintain nearly the same Nd isotopic composition within the same ocean. Further, the highly variable accumulation rates of ferromanganese sediments do not appear to cause any effects on Nd isotopic composition, as manganese nodules have extremely slow growth rates of a few millimeters per 10^6 years [35, 36], whereas hydrothermal crusts may grow as fast as 2 mm/1000 years [27,28]. Possible contributions to manganese nodules from diagenetically remobilized REE from underlying sediments also has no large local effects on $\epsilon_{Nd}(0)$. If diagenetic remobilization is a significant source of REE in manganese nodules, then underlying deep sea sediments must also be characterized by Nd isotopic values which are close to that of the ocean basin. Deep-sea red clays (RC-1, DSDP37-3-2 [37]) have $\epsilon_{Nd}(0)$ values similar to ferromanganese sediments in the same ocean, but the data base is too limited to draw any conclusions regarding their sources.

Nd isotopic measurements of Pacific seawater samples show a strong similarity to Pacific ferromanganese sediments. Seawater, with $\epsilon_{Nd}(0)$ values falling about midway in the spread exhibited by ferro-

manganese sediments, leads us to the conclusions that the source of Nd in Pacific ferromanganese sediments is from Nd dissolved in seawater, and that Pacific seawater is isotopically rather uniform with respect to Nd. These conclusions, coupled with the previous discussion on the isotopic uniformity of ferromanganese sediments in each ocean, lead us to infer that the Nd isotopic composition of seawater in the Atlantic, Indian, and Pacific Oceans are distinctly different from each other, but fairly uniform within each ocean. To test these conclusions directly, Nd isotopic measurements of a variety of seawater samples will have to be made.

In a previous study, O'Nions et al. [19] reported the Nd isotopic composition in ferromanganese nodules to be variable but concluded that the value of Nd in seawater was $\epsilon_{Nd}(0) \cong -3$. These workers attributed the variability to detritus included in the nodules but considered their data on Pacific nodules to be more representative of seawater. This was a reasonable conclusion, because $^{87}Sr/^{86}Sr$ measured in their Indian Ocean nodule was distinctly greater than the $^{87}Sr/^{86}Sr$ ratio for dissolved Sr in seawater. However, the Nd values reported by O'Nions et al. [19] for samples from each ocean lie well within the groupings reported here, yet our $^{87}Sr/^{86}Sr$ ratios are all very close to modern seawater $^{87}Sr/^{86}Sr$ ratios in spite of variable $\epsilon_{Nd}(0)$ values. The interpretation presented in this paper is in disagreement with the conclusions by O'Nions et al. [19] which reflect their more limited data base, the absence of a consideration of residence time for REE, as well as the magnitude of possible detrital contributions. A more recent abstract by Goldstein and O'Nions [38] on manganese nodules drew conclusions similar to those presented here.

To assess the effects of detrital contributions, consider mixtures (m) of two components A and B. The Nd composition is given by:

$$\epsilon^{m}_{Nd}(0) = \frac{(X_A)(C^{A}_{Nd})[\epsilon^{A}_{Nd}(0)] + (1 - X_A)(C^{B}_{Nd})[\epsilon^{B}_{Nd}(0)]}{(X_A)(C^{A}_{Nd}) + (1 - X_A)(C^{B}_{Nd})} \quad (1)$$

where X_A is the weight fraction of component A and C^{A}_{Nd} and C^{B}_{Nd} are the concentrations of Nd (in ppm) in components A and B. If we take the shift between Atlantic and Pacific samples to represent a detrital component (B) added to a seawater component (A) with $\epsilon^{A}_{Nd}(0) \cong -3$, we can calculate the value of $\epsilon^{B}_{Nd}(0)$ in the detrital component. We use $(1 - X_A) = 0.2$ as a reasonable limit on the weight fraction of detrital material in a manganese nodule (based on world averages for Al and Si abundances in nodules [39]) and a low value of $C^{A}_{Nd} = 100$ ppm Nd in the uncontaminated nodule. This yields:

$$[\epsilon^{B}_{Nd}(0) - \epsilon^{m}_{Nd}(0)]\, C^{B}_{Nd} = \frac{X_A C^{A}_{Nd}}{(1 - X_A)} [\epsilon^{m}_{Nd}(0) - \epsilon^{A}_{Nd}(0)]$$

$$\cong 3.6 \times 10^{3} \text{ (units of ppm)}$$

for the Atlantic Ocean where $\epsilon^{m}_{Nd}(0) \cong -12$. For $C^{B}_{Nd} \cong 35$ ppm, a high value for most crustal rocks, this yields $\epsilon^{B}_{Nd}(0) \cong -115$ which is close to the total growth of Nd over the history of the earth. The lowest observed $\epsilon_{Nd}(0)$ is about -30 and yields $C^{B}_{Nd} \cong 155$ ppm which is an excessively high value for possible detrital sources. It follows that the presence of detrital material in the manganese nodules cannot reasonably explain the observed differences between Pacific and Atlantic samples. If 20% by weight of a nodule is derived from an oceanic basalt with $\epsilon_{Nd}(0) \cong +10$ and $C_{Nd} \cong 10$ ppm, we obtain a shift of 0.36ϵ units. Some contributions from oceanic basalts and detrital material must obviously take place, but the above considerations show that the magnitude of their effects is likely to be less than an ϵ unit. We consider it most reasonable that the variations within an ocean basin reflect the dissolved content of Nd in different waters draining off of the various continental masses which are not completely mixed within the basin over the time scale for Nd deposition, and only a small contribution comes from oceanic magma sources.

Rapidly accumulating deposits of hydrothermal crusts and metalliferous sediments are associated with hydrothermal plumes ascending through mid-ocean ridge basalts (MORB). It has been demonstrated that hydrothermal leaching of MORB could supply the excess iron and manganese associated with hydrothermal crusts and metalliferous sediments from the observation that these and some other elements are depleted in the interiors of pillow basalts relative to their glassy margins [12]. Zelânov [40] reported local concentrations of Fe and Mn hydroxides as high

as 140 mg/l of seawater in water samples collected near the mouths of hot springs associated with the submarine Banu Wuhu volcano, compared with normal seawater concentrations for these elements of less than 60 μg/l [6]. Studies of Pb isotopes in metalliferous sediments indicate a volcanogenic source for this element also [26,41]. However, only two hydrothermal sediment samples from the Pacific Ocean studied here (MS-1, HC-1) with $\epsilon_{Nd}(0)$ about 2ϵ units greater than the manganese nodules show any indication of a possible basaltic contribution to the Nd isotopes. Contributions from oceanic basalts to the Nd composition of hydrothermal crusts and metalliferous sediments can be demonstrated by comparing Mn/Nd ratios and $\epsilon_{Nd}(0)$ in oceanic basalts with that in the hydrothermally deposited sediments. Typical MORB have Mn/Nd $\cong$ 150 (Mn $\cong$ 1500 ppm, Nd $\cong$ 10 ppm) and $\epsilon_{Nd}(0) \cong +10$ compared with a hydrothermal crust (HC-1) which has Mn/Nd $\cong$ 900 (Mn = 0.18% [30], Nd = 2.05 ppm) and $\epsilon_{Nd}(0) = -1.4$. Mn/Nd ratios indicate that almost all of the Nd in the hydrothermal crust could in principle have a basaltic source. However, from the mixing equation presented earlier, using $\epsilon_{Nd}(0) \cong +10$ for MORB and seawater with $\epsilon_{Nd}(0) \cong -3$, we calculate that the maximum mass fraction of the hydrothermal crust (sample HC-1) from basaltic sources must be less than about 5%. On the other hand, metalliferous sediment (MS-1) which has a much higher concentration of Nd (C_{Nd} = 20.7 ppm) must have a mass fraction of 35% of MORB to account for the observed ϵ value of -0.2 corresponding to a 3ϵ shift from our estimated ϵ value for Pacific seawater. However, Sr data for this sample (Table 4) cannot be quantitatively balanced by the mass fraction calculated for Nd, although the isotopic effect for Sr is in the expected direction for a sample diluted by MORB materials. A sample of MS-1 was also leached with HCl to remove $CaCO_3$ and the residue was analyzed and found to have $\epsilon_{Sr}(0) = +47$. This residue clearly has $\epsilon_{Sr}(0)$ which is from materials with $\epsilon_{Sr}(0)$ lower than seawater. However, a quantitative explanation of Nd and Sr relationships is difficult to make from the available data. Generally, if the Nd in metalliferous sediments is derived from Nd dissolved in hydrothermal solutions, then approximately 15% of the total Nd in these samples must come from Nd derived from basaltic sources. It is clear that the causes of variations within the oceans remain a major issue. Substantial contributions (~20%) to the dissolved load of Nd from primary oceanic sources may exist as assessed by these methods.

Sr isotopic data (this study, [7,41]) indicate that $\epsilon_{Sr}(0)$ values in these sediments are very close to seawater $\epsilon_{Sr}(0)$ values. We conclude, therefore, in agreement with other authors [7,26,31,41] that the source of REE, Sr, and possibly other elements is ambient seawater and was *not dominated* by local igneous sources. A small fraction of these elements (REE and Sr) may be added to hydrothermal crusts and metalliferous sediments possibly as a result of scavenging of seawater by Fe and Mn hydroxides when they are deposited from ascending solutions upon entering oxygenated seawater [29].

$f_{Sm/Nd}$ values have been measured for most samples. $f_{Sm/Nd}$ values for seawater range from -0.39 (this study) to -0.5 [2,5]. These values are typical of continental $f_{Sm/Nd}$ values [37]. Manganese nodules and hydrothermal ferromanganese deposits exhibit a range of $f_{Sm/Nd}$ from about -0.2 to -0.4. MN-19 from Lake Oneida has an $\epsilon_{Nd}(0)$ consistent with a continental source for its REE, yet has an extremely fractionated $f_{Sm/Nd}$ value (-0.159) relative to the probable $f_{Sm/Nd}$ value of its REE source material. The variation of $f_{Sm/Nd}$ exhibited by ferromanganese sediments is not consistent with a steady state model for the input versus output of elements in seawater. This indicates that complexities exist in the transport mechanisms of the REE into and out of seawater. Further study is needed in the mechanisms and rates of REE solution, transport, and precipitation before conclusions can be drawn from these variable enrichment factors.

T^{Nd}_{CHUR} ages have been calculated for the ferromanganese sediments and seawater analyzed here, using the measured $\epsilon_{Nd}(0)$ and $f_{Sm/Nd}$ values (Table 3). These calculations assume the $f_{Sm/Nd}$ values are characteristic of the sources of REE. T^{Nd}_{CHUR} ages calculated are variable but have averages which are distinct for each ocean, with the Pacific samples having the youngest ages and the Atlantic the oldest. Because it has been observed that $f_{Sm/Nd}$ is variable in ferromanganese sediments and not the same as the source values, these ages probably do not reflect the true source rock ages. If we use a typical $f_{Sm/Nd}$ value for a continental source of about -0.4 [37] we cal-

culate an average age for the Atlantic Ocean samples of about 1.20 AE, 0.85 AE for the Indian Ocean, and for the Pacific samples an age of 0.35 AE. We also get a much tighter clustering of the calculated ages using a continental $f_{Sm/Nd}$ value which is consistent with the clustering observed for $\epsilon_{Nd}(0)$ values. These ages are also younger than those calculated from measured $f_{Sm/Nd}$ values for the samples, but in either case, a distinctly older source for the REE in the Atlantic is clearly necessary to explain the difference between Atlantic and Pacific T^{Nd}_{CHUR} ages.

Reasonable constraints can be placed on the residence time of Nd in seawater from the data presented here, along with available concentration data for Nd in crustal rocks and the dissolved load in river water. Approximate limits of the residence time of Nd (τ_{Nd}) can be calculated from variations of the Na/Nd ratios in crustal rocks (CR) and river water (RW) relative to seawater (SW) Na/Nd and the residence time of Na in seawater ($\tau_{Na} = 4.8 \times 10^7$ yr [6]). We can calculate τ_{Nd} from the equation:

$$\tau_{Nd} = \tau_{Na}\left[\frac{(Na/Nd)_{CR}}{(Na/Nd)_{SW}}\right]$$

For $(Na/Nd)_{CR} \cong 1000$ and $(Na/Nd)_{SW} = 3.5 \times 10^9$ as presented earlier, we get $\tau_{Nd} \cong 15$ years as a lower limit. Studies by several authors [6,42,43], however, indicate that only a small percentage of Nd eroded from the continents enters the oceans as a dissolved component in river water. Using data from these authors, we get a range in $(Na/Nd)_{RW}$ from 3.0×10^4 to 1.5×10^5 (Na ≅ 6 ppm, Nd ≅ 40–200 × 10^{-6} ppm) and a range in τ_{Nd} from about 400 to 2000 years. Residence time calculations made by Goldberg et al. [2] based on roughly estimated fluxes of Nd into the oceans and the total dissolved content of Nd in the oceans yielded $\tau_{Nd} \cong 270$ years. A reliable value for the residence time of Nd is presently not available and may be substantially greater than previously estimated as indicated by Na/Nd ratios presented above. Clearly, more studies are needed to determine the fluxes of the REE to the oceans to further define the residence time of Nd. Isotopic data presented here allows us to put one more constraint on τ_{Nd}. As mentioned earlier, we observe a tight clustering of $\epsilon_{Nd}(0)$ in each ocean, but very marked distinctions between oceans. It is clear that to maintain these distinctions, the residence time of Nd must be considerably shorter than the mixing times between ocean basins. Beyond this, no other conclusions can be drawn from the data.

To obtain limitations on interocean mixing, we have for two ocean bodies 1 and 2 supplied by drainage from the respective land masses A and B, the following equations at steady state:

$$0 = \epsilon_A J_{A1j} - \epsilon_1 J_{13j} + \epsilon_2 C_{2j}\dot{W}_{12} - \epsilon_1 C_{1j}\dot{W}_{12}$$

$$0 = \epsilon_B J_{B2j} - \epsilon_2 J_{23j} - \epsilon_2 C_{2j}\dot{W}_{12} + \epsilon_1 C_{1j}\dot{W}_{12}$$

Here J_{A1j} and J_{B2j} are the fluxes of species j into oceans 1 and 2 from the sources A and B respectively. J_{13j} and J_{23j} are the rates of deposition of j(^{144}Nd in this case) from oceans 1 and 2 into the sediment layer, 3. $\dot{W}_{12}$ is the rate of exchange of water masses between 1 and 2. ϵ_1 and ϵ_2 are the ϵ values in each ocean. The ocean bodies are decoupled when $\dot{W}_{12} = 0$ which yields the condition $J'_{A1i} = J'_{13i}$ and $J'_{B2i} = J'_{23i}$ where the primes indicate this special decoupled case for an arbitrary species i. If the systems are only weakly coupled, then assuming that $C_{1j} \cong C_{2j}$ we obtain:

$$(\epsilon_1 - \epsilon_A) J'_{13j} \cong (\epsilon_2 - \epsilon_1) C_{1j}\dot{W}_{12}$$

$$(\epsilon_2 - \epsilon_B) J'_{23j} \cong (\epsilon_2 - \epsilon_1) C_{1j}\dot{W}_{12}$$

Using:

$$\frac{J'_{13j}}{C_{1j}W_1} = \frac{1}{\tau_{1j}}$$

for the mean residence time τ_{1j} in the decoupled water body of mass W_1, we get for the mixing time between 1 and 2 (τ_{12}) in terms of τ_{1j}:

$$\tau_{12} = \frac{W_1}{\dot{W}_{12}} \cong \frac{(\epsilon_2 - \epsilon_1)\tau_{1j}}{(\epsilon_1 - \epsilon_A)}$$

The difference between Atlantic and Pacific samples is $(\epsilon_2 - \epsilon_1) \cong 8\epsilon$ units. If $(\epsilon_1 - \epsilon_A) \cong 2$ as estimated by the dispersion for the Pacific for Nd and using a value for the residence time (τ_{1j}) of 500 years, this gives $\tau_{12} \cong 4\tau_{1j} \cong 4 \times 500$ years ≅ 2000 years. Estimating ϵ_A is difficult from the available data and it is not evident that this approach can yield reliable results for interocean mixing times.

6. Conclusions

Authigenic ferromanganese sediments indicate sharp and clear Nd isotopic compositional differences between the Atlantic, Pacific, and Indian Oceans. The composition of Nd measured in Pacific Ocean water is very close to ferromanganese sediments in the Pacific Ocean. We therefore conclude from ferromanganese sediment data that the isotopic composition of Nd in ocean water is characteristic of the water masses in each individual ocean basin. This reflects the composition of continental components in solution with some contributions from Nd from oceanic sources. This clear distinction should permit the application of the Nd isotopic composition in ocean water and chemical precipitates as a general tracer in oceanography. This characteristic difference between the Atlantic and Pacific Oceans corresponds to a difference in the relative abundance of ^{143}Nd between these water masses of only 10^6 atoms/g seawater.

Previous workers [18,19] have observed that a dominant continental component is necessary to explain the observed $\epsilon_{Nd}(0)$ values for authigenic marine sediments. However, it is difficult to assess from the available data what the average $\epsilon_{Nd}(0)$ value of continental material being supplied to the oceans is, and how it varies from ocean to ocean. If we consider North American shale (NAS) with $\epsilon_{Nd}(0) = -14.4$ [1] to represent average continental sources feeding the Atlantic Ocean and $\epsilon_{Nd}(0) = +10$ to represent average oceanic sources, then we can calculate that for the Atlantic Ocean there must be at least a 90% contribution from continental sources and only 10% from MORB to account for the average $\epsilon_{Nd}(0) \cong -12$ observed for this ocean. However, to account for variation of 2ϵ units in seawater by the addition of Nd from MORB or oceanic volcanic sources to continental material as represented by NAS would require a doubling of the oceanic contribution. At present it is not clear whether the observed variations which we attribute to seawater are a result of variations in the isotopic composition of the input of dissolved Nd from continental material or of major shifts in the proportion from oceanic sources. If we assume a similar value of 90% continentally derived Nd in the Pacific Ocean ($\epsilon_{Nd}(0) \cong -3$) as was obtained for the Atlantic using NAS, we calculate that the average $\epsilon_{Nd}(0)$ value for continental sources for the Pacific Ocean is about –4.5. This is a reasonable value when the ages of the continental material being drained into the Pacific from western North and South America are considered. There is, of course, considerably greater marine volcanic activity in the Pacific Ocean which could result in larger contributions to the REE from these sources. A minimum contribution of 55% continental Nd with NAS affinities is required to produce the observed $\epsilon_{Nd}(0)$ values in authigenic sediments from the Pacific Ocean.

Data for MN-18 from the Scotia Sea indicate that $\epsilon_{Nd}(0)$ in this sample is dominated by Nd with Pacific Ocean affinities in spite of a location more adjacent to the South Atlantic. This supports the view that ocean currents may be responsible for transporting REE from one water body to another. It may, therefore, be possible to determine ocean flow patterns and the effectiveness of such currents in transporting REE between water masses by measuring the Nd isotopic composition of seawater (either directly or indirectly) across observed Nd isotopic boundaries such as between the Scotia Sea and the South Atlantic Ocean.

Growth rates of deep-ocean manganese nodules are typically very slow. Typical growth rates average between 2 and 8 mm/10^6 years [35], making a nodule about 5 cm in diameter greater than 5×10^6 years old. The similarity of the $\epsilon_{Nd}(0)$ values in manganese nodules with that measured for seawater suggests that it may be possible to trace variations of Nd through time by sampling several layers within a nodule corresponding to a large time span and therefore to provide a basis for monitoring the flow of ocean waters over times of 10^6 years.

Acknowledgements

This study was initiated in 1978 as a result of the mutual interests of members of both the California Institute of Technology and Oregon State University. The analytical work was carried out at Caltech on samples prepared at OSU. The results comprised part of the requirements for a degree of Master of Science for D.J.P. who was a graduate student at OSU. D.J.P. would like to thank Malcolm McCulloch for providing the necessary laboratory instruction neeeded to con-

duct this research. Samples used in this study were provided by: J. Greenslate, J. Honnorez, F. McCoy, F. Manheim, W.S. Moore, J. Dymond, T. Walsh, and R. Senechal. J. Corliss helped us to obtain the seawater samples. This research was supported in part by grants from: NSF PHY 76-02724, NSF GX-28675, NSF OCE 77-11101; NASA NGL 05-002-188, and GSA 2382-78.

References

1 D.J. DePaolo and G.J. Wasserburg, Nd isotopic variations and petrogenetic models. Geophys. Res. Lett. 3 (1976) 249.
2 E.D. Goldberg, M. Koide, R.A. Schmitt and R.H. Smith, Rare earth distributions in the marine environment, J. Geophys. Res. 68 (1963) 4209.
3 T.R. Wildeman and L. Haskin, Rare-earth elements in ocean sediments, J. Geophys. Res. 70 (1965) 2905.
4 S.R. Taylor, Trace element abundances and the chondritic Earth model, Geochim. Cosmochim. Acta 28 (1964) 1273.
5 O.T. Høgdahl, S. Melson and B.T. Bowen, Neutron activation analysis of Lanthanide elements in seawater, Adv. Chem. Ser. 73 (1968) 308.
6 H.D. Holland, The Chemistry of the Atmosphere and Oceans (J. Wiley and Sons, New York, N.Y., 1978).
7 J. Dymond, J.B. Corliss, G.R. Hezth, C.W. Field, E.J. Dasch and H.H. Veeh, Origin of metalliferous sediments from the Pacific Ocean, Geol. Soc. Am. Bull. 84 (1973) 3355.
8 E. Bonatti, T. Kraemer and H. Rydell, Classification and genesis of submarine iron-manganese deposits, in: Ferromanganese Deposits on the Ocean Floor, D.R. Horn, ed. (IDOE Publ. NSF, 1972) 149.
9 D.Z. Piper, Rare earth elements in ferromanganese nodules and other marine phases, Geochim. Cosmochim. Acta 38 (1974) 1007.
10 G. Arrhenius and E. Bonatti, Neptunism and Vulcanism in the ocean, in: Progress in Oceanography 3, M. Sears, ed. (Pergamon Press, New York, N.Y., 1965).
11 K. Bostrom and M.N.A. Petersen, Precipitates from hydrothermal exhalations on the East Pacific Rise, Econ. Geol. 61 (1966) 1258.
12 J.B. Corliss, The origin of metal-bearing submarine hydrothermal solutions, J. Geophys. Res. 76 (1971) 8128.
13 A.M. Ehrlich, Rare earth abundances in manganese nodules, Ph.D. Thesis, Massachusetts Institute of Technology, Cambridge, Mass. (1968).
14 M.L. Bender, Mechanisms of trace metal remocal from the oceans, in: Ferromanganese Deposits on the Ocean Floor, D.R. Horn, ed. (IDOE Publ. NSF, 1972) 73.
15 D.J. DePaolo and G.J.Wasserburg, Inferences about magma sources and mantle structure from variations of $^{143}Nd/^{144}Nd$, Geophys. Res. Lett. 3 (1976) 743.
16 R.K. O'Nions, P.J. Hamilton and N.M. Evensen, Variations in $^{143}Nd/^{144}Nd$ and $^{87}Sr/^{86}Sr$ ratios in oceanic basalts, Earth Planet. Sci. Lett. 34 (1977) 13.
17 P. Richard, N. Shimizu and C.J. Allègre, $^{143}Nd/^{146}Nd$, a natural tracer: an application to oceanic basalts, Earth Planet. Sci. Lett. 31 (1976) 269.
18 D.J. DePaolo and G.J. Wasserburg, The sources of island arcs as indicated by Nd and Sr isotopic studies, Geophys. Res. Lett. 4 (1977) 465.
19 R.K. O'Nions, S.R. Carter, R.S. Cohen, N.M. Evensen and P.J. Hamilton, Pb, Nd and Sr isotopes in oceanic ferromanganese deposits and ocean floor basalts, Nature 273 (1978) 435.
20 G.P. Glasby, The geochemistry of manganese nodules from the Northwest Indian Ocean, in: Ferromanganese Deposits on the Ocean Floor, D.R. Horn, ed. (IDOE Publ. NSF, 1972) 93.
21 G.P. Glasby, Mechanisms of enrichment of the rarer elements in marine manganese nodules, Mar. Chem. 1 (1972-73) 105.
22 W. Raab, Physical and chemical features of Pacific deep sea manganese nodules and their implications to the genesis of nodules, in: Ferromanganese Deposits on the Ocean Floor, D.R. Horn, ed.(IDOE Publ. NSF, 1972) 31.
23 D.S. Cronan, Regional geochemistry of ferromanganese nodules in the World Ocean, in: Ferromanganese Deposits on the Ocean Floor, D.R. Horn, ed. (IDOE Publ. NSF, 1972) 19.
24 D.S. Cronan, Manganese nodules and other ferro-manganese oxide deposits, in: Chemical Oceanography 5, J.P. Riley and R. Chester, eds. (Academic Press, London, 1976) 217.
25 R.K. Sorem and R.H. Fewkes, Internal characteristics, in: Marine Manganese Deposits, G.P. Glasby, ed. (Elsevier, Amsterdam, 1977).
26 M. Bender, W. Broeker, V. Gornitz, U. Middel, R. Kay, S.S. Sun and P. Biscaye, Geochemistry of three cores from the East Pacific Rise, Earth Planet. Sci. Lett. 12 (1971) 425.
27 M.R. Scott, R.B. Scott, P.A. Rona, L.W. Butler and A.J. Norwalk, Rapidly accumulating manganese deposit from the median valley of the Mid-Atlantic Ridge, Geophys. Res. Lett. 1 (1974) 355.
28 W.S. Moore and P.R. Vogt, Hydrothermal manganese crusts from two sites near the Galapagos spreading axis, Earth Planet. Sci. Lett. 29 (1976) 349.
29 E. Bonatti, Metallogenesis at oceanic spreading centers, Annu. Rev. Earth Planet. Sci. 3 (1975) 401.
30 J.B. Corliss, M. Lyle, J. Dymond and K. Crane, The chemistry of hydrothermal mounds near the Galapagos Rift, Earth Planet. Sci. Lett. 40 (1978) 12.
31 J.R. Toth, Deposition of submarine hydrothermal manganese and iron, and evidence for input of volatile elements to the ocean, M.S. Thesis, Oregon State University, Corvallis, Oreg. (1977).
32 D.A. Papanastassiou, D.J. DePaolo and G.J. Wasserburg, Rb-Sr and Sm-Nd chronology and genealogy of mare basalts from the Sea of Tranquility, Proc. 8th Lunar Sci. Conf. (1977) 1639.

33 D.A. Papanastassiou and G.J. Wasserburg, Rb-Sr ages and initial strontium in basalts from Apollo 15, Earth Planet. Sci. Lett. 17 (1973) 324.
34 G.J. Wasserburg, D.A. Papanastassiou, E.V. Nenow and C.A. Bauman, A programmable magnetic field mass spectrometer with on-line data processing, Rev. Sci. Instr. 40 (1969) 288.
35 T.L. Ku, Rates of accretion, in: Marine Manganese Deposits, G.P. Glasby, ed. (Elsevier, Amsterdam, 1977).
36 J. Greenslate, Marine manganese concretion growth rates: Non-radiometric considerations, Geophys. Res. Lett. 5 (1978) 237.
37 M.T. McCulloch and G.J. Wasserburg, Sm-Nd and Rb-Sr chronology of continental crust formation, Science 200 (1978) 1003.
38 S.L. Goldstein and R.K. O'Nions, Nd and Sr isotopes in oceanic ferromanganese deposits, EOS 60 (1979) 281.
39 D.S. Cronan, Deep-sea nodules: distribution and geochemistry, in: Marine Manganese Deposits, G.P. Glasby, ed. (Elsevier, Amsterdam, 1977).
40 K.K. Zelanov, Iron and manganese in exhalations of the submarine Banu Wuhu volcano, Dokl. Akad. Nauk S.S.S.R. 155 (1964) 94.
41 E.J. Dasch, J.R. Dymond and G.R. Heath, Isotopic analysis of metalliferous sediment from the East Pacific Rise, Earth Planet. Sci. Lett. 13 (1971) 175.
42 J.-M. Martin, O. Høgdahl and J.C. Philippot, Rare earth element supply to the ocean, J. Geophys. Res. 81 (1976) 3119.
43 J.-M. Martin and M. Maybeck, Elemental mass-balance of material carried by major world rivers, Mar. Chem. 7 (1979) 173.
44 D.A. Papanastassiou and G.J. Wasserburg, Strontium isotopic anomalies in the Allende meteorite, Geophys. Res. Lett. 5 (1978) 595.

Earth and Planetary Science Letters, 50 (1980) 128–138
Elsevier Scientific Publishing Company, Amsterdam – Printed in The Netherlands

[6]

NEODYMIUM ISOTOPIC VARIATIONS IN SEAWATER [1]

DONALD J. PIEPGRAS and G.J. WASSERBURG
The Lunatic Asylum of the Charles Arms Laboratory, Division of Geological and Planetary Sciences, California Institute of Technology, Pasadena, CA 91125 (U.S.A.)

Received March 3, 1980
Revised version received June 13, 1980

New data for the direct measurement of the isotopic composition of neodymium in Atlantic Ocean seawater are compared with previous measurements of Pacific Ocean seawater and ferromanganese sediments from major ocean basins. Data for Atlantic seawater are in excellent agreement with Nd isotopic measurements made on Atlantic ferromanganese sediments and are distinctly different from the observed compositions of Pacific samples. These results clearly demonstrate the existence of distinctive differences in the isotopic composition of Nd in the waters of the major ocean basins and are characteristic of the ocean basin sampled. The average $\epsilon_{Nd}(0)$ values for the major oceans as determined by data from seawater and ferromanganese sediments are as follows: Atlantic Ocean, $\epsilon_{Nd}(0) \cong -12 \pm 2$; Indian Ocean, $\epsilon_{Nd}(0) \cong -8 \pm 2$; Pacific Ocean, $\epsilon_{Nd}(0) \cong -3 \pm 2$. These values are considerably less than $\epsilon_{Nd}(0)$ value sources with oceanic mantle affinities indicating that the REE in the oceans are dominated by continental sources. The difference in the absolute abundance of ^{143}Nd between the Pacific and Atlantic Oceans corresponds to $\sim 10^6$ atoms ^{143}Nd per gram of seawater. The correspondence between the $^{143}Nd/^{144}Nd$ in seawater and in the associated sediments suggests the possible application of this approach to paleo-oceanography.

Distinctive differences in $\epsilon_{Nd}(0)$ values are observed in the Atlantic Ocean between deep-ocean water associated with North Atlantic Deep Water and near-surface water. This suggests that North Atlantic Deep Water may be relatively well mixed with respect to Nd isotopic composition whereas near-surface water may be quite heterogeneous, reflecting different sources for surface waters relative to deep water. This suggests that it may be possible to distinguish the sources of water masses within an ocean basin on the basis of Nd isotopic composition.

The Nd isotopic variations in seawater are used to relate the residence time of Nd and mixing rates between the oceans.

1. Introduction

The purpose of this research was to determine directly the isotopic composition of neodymium in water from the Atlantic and Pacific Oceans. Due to the radioactive decay of $^{147}Sm(t_{1/2} = 1.06 \times 10^{11}$ years) into ^{143}Nd, crustal rocks have $^{143}Nd/^{144}Nd$ ratios which reflect their age and $^{147}Sm/^{144}Nd$ ratio. Terrestrial differentiation processes have segregated material into oceanic and continental crustal rocks with distinctive Sm/Nd and $^{143}Nd/^{144}Nd$ ratios [1–5]. Typical $\epsilon_{Nd}(0)$ values for mid-ocean ridge basalts (MORB) are +10 ($\epsilon_{Nd}(0)$ values are present-day deviations in parts in 10^4 from $^{143}Nd/^{144}Nd$ for a chondritic reference reservoir [1]). Continental rocks, however, generally have a range in $\epsilon_{Nd}(0)$ from 0 to −30. Rare earth elements (REE) dissolved in seawater must be derived from the weathering and dissolution of oceanic and/or continental rocks or by direct injections from the sub-oceanic mantle during submarine volcanism. The isotopic composition of Nd in seawater will, therefore, reflect the ages and $^{147}Sm/^{144}Nd$ ratios of these possible sources for the REE. The existence of distinct differences in the Nd isotopic composition between waters in the different oceans would have substantial implications for oceanographic studies and in understanding the geochemical behavior of the REE in the marine environment and their transport from the continents and

Division of Geological and Planetary Sciences, California Institute of Technology, Contribution No. 3376 (338).

from oceanic volcanism.

The concentration of Nd in seawater is 2 to 3 × 10^{-12} g/g, and the level of expected variations in the ^{143}Nd abundance corresponds to a difference of only 10^6 atoms per gram of seawater [6]. Such measurements are possible using several liters of seawater utilizing techniques currently available. It should be possible to carry out these measurements on 0.5- to 1-liter samples. To avoid working at these low levels, previous workers have attempted to infer the isotopic composition of Nd in seawater by using samples of chemical precipitates enriched in REE. DePaolo and Wasserburg [3] measured ^{143}Nd/^{144}Nd in a sample of Eocene fish debris which was found to have $\epsilon_{Nd}(0) = -9.2$. This was followed by a more extensive study by O'Nions et al. [7], who measured the Nd isotopic composition in manganese nodules and metalliferous sediments, mostly from the Pacific Ocean. O'Nions et al. reported variations between their Pacific and Indian Ocean samples, but attributed this variation to detrital contamination in their Indian Ocean sample and concluded that the oceans probably had fairly uniform $\epsilon_{Nd}(0)$ values between −2 and −4. Piepgras et al. [6] analyzed a variety of ferromanganese sediments from the Atlantic, Pacific, and Indian Oceans for Nd isotopic composition. They observed inter-ocean variations in the ferromanganese sediments which were quite large, and that samples within each ocean basin produced isotopic compositions of Nd which were characteristic of the ocean from which the sample came. It was shown that these variations could not be accounted for by detrital contamination as suggested by O'Nions et al. [7], but rather, must reflect differences in the dissolved load of Nd in the oceans. To support this conclusion, Piepgras et al. made direct Nd isotopic measurements on four seawater samples from the Pacific Ocean and found the seawater results to be the same as those for Pacific ferromanganese sediments. However, no data were presented on Atlantic Ocean water which would provide a clear test of their hypothesis. In this paper, we will present direct Nd isotopic measurements of Atlantic Ocean waters in an attempt to further clarify the conclusions drawn by Piepgras et al. regarding Nd isotopic variations in seawater.

2. Samples and analytical procedures

Seawater samples used in this study were collected from several locations in the Atlantic and Pacific Oceans (Table 1). Pacific samples, collected by K.

TABLE 1

Sample locations and results of Sm and Nd concentration measurements [a]

Sample	Depth (m)	Location	Nd (10^{-12} g/g)	Sm (10^{-12} g/g)	$\frac{^{147}Sm}{^{144}Nd}$
Atlantic Ocean					
OCE63-1-1	300	29°53′00″N, 76°14′12″W	2.00	0.462	0.140
OCE63-2-1	1000	27°57′14″N, 70°23′25″W	composition run only, see Table 3		
OCE63-2-2	2200	27°57′14″N, 70°23′25″W	2.57	0.516	0.121
OCE63-2-3	3400	27°57′14″N, 70°23′25″W	3.19	0.623	0.118
OCE63-3-1	50	27°01′42″N, 74°20′00″W	composition run only, see Table 3		
OCE63-4-2	4100	27°06′30″N, 74°21′00″W	composition run only, see Table 3		
Pacific Ocean [b]					
SW-1 [c]	1000	36°47′N, 122°48′W	3.23	0.630	0.118
SW-2	2400	36°50′N, 122°50′W	composition run only, see Table 3		
SW-3 [c]	1000	36°47′N, 122°48′W	composition run only, see Table 3		
SW-4a	2500	0°47′20″N, 86°07′21″W	2.24	0.416	0.112
SW-4b (duplicate)	2500	0°47′20″N, 86°07′21″W	composition run only, see Table 3		

[a] Precision is approximately 1% for concentration measurements.
[b] Data for Pacific samples from Piepgras et al. [6].
[c] SW-1 and SW-3 are separate aliquots of the same water sample.

Bruland and L. Gordon, have been described previously by Piepgras et al. Atlantic seawater samples were collected from locations in the Sargasso Sea by D. Piepgras during cruise 63 of the R/V "Oceanus" (Woods Hole) in May 1979. These samples were specifically collected for the purpose of carrying out Nd isotopic analyses. Atlantic samples include two vertical profiles of the water column.

Unfiltered samples of Atlantic seawater were collected using 30-liter Niskin bottles constructed from PVC and with Teflon-coated retraction springs. These were transferred in a closed environment to acid-cleaned polyethylene bottles for storage. Each sample was acidified on board with 100 ml high-purity 10*N* HCl. All samples were analyzed without prior filtration.

Chemical separation of the REE from the seawater samples has been described previously [8,6]. With the exception of two samples, laboratory separation of REE from the seawater samples for Nd isotopic analysis was carried out at Caltech. We studied the techniques at Oregon State University (OSU) under the guidance of Roberta Conard and John Corliss. REE separations for two samples were made at OSU. In samples for which Sm and Nd concentrations were determined, ^{150}Nd and ^{147}Sm spikes were added to the water prior to precipitation of the REE. This should eliminate any errors in concentration measurements due to possible yields of less than 100%.

Sm and Nd were separated from the REE precipitates using procedures described by Papanastassiou et al. [9]. Sample sizes for mass spectrometric analysis were typically 15×10^{-9} g Nd. Total chemistry blanks for Nd including REE precipitation are approximately 1×10^{-10} g. Samples were analyzed at ion beam intensities of $6.0–8.0 \times 10^{-12}$ A. This beam intensity was maintained for 6–8 hours while approximately 150 ratios were obtained for each sample. All isotopes of Nd were measured. For unspiked runs, isotope ratios were normalized to ^{150}Nd/^{142}Nd, and for spiked runs, normalization was to ^{146}Nd/^{142}Nd. Strontium was separated from aliquots of samples for Nd analysis by our standard ion exchange techniques [10] with blank levels of approximately 1×10^{-10} g.

Table 2 presents the results of isotopic measurements for the non-radiogenic isotopes of Nd. Excesses of ^{148}Nd, measured as ^{148}Nd/^{144}Nd, ranging from 15 to 47 ϵ-units were reported by Piepgras et al. [6]. These excesses were attributed to anthropogenic contamination resulting from the use of a ^{148}Nd tracer in the OSU laboratory where the REE precipitations were done. It was, therefore, necessary to carry out the subsequent precipitation procedures in our laboratory at Caltech where no ^{148}Nd is in use. REE were precipitated from two of the Atlantic samples at OSU (see Table 2) in order to observe their techniques. New reagents were used with the exception of Fe_2O_3 powder. ^{148}Nd excesses were still observed in these samples, but they were considerably smaller. However, REE separations made at Caltech using all new reagents have ^{148}Nd abundances that are normal within analytical uncertainties. All other non-radiogenic isotopes have normal abundances within analytical uncertainties as well, regardless of where the precipita-

TABLE 2

ϵ_{Nd} values for non-radiogenic Nd isotopes in Atlantic seawater samples [a]

Sample	ϵ_{142}	ϵ_{145}	ϵ_{146}	ϵ_{148}
OCE63-2-1 [b]	−0.2 ± 0.7	−1.5 ± 1.4	−0.9 ± 0.7	+0.9 ± 1.5
OCE63-2-2 [b]	0.0 ± 0.6	−0.2 ± 1.0	–	+0.3 ± 1.3
OCE63-3-1 [b]	+0.2 ± 0.6	+0.6 ± 1.4	−0.5 ± 1.5	+0.4 ± 2.4
OCE63-4-2 [b]	−0.3 ± 0.6	+0.3 ± 2.3	−0.3 ± 1.5	+1.2 ± 1.8
OCE63-1-1 [c]	−0.3 ± 0.6	−1.0 ± 0.9	–	+8.1 ± 0.7
OCE63-2-3 [c]	−0.5 ± 0.6	−1.0 ± 1.1	–	+2.7 ± 1.8

[a] Normal isotopic abundances have $\epsilon_{Nd} = 0$.
[b] REE separations made at Caltech.
[c] REE separations made at OSU.

tions were done. This clearly demonstrates our ability to detect differences as small as 10^5 atoms per gram of seawater in any isotope measured. It is therefore concluded, as before, that ^{143}Nd measurements were unaffected by this contamination. It should be stressed that the level of contamination which we have detected is too low to have any effect on Nd concentration values determined either by isotope dilution here at Caltech or by neutron activation analysis as done at OSU.

3. Data representation

Representation of Sm and Nd data follows that given by DePaolo and Wasserburg [1]. Measured $^{143}Nd/^{144}Nd$ ratios are presented as fractional deviations in parts in 10^4 (ϵ-units) from $^{143}Nd/^{144}Nd$ in a chondritic uniform reference reservoir (CHUR) as measured today:

$$\epsilon_{Nd}(0) = \left[\frac{(^{143}Nd/^{144}Nd)_M}{I_{CHUR}(0)} - 1\right] \times 10^4$$

where M is the ratio measured in the sample today, and $I_{CHUR}(0) = 0.511836$ is the $^{143}Nd/^{144}Nd$ in the CHUR reference reservoir today. An enrichment factor for $^{147}Sm/^{144}Nd$ in a sample relative to CHUR is given by:

$$f^{Sm/Nd} = \left[\frac{(^{147}Sm/^{144}Nd)_M}{(^{147}Sm/^{144}Nd)_{CHUR}} - 1\right]$$

where $(^{147}Sm/^{144}Nd)_{CHUR} = 0.1967$. Jacobsen and Wasserburg [11] have determined this new value for $(^{147}Sm/^{144}Nd)_{CHUR}$ from recent and more thorough studies of Sm and Nd in chondritic meteorites.

4. Results and discussion

Results of Nd isotopic measurements made on Atlantic and Pacific seawater samples are presented in Table 3. These are also plotted on a histogram in Fig. 1. $\epsilon_{Nd}(0)$ values for seawater samples are plotted on the top level of the histogram, manganese sediments in the middle and the ranges in $\epsilon_{Nd}(0)$ for possible sources of REE in seawater are indicated at the bottom. It is seen that the Atlantic and Pacific seawater samples lie in two distinct groups, the Atlantic samples

TABLE 3

Isotopic compositions of Nd and Sr in seawater samples [a]

Sample	$f^{Sm/Nd}$	$^{143}Nd/^{144}Nd$ [b]	$^{87}Sr/^{86}Sr$ [d]	ϵ_{Nd} (0)	ϵ_{Sr} (0)
OCE63-1-1	−0.288	0.511276 ± 30 [c]	0.70904 ± 5	−10.9 ± 0.6	+64.4 ± 0.9
OCE63-2-1	–	0.511163 ± 22		−13.1 ± 0.4	
OCE63-2-2	−0.385	0.511150 ± 33 [c]		−13.4 ± 0.6	
OCE63-2-3	−0.400	0.511145 ± 27 [c]		−13.5 ± 0.5	
OCE63-3-1	–	0.511346 ± 47		−9.6 ± 0.9	
OCE63-4-2	–	0.511135 ± 37		−13.7 ± 0.7	
SW-1	−0.400	0.511641 ± 36 [c]		−3.8 ± 0.7	
SW-2	–	0.511712 ± 25		−2.4 ± 0.5	
SW-3	–	0.511718 ± 25		−2.3 ± 0.5	
SW-4a	−0.431	0.511706 ± 34 [c]	0.70905 ± 5	−2.5 ± 0.7	+64.5 ± 0.9
SW-4b (duplicate)	–	0.511731 ± 28 [c]		−2.1 ± 0.5	
CIT seawater Sr standard [e]			0.70905 ± 1		+64.6 ± 0.2

[a] Nd data for SW-1, 2, 3, 4 from Piepgras et al. [6]. Reported errors are 2σ of the mean.
[b] Normalized to $^{150}Nd/^{142}Nd = 0.2096$.
[c] Spiked with ^{150}Nd and normalized to $^{146}Nd/^{142}Nd = 0.636151$.
[d] Normalized to $^{86}Sr/^{88}Sr = 0.1194$.
[e] Average of ten analyses [39]. The CIT seawater Sr standard was collected in the Atlantic Ocean in 1963 at 00°03'S, 34°49'W by Woods Hole Oceanographic Institution (V.T. Bowen, personal communication, 1963).

132

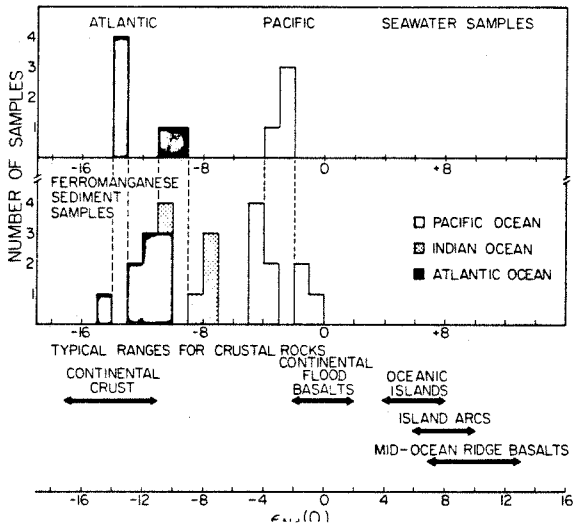

Fig. 1. Histogram of $\epsilon_{Nd}(0)$ values of seawater (top) and ferromanganese sediments (bottom). Possible sources of REE in seawater are referenced below the histogram. Data for Atlantic seawater are from this study. Pacfic seawater data are from Piepgras et al. [6]. Ferromanganese sediment data are from Piepgras et al. [6] and O'Nions et al. [7].

having the most negative $\epsilon_{Nd}(0)$ values. Furthermore, we observe that the range in $\epsilon_{Nd}(0)$ values for the Atlantic samples is the same as that of ferromanganese sediments from this ocean which were previously analyzed. This same type of relationship was made previously by Piepgras et al. [6] for Pacific seawater and ferromanganese sediments. These results clearly demonstrate that there are distinctive Nd isotopic variations between the oceans, and that the ferromanganese sediments closely reflect the Nd isotopic composition in each ocean basin. These results can best be explained by a relatively short residence time for Nd in the oceans relative to the rates of exchange between the oceans, coupled with the necessity for an older ($\gtrsim$1.5 AE) continental source for the Nd in the Atlantic samples relative to Pacific samples. It is remarkable that the ocean water and ferromanganese sediments in each ocean appear to lie in a rather restricted range. This suggests a rather thorough mixing of Nd within each ocean basin which requires better understanding.

Some heterogeneities within the Atlantic waters are indicated. The Atlantic seawater samples shown in Fig. 1 lie in two distinct groups. These differences appear to be related to water depth. Samples from water depths of 1000 m and greater show very uniform $\epsilon_{Nd}(0)$ of -13.5 ± 0.4. Two samples from near-surface depths (300 m and 50 m) have $\epsilon_{Nd}(0)$ values of -10.9 and -9.6 respectively. All deep water samples ($\geqslant$1000 m) reported here are from water masses associated with North Atlantic Deep Water which comprises the bulk of Atlantic Ocean water below approximately 1000 m. Our data suggest that North Atlantic Deep Water may have uniform Nd isotopic composition at least in the western Atlantic Ocean basin. Surface waters on the other hand, may be variable, depending largely on other sources for their observed isotopic compositions. It may therefore be possible to distinguish water masses within an ocean basin on the basis of Nd isotopic composition (e.g., Mediterranean water flowing into the Atlantic). Mechanisms for maintaining isotopic distinctions between water masses are not clear but must be related to the sources of surface waters, the mechanism of their injection into the oceans, and the circulation patterns and mixing mechanisms within the oceans. Clearly, a larger data base is needed to both substantiate these observations and to understand why the isotopic differences exist. The lack of a similar distinction for Pacific samples presented here may be due to inadequate sampling. A correlation between $\epsilon_{Nd}(0)$ and the known variations of temperature and salinity usually used to distinguish different water masses must be explored.

Strontium isotopic measurements have been made on aliquots of some of the seawater samples analyzed in this study. Results of these measurements are given in Table 3. Values for Atlantic and Pacific seawater are identical to the level of precision reported here of ± 1 ϵ-unit. This more precise value is in agreement with the results obtained by previous authors who have shown to a level of approximately ± 10 ϵ-units that the oceans have fairly uniform Sr isotopic composition [12–14]. We note that the total range of uncertainty in these older data is equal to the range of effects observed in the ^{143}Nd abundance. The uniformity of Sr isotopic composition of seawater and the heterogeneity of Nd isotopes reported here clearly indicate the relative residence times of these two elements compared to the rates of mixing in and between the oceans.

The bottom of Fig. 1 indicates typical $\epsilon_{Nd}(0)$ values of possible sources of REE in the oceans. Comparison of seawater and ferromanganese sediment data in Fig. 1 with possible sources clearly shows that substantial contributions from continental sources are necessary to produce the observed $\epsilon_{Nd}(0)$ values in the marine environment. Contributions from continental sources account for at least 80% of the Nd in the Atlantic Ocean and a minimum of 50% in the Pacific Ocean. Differences in the $\epsilon_{Nd}(0)$ values between the Pacific and Atlantic Oceans may be due to differences in the $\epsilon_{Nd}(0)$ values of the continental sources directly supplying REE to each of these oceans and without significant transport of REE between the oceans. Another possibility is that the $\epsilon_{Nd}(0)$ values in the continental sources are the same for both oceans, with the Pacific Ocean having much larger contributions (as much as 50%) from oceanic mantle sources with $\epsilon_{Nd}(0) \cong +10$ [6]. Continental drainage patterns indicate a far greater drainage for fresh water into the Atlantic Ocean relative to the Pacific Ocean [15]. Consideration of this observation suggests a third alternative for explaining Nd isotopic differences between the oceans. The observed $\epsilon_{Nd}(0)$ for Pacific water may reflect a large contribution of oceanic mantle sources ($\epsilon_{Nd}(0) \cong +10$) mixed with Atlantic waters ($\epsilon_{Nd}(0) \cong -12$) with only small, direct contributions into the Pacific basin from older continental sources. However, no marine materials (sediments or water) have been analyzed as yet which have $\epsilon_{Nd}(0)$ values greater than zero. This indicates that submarine volcanic sources (or hydrothermal systems) cannot play a dominant role and suggests that dilution of Nd from continental sources draining into each ocean basin combined with Nd having $\epsilon_{Nd}(0) > 0$ from oceanic mantle sources is the most likely explanation for negative $\epsilon_{Nd}(0)$ values observed in seawater and in associated marine deposits. Some contributions from oceanic mantle sources with positive $\epsilon_{Nd}(0)$ values are likely, however. The best place to look for positive $\epsilon_{Nd}(0)$ values in the marine environment may be in waters emanating from deep-sea hydrothermal springs associated with mid-ocean ridge spreading centers such as those observed at the Galapagos Rift [16] and 21°N on the East Pacific Rise. Evidence for contribution from a mid-ocean ridge type mantle source was found in a hydrothermal crust from the Galapagos region and in a metalliferous sediment from the East Pacific Rise by Piepgras et al. [6]. These workers observed a shift in the $\epsilon_{Nd}(0)$ values of these two samples of approximately 2 ϵ-units from average values for ambient Pacific seawater toward more radiogenic values as would be expected for mid-ocean ridge-type mantle contributions.

Chow and Patterson [17,18] measured the isotopic composition of lead in manganese nodules and other pelagic sediments. Direct measurements of the isotopic composition of lead in seawater has not yet been done because of the low concentrations of lead in seawater (1×10^{-12} g/g in deep waters [19]) and the enormous problems associated with Pb contamination [20]. These concentrations are comparable to those of Nd in seawater, but contamination problems for Nd are small by comparison with lead contamination. In general, leads in Atlantic manganese nodules were more radiogenic than leads in Pacific manganese nodules, consistent with an older continental source for Atlantic leads. Chow and Patterson concluded that the source of lead in pelagic sediments was weathered and relatively ancient continental rocks which contain leads with high $^{238}U/^{204}Pb$ and rather diverse isotopic compositions. They estimated that only about 10% of the lead entering the oceans may have come from young oceanic mantle sources. Nd isotopic variations in the oceans are very similar to patterns of lead isotopic variations found by Chow and Patterson.

REE abundance patterns in seawater indicate that the REE balance is controlled to some extent by precipitation into manganese nodules. This is best indicated by the presence of positive cerium anomalies in nodules and a corresponding negative Ce anomaly in seawater [8,21,22]. Enrichment factors ($f^{Sm/Nd}$) for Sm and Nd have been determined for several seawater samples (Table 3). With the exception of one sample, all have f values between −0.385 and −0.431. One sample (OCE63-1-1) has $f^{Sm/Nd} = -0.288$. Ferromanganese sediments have highly variable f values (−0.197 to −0.415 [6]) with an average of approximately −0.270. (Data from Piepgras et al. [6] has been corrected for the new $(^{147}Sm/^{144}Nd)_{CHUR}$ given in the section on data representation.) The difference in f values between seawater and ferromanganese sediments is of a similar nature but much smaller than the previously observed cerium differences. North American Shale has $f^{Sm/Nd} = -0.390$ [23] and is considered to

represent the average continental source of REE in the oceans. If this is the correct value for $f^{Sm/Nd}$ in the dissolved component of REE runoff from the continents, then steady state considerations indicate that ferromanganese sediments cannot represent the only major sink for REE in the oceans. Clearly, there must be other substantial sedimentary deposits or other possible sinks in the oceans which have f values (and Ce abundances) which would balance their abundances in ferromanganese deposits with those in seawater. Ocean floor basalts could be one possible sink. Ludden and Thompson [24,25] showed enrichments of the REE in weathered basalts by as much as four times over fresh ocean floor basalts. This, however, has not been substantiated by Nd isotopic studies, which show no effects due to seawater alteration on their Nd isotopic composition [7]. It may, however, be necessary to reassess our estimates of f values in the dissolved load of continental runoff. A study of REE and Nd isotopes dissolved in major world rivers offers the best promise of characterizing the sources of REE in the oceans and should provide a starting point for both isotopic composition and f values from continental sources which may be traced through the marine environment.

In an attempt to determine paleo-isotopic variations of Nd in seawater over short time scales (<30 m.y.), we have analyzed surface and central layers of a Pacific manganese nodule (MN139). The growth rate of this nodule has been determined by ^{10}Be and uranium series methods to be 1–2 mm/10^6 years [26]. From this information, the time span represented by this nodule is estimated to be at least 19 m.y. Results of Nd isotopic analyses are given in Table 4. $\epsilon_{Nd}(0)$ values for the 1-mm and 36-mm layers are not significantly different to indicate changes in the REE sources in the Pacific Ocean during this time interval.

TABLE 4

Results of Nd isotopic measurements in two layers of a Pacific Ocean manganese nodule (MN139)

Depth of layer (mm)	$^{143}Nd/^{144}Nd$	ϵ_{Nd} (0)
0– 1	0.511651 ± 20	−3.6 ± 0.4
36–37	0.511597 ± 24	−4.6 ± 0.5

Neodymium isotopic variations over longer time scales would be expected, however. Sr isotopic variations in seawater during Phanerozoic time have been documented [27,28] and a similar approach as used for Sr paleo-isotopic research could be applied to Nd isotopic studies. If one considers the hypothetical Pangean supercontinent, the surrounding Panthalassa Ocean should have had a fairly uniform Nd isotopic composition as there would have been no isolation of water masses by continental barriers which would prevent mixing. Authigenic and pelagic sediments deposited in this ocean should reflect this, and the isotopic compositions may be preserved in the sedimentary record. Isolation of water masses by the formation of interior seas and new oceans (i.e., the Tethys Sea and the Atlantic Ocean) as a result of continental drift and seafloor spreading rearranging the configuration of the continental land masses would produce drainage patterns which are unique for each body of water into which they flow. These isolated seas would have Nd isotopic compositions characteristic of the waters issued from the adjacent continental drainage systems and would not be mixed with the larger oceans. The isotopic composition of individual seas would most likely be different from one water mass to another as observed in today's oceans as well as being different from Panthalassa. The Nd isotopic composition of paleo-seas, if preserved in the sedimentary record, should provide a crude reconstruction of surface drainage patterns and the degree of isolation of ocean basins at times in the geologic past corresponding to changes in the configuration of the continents.

Measurements of Sm and Nd concentrations are given in Table 1. The total range in concentration of Nd reported here for the North Atlantic is from 2.0×10^{-12} g/g in surface waters to 3.2×10^{-12} g/g in deep waters. In general, concentrations increase with depth. This is very similar to concentration profiles of other trace elements (Zn, Cu, Ni, Cd) which have been measured in seawater [29–31]. According to these authors, the depletion of trace metals in surface waters is attributed to uptake of these elements by the activity of organisms. Removal of Nd and other trace elements by particulates must also be considered. From studies of radionuclides of the ^{238}U decay series, it is evident that particulate matter is the major agent for removal of trace elements in surface waters, and probably at

depth in the oceans as well [32].

Similarity of the geochemical behavior of plutonium to that of neodymium suggests that Nd isotopic studies may be useful in environmental research. Pu is a highly radioactive waste product in nuclear reactors and is considered to be very toxic in the environment. Because of some similarities between Nd, Sm, and Pu, it is possible that one could contribute to understanding of the transport of Pu in the river and marine environments by studying the transport characteristics of Nd. However, there are distinct differences between the solution chemistry of Pu and the REE which may seriously complicate the issue. Studies on the oxidation state of Pu in seawater [33,34] indicate that the solution chemistry of this element is complex and not well understood. In addition, there is very little information on the geochemical behavior of Nd in aqueous environments so that a prediction of the coherence of Nd and Pu in natural systems is not yet possible. It would be very useful to do comparative studies of Nd and Pu in rivers and estuaries where the behavior of plutonium is known in order to establish whether correlations between Nd and Pu can be made. If the Nd behavior is found to follow Pu, then knowledge of Nd transportation may be used to predict the behavior of Pu in regions where Pu has not been studied.

It may be possible to use the isotopic data presented here to estimate mixing times between the oceans and the residence time of Nd in the oceans. The steady state equations for a simple two-box model were given by Piepgras et al. [6]. In that work the approach was to use estimates for the residence time of Nd, however, this does not appear to be appropriate. Let us assume two ocean bodies, 1 and 2, each of which is homogeneous. Let them be supplied by net "drainages" from land masses A and B, respectively, with Nd isotopic composition ϵ_A and ϵ_B, where the injection of Nd from oceanic volcanic sources is included. Let J_{13j} and J_{23j} be the rates of deposition of species j (in this case, Nd) from oceans 1 and 2 into a sediment layer, 3, which is the sink for this species. Take $\dot{W}_{12}$ to be the rate of transport and mixing of water from ocean 1 into ocean 2 and ϵ_1, ϵ_2 to be the Nd isotopic composition in ϵ-units in each ocean. Then, the exact solutions at steady state are:

$$0 = \epsilon_A J_{A1j} - \epsilon_1 J_{13j} + (\epsilon_2 C_{2j} - \epsilon_1 C_{1j}) \dot{W}_{12} \qquad (1)$$

for ocean 1.

$$0 = \epsilon_B J_{B2j} - \epsilon_2 J_{23j} - (\epsilon_2 C_{2j} - \epsilon_1 C_{1j}) \dot{W}_{12} \qquad (2)$$

for ocean 2. Here, J_{A1j} and J_{B2j} are the fluxes of species j from land masses A and B into oceans 1 and 2, respectively, and C_{1j}, C_{2j} are the concentrations of j in oceans 1 and 2. Combining equations (1) and (2) gives the coupled equation for both oceans:

$$0 = \epsilon_A J_{A1j} + \epsilon_B J_{B2j} - \epsilon_1 J_{13j} - \epsilon_2 J_{23j} . \qquad (3)$$

We also have at steady state:

$$0 = J_{A1j} - J_{13j} + (C_{2j} - C_{1j}) \dot{W}_{12} \qquad (4)$$

$$0 = J_{B2j} - J_{23j} - (C_{2j} - C_{1j}) \dot{W}_{12} \qquad (5)$$

For the case where $\dot{W}_{12} = 0$ we note that for ocean 1, $J_{A1j} = J_{13j}$ and, therefore, $\epsilon_A = \epsilon_1$. The residence time τ in ocean 1 for species j is:

$$\tau_{1j} = \frac{C_{1j} W_1}{J_{A1j}} \qquad (6)$$

The same relationships also hold for ocean 2. This describes the decoupled situation for isolated ocean basins.

For the case where $\dot{W}_{12}$ *does not* equal zero, we solve equation (4) for J_{13j}, and substituting into equation (1) yields:

$$\frac{C_{2j} W_1}{J_{A1j}} = \frac{(\epsilon_A - \epsilon_1)}{(\epsilon_1 - \epsilon_2)} \frac{W_1}{\dot{W}_{12}} \qquad (7)$$

where W_1 is the mass of water in ocean 1. Insofar as C_{2j} is not greatly different from C_{1j}, we can substitute C_{1j} for C_{2j} and then the left-hand side of equation (7) is equal to the residence time, τ_{1j}, of species j in ocean 1. The Antarctic Circumpolar Current is the dominant flow between the oceans and will be called $\dot{V}_{12}$, with a value between 1 and 1.5×10^8 m^3/s [35–37]. We take the Atlantic ($\sim 3.5 \times 10^{17}$ m^3) to be one ocean and consider the Pacific, Indian, etc., as the second ocean ($\sim 10^{18}$ m^3). Let us assume that the entrainment efficiency for mixing Pacific water into the Atlantic due to the Antarctic Circumpolar Current is q, then:

$$\dot{W}_{12} = q \dot{V}_{12} \qquad (8)$$

Hence:

$$\tau_{1j} = \frac{(\epsilon_A - \epsilon_1) W_1}{(\epsilon_1 - \epsilon_2) q \dot{V}_{12}} \qquad (9)$$

For the Atlantic and Pacific Oceans, $W_1/\dot{V}_{12}$, are about 100 years and 280 years, respectively. The maximum value for the primary input source is $\epsilon_{MORB} \approx +10$ ϵ-units which gives 404 years $\geqslant q \times \tau_{Pac.Nd}$ for the Pacific. For the Atlantic, the primary input source must have $\epsilon_A \geqslant -25$ ϵ-units for a 2.5-AE crustal source or a maximum value near that of North American Shale composite (NAS) with $\epsilon_{NAS} \approx -14.4$ ϵ-units. This gives 26 years $\leqslant q\,\tau_{Atl.Nd} \leqslant 144$ years. In this treatment the mixing efficiency remains unspecified, however, for values of q close to unity, a residence time of less than 100 years is indicated. The existence of more complete data on the isotopic composition of Nd from continental sources and in the different water masses may justify a more complex and realistic treatment of the residence time and mixing problems.

The possibility of complete removal of REE from seawater prior to mixing between water bodies must be considered. This may be accomplished by adsorption onto particulate matter, including fecal pellets of marine organisms [32] which carry the REE into the sedimentary layer. Reactive natural radionuclides such as ^{210}Pb and ^{234}Th are rapidly removed on particles along the traverse of a stream and in the estuarine zone before reaching the open ocean [38]. This may also be true for the REE, but this study and work by Chow and Patterson [17,18] clearly indicate a dominant continental component for the REE and Pb in marine sediments and seawater suggesting that at least some of these very insoluble trace elements are capable of breaching the estuarine environment and entering the oceans. Whether the REE and Pb are carried into the oceans in solution or adsorbed onto particulate matter is unknown and requires further study. More attention must be given to removal mechanisms of the REE from seawater. It is possible that even though mixing of the Atlantic and Pacific Oceans is taking place, the REE are removed by adsorption onto particulates before they are retained by the Antarctic Circumpolar Current (K.K. Turekian, personal communication).

5. Conclusions

We have firmly established that there are distinct Nd isotopic variations in seawater and that the $\epsilon_{Nd}(0)$ values observed are characteristic of the ocean basin sampled. While the difference in the absolute abundance of ^{143}Nd between the Atlantic and Pacific Oceans is only $\sim 10^6$ atoms per gram of seawater, the isotopic effects can be readily measured. The dominant source of REE in the oceans has been shown to be from the weathering of continental crust with relatively small contributions from rocks with oceanic affinities. However, to provide a complete understanding of the sources and transport of REE in the oceans, a more thorough knowledge of continental source of REE to the oceans from river input is necessary.

Isotopic differences observed between surface waters and deep waters in the Atlantic Ocean suggest that the Nd isotopic composition may be useful for distinguishing the injection and mixing of water masses in an ocean basin. If this is substantiated by further data, considerable understanding of the physical mixing processes of water masses may be realized. The existence of Nd isotopic distinctions between different ocean basins has been used to place constraints on the residence time of Nd in seawater. However, more information is needed on the solution chemistry and removal mechanisms of the REE in seawater before any conclusions can be made regarding mixing rates in the oceans on the basis of Nd isotopic composition. The Nd isotopic composition of modern ambient seawater appears to be rather accurately reflected in ferromanganese sediments. It is possible that this may prove to be more generally true for a wider variety of chemical sediments including carbonates. If the isotopic composition of ambient "local" seawater is preserved in ancient chemical sediments, it may be possible to use the ^{143}Nd isotopic abundance in paleo-oceanographic studies and in testing models of the geometrical configurations resulting from continental drift.

Acknowledgements

We would like to thank William Schmitz of the Woods Hole Oceanographic Institution and Jim Price of the University of Rhode Island as well as the crew of the R/V "Oceanus" for providing us with the necessary ship time needed to collect the Atlantic water samples. John Corliss and Roberta Conard of

Oregon State University provided valuable assistance in teaching us how to carry out the bulk chemical preparations of the samples. T.L. Ku of the University of Southern California provided us with the manganese nodule (MN139) analyzed in this study. This work has benefited greatly from lengthy discussions with K. Turekian, who reviewed this manuscript. We also wish to thank C. Wunsch, B. Schaule, and C. Patterson for invaluable comments. The results of this study were first presented in 1979 at the annual meeting of the Geological Society of America, San Diego, California [40]. This research was supported in part by grants from NSF PHY 76-83685 and NASA NGL 05-002-188.

References

1 D.J. DePaolo and G.J. Wasserburg, Nd isotopic variations and petrogenetic models, Geophys. Res. Lett. 3 (1976) 249–252.
2 D.J. DePaolo and G.J. Wasserburg, Inferences about magma sources and mantle structure from variations of $^{143}Nd/^{144}Nd$, Geophys. Res. Lett. 3 (1976) 743–746.
3 D.J. DePaolo and G.J. Wasserburg, The sources of island arcs as indicated by Nd and Sr isotopic studies, Geophys. Res. Lett. 4 (1977) 465–468.
4 P. Richard, N. Shimizu and C.J. Allègre, $^{143}Nd/^{146}Nd$, a natural tracer: an application to oceanic basalts, Earth Planet. Sci. Lett. 31 (1976) 269–278.
5 R.K. O'Nions, P.J. Hamilton and N.M. Evensen, Variations in $^{143}Nd/^{144}Nd$ and $^{87}Sr/^{86}Sr$ ratios in oceanic basalts, Earth Planet. Sci. Lett. 34 (1977) 13–22.
6 D.J. Piepgras, G.J. Wasserburg and E.J. Dasch, The isotopic composition of Nd in different ocean masses, Earth Planet. Sci. Lett. 45 (1979) 223–236.
7 R.K. O'Nions, S.R. Carter, R.S. Cohen, N.M. Evensen and P.J. Hamilton, Pb, Nd and Sr isotopes in oceanic ferromanganese deposits and ocean floor basalts, Nature 273 (1978) 435–438.
8 E.D. Goldberg, M. Koide, R.A. Schmitt and R.H. Smith, Rare earth distributions in the marine environment, J. Geophys. Res. 68 (1963) 4209–4217.
9 D.A. Papanastassiou, D.J. DePaolo and G.J. Wasserburg, Rb-Sr and Sm-Nd chronology and genealogy of mare basalts from the Sea of Tranquility, Proc. 8th Lunar Sci. Conf. (1977) 1639–1672.
10 D.A. Papanastassiou and G.J. Wasserburg, Rb-Sr ages and initial strontium in basalts from Apollo 15, Earth Planet. Sci. Lett. 17 (1973) 324–337.
11 S.B. Jacobsen and G.J. Wasserburg, Sm-Nd isotopic systematics of chondrites, in: Lunar and Planetary Science XI (1980) in press (abstract).
12 G. Faure, P.M. Hurley and J.L. Powell, The isotopic composition of strontium in surface water from the North Atlantic Ocean, Geochim. Cosmochim. Acta 29 (1965) 209–220.
13 E.I. Hamilton, The isotopic composition of strontium in Atlantic Ocean water, Earth Planet. Sci. Lett. 1 (1966) 435–436.
14 V.R. Murthy and E. Beiser, Strontium isotopes in ocean water and marine sediments, Geochim. Cosmochim. Acta 32 (1968) 1121–1126.
15 M.I. Budyko, Climate and Life (Academic Press, New York, N.Y., 1974) 508 pp.
16 J.B. Corliss, J. Dymond, L.I. Gordon, J.M. Edmond, R.P. von Herzon, R.D. Ballard, K. Green, D. Williams, A. Bainbridge, K. Crane and T.H. van Andel, Submarine thermal springs on the Galapagos Rift, Science 203 (1979) 1073–1083.
17 T.J. Chow and C.C. Patterson, Lead isotopes in manganese nodules, Geochim. Cosmochim. Acta 17 (1959) 21–31.
18 T.J. Chow and C.C. Patterson, The occurrence and significance of lead isotopes in pelagic sediments, Geochim. Cosmochim. Acta 26 (1962) 263–308.
19 B. Schaule and C.C. Patterson, Lead concentrations in the northeast Pacific Ocean: evidence for global anthropogenic perturbations (in preparation).
20 C. Patterson, Lead in seawater, Science 183 (1974) 553–554.
21 O.T. Høgdahl, S. Melson and V.T. Bowen, Neutron activation analysis of Lanthanide elements in seawater, Adv. Chem. Ser. 73 (1968) 308–325.
22 D.Z. Piper, Rare earth elements in ferromanganese nodules and other marine phases, Geochim. Cosmochim. Acta 38 (1974) 1007–1022.
23 M.T. McCulloch and G.J. Wasserburg, Sm-Nd and Rb-Sr chronology of continental crust formation, Science 200 (1978) 1003–1011.
24 J.N. Ludden and G. Thompson, Behaviour of rare earth elements during submarine weathering of tholeiitic basalt, Nature 274 (1978) 147–149.
25 J.N. Ludden and G. Thompson, An evaluation of the behavior of the rare earth elements during the weathering of sea-floor basalt, Earth Planet. Sci. Lett. 43 (1979) 85–92.
26 T.L. Ku, A. Omura and P.S. Chen, ^{10}Be and U-series isotopes in manganese nodules from the central North Pacific, in: Marine Geology and Oceanography of the Pacific Manganese Nodule Province, J.L. Bischoff and D.Z. Piper, eds. (Plenum Press, New York, N.Y., 1979) 791–814.
27 Z.E. Peterman, C.E. Hedge and H.A. Fourtelot, Isotopic composition of strontium in seawater throughout Phanerozoic time, Geochim. Cosmochim. Acta 34 (1970) 105–120.
28 E.J. Dasch and P.E. Biscaye, Isotopic composition of strontium in Cretaceous-to-Recent, pelagic foraminifera, Earth Planet. Sci. Lett. 11 (1971) 201–204.
29 M.L. Bender and C. Gagner, Dissolved copper, nickel,

and cadmium in the Sargasso Sea, J. Mar. Res. 34 (1976) 327–339.
30 E.A. Boyle, F.R. Sclater and J.M. Edmond, The distribution of dissolved copper in the Pacific, Earth Planet. Sci. Lett. 37 (1977) 38–54.
31 K.W. Bruland, Oceanographic distributions of cadmium, zinc, nickel, and copper in the North Pacific, Earth Planet. Sci. Lett. 47 (1980) 176–198.
32 K.K. Turekian, The fate of metals in the oceans, Geochim. Cosmochim. Acta 41 (1977) 1139–1144.
33 D.M. Nelson and M.B. Lovett, Oxidation state of plutonium in the Irish Sea, Nature 276 (1978) 599–601.
34 S.R. Aston, Evaluation of the chemical forms of plutonium in seawater, Mar. Chem. 8 (1980) 319–325.
35 H.U. Sverdrup, M.W. Johnson and R.H. Fleming, The Oceans (Prentice-Hall, New York, N.Y., 1942) 1087 pp.
36 W.D. Nowlin, Jr., T. Whitworth III and R.D. Pillsbury, Structure and transport of the Antarctic Circumpolar Current at Drake Passage from short-term measurements, J. Phys. Oceanogr. 7 (1977) 788–802.
37 H.L. Bryden and R.D. Pillsbury, Variability of deep flow in the Drake Passage from year-long current measurements, J. Phys. Oceanogr. 7 (1977) 803–810.
38 K.K. Turekian, The fate of metals in estuaries, in: Estuaries, Geophysics, and the Environment (National Academy of Sciences, Washington, D.C., 1977) 127 pp.
39 D.A. Papanastassiou and G.J. Wasserburg, Strontium isotopic anomalies in the Allende meteorite, Geophys. Res. Lett. 5 (1978) 595–598.
40 D.J. Piepgras and G.J. Wasserburg, Oceanographic implications of Nd isotopic variations in seawater, Geol. Soc. Am. Annu. Meet., San Diego, Calif. (1979) 495 (abstract).

16 July 1982, Volume 217, Number 4556 SCIENCE

Isotopic Composition of Neodymium in Waters from the Drake Passage

Donald J. Piepgras and G. J. Wasserburg

Summary. The isotopic composition of neodymium has been determined in seawaters from the Drake Passage. The Antarctic Circumpolar Current, which controls interocean mixing, flows through this passage. The parameter $\epsilon_{Nd}(0)$, which is a function of the ratio of neodymium-143 to neodymium-144, is found to be uniform with depth at two stations with a value which is intermediate between the values for the Atlantic and the Pacific and indicates that the Antarctic Circumpolar Current consists of about 70 percent Atlantic water. Cold bottom water from a site in the south central Pacific has the neodymium isotopic signature of the waters in the Drake Passage. By using a box model to describe the exchange of water between the Southern Ocean and the ocean basins to the north together with the isotopic results, an upper limit of approximately 33 million cubic meters per second is calculated for the rate of exchange between the Pacific and the Southern Ocean. Concentrations of samarium and neodymium were also determined and found to increase approximately linearly with depth. These results suggest that neodymium may be a valuable tracer in oceanography and may be useful in paleo-oceanographic studies.

Studies of many oceanographic problems have been made with short-lived radionuclides such as ^{3}H, ^{14}C, ^{210}Pb, ^{226}Ra, and ^{230}Th. Because some of these nuclides have half-lives which are short relative to the time scales of the processes studied, they have been used, in conjunction with other hydrographic measurements, as tracers for studying oceanic circulation paths, mixing rates, and the chemical behavior and distribution of associated stable elements in seawater. One problem of interest to oceanographers is that of determining mixing rates in and between the oceans. Estimates of oceanic mixing rates are not well constrained, but ^{14}C studies (*1*) indicate that at least 1500 years are required for the exchange of deep water with the mixed layer. A longer time may be required for the exchange of deep waters between ocean basins. A minimum time of ~ 150 years to mix the world oceans is obtained by assuming that the Pacific Ocean is emptied by the flow through the Drake Passage and mixed with the Atlantic.

The isotopic compositions of elements connected to long-lived radioactive decay may also be useful as tracers for studying large-scale mixing in the oceans and chemical processes affecting their distribution in seawater if the elements have (i) isotopically distinct source regions and (ii) sufficiently short residence times in the water column compared to the time scale of interocean mixing. Analysis of deep-sea sediments showed that the lead, strontium, and neodymium which are supplied to the Atlantic Ocean from crustal rocks are isotopically distinct from those which are injected into the Pacific (*2–4*). The concentration of strontium in seawater [~ 8 parts per million (*5*)] is only a factor of 10 to 50 less than the average abundances in oceanic and continental crust. This indicates that Sr has a relatively long residence time (~ 10^{6} years) in seawater. As a consequence, $^{87}Sr/^{86}Sr$ is uniform in the different oceans (*6, 7*) even though there are several isotopically distinct sources of the element. Therefore, the Sr isotopic composition of seawater is not suitable as a large-scale oceanographic tracer but may be useful as a tracer in the immediate environment of Sr injection. The variations of $^{87}Sr/^{86}Sr$ observed in deep-sea sediments are then ascribed totally to the composition of the detrital material imparted at the source.

In contrast, the concentrations of Nd and Pb in deep waters are about 3×10^{-6} ppm (*4, 7, 8*, and this study) and 1×10^{-6} ppm (*9*), respectively. These are about 10^{-6} to 10^{-7} times the Nd and Pb concentrations in average oceanic and continental crustal rocks, indicating that these elements have very short residence times in seawater. In the case of Nd, the available data on rare earth elements in river water indicate that only a small proportion of the Nd weathered from crustal rocks enters rivers in solution (*5, 10*). However, Nd concentrations in rivers are 10 to 50 times those in seawater, which still implies a relatively short Nd residence time. Significant transport of rare earths to the oceans may be carried from the atmosphere by dust. As a result of the short residence times of Pb and Nd and their distinctive source characteristics, the oceans are not well mixed with respect to Nd and Pb isotopic compositions, indicating their usefulness as oceanographic tracers. In this article we discuss our results for Nd and its use in this way.

The abundance of ^{143}Nd in nature increases through geologic time due to the α-decay of ^{147}Sm (half-life $\tau_{1/2} = 1.08 \times 10^{11}$ years). Chemical fractionation of Sm and Nd during the formation of the continental crust relative to the depleted oceanic mantle results in differences in the isotopic composition of Nd in these lithic sources which reflect their age and Sm/Nd ratio (*11*). The change in ^{143}Nd is commonly related to the nonradiogenic isotope ^{144}Nd, and for convenience, because the differences are small, represented by $\epsilon_{Nd}(0) = [(^{143}Nd/^{144}Nd)_{measured}/(0.511847) - 1] \times 10^{4}$, where 0.511847 is the present-day average $^{143}Nd/^{144}Nd$ ratio in chondritic meteorites (*12*). These values reflect natural variations due only

Donald J. Piepgras is a graduate student in geochemistry and G. J. Wasserburg is John D. MacArthur Professor of Geology and Geophysics in the Division of Geological and Planetary Sciences, California Institute of Technology, Pasadena 91125.

0036-8075/82/0716-0207$01.00/0

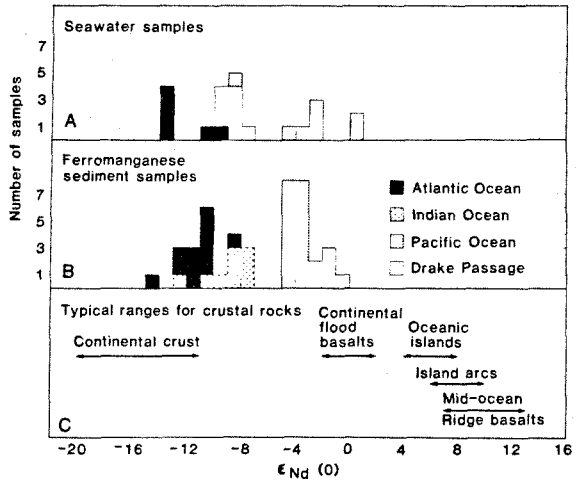

Fig. 1. Histograms of $\epsilon_{Nd}(0)$ values of (A) seawater and (B) ferromanganese sediments. Possible sources of rare earth elements in seawater and their typical $\epsilon_{Nd}(0)$ values are indicated in (C). Note the correspondence between the values of $\epsilon_{Nd}(0)$ in ferromanganese sediments and seawater from the respective oceans. Data for the Drake Passage are from this study. Atlantic seawater data are from Piepgras and Wasserburg (*7*). Pacific seawater data are from this study and Piepgras *et al.* (*4*). Ferromanganese sediment data are from Piepgras *et al.* (*4*), O'Nions *et al.* (*13*), Goldstein and O'Nions (*14*), and Elderfield *et al.* (*52*).

to the radioactive decay of ^{147}Sm and have been corrected for instrumental and natural mass fractionation. Typical ranges of $\epsilon_{Nd}(0)$ are shown in Fig. 1 for a variety of continental and oceanic crustal and mantle reservoirs which are potential sources of rare earth elements to the oceans. Neodymium isotopes measured in seawater would be blends of the Nd isotopic compositions from these reservoirs.

Recent studies have shown distinct differences in the $^{143}Nd/^{144}Nd$ ratio in seawater between the major ocean basins but only small differences within individual ocean basins (*4*, *7*). This was inferred from measurements on ferromanganese sediments and direct measurements on seawater. O'Nions *et al.* (*13*) measured the Nd isotopic composition of ferromanganese sediments in the Pacific and Indian oceans. They observed variations between samples from these two oceans but concluded that this was due to a detrital component in their Indian Ocean sample and that the oceans were a relatively well-mixed reservoir for Nd with a $^{143}Nd/^{144}Nd$ ratio corresponding to $\epsilon_{Nd}(0) \approx -3$. Piepgras *et al.* (*4*) made isotopic measurements on ferromanganese sediments from the Pacific, Indian, and Atlantic oceans. They found differences in the Nd isotopic composition of the ferromanganese sediments and inferred that these differences were characteristic of the individual ocean basins. These results and data from O'Nions *et al.* (*13*) are shown in Fig. 1B. A recent study by Goldstein and O'Nions (*14*) of Nd isotopes in ferromanganese sediments obtained by a similar sampling of the oceans confirmed the results of Piepgras *et al.* (*4*). Direct Nd isotopic measurements in Pacific (*4*) and Atlantic (*7*) seawater (Fig. 1A) showed that the data on ferromanganese sediments for these oceans rather accurately reflected the Nd isotopic composition of modern seawater in the respective basins. There are no direct Nd isotopic measurements in Indian Ocean seawater, but a value for $\epsilon_{Nd}(0)$ can be inferred from ferromanganese sediment data. Estimated average $\epsilon_{Nd}(0)$ values for these oceans are: Pacific Ocean, −3; Indian Ocean, −8; and Atlantic Ocean, −12. Differences in $\epsilon_{Nd}(0)$ were also observed between surface water and deep water (> 1000 meters) in the North Atlantic (*7*) and were attributed to the existence of different sources of Nd. On the average, however, $\epsilon_{Nd}(0)$ was found to be fairly uniform within individual ocean basins in comparison to the differences between basins. A comparison of the $\epsilon_{Nd}(0)$ values with those in possible sources of rare earth elements in seawater (Fig. 1C) shows that the Nd in seawater is derived predominantly from continental sources [$\epsilon_{Nd}(0) < 0$], with only small contributions from sources with oceanic mantle affinity [$\epsilon_{Nd}(0) \approx 10$]. The more negative $\epsilon_{Nd}(0)$ values observed in the Atlantic compared to the Pacific point to the dominance of an old continental source (having a low average Sm/Nd ratio) relative to young, mantle-derived materials for Nd injections into the Atlantic Ocean (see Table 1). This is in agreement with the fact that ~ 70 percent of the world continental drainage flows into the Atlantic.

Geological processes affecting Sm and Nd systematics have also resulted in chemical fractionation of U and Pb, causing differences in Pb isotopic compositions of various lithic sources. Thus there are several possible sources of Pb in seawater with distinctive isotopic compositions, and significant Pb isotopic variations in marine sediments have been observed. Chow and Patterson (*2*) found that Pb in Atlantic ferromanganese sediments was more radiogenic than that in Pacific sediments; this is consistent with an older continental source for the Atlantic Pb and is supported by the Nd results. Direct measurement of Pb isotopes in seawater is difficult because of contamination from industrial Pb during collection and handling of samples (*15*). There are no data for Pb isotopes in deep ocean waters. Data for Pb in seawater from coastal regions (*16*) and Pacific and Atlantic surface waters (*17*) reveal large variations in Pb isotopic composition which can be traced to anthropogenic input. The data base is insufficient for distinguishing Atlantic and Pacific characteristics, but recent anthropogenic effects have probably altered the natural distribution of Pb in surface seawater, making it difficult to compare these seawater measurements and data on deep-sea sediments.

Because of the difference in $\epsilon_{Nd}(0)$ between the Atlantic and Pacific oceans, it should be possible to use the Nd isotopic composition to monitor the exchange and mixing of water between these oceans. The Drake Passage is the only region where significant transport of water can take place between the Atlantic and Pacific basins, and it is presumed that some Pacific water is entrained into the Atlantic after entry through the Drake Passage, where there is a net eastward flow of water at ~ 130 sverdrups (1 Sv = 10^6 cubic meters per second) (*18*). We determined the isotopic composition of Nd in water flowing through the Drake Passage and compared it with results for the Atlantic and Pacific oceans. Because of the eastward transport through the Drake Passage, we expected to find Pacific signatures in the Nd isotopic composition of water flowing through this region. We will put forward some ideas derived from limited data on Nd isotopic variations which appear to be pertinent to problems of large-scale transport and mixing of the oceans. This represents an initial exploration of these problems with a new isotopic tracer. The data presented are a small supplement to the extensive and diverse observations made by oceanographers for many decades and can only be interpreted within the larger framework of oceanographic studies.

Sampling

Samples were collected during leg 11 of cruise 107 of the R.V. *Atlantis II* from vertical profiles of the water column at several stations in the Drake Passage and southeast Pacific. Water samples collected by K. Bruland from vertical profiles at two stations in the Central Pacific and material collected by Bruland from a sediment trap were analyzed in order to extend the data base and study the contribution of particles to the rare earth elements in seawater. Locations and depths for individual samples are shown in Table 1 and Fig. 2. Station 315 is south of the Antarctic polar front, which was located at about 58°S in the Drake Passage during this cruise (*19*). Station 327 is slightly to the north of the polar front.

Ten-liter samples were collected in Teflon-coated GO-FLO water samplers (*20*). They were transferred in a closed environment to cleaned polyethylene storage bottles and acidified with 25 milliliters of high-purity 10 normal HCl. Five-liter subsamples were analyzed for Sm and Nd concentrations and Nd isotopic composition. If only elemental concentrations were needed, the sample size could be reduced to 0.5 liter. The chemical separation of the rare earths and mass spectrometric techniques have been described (*4*, *7*). Samples collected by Bruland in the Central Pacific were filtered before analysis; the Drake Passage samples were analyzed without filtration. Data of Biscaye and Ettriem (*21*) for the North Atlantic show particle concentrations of 5 to 6 micrograms per liter averaged over the entire water column. Assuming an Nd concentration of 30 ppm in the particulate phase, about 200 picograms of Nd per liter of seawater would come from particles. As the total concentration of Nd in seawater is ten times larger than this, we assume it to be primarily in solution. Data for rare earths in pteropod tests in the South Atlantic (*22*) indicate much lower concentrations of Nd (< 5 ppm). The concentration of particles changes with depth, having a maximum at the surface and ocean bottoms which is four to five times the average (*21*). Therefore a substantial percentage of the Nd in near-surface waters could be adsorbed onto particles, but a correlation between particle distributions and Nd concentration changes with depth cannot be made at present. Although we have not compared filtered and unfiltered seawater samples from the same locations, Piepgras *et al.* (*4*) measured filtered and unfiltered samples from different locations in the Pacific and found similar concentrations; an unfiltered sample from the Galápagos Rise area had a slightly lower Nd concentration than filtered samples collected off California. Differences between filtered and unfiltered samples will need more attention and the chemical state of rare earth elements in seawater needs to be better defined, particularly with regard to the role of adsorption on sols and particles.

Results

Results of our Nd isotopic measurements on seawater samples from the Drake Passage and the Central Pacific are shown in Table 1 and Figs. 1 and 3. In addition to isotopic measurements, Sm and Nd concentrations were measured to ± 0.1 percent or better, and these results are shown in Table 1 and Fig. 4. These concentration data are also of importance in considering the origin, transport, and deposition of the rare earth elements.

The results for samples from station 315 show $\epsilon_{Nd}(0)$ values which are fairly uniform at all depths, ranging from −8.4 to −9.1 (Fig. 3A). Concentrations of Sm and Nd at station 315, however, increase with depth by a factor of ~ 2. Figure 4A shows that the Nd concentration increases approximately linearly with depth. The isotopic compositions are independent of concentration at this station. Station 327 is located north of the Antarctic polar front and two samples from this station have $\epsilon_{Nd}(0) = -9.2$ and −8.2. Measurements of the Nd concentration in three samples from station 327 show an approximately linear increase with depth (Fig. 4A) and a concentration gradient about a factor of 3 lower than that observed for station 315. Two samples from stations in the general vicinity of the Drake Passage were also analyzed (Fig. 3A). Station 261 is about 700 kilometers west of the coast of Chile in the Humboldt Plain and far north of the Drake Passage, and the sample has $\epsilon_{Nd}(0) = -7.9$. Station 292 is west of the Drake Passage in the Bellingshausen Plain within the Antarctic Circumpolar Current, and has $\epsilon_{Nd}(0) = -8.2$.

These data show that the Nd isotopic composition of seawater in the Drake Passage and in the deep waters of the Bellingshausen Plain is nearly uniform with depth and geographic location and that the concentration increases linearly with depth. The Antarctic polar front, which divides the transect along which the samples were taken, has no observable effect on the distribution of isotopic compositions of Nd in the Drake Passage. Further, the deep water in the Humboldt Plain northwest of the passage is indistinguishable in terms of Nd iso-

Table 1. Sample locations and results of Sm and Nd measurements in samples from the Drake Passage and the Pacific Ocean. Errors for concentration measurements are ~ 0.05 percent for Nd and ~ 0.1 percent for Sm. The $^{143}Nd/^{144}Nd$ ratio was determined in samples spiked with ^{150}Nd and normalized to $^{146}Nd/^{142}Nd = 0.636151$. Reported errors are 2 standard deviations from the mean.

Station	Depth (m)	Location	Nd (10^{-12} g/g)	Sm (10^{-12} g/g)	$^{147}Sm/^{144}Nd$	$^{143}Nd/^{144}Nd$	$\epsilon_{Nd}(0)$
315	50	61°01′10″S, 62°15′21″W	1.85	0.347	0.109	0.511381 ± 50	−9.1 ± 1.0
	800		2.30	0.432	0.113	0.511388 ± 39	−9.0 ± 0.7
	2000		3.25	0.610	0.113	0.511418 ± 38	−8.4 ± 0.7
	3600		4.21	0.800	0.115	0.511389 ± 21	−8.9 ± 0.4
327	50	56°27′55″S, 66°33′01″W	1.19				
	650		1.31			0.511375 ± 40	−9.2 ± 0.8
	1900		1.93			0.511429 ± 33	−8.2 ± 0.6
261	3900	47°47′33″S, 83°16′31″W	3.69	0.683	0.112	0.511444 ± 26	−7.9 ± 0.5
292	5050	60°54′02″S, 89°24′23″W	4.09			0.511430 ± 28	−8.2 ± 0.6
31	30	20°00′S, 159°59′W	0.411			0.511861 ± 39	0.3 ± 0.8
	2800		2.57			0.511617 ± 36	−4.5 ± 0.7
	4500		3.68			0.511435 ± 29	−8.1 ± 0.6
17	2000	14°41′N, 160°01′W				0.511848 ± 24*	0.0 ± 0.5
Sediment trap	580	36°44′42″N, 122°45′12″W	3.2 ppm†	0.60 ppm†	0.113		

*Unspiked, normalized to 146/142 as above. †The Sm and Nd were determined in an aliquot of the total sample; errors are ~ 5 percent.

topic composition from the waters in the Drake Passage.

Two profiles from the Central Pacific were analyzed (Table 1 and Figs. 3C and 4C). At station 31, $\epsilon_{Nd}(0)$ decreases with depth from 0.3 at 30 m to −8.1 at 4500 m. A sample from 2000 m at station 17 has $\epsilon_{Nd}(0) = 0.0$, compared to a value of −4.5 for a sample at 2800 m at station 31. These results show large differences in Nd isotopic composition between waters within the Central Pacific as well as between the Central Pacific and the Drake Passage. At least in the region of station 31, the Pacific now has a source of Nd near the sea surface which is more radiogenic than indicated by ferromanganese sediment data in this area (*4*, *14*) or from seawater in the eastern Pacific (*7*). Comparison of $\epsilon_{Nd}(0)$ for the Central Pacific sample from 4500 m at station 31 [$\epsilon_{Nd}(0) = -8.1$] with values from the Drake Passage (Fig. 3A) shows them to be indistinguishable and indicates that this sample represents Antarctic Bottom Water underlying middle and deep Pacific water. This bottom water sample was collected with the hope of obtaining northward spreading Antarctic Bottom Water (*23*).

The Nd concentration profile at station 31 (Fig. 4C) shows an approximately linear increase with depth, as observed at other stations. The sample from 30 m has the lowest Nd concentration yet measured in seawater. In addition to the seawater samples, a sample of particulate matter from a sediment trap suspended at a depth of 580 m in the eastern North Pacific was analyzed for Sm and Nd and showed an Nd concentration of ~ 3 ppm and a $^{147}Sm/^{144}Nd$ ratio similar to that in seawater. This low concentration supports the argument that suspended material does not contribute significantly to the Nd content of unfiltered seawater.

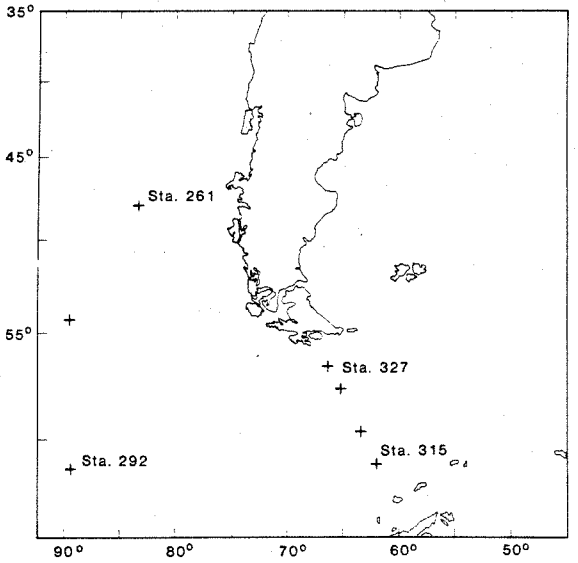

Fig. 2. Map showing locations of water sampling sites in the Drake Passage and southeast Pacific for Nd analysis. Stations for which Nd data were obtained in this study are labeled.

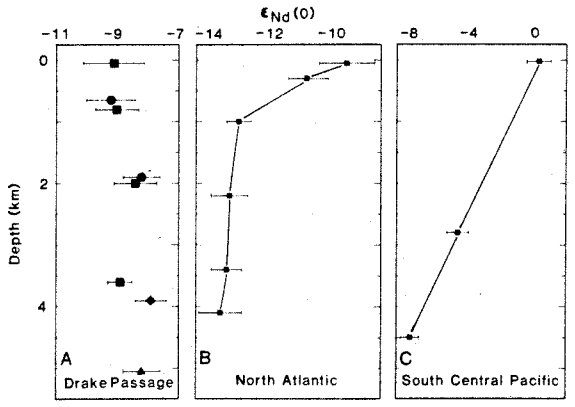

Fig. 3. Value of $\epsilon_{Nd}(0)$ as a function of water depth in (A) the Drake Passage, (B) the North Atlantic, and (C) the south central Pacific (station 31). North Atlantic data are from Piepgras and Wasserburg (*7*). Symbols in (A): (■) station 315; (●) station 327; (◆) station 261; (▲) station 292.

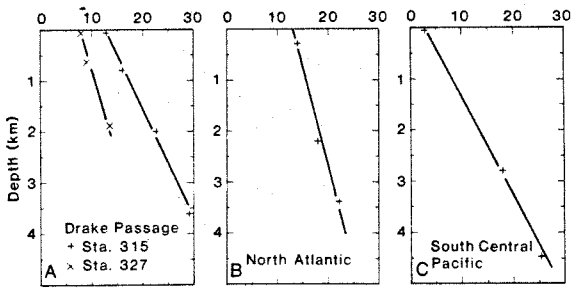

Fig. 4. Neodymium concentration as a function of depth in (A) the Drake Passage (stations 315 and 327), (B) the North Atlantic, and (C) station 31 in the south central Pacific. North Atlantic data are from Piepgras and Wasserburg (*7*). Errors on data points are negligible compared to the size of the symbols.

Discussion

The $\epsilon_{Nd}(0)$ values for the Drake Passage shown in Fig. 1 are close to −9. These values lie in the direction of more ancient continental sources than the Pacific and are far removed from young oceanic mantle-type sources, for which $\epsilon_{Nd}(0) \approx 10$. They are intermediate between North Atlantic and mid-depth Pacific values and closer to the Atlantic values, and they are similar to and possibly slightly lower than the values inferred for the Indian Ocean. From these data we conclude that the water flowing out of the Pacific sector of the Southern Ocean and into the Atlantic sector has Nd which is dominantly of Atlantic or Indian Ocean origin rather than dominantly of Pacific origin.

Bottom waters of the Bellingshausen Plain to the west of the Drake Passage and the Humboldt Plain west of central Chile far north of the Antarctic Convergence have the same $\epsilon_{Nd}(0)$ as the Drake Passage. These data show a coherence in Nd isotopic composition for the Southern Ocean and support its identification as a distinctive water body. In addition, a sample of cold bottom water from the Central Pacific has the same value of $\epsilon_{Nd}(0)$ as the Drake Passage, which identifies this bottom water with a northward

spreading part of the Southern Ocean. These results are in agreement with observations by Reid and Lynn (*24*) and Reid (*25*), who showed that waters having physical oceanographic properties with Atlantic characteristics are preserved in the bottom waters of the Pacific Ocean. The oceanography of the Southern Ocean is reviewed in (*26*). More generally, our results support extensive observations of physical oceanographic properties which identify the Southern Ocean as a distinct water mass that is preserved in the bottom waters over extensive regions of the world ocean [see color plates in Dietrich *et al.* (*27*)].

If we assume that the water in the Drake Passage consists only of mixtures of Atlantic and Pacific seawater (ignoring fresh water) and that the Nd concentrations in these waters are equal, we can estimate the relative amounts of water contributed by these sources which would yield $\epsilon_{Nd}(0) \approx -9$. Using the estimates of $\epsilon_{Nd}(0)$ for the two oceans given earlier, we calculate that about 70 percent of the water flowing through the Drake Passage into the Atlantic Ocean is of Atlantic origin. Allowing for errors in our estimates of $\epsilon_{Nd}(0)$ for the Atlantic and Pacific oceans, a lower limit of at least 50 percent Atlantic water is required to balance the Nd isotopic data for the Drake Passage. The Pacific contribution to the Nd budget appears to be smaller than or equal to that of the Atlantic.

This balance, however, is in disagreement with some views based on physical oceanographic observations which indicate that the Pacific should dominate the water properties of this region. The salinity maximum in the Drake Passage has been reported to be 34.725 per mil (*28*, *29*), which we confirmed at our stations. If we use this salinity maximum for the Drake Passage and Montgomery's (*30*) values for the mean salinities of the Atlantic ($\approx$ 34.9 per mil) and the Pacific ($\approx$ 34.6 per mil), then at least 60 percent of the water in the Drake Passage should be of Pacific origin if only Pacific and Atlantic mixtures are considered. As there is a substantial contribution of fresh water to the Southern Ocean, it is not clear that Drake Passage water may be considered as a mixture of components having the mean salinity characteristics of the Atlantic and Pacific. Heat budget calculations by Hastenrath (*31*) indicate that there must be a net heat transfer from the Pacific to the Atlantic. Stommel (*32*), using data from Hastenrath (*31*), indicates that the South Pacific Ocean supplies heat dominantly by mass flow to the South Atlantic and that the transfer takes place through the Drake Passage [see figure 1 in (*32*)]. However, the available heat budget data are subject to large uncertainties and may not be a reliable indicator of the mass flow and hence the relative sources of water in the Drake Passage. We also considered the possibility that the Nd isotopic compositions in the Southern Ocean are controlled by contributions of dissolved Nd from Antarctica. Using an estimate for the runoff from Antarctica of 0.075 Sv (*33*) and an upper limit of 40 nanograms per liter for the Nd concentration in fresh water (*10*), we estimated the transport of dissolved Nd to the Southern Ocean from Antarctica as 3 grams per second. Gordon (*26*) estimates a rate of exchange of ~ 20 Sv between the Atlantic and Southern oceans. If deep water has an average Nd concentration of 3 ng/liter, the transport of dissolved Nd from the Atlantic to the Southern Ocean is ~ 63 g/sec. The value calculated for the Nd flux from Antarctica is only 5 percent of this, indicating that runoff from Antarctica is not an important source of Nd in the Southern Ocean. We conclude that, unless there is another source of rare earths in the Southern Ocean (possibly atmospheric dust), less than 50 percent of the water flowing through the Drake Passage is from the Pacific and the salt and heat budgets of the region should be reconsidered.

Figure 3 shows rather uniform values of $\epsilon_{Nd}(0)$ with depth in the Drake Passage, in contrast to the data for the North Atlantic (*7*) and the south central Pacific. This indicates that the addition of Nd to Southern Ocean waters from other source regions (Pacific, Indian, and Atlantic oceans) must be slow relative to the residence time and vertical mixing rates of Nd in the Southern Ocean.

The changes in Nd isotopic composition with depth in the profiles from the North Atlantic (Fig. 3B) and south central Pacific (Fig. 3C) indicate that the profiles consist of water layers with different sources. The Atlantic data suggest a sill of water, possibly Mediterranean, underlain by North Atlantic deep water with some mixing. The Pacific data appear to represent mixtures of Southern Ocean water with what we infer to be more typical shallow or intermediate Pacific water. The limited data do not permit better identification of the sources of water in the profiles, but they indicate well-defined isotopic characteristics which may be used to characterize water masses and which are unaffected by changes in salinity due to evaporation or dilution with rainwater.

Box Model

We constructed a six-box model in order to characterize the mixing of the Southern, Atlantic, Indian, and Pacific oceans. Figure 5 depicts the model and the exchange paths. We divided the Southern Ocean into boxes 1, 2, and 3, adjacent to the Atlantic, Indian, and Pacific oceans, represented by boxes 1′, 2′, and 3′, respectively. This subdivision is to account for interactions with the other oceans. [Georgi (*28*) presented data for a series of transects of the Southern Ocean including the Drake Passage and regions south of Africa and New Zealand, which have boundaries between the Southern Ocean and major ocean basins to the north. He showed that salinity in the Southern Ocean decreases from a maximum south of Africa to a minimum in the Drake Passage and interpreted this as resulting from successive interactions with the Atlantic, Indian, and Pacific oceans.] Flow between the Southern Ocean boxes is constrained to be unidirectional and toward the east by the Antarctic Circumpolar Current. Flow between the Southern Ocean and the major oceans to the north is two-directional and constrained to be between adjacent primed and unprimed boxes only, as shown in Fig. 5. If we assume that there are no sources of Nd within the Southern Ocean, then for box 1 at steady state we have

$$0 = \epsilon_3 C_3 \dot{W}_{31} - \epsilon_1 C_1 \dot{W}_{12} + \epsilon_{1'} C_{1'} \dot{W}_{1'1} - \epsilon_1 C_1 \dot{W}_{11} \quad (1)$$

where the ϵ's are the Nd isotopic compositions, the C's are Nd concentrations, and the $\dot{W}_{ij}$ are rates of volume transport of water from box i to box j. Taking the flow of the Antarctic Circumpolar Current to be uniform, we have $\dot{W}_{12} = \dot{W}_{23} = \dot{W}_{31}$. Letting $\dot{W}_{11'} = \dot{W}_{1'1}$ and taking the C's to be approximately equal, we find that Eq. 1 reduces to

$$0 \approx (\epsilon_3 - \epsilon_1)\dot{W}_{12} - (\epsilon_1 - \epsilon_{1'})\dot{W}_{11'} \quad (2)$$

Similarly, for boxes 2 and 3, respectively

$$0 \approx (\epsilon_1 - \epsilon_2)\dot{W}_{12} - (\epsilon_2 - \epsilon_{2'})\dot{W}_{22'} \quad (3)$$

$$0 \approx (\epsilon_2 - \epsilon_3)\dot{W}_{12} - (\epsilon_3 - \epsilon_{3'})\dot{W}_{33'} \quad (4)$$

With the available data base this box model is underdetermined, but we estimated $\epsilon_{Nd}(0)$ for the undetermined Southern Ocean boxes in order to calculate an upper limit for the rate of exchange between the Southern Ocean and the Pacific ($\dot{W}_{33'}$). We may obtain bounds

on the unknown ϵ values by assuming that $0 \leq \dot{W}_{ii'}/\dot{W}_{12} \leq 1$. This yields equations of the form $0 \leq (\epsilon_i - \epsilon_j)/(\epsilon_{j'} - \epsilon_{i'}) \leq 1$. Taking $\epsilon_3 = -9$, $\epsilon_{3'} = -3$, and $\epsilon_{2'} = -8$, we get $-9.25 \geq \epsilon_2 \geq -10.5$. Using this result in Eq. 4 and taking $\dot{W}_{12} = 130$ Sv, we calculate an upper limit of $\dot{W}_{33'} \approx 33$ Sv for the flow rate between the Pacific and Southern oceans. From this we obtain a lower limit of ~ 800 years for the mean time for exchange between the Atlantic and Pacific. The most sensitive parameters are the values of $\epsilon_{Nd}(0)$ associated with the different segments of the Southern Ocean. If the difference between these values goes to zero, then mixing, as constrained by these approximations, cannot occur, and it would be necessary to consider concentration differences as well.

Transport of Neodymium in the Water Column

In contrast to the differences in $\epsilon_{Nd}(0)$ in the water column at different locations, Nd concentration profiles all exhibit approximately linear increases with depth. Samples where the Sm concentration was measured yielded a constant $^{147}Sm/^{144}Nd$ of ~ 0.11 at all levels. This is similar to $^{147}Sm/^{144}Nd$ in continental crustal rocks but much lower than the ratio (0.1967) in a chondritic uniform reservoir (*34*), indicating that the same processes control the vertical transport of Sm and Nd in the water column at the different sampling locations in the oceans.

Potential temperature versus salinity (*T-S*) diagrams for stations 315 and 327 in the Drake Passage and station 31 in the Pacific are shown in Fig. 6. The diagrams for stations 315 and 327 indicate that four components of water having distinctive temperature and salinity characteristics are involved in mixing. In general, these *T-S* relations indicate that lateral as well as vertical transport must play an important role. The points in Fig. 6 representing the sampling for Nd do not lie on straight-line segments in the *T-S* diagram. The samples from the three lower depths at station 315 appear to be on a linear segment, while those from the other stations lie on divergent trends. As pointed out by Craig (*35*), colinearity on the *T-S* diagram is a necessary condition for treating element distribution in terms of a two-component mixing model. However, $\epsilon_{Nd}(0)$ is uniform at stations 315 and 327, indicating only one component of Nd in the water column in the Drake Passage. From the *T-S* diagram for station 31 we infer that there are at least four components of water involved in mixing at this location, whereas the $\epsilon_{Nd}(0)$ data indicate mixing of two components of Nd, one with $\epsilon_{Nd}(0) \approx -8$ and the other with $\epsilon_{Nd}(0) \approx 0$. The different *T-S* relations at these stations are also in contrast with the linear Nd concentration profiles at all stations analyzed. These observations indicate that the distribution and transport of Nd in seawater are not dependent on the factors that directly influence local temperature and salinity variations.

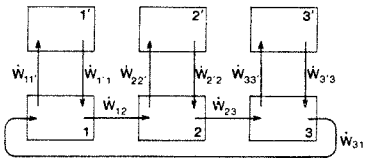

Fig. 5. Box model for mixing in the Southern Ocean. The Southern Ocean is divided into three boxes (1, 2, and 3) adjacent to the Atlantic (1'), Indian (2'), and Pacific (3') oceans, respectively.

Any explanation for the observed distribution of Nd in the water column must be considered in the context of the numerous studies of other trace element distributions in the oceans. We therefore outline some key observations related to the problem of trace element transport. A number of stable elements (Zn, Ni, Cd, and Ba) increase with depth in a complex fashion (*36–39*). For example, Ba increases to a maximum at about 2 km and then remains relatively constant or decreases toward the bottom (*38, 39*). These elements are found to correlate with nutrient profiles in the oceans, indicating that their distribution is controlled by uptake into planktonic organisms in surface waters with subsequent re-solution in deep waters. The sources of the individual elements and their transport have been subjects of study for three decades. A key to some of the transport processes that may occur in the marine environment has come from study of abundances of the decay products of U and Th (*40*). These decay series are important because some of the nuclides are at extremely low concentrations due to their removal from solution. For example, from the near absence of ^{232}Th in seawater and the presence of the daughter ^{228}Th ($\tau_{1/2}$ = 1.9 years) it is inferred that the more soluble intermediate daughter ^{228}Ra ($\tau_{1/2}$ = 5.7 years) is transported from coastal waters into the surface ocean waters to provide the source of ^{228}Th with a lateral transport time scale of ~ 20 years. Dissolved U has a relatively high and uniform concentration in seawater (~ 3 μg/liter) (*41*), but one of its daughters, ^{230}Th ($\tau_{1/2} = 7.7 \times 10^4$ years), has a very low concentration, well below secular equilibrium (~ 10^{-3}) (*42*). Recent experiments (*43*) showed the dissolved ^{230}Th to increase regularly with depth in an approximately linear manner. These data can be explained by constant production of ^{230}Th throughout the water column from ^{238}U decay [^{238}U ($\tau_{1/2} = 4.5 \times 10^9$ years) → ^{234}Th ($\tau_{1/2}$ = 24 days) → ^{234}U ($\tau_{1/2} = 2.4 \times 10^5$ years) → ^{230}Th ($\tau_{1/2} = 7.7 \times 10^4$ years) → ^{226}Ra ($\tau_{1/2} = 1.6 \times 10^3$ years)] with subsequent adsorption of ^{230}Th on particulate matter, which settles to the bottom (*40, 42*). For some nuclides from this decay series such as ^{210}Pb there are direct observations of the proportions associated with particles (~ 10 percent) and in solution (~ 90 percent) (*44*). In addition to scavenging from solution and particle settling, there is evidence for element transport from the sediments into the water column over at least a few hundred meters from the bottom. This is demonstrated by the presence of excess ^{222}Rn ($\tau_{1/2}$ = 3.8 days) (*45*) as well as ^{228}Ra and ^{228}Th (from decay of dissolved ^{228}Ra) (*46*) in the lower levels of the deep sea. There is in general no direct connection between the processes controlling these short-lived nuclides and the more abundant stable elements; however, Chan *et al.* (*39*) showed an excellent correlation between Ra (~ 6×10^{-14} grams per kilogram) and Ba (~ 10^{-5} grams per kilogram) in regions above a bottom layer for basins in widely different areas.

These observations indicate that the concentration and isotopic composition of Nd may depend on scavenging by particles, re-solution from particles, and re-solution from sediments at the sea bottom. The regular change of Nd concentration with depth [similar to that of Cu (*36*) and ^{230}Th (*43*)] cannot be due simply to scavenging as there is no steady source such as that for ^{230}Th. Removal of Nd from near-surface waters by settling particles with continuous re-solution during settling coupled with vertical transport or circulation might provide a net effective local source. Some workers have formally used an arbitrary constant source function for elements such as Ba (which has a long residence time) in the water column in order to explain the concentration as a function of depth: The source term presumably results from dissolution of particles ($CaCO_3$) containing Ba, a mechanism suggested by Turekian *et al.* (*22*). We do not find an a priori basis for assuming a

uniformly distributed source for Nd (which has a short residence time) in the water column. In addition, if the time scale for removal is short [20 years, as indicated from Th data (*43*)], this would result in rapid removal of Sm and Nd during the history of a water mass.

Theoretical analyses of element distribution in ocean water due to these processes are primarily based on transport models that involve diffusion (with eddy diffusion parameter $\kappa \sim 1$ square centimeter per second and upward advective velocity $w \sim 10^{-5}$ cm/sec). These phenomenological transport models are based on the view that there is an upward component of velocity in the ocean from the cold deep waters that balances the downward diffusion of heat from the warm surface layers (*47*). This approach has led to a set of abyssal recipes (*48*). Craig has discussed this class of models (*35*) as well as the problem of scavenging for the case of Cu (*49*).

The usual form of the one-dimensional equations at steady state for θ (either temperature or salinity) is

$$0 = \kappa \frac{\partial^2 \theta}{\partial z^2} - w \frac{\partial \theta}{\partial z} \quad (5)$$

For the concentration of species i in solution (C_i) the equation becomes

$$0 = \kappa \frac{\partial^2 C_i}{\partial z^2} - w \frac{\partial C_i}{\partial z} - (\lambda_i + \psi_i) C_i + P_i \quad (6)$$

Here z is the height upward from the ocean bottom, P_i is the local generic production rate of species i, and $\lambda_i + \psi_i$ are the decay constant plus adsorption rate. These transport equations, which require layers at the upper and lower boundaries to satisfy continuity, have been used extensively as a basis for discussing observational data. By fitting either temperature or salinity to Eq. 5 over regions where temperature and salinity are linearly correlated, the parameter (κ/w) is determined, and by using the known concentration of species i the source term P_i can be explicitly calculated (*35*) (it is usually taken to be a constant).

In explicitly considering transport with sequestering on particles that are raining out, we derive the one-dimensional equation for species i

$$\frac{\partial C_i}{\partial \tau} + \frac{\partial m_p C_{pi}}{\partial \tau} = \kappa \frac{\partial^2 C_i}{\partial z^2} - w \frac{\partial C_i}{\partial z} + \frac{\partial m_p C_{pi} v}{\partial z} - \lambda_i (C_i + m_p C_{pi}) + P_i \quad (7)$$

where C_{pi} is the concentration of i on particulate matter, m_p is the mass of particles per gram of seawater, and v is their characteristic settling velocity in the rising advective stream. We have neglected particle diffusion, but if it were included C_i in the first term on the right should be $C_i + m_p C_{pi}$. For ^{234}Th, which is dominantly associated with particles, $C_i \rightarrow 0$ (*50*).

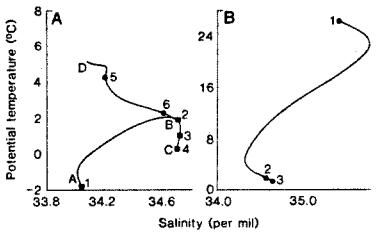

Fig. 6. Potential temperature versus salinity diagrams for stations 315, 327, and 31. (A) Drake Passage. Station 315 follows points ABC. Boxes labeled 1 to 4 correspond to Nd samples at 50, 800, 2000, and 3600 m, respectively. Station 327 follows points DB, and circles labeled 5 and 6 correspond to Nd samples at 650 and 1900 m, respectively. The *T-S* data are for 50-m intervals from CTD casts. (B) South central Pacific, station 31. Points 1 to 3 correspond to Nd samples at 30, 2800, and 4500 m, respectively. The shape of this curve is inferred from eight *T-S* measurements made at this station.

If there is quasi-equilibrium partitioning between the adsorbed and dissolved species of the form $C_{pi}/C_i = \alpha$ (a constant), the settling velocity v is constant, there is no true in situ source, and the species are stable, then the steady-state equation becomes

$$0 = \kappa \frac{\partial^2 C_i}{\partial z^2} - w \frac{\partial C_i}{\partial z} + \alpha v \frac{\partial m_p C_i}{\partial z} = \frac{\partial}{\partial z} \left[\kappa \frac{\partial C_i}{\partial z} - (w - \alpha v m_p) C_i \right] \quad (8)$$

The expression in brackets is the downward net flux, which is constant at steady state.

Comparison of this result with Eq. 6 shows that the coefficient of $\partial C_i/\partial z$ in Eq. 8 is $-w + \alpha v m_p$ rather than $-w$. If $\alpha v m_p$ is comparable to w, then the advective velocity terms are not the same for species whose transport involves particle settling and the transport equations for salinity and temperature. In such cases Eqs. 5 and 8 may be decoupled. If we use a Stokes velocity of $8 \times 10^{-5} D^2$ cm/sec for particles of diameter D micrometers and take $\alpha m_p \sim 10^{-1}$ (9 percent adsorbed on particles), then for 3-μm particles we get $\alpha v m_p \sim 7 \times 10^{-5}$ cm/sec. The advective velocity in Eq. 5 is usually taken as $w \sim 10^{-5}$ cm/sec. It follows that if only a few percent is adsorbed in equilibrium on grains, the settling term may govern the transport. The characteristic length then becomes $\kappa/\langle(\alpha v m_p - w)\rangle$ ($\langle\ \rangle$ indicates the average value). For attenuation by a factor of e for a depth of 4 km and $\kappa \sim 1$ cm^2/sec we obtain $\langle(\alpha v m_p - w)\rangle \sim 3 \times 10^{-6}$ cm/sec. For $(\alpha v m_p - w) C_i$ = constant, the concentration is a linear function of depth, and the distribution of particles is hyperbolic. According to this model (Eq. 8), the Nd data require that the net downward flux be less than $(\alpha v m_p - w) C_i$. If equilibration is not achieved, then C_{pi}/C_i is not constant and the falling grain may continue to sequester material from solution. In this case $d(m_p C_{pi}) = -\psi_i m_p C_i dz/v$ if the particulate mass is constant. Substituting this in Eq. 7 at steady state gives a result analogous to Eq. 6 and does not yield an advective term that competes with w. The Nd isotopic and concentration data are not yet sufficient to test these models or to establish whether linear mixing requires linear behavior between T and S. It appears that, in order to understand the distribution of Nd and related elements, a detailed comparison of experimental data, taking into account the vertical distribution of particles, will be needed to assess the validity of the class of models described by Eq. 7.

If Nd and other rare earth elements were injected from bottom sediments, they would be distributed over a scale of only a few hundred meters from the sea floor on an appropriate short time scale, as indicated by the transport coefficients from Rn and Ra studies (*45*, *46*). The time for Nd injected from the bottom to reach the surface must be ~ 1000 years. The isotopic differences observed in some profiles indicate preservation of intrinsic differences in Nd. In contrast, the regular behavior of the Nd concentration suggests continuous mixing or exchange between surface and bottom waters on a short time scale. A complex transport mechanism involving precipitation of Nd from solution, scavenging by particles, and re-solution of bottom materials is suggested above. Layering of mid-depth water masses is known to occur in the ocean and must play an important role. A large contribution from the sediments would imply that the observed Nd in solution was not directly related to the dissolved Nd from the continents but resulted from a dissolution-precipitation-saltation process. Such considerations could alter the model of simple uniform ocean basins that we proposed on the basis of the isotopic composition data.

Conclusions

Water flowing through the Drake Passage has an average Nd isotopic composition corresponding to $\epsilon_{Nd}(0) \approx -9$. The $\epsilon_{Nd}(0)$ values reported here indicate that one-half to two-thirds of the Nd in these waters is of Atlantic origin and at most one-half is of Pacific origin. These sources of the water mass do not agree with those based on the estimated salt budget for the Drake Passage or on heat transport considerations. From the Nd data reported here, the Antarctic Circumpolar Current is dominated by Atlantic water, which it spreads to other ocean basins and recirculates back into the Atlantic. These observations are in qualitative agreement with those of Reid and Lynn (*24*) and Reid (*25*), who inferred the presence of Atlantic water in the Indian and Pacific oceans from physical properties of the water and concluded that the Antarctic Circumpolar Current spreads the Atlantic water to other ocean basins, but made no quantitative estimates of the amount of Atlantic water in the Circumpolar Current.

Concentrations of Sm and Nd in the water column show an approximately linear increase with depth in the Drake Passage and at other locations. This is similar to results for Cu (*36*). The concentration gradient requires some means of transport and replenishment of these elements in the water column on a short time scale. This transport appears to be governed by settling and re-solution of particles. If replenishment of ND in the bottom waters is due to re-solution of the underlying sediments, the Nd isotopic composition must reflect materials previously deposited rather than recent continental drainage. The concentration data are difficult to explain by the simple model used to discuss the isotopic data. Further advances will require an understanding of transport characteristics of rare earth elements in the ocean.

An upper limit of 33 Sv for the rate of exchange between the Pacific and Southern oceans has been calculated on the basis of a box model describing Nd transfer between the oceans. At present, the model is underdetermined, but with more data for the Nd isotopic composition of Southern Ocean waters, it may be possible to put further constraints on the rates of exchange between the Southern Ocean and ocean basins to the north.

Insofar as the differences observed in $\epsilon_{Nd}(0)$ between the Atlantic and the Pacific reflect the rate of water exchange between these oceans, then this must be controlled by the flow through the Drake Passage. We may imagine that as the passage was opened in late Oligocene time (*51*), the degree of isotopic difference decreased. If the Nd isotopic composition of seawater is preserved in sediments over geologic time, it may be possible to study the degree of isolation of earlier oceans under different arrangements of the continents. This has considerable interest in terms of determining the disposition of earlier ocean basins and may possibly be used to trace the flow of major paleo-ocean currents. In the case of the Southern Ocean, we believe that the dominant source must be North Atlantic deep water. The changes of such flow over the past few million years may be of use in understanding climate change.

References and Notes

1. H. Craig, *Proc. 2nd U.N. Int. Conf. Peaceful Uses At. Energy* **18**, 358 (1958); in *Earth Science and Meteoritics*, J. Geiss and E. D. Goldberg, Eds. (North-Holland, Amsterdam, 1963), p. 103; W. S. Broecker, R. Gerard, M. Ewing, B. Heezen, *J. Geophys. Res.* **65**, 2903 (1960).
2. T. J. Chow and C. C. Patterson, *Geochim. Cosmochim. Acta* **17**, 21 (1959); *ibid.* **26**, 263 (1962).
3. E. J. Dasch, *ibid.* **33**, 1521 (1969).
4. D. J. Piepgras, G. J. Wasserburg, E. J. Dasch, *Earth Planet. Sci. Lett.* **45**, 223 (1979).
5. H. D. Holland, *The Chemistry of the Atmosphere and Oceans* (Wiley, New York, 1978); G. W. Brass and K. K. Turekian, *Earth Planet. Sci. Lett.* **34**, 165 (1977); K. K. Turekian, in *Handbook of Geochemistry*, K. H. Wedepohl, Ed. (Springer-Verlag, New York, 1969), vol. 1, chap. 10.
6. G. Faure, P. M. Hurley, J. L. Powell, *Geochim. Cosmochim. Acta* **29**, 209 (1965); V. R. Murthy and E. Beiser, *ibid.* **32**, 1121 (1968); E. I. Hamilton, *Earth Planet. Sci. Lett.* **1**, 435 (1966).
7. D. J. Piepgras and G. J. Wasserburg, *Earth Planet. Sci. Lett.* **50**, 128 (1980).
8. E. D. Goldberg, M. Koide, R. A. Schmitt, R. H. Smith, *J. Geophys. Res.* **68**, 4209 (1963); O. T. Høgdahl, S. Melson, V. T. Bowen, *Adv. Chem. Ser.* **73**, 308 (1968); A. Masuda and Y. Ikeuchi, *Geochem. J.* **13**, 19 (1979).
9. B. K. Schaule and C. C. Patterson, in *Proceedings of an International Experts Discussion on Lead*, M. Branica, Ed. (Pergamon, Oxford, 1978), p. 31; *Earth Planet. Sci. Lett.* **54**, 97 (1981).
10. J.-M. Martin and M. Meybeck, *Mar. Chem.* **7**, 173 (1979).
11. D. J. DePaolo, *Eos* 62, 137 (1981).
12. ——— and G. J. Wasserburg, *Geophys. Res. Lett.* **3**, 249 (1976).
13. R. K. O'Nions, S. R. Carter, R. S. Cohen, N. M. Evensen, P. J. Hamilton, *Nature (London)* **273**, 435 (1978).
14. S. L. Goldstein and R. K. O'Nions, *ibid.* **292**, 324 (1981).
15. C. Patterson, *Science* **183**, 553 (1974).
16. ———, D. M. Settle, B. Glover, *Mar. Chem.* **4**, 305 (1976); V. J. Stukas and C. S. Wong, *Science* **211**, 1424 (1981).
17. A. Ng, B. Schaule, K. Bruland, C. C. Patterson (unpublished manuscript, 1981).
18. H. L. Bryden and R. D. Pillsbury, *J. Phys. Oceanogr.* **7**, 803 (1977); W. D. Nowlin, Jr., T. Whitworth III, R. D. Pillsbury, *ibid.*, p. 788.
19. The position of the polar front was determined from expendable bathythermograph and conductivity, temperature, depth (CTD) data taken during the cruise by M. S. McCartney (in preparation).
20. K. W. Bruland, R. P. Franks, G. A. Knauer, J. H. Martin, *Anal. Chim. Acta* **105**, 233 (1979).
21. P. E. Biscaye and S. L. Ettriem, *Mar. Geol.* **23**, 155 (1977).
22. K. K. Turekian, A. Katz, L. Chan, *Limnol. Oceanogr.* **18**, 240 (1973).
23. K. Bruland, personal communication.
24. J. L. Reid and R. L. Lynn, *Deep-Sea Res.* **18**, 1063 (1971).
25. J. L. Reid, in *Evolution of Physical Oceanography*, B. A. Warren and C. Wunsch, Eds. (MIT Press, Cambridge, Mass., 1981), p. 70.
26. A. L. Gordon, *Antarct. Oceanol. I* **15**, 169 (1971).
27. G. Dietrich, K. Kalle, W. Krauss, G. Siedler, *General Oceanography: An Introduction* (Wiley, New York, ed. 2, 1980).
28. D. T. Georgi, *J. Geophys. Res.* **86**, 6556 (1981).
29. A. E. Bainbridge, Ed., *GEOSECS Atlantic Expedition*, vol. 2, *Sections and Profiles* (National Science Foundation, Washington, D.C., 1980).
30. R. B. Montgomery, *Deep-Sea Res.* **5**, 134 (1958).
31. S. Hastenrath, *J. Phys. Oceanogr.* **10**, 159 (1980).
32. H. Stommel, *Proc. Natl. Acad. Sci. U.S.A.* **77**, 2377 (1980).
33. V. I. Kozoun *et al.*, *World Water Balance and Water Resources of the Earth* (U.S.S.R. National Committee for the International Hydrological Decade, Leningrad, 1974).
34. S. B. Jacobsen and G. J. Wasserburg, *Earth Planet. Sci. Lett.* **50**, 139 (1980).
35. H. Craig, *J. Geophys. Res.* **74**, 5941 (1969).
36. E. A. Boyle, F. R. Sclater, J. M. Edmond, *Earth Planet. Sci. Lett.* **37**, 38 (1977); K. W. Bruland, *ibid.* **47**, 176 (1980).
37. F. R. Sclater, E. Boyle, J. M. Edmond, *ibid.* **31**, 119 (1976); E. A. Boyle, F. Sclater, J. M. Edmond, *Nature (London)* **263**, 42 (1976); K. W. Bruland, G. A. Knauer, J. H. Martin, *Limnol. Oceanogr.* **23**, 618 (1978).
38. T. J. Chow and E. D. Goldberg, *Geochim. Cosmochim. Acta* **20**, 192 (1960); K. K. Turekian and D. G. Johnson, *ibid.* **30**, 1153 (1966); K. Wolgemuth and W. S. Broecker, *Earth Planet. Sci. Lett.* **8**, 372 (1970); M. P. Bacon and J. M. Edmond, *ibid.* **16**, 66 (1972); M. Bernat, T. Church, J. C. Allègre, *ibid.*, p. 75.
39. L. H. Chan, J. M. Edmond, R. F. Stallard, W. S. Broecker, Y. C. Chung, R. E. Weiss, T. L. Ku, *Earth Planet. Sci. Lett.* **32**, 258 (1976).
40. "GEOSECS collected papers: 1972–1973," H. Craig, Ed., *Earth Planet. Sci. Lett.* **23**, 1 (1974); "GEOSECS collected papers: 1973–1976," H. Craig and K. K. Turekian, Eds., *ibid.* **32**, 217 (1976).
41. E. Rona, L. O. Gilpatrick, L. M. Jeffrey, *Trans. Am. Geophys. Union* **37**, 697 (1956); K. K. Turekian and L. H. Chan, in *Activation Analysis in Geochemistry and Cosmochemistry*, A. O. Brunfelt and E. Steinnes, Eds. (Universitetsforlaget, Oslo, 1971), p. 311; B. S. Amin, S. Krishnaswami, B. L. K. Somayajulu, *Earth Planet. Sci. Lett.* **21**, 342 (1974).
42. W. S. Moore and W. M. Sackett, *J. Geophys. Res.* **69**, 5401 (1964).
43. Y. Nozaki, Y. Horibe, H. Tsubota, *Earth Planet. Sci. Lett.* **54**, 203 (1981).
44. B. L. K. Somayajulu and H. Craig, *ibid.* **32**, 268 (1976).
45. J. L. Sarmiento, H. W. Feely, W. S. Moore, A. E. Bainbridge, W. S. Broecker, *ibid.* **32**, 357 (1976); R. M. Key, N. L. Guinasso, Jr., D. R. Schink, *Mar. Chem.* **7**, 221 (1979).
46. W. S. Moore, *J. Geophys. Res.* **74**, 694 (1969); J. K. Cochran, *Earth Planet. Sci. Lett.* **49**, 381 (1980).
47. H. Stommel, *Deep-Sea Res.* **5**, 80 (1958).
48. W. H. Munk, *ibid.* **13**, 707 (1966).
49. H. Craig, *Earth Planet. Sci. Lett.* **23**, 149 (1974).
50. S. G. Bhat, S. Krishnaswamy, D. Lal, Rama, W. S. Moore, *ibid.* **5**, 483 (1969).
51. J. P. Kennett, *J. Geophys. Res.* **82**, 3843 (1977).
52. H. Elderfield, C. J. Hawkesworth, M. J. Greaves, *Geochim. Cosmochim. Acta* **45**, 513 (1981).

53. We thank M. S. McCartney of Woods Hole Oceanographic Institution for providing us with the ship time needed to collect the Drake Passage samples and for supplying the results of the CTD measurements made during the cruise. We appreciate the cooperation of the crew of the R.V. *Atlantis II* during the cruise. We are grateful to K. Bruland for his generous efforts to supply us with the Pacific samples and his continuous support for our work. Numerous discussions with him have greatly aided us in this work. This manuscript has also benefited from discussions with W. S. Broecker, P. Goldreich, A. Piola, J. L. Reid, M. C. Stordal, and C. Wunsch. We thank K. K. Turekian for his careful and scholarly review and for calling our attention to the importance of "particulates" in the transport of trace elements in the marine environment. Comments of an anonymous reviewer have also improved this article. This research was supported in part by grants NSF OCE-8108595, NASA NGL 05-002-188, and NSF PHY 79-23628. Division contribution number 3639 (397). This study was carried out at the Lunatic Asylum of the Charles Arms Laboratory.

JOURNAL OF GEOPHYSICAL RESEARCH, VOL. 88, NO. C10, PAGES 5997–6006, JULY 20, 1983

Influence of the Mediterranean Outflow on the Isotopic Composition of Neodymium in Waters of the North Atlantic

D. J. PIEPGRAS AND G. J. WASSERBURG

The Lunatic Asylum of the Charles Arms Laboratory, Division of Geological and Planetary Sciences, California Institute of Technology, Pasadena, California 91125

The isotopic composition of neodymium in the water column of the eastern North Atlantic near the Strait of Gibraltar has been determined for several depths. The data show that the Mediterranean outflow results in a significant shift in $\varepsilon_{Nd}(0)$ toward more radiogenic values of $^{143}Nd/^{144}Nd$ in the water column at a 1000-m depth. This corresponds to a depth in the neighborhood of the salinity maximum associated with the Mediterranean outflow. The core of the Mediterranean outflow gives $\varepsilon_{Nd}(0) = -9.8$, as compared to $\varepsilon_{Nd}(0) \approx -12$ in overlying and underlying waters, demonstrating that the Mediterranean waters are distinct from the Atlantic. From mixing considerations we estimate that pure Mediterranean waters have $\varepsilon_{Nd}(0) \approx -6$. Possible sources of this relatively radiogenic Nd could be from drainage of young continental terranes or the injection of remobilized Nd from deep-sea sediments that have a young radiogenic volcanic component. New data from a depth profile in the western Atlantic is presented. Comparison of Nd data for the eastern North Atlantic with that for the western North Atlantic shows fundamental differences in the water column structures for $\varepsilon_{Nd}(0)$. While both regions show a pronounced maximum in $\varepsilon_{Nd}(0)$, the western basin maximum occurs at the near surface rather than at 1000 m. In addition, deep waters of the eastern basin are found to be more radiogenic than the western basin. These differences indicate several sources of isotopically distinct Nd in the North Atlantic. The deep waters of the North Atlantic (>1000 m) have the lowest values of $\varepsilon_{Nd}(0)$ measured in the oceans. We believe that the source of these low $\varepsilon_{Nd}(0)$ values, which we associate with North Atlantic deep water, is either from freshwater drainage off the Precambrian shields of North America and Asia into the Arctic Ocean or from the injection of 'older,' continentally derived REE from deep-sea sediments. Sm and Nd concentrations are found to increase with depth and $\varepsilon_{Nd}(0)$ changes with depth, indicating both vertical and lateral transport processes from different sources. This suggests a surface source of Nd and injection of REE into the water column from deep-sea sediments or large-scale bottom currents with high REE concentrations.

INTRODUCTION

In this study we have examined the effect of the Mediterranean outflow on the isotopic composition of neodymium in the water column of the eastern North Atlantic. Because of the very long half-life of ^{147}Sm ($t_{1/2} = 1.06 \times 10^{11}$ years) and the short cycling time of the rare earth elements (REE) in the oceans, compared to mixing between the oceans, the ratio $^{143}Nd/^{144}Nd$ is variable in seawater. This variation reflects the $^{143}Nd/^{144}Nd$ ratio in the source terranes that supply the REE to the oceans. The $^{143}Nd/^{144}Nd$ ratio is used as a tracer for studying the transport of REE in the oceans and may be used for studying the origin of different water masses. A summary of the observations and current ideas in this field may be found in an article by *Piepgras and Wasserburg* [1982]. The Nd isotopic data presented in this paper will be given in units of $\varepsilon_{Nd}(0)$.

$$\varepsilon_{Nd}(0) = \left[\frac{(^{143}Nd/^{144}Nd)_{measured}}{0.511847} - 1 \right] \times 10^4 \qquad (1)$$

where 0.511847 is the present-day $^{143}Nd/^{144}Nd$ ratio in a chondritic reservoir [*DePaolo and Wasserburg*, 1976; *Jacobsen and Wasserburg*, 1980].

Recent studies have clearly established that there are distinct differences in the Nd isotopic composition between the different oceans [*Piepgras et al.*, 1979; *Piepgras and Wasserburg*, 1980; *Goldstein and O'Nions*, 1981; *Piepgras and Wasserburg*, 1982]. In addition to the interocean Nd isotopic variations, smaller but distinct variations occur within individual ocean basins. Results from previous studies of Nd isotopic measurements for vertical profiles in the Sargasso Sea and the Central Pacific [*Piepgras and Wasserburg*, 1980, 1982] are shown in Figure 1 *a* and *c*. In addition to these results, additional data has been obtained for another Atlantic profile at station 30 (36°N, 62° W) and are shown in Figure 1*b*. The results for station 30 indicate a uniform deepwater isotopic composition of $\varepsilon_{Nd}(0) \approx -14$, in agreement with data for the Sargasso Sea. All of these profiles indicate a source of REE at the surface which is distinct from that for the respective deep waters. This demonstrates lateral as well as vertical transport of the REE. In the Pacific profile the bottom water at this station has been identified, on the basis of its Nd composition, to have spread northward from the southern ocean [*Piepgras and Wasserburg*, 1982]. Isotopic heterogeneity in the water column is not ubiquitous, however. The southern ocean in the vicinity of the Drake Passage has uniform $^{143}Nd/^{144}Nd$ in the water column, corresponding to $\varepsilon_{Nd}(0) \approx -9$ and a linear gradient in Nd concentration, leading to the conclusion that it is isotopically, but not chemically, well mixed [*Piepgras and Wasserburg*, 1982]. Results of these various studies indicate that it should be possible to monitor the effects of injection of REE on the water column in regions where the injected REE can be characterized isotopically.

We have chosen to look at the effects of the Mediterranean outflow on the Nd isotopic composition in the water column of the eastern North Atlantic. The Mediterranean outflow

Paper number 3C0468.
0148-0227/83/003C-0468505.00

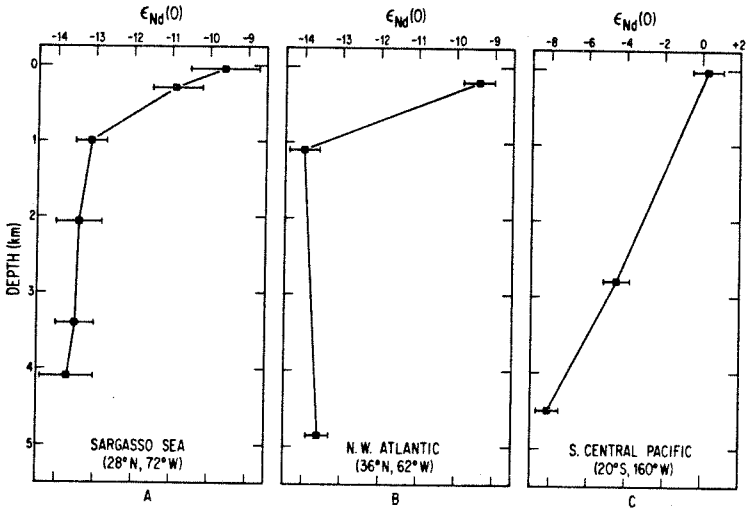

Fig. 1. $\epsilon_{Nd}(0)$ as a function of depth in the (A) Sargasso Sea (*Piepgras and Wasserburg*, 1980]. (B) western North Atlantic at A-II. 109-1, station 30 (this study), and (C) south central Pacific [*Piepgras and Wasserburg*, 1982]. The Sargasso Sea data is a composite of several closely spaced stations. The location given in the figure for these samples is the approximate mean position of all stations from the Sargasso Sea.

has a profound influence on the temperature and salinity characteristics of the Atlantic. The high evaporation rate in the Mediterranean Sea produces water masses with salinities greater than 38‰. Some of this dense, saline water spills into the Atlantic over the Gibraltar sill at a rate of about 1.04×10^6 m^3/s [*Tchernia*, 1980]. This outflow is replaced by an inflow of less saline Atlantic surface water at a rate of about 1.11×10^6 m^3/s, which balances the outflow and net evaporation losses of water in the Mediterranean. The dense Mediterranean outflow water moves downward along the continental slope, mixing with Atlantic water as it sinks to a depth of ~1000 m, where it reaches water of the same density. At this level it spreads out across the Atlantic, resulting in an intermediate-depth salinity maximum, which is the characteristic feature of the core of upper North Atlantic deep water [*Dietrich et al.*, 1980]. The Mediterranean outflow also results in the Atlantic having a warmer median temperature than the Pacific [*Knauss*, 1978]. The influx of Atlantic water is the largest source of water to the Mediterranean, and it might be expected that this component would dominate the Nd isotopic character of the Mediterranean. If the isotopic composition of Nd in the outflowing Mediterranean water can be distinguished from Nd in the Atlantic water it flows into, then a source of isotopically distinct Nd to the Mediterranean would be required. This condition would allow simple modeling of the REE transport

TABLE 1. Sample Locations and Results of Sm and Nd Measurements

Depth, m	Nd, 10^{-12} g/g	Sm, 10^{-12} g/g	$\frac{^{147}Sm}{^{144}Nd}$	$\frac{^{143}Nd}{^{144}Nd}$	$\epsilon_{Nd}(0)$
A-II, 109-1, Station 95 (36°17'41"N, 10°02'27"W), Eastern North Atlantic					
Surface	1.80	0.376	0.126	0.511264 ± 33	−11.4 ± 0.7
200	2.01	0.417	0.125	0.511208 ± 19	−12.5 ± 0.4
500	2.26	0.473	0.126	0.511240 ± 30	−11.9 ± 0.6
800	2.48	0.528	0.128	0.511304 ± 28	−10.6 ± 0.5
1000	2.34	0.519	0.134	0.511348 ± 29	−9.8 ± 0.6
1000	2.35	—	—	0.511334 ± 20	−10.0 ± 0.4
1150	2.61	0.532	0.127	0.511251 ± 28	−11.7 ± 0.5
1300	2.49	0.533	0.129	0.511253 ± 26	−11.6 ± 0.6
2000	2.46	0.498	0.122	0.511221 ± 20	−12.2 ± 0.4
3000	2.84	0.556	0.118	0.511208 ± 25	−12.5 ± 0.5
4000	3.33	0.644	0.117	0.511245 ± 22	−11.8 ± 0.4
A-II, 109-1, Station 101 (36°45'15"N, 08°36'20"W), Gulf of Cadiz					
650	5.16			0.511340 ± 20	−9.9 ± 0.4
A-II, 109-1, Station 30 (36°15'38"N, 61°58'27"W), Western North Atlantic					
200	1.96	—	—	0.511365 ± 20	−9.4 ± 0.4
1100	2.60	—	—	0.511128 ± 21	−14.0 ± 0.4
4850	9.01	—	—	0.511153 ± 16	−13.6 ± 0.3

The $^{143}Nd/^{144}Nd$ ratios were determined in samples spiked with ^{150}Nd and normalized to $^{146}Nd/^{142}Nd = 0.636151$. Reported errors are two standard deviations from the mean. 2σ errors for concentration measurements are ~ 0.05% for Nd and ~ 0.1% for Sm.

TABLE 2. Hydrographic Data for Eastern North Atlantic Samples

Depth, m	Salinity, ‰	O_2, μM/kg	Phosphate, μM/kg	Nitrate, μM/kg	Silicate, μM/kg
A-II, 109-1 Station 95 (36°17'41"N, 10°02'27"W) Eastern North Atlantic					
Surface	36.545	230	0.01	0.20	1.34
200	35.891	222	0.33	5.82	2.74
500	35.651	198	0.81	13.97	6.56
800	36.019	184	0.85	14.33	8.76
1000	35.961	184	0.98	16.24	10.97
1150	36.057	186	0.96	16.04	11.46
1300	36.020	193	0.96	15.90	11.74
2000	35.210	238	1.18	18.44	19.48
3000	35.063	238	1.33	20.29	33.35
4000	34.903	240	1.44	21.55	44.90
A-II, 109-1, Station 101 (36°45'15"N, 08°36'20"W), Gulf of Cadiz					
650	36.587	—	—	—	—
A-II, 109-1, Station 30 (36°15'38"N, 61°58'27"W), Western North Atlantic					
200	36.523	224	0.11	3.06	1.59
1100	35.063	218	1.08	19.69	13.39
4850	34.896	263	1.24	18.97	35.59

to and in the Mediterranean and the exchange of REE with the Atlantic. Therefore, we feel that a study of the Mediterranean outflow will give us insights to the influence it has on the REE distribution in the Atlantic Ocean and also on REE transport processes within the Mediterranean Sea. At certain locations the high-salinity character of the Mediterranean outflow allows easy identification of this water mass, making correlation of water samples with water source type definitive.

SAMPLING AND ANALYTICAL PROCEDURES

Seawater samples were collected for Nd isotopic analysis during cruise 109-1 of the RV *Atlantis II* from several locations along 36°N latitude. Samples reported in the present study are from three stations, two of which are from the vicinity of the Mediterranean outflow and one from the western basin. Sample locations are given in Table 1. Ten-liter samples of seawater were collected from various depths in the water column, using Go-Flo and Nisken water sampling devices. The sampling depths were chosen on the basis of salinity profiles determined from CTD (conductivity, temperature, and depth) casts to insure a well-bracketed sampling of the Mediterranean outflow. Surface samples were collected in a plastic bucket from the bow of the ship. In an effort to minimize contamination of surface water surrounding the ship, the pumping of water from bilges and desalination plants was shut down prior to arrival on stations. Aliquots of the seawater samples were taken for the shipboard analysis of salinity, oxygen, and nutrient concentrations. The remainder of each sample was stored in polyethylene containers and acidified with 25 ml, high-purity 10 N HCl. All samples were analyzed for Nd isotopic composition and Sm and Nd concentration by using unfiltered 4-l subsamples. The reagents, analytical techniques, and mass spectrometry have been described elsewhere [*Piepgras et al.*, 1979].

RESULTS

Table 2 lists the results of hydrographic measurements of salinity, oxygen, and nutrients made on water samples collected for Sm and Nd analysis. Potential temperature (θ) and salinity (S) data acquired from CTD measurements are plotted in θ-S diagrams in Figure 2 for all stations from which samples have been analyzed for Sm and Nd. The θ-S diagram for station 95 (Figure 2*a*) contains two segments with nearly linear θ-S relationships. The first segment lies between the surface and about 500 m. The second linear segment extends from 1200 m to the ocean bottom (4700 m). Between 500 m and 1200 m, the θ-S diagram is characterized by a rather large increase in salinity from 35.656‰ to 36.148‰ and a relatively small drop in potential temperature from 11.4°C to 9.9°C. This unique section of the θ-S diagram results from the addition of warm, saline waters flowing out from the Mediterranean Sea into the North Atlantic. Although the detailed structure between 500 and 1200 m shows some complexity, we will refer to samples lying within this interval as from the core of the Mediterranean outflow. From salinity considerations this core can be extended to about 1400-m depth. The θ-S diagram for station 101 (Figure 2*b*) is similar to the upper portion of the θ-S diagram for station 95. Potential temperature and salinity both decrease from the surface to a depth of about 400 m and then increase to the bottom. This increase in potential temperature and salinity below 400 m is interpreted as the result of outflowing Mediterranean water. There are four samples located within the Mediterranean core at station 95 (800, 1000, 1150, and 1300 m) and one sample at station 101 (650 m).

Salinity and dissolved oxygen profiles generated from CTD measurements are shown in Figure 3. At station 95 (Figure 3*a*), salinity is observed to decrease from a surface maximum of ~36.5‰ to a value of ~35.6‰ at 500 m. Between 500 m and 1200 m, salinity increases with maxima at 800 and 1200 m of ~36.1‰. Below 1200 m, the salinity decreases to the deepwater minimum value of ~34.9‰. Dissolved oxygen shows a near-surface maximum of 271 μM/kg at 40 m. It then decreases to a minimum of 1000 m of 178 μM/kg. Below 1000 m, dissolved oxygen values increase to a deepwater maximum of 249 μM/kg at 2600 m. Below this depth, the dissolved oxygen content remains nearly constant to the ocean bottom. The Mediterranean outflow is identified both by the salinity maxima between 500 and 1400 m and the oxygen minimum centered at 1000 m. At station 101 (Figure 3*b*), salinity decreases from a surface maximum of ~36.5‰ to ~35.7‰ at 400 m. Below 400 m, it increases to a bottom

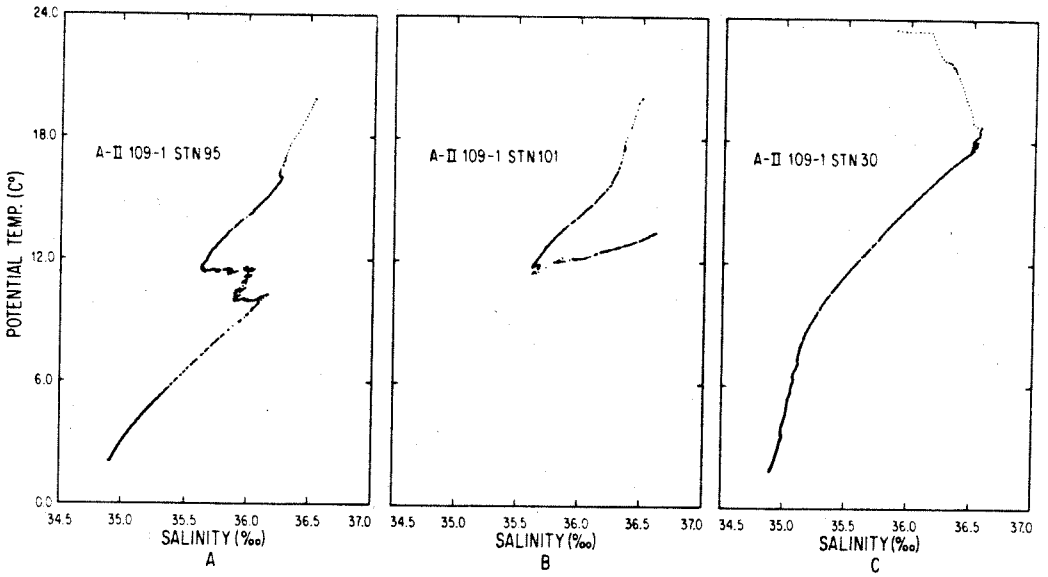

Fig. 2. Potential temperature vs. salinity at (A) station 95, (B) station 101 and (C) station 30. The scale is the same for all three θ-S diagrams.

value of ~36.6‰. This increase is a result of the Mediterranean outflow. The oxygen profile has a near-surface maximum at 40 m and then decreases to a bottom value of ~194 μM/kg.

The nutrient concentrations for samples collected at station 95 are plotted in Figure 4. PO_4^{3-} and NO_3^- increase rapidly with depth through the upper 500 m of the water column. Below 500 m, they increase gradually to the bottom. Silicate maintains a fairly constant rate of increase at all levels in the water column. All of the nutrient profiles exhibit some perturbations in their concentration gradients at the level of the Mediterranean outflow.

Our results for Sm and Nd concentrations and Nd isotopic abundances are given in Table 1. All of the isotopic results for station 95 are within the range of $\varepsilon_{Nd}(0)$ values for the Atlantic Ocean that have been previously reported [*Piepgras and Wasserburg*, 1980]. The isotopic results for Nd at station 95 are plotted as a function of depth on Figure 5. It is seen from inspection of Figure 5 that $\varepsilon_{Nd}(0)$ varies with depth by 2.7 ε units. The top 500 m of the water column has $\varepsilon_{Nd}(0)$ ranging from -11.4 ± 0.7 to -12.5 ± 0.4. Below 500 m, $\varepsilon_{Nd}(0)$ increases to more radiogenic values, reaching a maximum of -9.8 ± 0.6 at 1000 m. A repeat analysis of the 1000-m sample has $\varepsilon_{Nd}(0) = -10.0 \pm 0.4$, indicating the

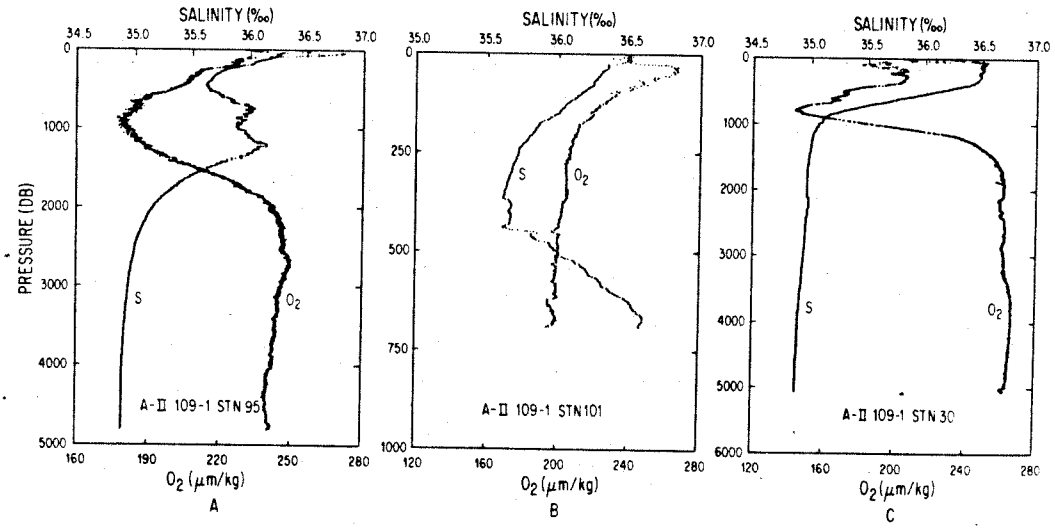

Fig. 3. Salinity and dissolved oxygen as a function of pressure (A) station 95, (B) station 101 and (C) station 30. The high-salinity tongue of the Mediterranean outflow is clearly seen in the profiles for stations 95 and 101.

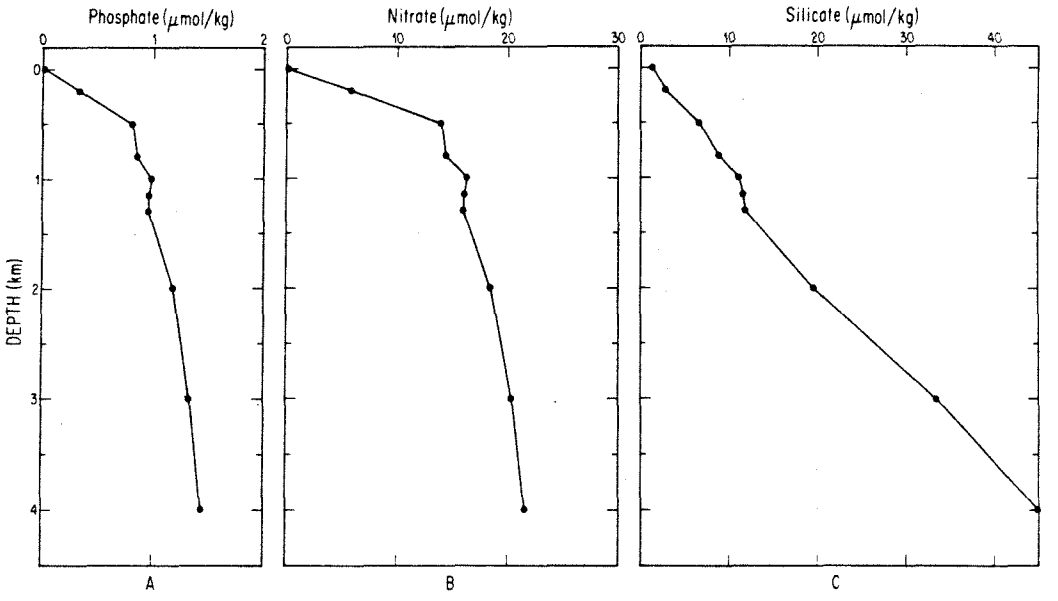

Fig. 4. Nutrient concentrations as a function of depth at station 95: (A) phosphate, (B) nitrate, and (C) silicate. The influence of the Mediterranean outflow can be observed on all of these profiles.

reproducibility of our methods. Below 1000 m, $\epsilon_{Nd}(0)$ is lower again. At the 1150-m depth, $\epsilon_{Nd}(0) = -11.7 \pm 0.5$ and remains nearly constant at this value to 4000 m. One sample from station 101 at a depth of 650 m lies within the core of the Mediterranean outflow water and has $\epsilon_{Nd}(0) = -9.9 \pm 0.4$.

Results of Sm and Nd concentration measurements for station 95 are shown on Figure 6. In general the concentrations of both Sm and Nd increase with depth. The Nd concentration ranges from 1.80×10^{-12} g/g at the surface to 3.33×10^{-12} g/g at 4000 m. Sm ranges between 0.375×10^{-12} g/g and 0.644×10^{-12} g/g in this depth interval. There are irregularities in this trend at depths between 800 and 2000 m where the concentrations of both Sm and Nd are observed to oscillate. Below 2000 m, the Nd concentration exhibits an approximately linear increase with depth. Very little variation in the Sm/Nd ratio is observed in the water column, as indicated by the nearly uniform $^{147}Sm/^{144}Nd$ ratios given in Table 1. The bottom sample from station 101 at 650 m has a high Nd concentration of 5.16×10^{-12} g/g.

The θ-S diagram for station 30 is plotted in Figure 2*c*. Salinity is observed to increase with decreasing potential temperature until a salinity maximum of ~36.5‰ is reached, which occurs between 50 and 200 m in the water column. Below the salinity maximum, both θ and S decrease to the bottom. A slight bend in the θ-S curve below the salinity maximum indicates that a total of four components are involved in mixing at this location. For station 30, salinity and oxygen are plotted versus depth on Figure 3*c*. Salinity increases with depth to a broad, near-surface maximum between 50 and 200 m of ~36.5‰. Below 200 m, salinity decreases to the bottom. If Mediterranean outflow water were present, we would expect to see a salinity maximum at a depth of ~1000 to 1200 m. However, this is not observed, and we conclude that there is no Mediterranean component at this westerly station. Oxygen has a near-surface maximum of ~233 μM/kg at 50 m and an intermediate-depth minimum of ~145 μM/kg at ~800 m. O_2 then increases to ~260 μM/kg at 1800 m. Below this depth, O_2 is fairly uniform.

Nd concentrations and isotopic abundances for samples from station 30 are given in Table 1. The isotopic data are presented in Figure 1*b* and are almost indistinguishable from the observations in the Sargasso Sea. Nd at station 30

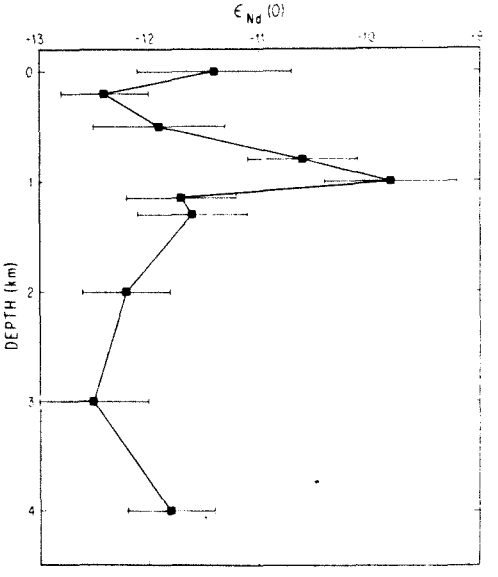

Fig. 5. $\epsilon_{Nd}(0)$ as a function of depth at station 95 in the eastern North Atlantic. Notice the maximum in $\epsilon_{Nd}(0)$ at 1000 m. The error bars represent the 2σ errors on the isotopic measurements.

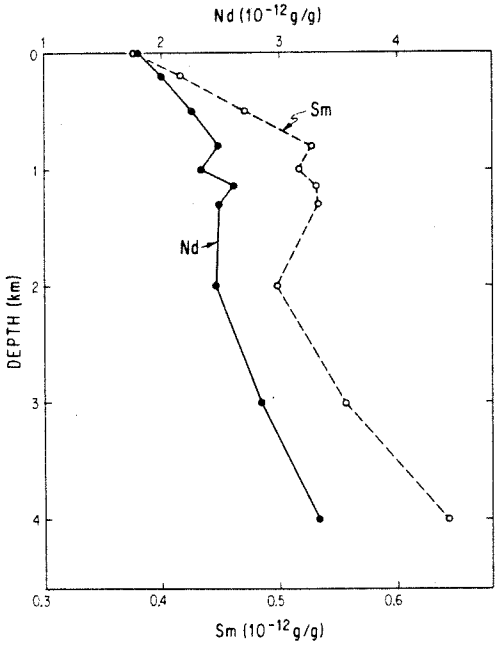

Fig. 6. Sm (open circles) and Nd (solid circles) as a function of depth at station 95. Notice the similarity in the form of this curve in the depth region near 1000 m with that for salinity in Figure 5.

exhibits increasing concentration with depth. The bottom value of 9.01×10^{-12} g/g is the highest Nd concentration yet measured in ocean waters.

DISCUSSION

The total range in $\varepsilon_{Nd}(0)$ observed at station 95 is small; however, we find the shift in $\varepsilon_{Nd}(0)$ toward more radiogenic values in two samples (800 m and 1000 m) associated with the core of the Mediterranean outflow to be significant. With the exception of the surface sample, the 2σ errors on the 800- and 1000-m samples do not overlap with those measurements at other depths, clearly indicating a source of Nd in these samples which is different from that in overlying and underlying waters. The maximum in $\varepsilon_{Nd}(0)$ at 1000 m, shown in Figure 5, correspond to approximately a 2-ε unit shift from $\varepsilon_{Nd}(0)$ values in overlying and underlying waters. We believe this shift to be a direct result of Mediterranean water having $\varepsilon_{Nd}(0) \geq -9.8$ intruding into a nearly uniform layer of North Atlantic water having $\varepsilon_{Nd}(0) \approx -12$. One sample from station 101 (650 m) in the Gulf of Cadiz represents Mediterranean outflow water as it is sinking down the continental slope. The value of $\varepsilon_{Nd}(0) = -9.9 \pm 0.4$ in this sample is consistent with our conclusions about the source of the isotopic shift found at station 95.

Two samples (1150 m and 1300 m) associated with the Mediterranean core as defined by the θ-S diagram in Figure 2 have $\varepsilon_{Nd}(0) = -11.7 \pm 0.5$ and -11.6 ± 0.6, respectively. These values are similar to other deepwater values at this station. We find this surprising because these samples lie very close to the salinity maximum associated with the Mediterranean outflow. It is not clear why there should be an abrupt decrease in $\varepsilon_{Nd}(0)$ below 1000 m while still being within the Mediterranean core, and we cannot explain this anomaly. Possibly, it is related to differences in the relative 'diffusion' rates of Nd, temperature, and salinity. In principle, however, $\varepsilon_{Nd}(0)$ can be decoupled from either temperature or salinity. This is because the isotopic composition of a mixture of two components is dependent on both the isotopic composition and Nd concentration of the end members being mixed. The relationship for the salinity (S_m) in a two-component mixture (S_1 and S_2) is given by

$$S_m = X S_1 + (1 - X)S_2 \tag{2}$$

where X is the weight fraction of component 1 in the mixture. For $\varepsilon_{Nd}(0)$ the relationship is given by

$$\varepsilon_M = \frac{XC_1\varepsilon_1 + (1 - X)C_2\varepsilon_2}{XC_1 + (1 - X)C_2} \tag{3}$$

where the C's are the concentration per gram of Nd in the pure components. In a case, such as the Mediterranean outflow, where a high-salinity, low-Nd concentration component is mixing with a lower-salinity, higher-Nd component, it can be shown, from the above relationships, that $\varepsilon_{Nd}(0)$ in mixtures of these components will initially approach the $\varepsilon_{Nd}(0)$ value in the end member having the higher Nd concentration more rapidly than the salinity approaches

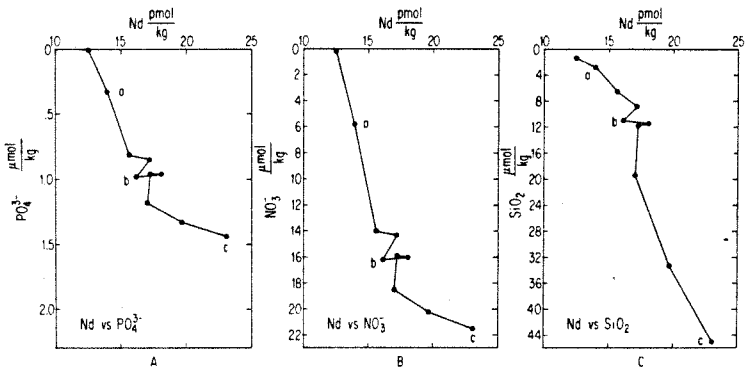

Fig. 7. Nd concentrations vs. (A) PO_4^{3-}, (B) NO_3^-, and (C) SiO_2 for station 95. For reference, the points labeled a, b, and c correspond to the depths 200, 1000, and 4000 m, respectively.

the corresponding salinity end member. The Nd concentration difference in the end members at station 95, however, is not sufficient to produce the decrease in $\varepsilon_{Nd}(0)$ observed at 1150 m. We do note that the data for station 30 are consistent with this explanation of the decoupling of salinity and $\varepsilon_{Nd}(0)$.

Estimates of the proportion of the Mediterranean component in the outflow waters at station 95 can be made from the salinity data. At the depth of the salinity maximum in the eastern basin corresponding to the Mediterranean core, the western Atlantic basin has $S \approx 35‰$. Using this value for a pure North Atlantic component, and taking $S = 38.4‰$ for the pure Mediterranean component [*Dietrich et al.*, 1980], we estimated, from the salinity corresponding to the maximum in $\varepsilon_{Nd}(0)$ at station 95, an ~30% Mediterranean component in the outflow core. Another method for estimating the fraction of Mediterranean water present is the conservative tracer 'NO' ('NO' = $O_2 + 9NO_3^-$) [*Broecker and Takahashi*, 1980]. From this approach we also calculate an ~30% Mediterranean component in the outflow at station 95, which agrees with that calculated from the salinity.

Although we have not made a direct measurement of Nd in Mediterranean water, it is possible to estimate its Nd isotopic composition. The Mediterranean component is diluted primarily by North Atlantic surface water ($\varepsilon_{Nd}(0) = -11.4$ at station 95), which enters the Mediterranean through the Straits of Gibraltar. If the core of the Mediterranean outflow at station 95 has about a 30% Mediterranean component, with the remaining component being primarily North Atlantic surface water, and assuming approximately equal Nd concentrations, then this would imply that pure Mediterranean component would have $\varepsilon_{Nd}(0) \sim -6$. *Elderfield and Greaves* [1982] analyzed a sample of biogenic carbonate from the Mediterranean and found $\varepsilon_{Nd}(0) = -7.1$; this supports our estimate for $\varepsilon_{Nd}(0)$ in the Mediterranean Sea. However, it is not a direct determination, and since our estimates of the proportions of pure Mediterranean water at station 95 could be in error, measurements of Nd in Mediterranean waters must be made to determine the actual composition. This has not yet been possible because of the lack of availability of expeditions.

The water budget of the Mediterranean Sea is dominated by the influx of Atlantic water, yet the Nd isotopic results reported here clearly indicate a source of Nd in the Mediterranean with an isotopic composition that differs from the Atlantic. Using a box model to describe the steady state conditions for Nd in the Mediterranean, we have

$$O = C_A \dot{W}_{AM} - C_M \dot{W}_{MA} + J_C - J_S \quad (4)$$

$$O = C_A \varepsilon_A \dot{W}_{AM} - C_M \varepsilon_M \dot{W}_{MA} + J_C \varepsilon_C - J_S \varepsilon_M \quad (5)$$

where the subscript A represents the Atlantic and M the Mediterranean. The C's are concentrations of Nd; the ε's are the isotopic compositions; $\dot{W}_{ij}$ represents the volume rate of water flow between the Atlantic and Mediterranean in the directions indicated by the subscripts; J_S is a sink term for Nd in the Mediterranean; and J_C is the net flux of Nd into the Mediterranean from sources other than the Atlantic that are characterized by isotopic compositions ε_C. It can be seen from (4) and (5) that if $J_C = 0$ then $\varepsilon_A = \varepsilon_M$ and there would be no difference in the isotopic composition of Nd in the Mediterranean from the Atlantic. There is a difference observed, however, indicating that J_C is nonzero. Solving (4) for J_S, and substituting this result into (5), we have

$$J_C = \frac{(\varepsilon_A - \varepsilon_M)}{(\varepsilon_M - \varepsilon_C)} C_A \dot{W}_{AM} \quad (6)$$

For estimating J_C we will use data from *Tchernia* [1980] for our estimates of the Mediterranean water budget. We can put reasonable limits on ε_C. Since $\varepsilon_M > \varepsilon_A$, it follows that $\varepsilon_C > \varepsilon_M$. A strict upper limit for ε_C must be ~+12, a high value for midocean ridge basalts. If we assume $\varepsilon_A \approx -12$, $\varepsilon_M \approx -7$, $C_A \approx 2 \times 10^{-12}$ g/g, and $\dot{W}_{AM} = 1.11 \times 10^6$ m^3/s, then using the above limits for ε_C, $J_C \geq 0.58$ g Nd/s. It is reasonable to assume that Nd concentrations in the Black Sea would be of the same order of magnitude as oceanic concentrations. Therefore, the flux of Nd from the Black Sea inflow of 6.35×10^3 m^3/s should be negligible in comparison to the total flux J_C. If all of the Nd that had ε_C were supplied by runoff (1.11×10^4 m^3/s), then the dissolved concentration of Nd in these waters must be greater than $\sim 53 \times 10^{-12}$ g/g. This is close to the value for dissolved concentrations levels of $\sim 40 \times 10^{-12}$ g/g, measured for river waters by *Martin and Maybeck* [1980]. However, negative values of $\varepsilon_{Nd}(0)$ seem more likely for continental drainages. For example, North American shale has $\varepsilon_{Nd}(0) = -14.4$ [*DePaolo and Wasserburg*, 1976]. Data from *Goldstein and O'Nions* [1982] for river-suspended loads have $\varepsilon_{Nd}(0) = -9.3$ to -16.2. Data by M. Stordal (personal communication, 1982) for both suspended and dissolved loads in the Mississippi River have $\varepsilon_{Nd}(0) \sim -12$. These values of $\varepsilon_{Nd}(0)$ in continental drainages are clearly too negative to produce the appropriate isotopic value in the Mediterranean required by our data. If we considered a high value of $\varepsilon_{Nd}(0) = -3$ for the continental drainages into the Mediterranean (ε_C), then the Nd concentration in the continental runoff must be $\sim 250 \times 10^{-12}$ g/g. If instead of the calculated value for ε_M we assume that our observed value of -9.8 for $\varepsilon_{Nd}(0)$ in the Mediterranean outflow represents the lowest possible value in undiluted Mediterranean water, then for $\varepsilon_C \lesssim +12$, $J_C \gtrsim 0.22$ g Nd/s, and the dissolved concentration in runoff must be $\gtrsim 20 \times 10^{-12}$ g/g. A lower value of $\varepsilon_C = -6$ would result in a runoff concentration of $\sim 115 \times 10^{-12}$ g/g. The negative values of ε_C used in the above two cases yield runoff concentrations for Nd that are high in comparison to the river water values given by Martin and Maybeck. However, the present data base for REE in river waters is small, so this apparent discrepancy may not be real. Such values for ε_C in runoff would indicate that rivers in this region are draining a young continental terrane possibly characterized by a late Precambrian basement ($T \lesssim 0.9$ Ae) and younger volcanic terranes. If ε values in runoff were much more negative than the ε_C values used in the two cases above, excessively high concentrations of Nd in the runoff would be required. This would require a source of Nd additional to that of continental drainages. One possible source may be the injection of Nd remobilized from volcanogenic deep-sea sediments in the Mediterranean basin. Volcanic ash layers are common in eastern Mediterranean sediments [*Ryan*, 1971] and could represent a source of soluble and relatively radiogenic Nd necessary to shift the isotopic composition of incoming Atlantic water. Direct measurements of Nd in major drainages into the Mediterranean are needed to determine the relative importance of sources.

The deepwater $\varepsilon_{Nd}(0)$ values at station 95 (Figure 5)

contrast with those from the western basin of the North Atlantic. The values of −13 to −14 in the western Atlantic (Figure 1*a*, *b*) are significantly lower than the $\varepsilon_{Nd}(0)$ values of ~−12 in the deep layer at station 95. On the basis of Nd isotopic signatures alone, the deep waters of the eastern and western basins of the Atlantic Ocean thus appear to be distinguishable. The low values of $\varepsilon_{Nd}(0)$ in the deep waters are assumed to be a feature of North Atlantic deep water [*Piepgras and Wasserburg*, 1980]. If the source of North Atlantic deep water were the same for both the eastern and western basins, then one might expect that the isotopic composition of Nd associated with this water mass should be identical in both basins. The difference in isotopic composition implies that subsequent to the formation of North Atlantic deep water there have been modifications in the deep waters of the eastern and western basins that have resulted in a divergence of their isotopic characters. Presumably, injection of waters having distinctive isotopic compositions results in the eastern basin having more radiogenic values of $\varepsilon_{Nd}(0)$ than the western basin. At present, it is not possible to determine whether only one or both basins have undergone modification, or if North Atlantic deep water represents a unique or homogenous source. We note, however, that the $\varepsilon_{Nd}(0)$ value in the Mediterranean outflow ($\varepsilon_{Nd}(0) = -9.8$) could be considered a possible source of radiogenic Nd for modifying the eastern basin values. The more radiogenic ε values in the eastern basin may also be, in part, due to a larger southern component (Antarctic bottom water) than found in the western basin. A southern component would have $\varepsilon_{Nd}(0) \approx -9$ [*Piepgras and Wasserburg*, 1982]. *Broecker* [1979] suggested using SiO_2 or 'NO' for estimating the magnitude of the southern component. The proportion of a southern component, as determined from SiO_2, is as high as ~40% in the deepest waters, compared with ~30% as determined from 'NO.' Eastern basin silicate values may be anomalously high, however, because of silica dissolution [*Broecker and Takahashi*, 1980]. As sampled during this cruise, no difference in 'NO' values is observed between deep waters in the eastern and western basins. It is therefore not clear what influence Antarctic bottom water has on the isotopic differences observed between the eastern and western basins. The isotopic differences may also reflect a difference in the mean isotopic compositions of the sediments between the eastern and western basins if injections of REE from sediments into overlying waters are considered as an important source of these elements in the oceans.

The isotopic signature we attribute to the Mediterranean outflow ($\varepsilon_{Nd}(0) = -9.8$) at 1000 m is indistinguishable from the maximum in $\varepsilon_{Nd}(0)$ in the near-surface waters of the Sargasso Sea ($\varepsilon_{Nd}(0) = -9.6$) and at station 30 ($\varepsilon_{Nd}(0) = -9.4$). It is clear from the differences in depth in the water column at which these maxima are observed that the source of the relatively radiogenic Nd in the surface waters of the western basin is different from that observed for the Mediterranean outflow at station 95. The near-surface maxima in the western basin suggest that Nd of this isotopic composition is being transported by the Gulf Stream system. The presence of different sources of REE having the same Nd isotopic character indicates that we must be cautious in identifying water masses on the basis of Nd isotopic characteristics alone.

Sm and Nd concentrations at station 95 are shown in Figure 6. The general trend in the concentration profiles is toward higher concentration with increasing water depth. While there is no apparent relationship between Sm and Nd concentrations and Nd isotopic compositions in the water column here, like $\varepsilon_{Nd}(0)$, these concentration profiles are influenced by the Mediterranean outflow. In the core of this outflow the Sm and Nd concentrations appear to imitate the salinity in that they oscillate with the highs in the Sm and Nd concentrations corresponding to the high-salinity portions of the curve and the lows corresponding to lower salinity. Outside the region of the Mediterranean core, Sm and Nd increase in concentration downward in an approximately linear manner. Except within the core of Mediterranean water, the concentration gradient reported here is similar to concentration profiles measured in other parts of the world ocean [*Piepgras and Wasserburg*, 1982]. The presence of a concentration gradient requires some type of particle transport to deplete the surface and enrich the deep waters. The nature of these particles and the mechanism by which they transport REE have not been identified, and they require further study. A general discussion of vertical transport on sequestering particles and redissolution has been given by *Piepgras and Wasserburg* [1982]. It should be made clear, however, that the isotopic data require a source of Nd in the deep waters in addition to that transported from the surface on settling particles.

Elderfield and Greaves [1982] have measured REE concentrations for filtered seawater in a profile from the eastern North Atlantic, located at approximately 28°N, 26°W in a region that is also influenced by the Mediterranean outflow. However, they did not report any Nd isotopic composition data for these waters. Comparison of their Sm and Nd data with ours for station 95 show the profiles to be very similar, but in general the concentration levels at our station are 20–30% lower at comparable depths than reported by Elderfield and Greaves; $^{147}Sm/^{144}Nd$ ratios at these two localities also differ. Calculated $^{147}Sm/^{144}Nd$ ratios from the data of Elderfield and Greaves range from 0.106 to 0.126, with the exception of one sample (200 m) that has $^{147}Sm/^{144}Nd = 0.173$. By comparison, our $^{147}Sm/^{144}Nd$ ratios vary between 0.117 and 0.134, with no outlying values. One notable exception to the similarity in the Sm and Nd concentration profiles of these two stations is the surface enrichments of Sm and Nd, reported by Elderfield and Greaves. We find no eivdence of a surface enrichment of Sm and Nd at station 95, but rather the surface has the lowest concentrations. The reasons for this difference are not known but may be related to higher levels of dust fallout from the Sahara at their station, as suggested by Elderfield and Greaves. Alternatively, the difference between the surface concentrations of these two stations could be a result of the collection and filtration methods used. The lessons learned from lead studies in seawater [*Patterson*, 1974] have clearly demonstrated the problem of sample contamination during collection of water samples for trace metal analysis, especially in the surface waters surrounding a ship on station. We believe the levels of contamination for the REE are far below those observed for elements like Pb, Cu, and Zn, which are widely used industrially. We have carried out our sampling and analytical procedures with considerable care and believe that the regularity of our results indicate that they are not reasonably due to contamination. Nonetheless, the potential for contamination effects should always be considered when interpreting any trace element data in seawater.

Comparison of Nd concentrations versus nutrient concentrations provides an indication of a source of dissolved Nd from bottom sediments. The transport of many trace elements in the deep sea is often correlated with nutrient profiles [see *Bruland*, 1980, for several examples]. Increases in nutrient concentrations with depth are believed to be associated with the dissolution of settling particles [*Bruland*, 1980]. Thus a positive linear correlation between a trace element and nutrients implies that the same processes act to transport the correlated species. Samples from station 95 were analyzed for nutrient concentrations to compare directly with Sm and Nd concentration levels; Nd vs. PO_4^{3-}, NO_3^-, and SiO_2 are plotted in Figure 7. The upper 500 m of the water column show an approximately linear correlation between nutrient levels and Nd concentrations, as indicated in Figure 7. From the strong correlation in the upper portions of the water column between Nd and nutrients it can be argued that the same processes are acting to transport the REE through the water column. Samples within the Mediterranean outflow core (800 to 1300 m) do not exhibit a linear correlation between Nd and nutrients. This is probably a result of complex mixing processes between core waters and surrounding waters. There is a marked change in slope of Nd versus either PO_4^{3-} (Figure 7*a*) or NO_3^- (Figure 7*b*) in the deep waters below the Mediterranean outflow relative to waters above the outflow. A linear correlation is still observed in these samples, however. The change in slope below the Mediterranean core is a result of there being a relatively greater rate of increase with depth in the concentration of Nd as compared to PO_4^{3-} or NO_3^- in the deep waters. Injection of REE remobilized from deep-sea sediments seems the most likely source of this 'excess' Nd in the deep waters, although it could imply a more rapid depletion of nutrients relative to the REE in the particulate phase during dissolution of settling particles in the deep waters. For Nd versus SiO_2 (Figure 7*c*) there is also a change in slope below the Mediterranean core. In this case, however, SiO_2 concentrations are found to increase in relation to Nd, indicating a source of 'excess' silica relative to Nd in the deep waters. The higher silica values in the deep water could be the result of larger southern ocean contributions to the dissolved silica budget in the eastern basin of the North Atlantic relative to the western basin. Resolution in the deep ocean of silica tests having very low Nd concentrations may also be indicated. In either case the deep waters of the eastern basin appear to have a different source of REE from that in overlying shallower waters. This observation is compatible with the idea that deep-sea sediments represent a source of REE in the deep ocean. Laterally transported Nd in bottom currents having high Nd concentrations may also be a source of this deep-water excess.

The source of relatively nonradiogenic Nd in the deep waters of the North Atlantic remains to be determined. Two possibilities are runoff from Precambrian terranes into the Arctic Ocean and mobilization of REE in deep-sea sediments. Based on data for composite samples from the Canadian Shield [*McCulloch and Wasserburg*, 1978], runoff from Archean terranes would be expected to have $\epsilon_{Nd}(0) \leq -25$. If freshwater injections from North America and Asia into the Arctic are characterized by such low values of $\epsilon_{Nd}(0)$, then this component should be easily identified in Arctic Ocean waters. A northerly source for Nd associated with North Atlantic deep water would require extensive lateral transport of Nd in the North Atlantic and would indicate that bottom currents are supplying the 'excess' Nd to the deep waters.

REE could be supplied to the deep waters by injection from deep-sea sediments having Nd that is isotopically less radiogenic than that presently being supplied at the near surface of the oceans. This process has already been suggested as an important source of copper in the deep ocean [*Craig*, 1974; *Boyle et al.*, 1977]. These workers argue that scavenging takes place at all levels in the water column, and therefore a source of copper at the bottom is required to maintain the higher concentrations in the deep waters. This argument can also be made for Nd and other REE, since they display concentration gradients similar to those found for copper. We have already presented evidence from Nd concentrations vs. nutrient correlations for a deepwater source of Nd. Lateral as well as vertical transport is most evident from the difference in isotopic composition between deep and surface waters observed at many locations, which may also indicate a deepwater source of Nd. In addition, arguments can be made for the injection of Nd from sediments from mass balance considerations. Based on concentrations of 40 ng/kg of Nd dissolved in rivers [*Martin and Maybeck*, 1980] and a net annual discharge of 4.6×10^{19} cc/yr [*Holland*, 1978], a residence time of ~2200 years is obtained with respect to river input. This residence time is too long to be compatible with Nd observations in the oceans. In order to maintain the observed Nd isotopic variations in the oceans, we estimate that the oceanic REE residence times must be on the order of a few hundred years or less. From *Elderfield and Greaves* [1982] the residence time is ~750 years with respect to atmospheric dust input. This assumes that all of the Nd in the dust is soluble, which we believe is unlikely. If 10% of the atmospheric Nd were soluble, an ~7500-year residence time is indicated. *Goldstein and O'Nions* [1982] analyzed dust samples from the eastern Atlantic and western Pacific and found a limited range of isotopic composition from $\epsilon_{Nd}(0) = -9.1$ to -10.1. These values are too radiogenic to be the source of deepwater Nd. This further indicates that atmospheric dust may only be of local importance as a source of REE in the oceans. All of these considerations strongly indicate that a source of dissolved Nd from bottom sediments may be necessary to bring the dissolved oceanic REE budget into balance. However, Nd isotopic data from *Goldstein and O'Nions* [1981] for Atlantic deep-sea sediments exhibit a wide range of $\epsilon_{Nd}(0)$ from -3.4 to -12.3. Most of their values for Atlantic sediments are much more radiogenic than in overlying waters and in typical Atlantic Fe-Mn nodules. This would indicate that deep-sea sediments are not the source of Nd in the deep Atlantic waters, unless differential dissolution of older continental components can occur. We conclude that while the dominantly continental nature of Nd in ocean waters is well established, the detailed sources of Nd in the oceans are not yet established; and we are not yet able to identify and assess the importance of processes active at the sediment-seawater interface that may affect the REE budget of the oceans.

CONCLUSIONS

Nd isotopic results presented here have established that the outflow of Mediterranean water into the Atlantic is characterized by a shift in isotopic composition correspond-

ing to $\varepsilon_{Nd}(0) \geq -9.8$ for Mediterranean waters. This outflow is seen as a shift toward more radiogenic values of $^{143}Nd/^{144}Nd$ in the water column of the eastern North Atlantic at a water depth of 1000 m relative to overlying and underlying waters that have $\varepsilon_{Nd}(0) \approx -12$. This shift of two ε units coincides with the core of the Mediterranean outflow as identified from salinity measurements. We estimate the isotopic composition of Mediterranean water to be $\varepsilon_{Nd}(0) \approx -6$ to -7. The source of Nd with this isotopic composition may be runoff from a relatively young continental terrane or injection of Nd from deep-sea sediments that have significant young volcanogenic components. Though the Nd isotopic component of water associated with the Mediterranean outflow is indistinguishable from that in the near-surface waters of the western Atlantic, we have concluded that they must reflect different sources of Nd.

The deep waters from the eastern basin of the North Atlantic are isotopically distinguishable from the deep waters in the western basin. This may indicate inhomogeneity in the North Atlantic deep water sources or modification of waters in the eastern and/or western basins subsequent to the formation of this water mass. If Nd in the deep waters is supplied from sediments, the isotopic differences between the eastern and western basins could reflect sediments that have an 'older' Nd component in the western basin relative to the eastern basin.

The bulk of waters in the North Atlantic are characterized by lower values of $\varepsilon_{Nd}(0)$ (-11.5 to -14.0), indicating that there must be a major source of REE injections we have not identified. The source of low $^{143}Nd/^{144}Nd$ in the North Atlantic deep water may be runoff from Precambrian shields of North America and Asia into the Arctic Ocean, or possibly injection of the REE from some old component in bottom sediments into the overlying water column.

Comparison of Nd concentration data with corresponding nutrient data for station 95 has been made. Linear correlations between Nd and PO_4^{3-}, NO_3^-, and SiO_2, respectively, are observed in waters above and below the Mediterranean outflow core. On the basis of a difference in slope of these correlations above and below the outflow core, we have concluded that there is a source of 'excess' Nd in the deep waters at this station. We suggest that the source of this 'excess' Nd is the injection of REE from deep-sea sediments into the overlying water column.

Acknowledgments. We thank C. Wunsch and M. S. McCartney for providing ship time in the Atlantic. We appreciate the cooperation of the crew of the RV *Atlantis II* during the collection of the samples. B. Lowman and J. Jennings performed the nutrient analyses. This study has benefited greatly from many discussions with M. Stordal. We would also like to thank T. Takahashi and C. G. H. Rooth for their suggestions on improving the manuscript. This research was supported by grant NSF OCE-8108595. Basic laboratory operations were supported by NASA NGL-05-002-188. This is contribution 3803 (425) of the Division of Geological and Planetary Sciences, California Institute of Technology.

REFERENCES

Boyle, E. A., F. Sclater, and J. M. Edmond, The distribution of dissolved copper in the Pacific, *Earth Planet. Sci. Lett.*, *37*, 38–54, 1977.

Broecker, W. S., A revised estimate for the radiocarbon age of North Atlantic Deep Water, *J. Geophys. Res.*, *84*, 3218–3226, 1979.

Broecker, W. S., and T. Takahashi, Hydrography of the Central Atlantic—3, The North Atlantic deep-water complex, *Deep-Sea Res.*, *27A*, 591–613, 1980.

Bruland, K. W., Oceanographic distributions of cadmium, zinc, nickel, and copper in the North Pacific, *Earth Planet. Sci. Lett.*, *47*, 176–198, 1980.

Craig, H., A scavenging model for trace elements in the deep sea, *Earth Planet. Sci. Lett.*, *23*, 149–159, 1974.

DePaolo, D. J., and G. J. Wasserburg, Nd isotopic variations and petrogenetic models, *Geophys. Res. Lett.*, *3*, 249–252, 1976.

Deitrich, G., K. Kalle, W. Krauss, and G. Sielder, *General Oceanography: An Introduction*, 2nd ed., John Wiley, New York, 1980.

Elderfield, H., and M. J. Greaves, The rare earth elements in seawater, *Nature*, *296*, 214–219, 1982.

Goldstein, S. L., and R. K. O'Nions, Nd and Sr isotopic relationships in pelagic clays and ferromaganese deposits, *Nature*, *292*, 324–327, 1981.

Goldstein, S. L., and R. K. O'Nions, Nd isotopic study of river particulates, atmospheric dusts, and pelagic sediments (abstract), *Eos Trans. AGU*, *63*, 352–353, 1982.

Holland, H. D., *The Chemistry of the Atmosphere and Oceans*, John Wiley, New York, 1978.

Jacobsen, S. B., and G. J. Wasserburg, Sm-Nd isotopic evolution of chondrites, *Earth Planet. Sci. Lett.*, *50*, 139–155, 1980.

Knauss, J. A., *Introduction to Physical Oceanography*, Prentice-Hall, Englewood Cliffs, New Jersey, 1978.

Martin, J. -M., and M. Maybeck, Elemental mass-balance of material carried by major world rivers, *Mar. Chem.*, *7*, 173–206, 1980.

McCulloch, M. T., and G. J. Wasserburg, Sm-Nd and Rb-Sr chronology of continental crust formation, *Science*, *200*, 1003–1011, 1978.

Patterson, C. C., Lead in seawater, *Science*, *183*, 553–554, 1974.

Piepgras, D. J., and G. J. Wasserburg, Neodymium isotopic variations in seawater, *Earth Planet. Sci. Lett.*, *50*, 128–138, 1980.

Piepgras, D. J., and G. J. Wasserburg, Isotopic composition of neodymium in waters from the Drake Passage, *Science*, *217*, 207–214, 1982.

Piepgras, D. J., G. J. Wasserburg, and E. J. Dasch, The isotopic composition of Nd in different ocean masses, *Earth Planet. Sci. Lett.*, *45*, 223–236, 1979.

Ryan, W. B. F., Stratigraphy of Late Quarternary sediments in the eastern Mediterranean, in *The Mediterranean Sea: A Natural Sedimentation Laboratory*, edited by D. J. Stanley, pp. 149–169, Dowden, Hutchinson and Ross, Stroudsburg, Pa., 1971.

Tchernia, P., *Descriptive Regional Oceanography*, Pergamon, New York, 1980.

(Received September 20, 1982;
revised March 14, 1983;
accepted March 15, 1983.)

OCEANOGRAPHIC IMPLICATIONS OF Nd ISOTOPIC VARIATIONS IN SEAWATER

PIEPGRAS, Donald J. and WASSERBURG, G. J., The Lunatic Asylum of the Charles Arms Laboratory, Division of Geological and Planetary Sciences, California Institute of Technology, Pasadena, California 91125

Distinctive Nd isotopic variations have been observed in authigenic ferromanganese sediments from the Pacific, Indian, and Atlantic Oceans. Inter-ocean variations are quite large. Average $\varepsilon_{Nd}(0)$ values for ferromanganese sediments analyzed for each ocean are as follows: Atlantic Ocean, $\varepsilon_{Nd}(0)\cong-12$; Indian Ocean, $\varepsilon_{Nd}(0)\cong-8$; Pacific Ocean, $\varepsilon_{Nd}(0)\cong-3$. These values are far less than $\varepsilon_{Nd}(0)$ values of source rocks with oceanic affinities, which typically have $\varepsilon_{Nd}(0)\cong+10$. The magnitude of variation within each ocean is only about ±2 ε units. Direct measurements of the Nd isotopic composition of seawater presently being made in waters from the Pacific and Atlantic Oceans appear to agree well with the range observed in ferromanganese sediments. It is therefore believed that the Nd isotopic variations observed in ferromanganese sediments represent true variations in the dissolved load of Nd in the oceans. These variations reflect primarily the age and $^{147}Sm/^{144}Nd$ ratios of the continental masses being sampled, which are believed to be the major sources of REE in seawater. The observation of these Nd isotopic variations indicates that the residence time of Nd in seawater must be very short relative to the mixing rates between oceans. Nd isotopic studies in ferromanganese sediments and seawater should, therefore, be useful as a monitor of ocean currents and inter-ocean mixing times. Nd isotopic analysis of concentric layers of ferromanganese nodules may be useful for tracing variations of Nd in the oceans over the last several million years. Data for Pacific and Atlantic seawater will be presented along with data for selected ferromanganese sediments.

Nd ISOTOPIC COMPOSITION AS AN OCEANOGRAPHIC TRACER

D. J. Piepgras
G. J. Wasserburg (The Lunatic Asylum, Division of Geological and Planetary Sciences, California Institute of Technology, Pasadena, CA 91125

Direct Nd isotopic measurements have been made on several samples of seawater from Atlantic and Pacific Oceans. Results clearly indicate distinctive differences in the isotopic composition of Nd in the waters of these two oceans. $\varepsilon_{Nd}(0)$ values for samples from two sites in the Atlantic Ocean are -13.5 and -10.9. Four samples from two sites in the Pacific Ocean have $\varepsilon_{Nd}(0)$ values ranging from -2.1 to -3.8. These values lie wholly within the ranges in $\varepsilon_{Nd}(0)$ observed for ferromanganese sediments in the respective oceans (Piepgras et al, in press; O'nions et al, 1978). Average $\varepsilon_{Nd}(0)$ values for each ocean as determined by data from ferromanganese sediments and seawater are as follows: Atlantic Ocean, $\varepsilon_{Nd}(0) \cong -12$; Indian Ocean, $\varepsilon_{Nd}(0) \cong -8$; Pacific Ocean, $\varepsilon_{Nd}(0) \cong -3$. The dispersion within each ocean is only about $\pm 2\,\varepsilon$ units. These variations amount to a difference in the relative abundance of ^{143}Nd between the Atlantic and Pacific Oceans of only 10^6 atoms $^{143}Nd/g$ of seawater. Source rocks with oceanic affinities have a fairly uniform $\varepsilon_{Nd}(0) \cong +10$, a value which is considerably higher than those observed for ferromanganese sediments and seawater. We believe that the observed Nd isotopic variations represent differences in the dissolved load of Nd in the oceans which are a result of a short residence time of Nd in seawater and reflect primarily the age and $^{147}Sm/^{144}Nd$ ratios of the continental masses being sampled. Continental rocks are considered to be the major source of Nd in seawater with some contributions (~15-30%) from oceanic sources. Nd isotopic variations in seawater should, therefore, be useful as a natural tracer for monitoring inter-ocean mixing times. Nd isotopic analysis of concentric layers of ferromanganese nodules may be useful for determining fluctuations in the sources of REE which may have caused variations of Nd in the oceans over the past several million years. Data for Atlantic and Pacific seawater and selected ferromanganese sediments will be presented.

NEODYMIUM ISOTOPES IN DRAKE PASSAGE WATERS

D. J. Piepgras (Div. of Geological & Planetary Sciences, Calif. Inst. Tech., Pasadena, CA 91125
G. J. Wasserburg

Nd isotopic measurements were made on seawater flowing through the Drake Passage collected during Cruise #107 of RV Atlantis II. The results for a vertical profile south of the Antarctic Convergence show uniform ε_{Nd} and a decrease in Nd concentration in near surface waters. Results are as follows: 50M, ε_{Nd}=-9.1±1.0, C_{Nd}=1.85x10^{-12}g/g; 2000M, ε_{Nd} = -8.4±0.7, C_{Nd} = 3.25x10^{-12}g/g; 3600M, ε_{Nd}=-8.9±0.4, C_{Nd}= 4.21x10^{-12}g/g. These ε_{Nd} values clearly demonstrate that water flowing out of the Pacific sector of the Southern Ocean is dominated by Atlantic Nd (ε_{Nd}≃-12) rather than Pacific Nd (ε_{Nd}≃-3). Uniform ε_{Nd} in the Drake Passage is in contrast with ε_{Nd} stratification in the N Atlantic suggesting that the Southern Ocean is well "stirred" on the time scale of Nd residence time. Based on isotopic data reported here the Antarctic Circumpolar Current appears to be dominated by water of Atlantic origin which it spreads around to the Indian and Pacific and finally recirculates back into the Atlantic. 2/3 of the water flowing through the Drake Passage appears to be of Atlantic origin. We have constructed a 6 box model describing exchange between the Southern Ocean and Atlantic, Indian and Pacific. The Southern Ocean is divided into 3 boxes corresponding to portions adjacent to the respective regions of exchange given above. Exchange of the Pacific with the Southern Ocean is given by $[(\varepsilon_{SOI}C_{SOI}-\varepsilon_{SOP}C_{SOP})/(\varepsilon_{SOP}C_{SOP}-\varepsilon_{P}C_{P})] \cdot W_{ACC}$ where $\varepsilon_{SOI}C_{SOI}$, $\varepsilon_{SOP}C_{SOP}$ are the respective ε_{Nd} and Nd concentrations of the Southern Ocean adjacent to the Indian and Pacific, $\varepsilon_{P}C_{P}$ is ε_{Nd} and Nd concentration of the Pacific and W_{ACC} is the total flow of the Antarctic Circumpolar Current. Taking concentrations to be equal and substituting reasonable values into this equation we get an exchange rate between the Pacific and Southern Oceans of $\leq 20 \times 10^{6} m^{3} s^{-1}$. The results of this study suggest that Nd isotopic composition is a useful oceanographic tracer.

Isotopic Composition of Sr and Nd in Hydrothermal Solutions from 21°N, EPR and Guaymas Basin

D. J. PIEPGRAS and G. J. WASSERBURG (Div. of Geol. and Planet. Sci., Calif.Inst.of Tech.,Pasadena,CA 91125)

We have determined concentrations and isotopic compositions of Sr and Nd in hydrothermal fluids from 21°N, EPR and Guaymas Basin. This study represents the first effort to measure the Nd I.C. in hydrothermal solutions. Endmember samples (T=350°C) from 21°N exhibit a small range in ε_{Sr} values from -13.4 to -15.7. Correcting to C_{Mg}=0, the pure hydrothermal solutions are estimated to have ε_{Sr}≈-18. These results indicate that the fluids have undergone extensive but not complete exchange with Sr in the depleted oceanic crust (ε_{Sr}≈ -30). C_{Sr} ranges from 5.8 to 8.7 ppm and is similar to seawater (7.6 ppm) indicating that there must be buffering. Hydrothermal solutions from Guaymas Basin (T=315°C) rise through several hundred meters of sediment before reaching the sea floor. One sample from here has ε_{Sr}=+5.8, indicating that the solutions have reacted first with oceanic crust and then sediments. The high Sr concentration in this sample (19.3 ppm) is consistent with late stage interaction between the ascending fluid and carbonate rich sediments.

Nd shows a wide range in concentrations and isotopic compositions in solutions from 21°N. C_{Nd} ranges from 20-336 pg/g, a factor of 3-50 lower than reported by Michard et al. [1983] for solutions from 13°S, EPR. ε_{Nd} ranges from -3.6 to +7.9. The data clearly show substantial contributions of Nd from depleted oceanic crust to many of the samples analyzed. In spite of enrichments in Nd of up to 100 times seawater, none of the samples have ε_{Nd} values equal to MORB (ε_{Nd}≈+10). One sample from Guaymas Basin has ε_{Nd}=-11.4 consistent with leaching of Nd from sediments derived from old, continental sources. There is some inconsistency in the Nd isotopic data indicating that there is a possibility of contamination during sampling and/or handling of the solutions.

Neodymium Isotopic Constraints on Rare Earth and Trace Element Transport in the Oceans

D. J. PIEPGRAS and G. J. WASSERBURG (Div. of Geol. and Planet. Sci., Calif.Inst.of Tech.,Pasadena,CA 91125)

Nd isotopic and concentration data for several vertical profiles of the water column in the Atlantic put constraints on the transport of rare earth elements in the oceans, and may have implications for the transport of other trace elements as well. The data challenges the validity of vertical transport models for trace element distribution in the oceans which do not take into account significant horizontal transport. The Nd isotopic composition in the water column of the western N. Atlantic exhibits a relatively large shift of 2 to 3 ε-units in the depth interval from 800 to 1000 m. Below this depth at mid latitudes in the N. Atlantic the water column has uniform $\varepsilon_{Nd} \cong -13.5$ compared to $\varepsilon_{Nd} \cong -10.9$ to -9.4 at depths $\leq$ 800 m. This sharp difference in ε_{Nd} indicates that there is only limited exchange of Nd across this 200 m interval of the water column. To maintain this difference, there must be significant lateral transport of Nd from at least two different sources. REE in North Atlantic Deep Water (NADW) comprise one source that is being transported laterally southward from polar regions underneath upper water having a different source of Nd with an isotopic composition distinct from underlying NADW. The lateral transport concept is supported by new Nd isotopic data for the western equatorial Atlantic where a shift toward more radiogenic ε_{Nd} values is observed in the bottom waters, indicating the presence of northward spreading Antarctic Bottom Water ($\varepsilon_{Nd} \cong -9$) underneath southward spreading NADW. Though Nd fluxes from sediments may be an important source in deep waters, these new data indicate it is not the only source. Lateral transport of Nd is indicated at other locations in the Atlantic and Pacific, as well. Features such as observed maxima in trace element and nutrient profiles from the Atlantic may also be related to lateral transport phenomena, consistent with the Nd isotopic observations reported here.

Appendix X: An ion exchange technique for the separation of REE from seawater using Chelex 100 chelating resin

For samples collected during the Transient Tracers in the Oceans Tropical Atlantic Study (TTO/TAS) a new method for the shipboard separation of the REE was developed and tested. The method is based on an ion exchange technique using a chelating resin which has proven successful for the separation of a variety of trace elements from seawater for concentration analysis (for example, see Bruland et al. [1979]). The first determinations of rare earth concentrations in seawater using a similar extraction technique was made by DeBaar et al. [1983], and a detailed description of their procedure has been presented by DeBaar [1983]. A similar method, but with some modifications, was used for the shipboard extraction of REE from seawater samples collected during the TTO/TAS expedition. The modifications were designed primarily to simplify the chemical procedures at sea and to keep procedural blanks at a minimum. Approximately half of each sample collected was used for the shipboard REE extraction while the other half was stored in a plastic container and acidified for later extraction and analysis by the Fe coprecipitation method to allow for comparison between the two extraction techniques.

Chelex-100, the chelating resin used for this method, is a weakly acidic cationic exchanger manufactured by BIORAD Laboratories. This resin contains iminodiacetate (IMDA) ions on a styrene divinylbenzene copolymer base. The basic functional groups are:

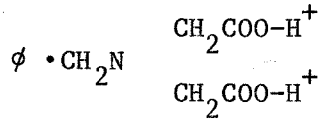

These IMDA ions act as chelating groups in binding metal ions. Thompson [1962] has determined the stability constants for binding REE to IMDA. The log K_1 values range from 5.88 to 7.61 indicating that the resin should have very high selectivity for rare earth ions.

Chelex-100 extraction technique. Columns were made from 1.5cm diameter polyethylene tubing inserted into plastic hose connectors on either end, with a porous polyethylene frit placed inside one end of the column. The Chelex-100 resin (200-400 mesh) was pre-cleaned by daily suspensions in 4N HCl for about two weeks followed by several rinses with quartz distilled H_2O. The columns were packed with resin to a water adjusted height of 7cm. Water was flushed through the columns until the pH of the effluent matched that of the added water. Approximately 5ml H_2O was left on top of the resin and the ends of the columns were sealed to prevent the resin from drying out before being used. Each column was individually packed in a heat sealed plastic bag and stored in an upright position until ready for use.

On board ship, about four liter samples of seawater were transferred directly after collection to polyethylene aspirator bottles and spiked with pre-weighed ^{150}Nd and ^{147}Sm spikes. The samples and spikes were allowed to equilibrate for about 12 hours before beginning the extraction. The rocking of the ship allowed for continuous stirring of the sample during the equilibration period. After equilibration, the sample bottles were connected to the columns with clean plastic tubing and the water was drawn through the resin at ambient seawater pH (~8) using a peristaltic pump down stream from the column. A small amount of seawater from each sample was allowed to remain on each column after the samples had been pumped through the resin, and the columns were then resealed and stored as above for return to the laboratory. At no times after collection were the samples exposed to

the air or laboratory environment on board the ship. After return to the laboratory, the remaining sample on each column was passed through by gravity flow. The columns were then flushed with 30ml H_2O to remove excess salts. The REE were eluted using 20ml 4N HNO_3 and evaporated to dryness. The remaining chemical procedures used to separate Sm and Nd are identical to those used for the iron precipitates and are presented in Appendix 1 and 2. The procedural blank for the Chelex-100 separation is about 25pg for Nd.

The procedure used here differs in several respects from that used by DeBaar [1983] for the REE and others for trace elements. Most workers convert the chelating resin to the ammonia form after cleaning the resin. This has not been done here because column blanks of ~100pg were measures on columns converted to the ammonia form. This may have been due to the use of relatively dirty NH_4OH but the blank of this reagent was not checked. Instead, the resin was left in the hydrogen form and adjusted with water only. In addition, the seawater samples were pumped through the columns at ambient pH (the amount of acid in the spikes is not sufficient to affect the pH of the sample). In DeBaar's procedure the pH of the sample is adjusted to ~6 before being pumped through the resin. There are two reasons for the lower pH, 1) there is less retention of Ca on the column, and 2) DeBaar [1983] has determined on the basis of radiotracer studies that there is a peak in the REE yields at this pH. Radiotracer experiments at ambient seawater pH in this lab have resulted in yields ≥90%. Since the samples are spiked before the chemistry is performed, concentration determinations will not be sensitive to overall yields. Not adjusting the pH of the samples simplifies the procedure at sea and reduces overall blanks due to a reduction in the amount of reagents used in the process. Another difference in the method used here is that the columns have not been rinsed with an

acetate buffer solution after the seawater has been pumped through the resin. The purpose of the acetate buffer is to remove excess salts from the column before eluting the REE. The remaining chemistry necessary to separate the Sm and Nd fractions achieves the same purpose, thus reducing once again the number of reagents used in the procedure.

Comparison between the Chelex-100 extraction technique and the Fe coprecipitation technique has been made for only two samples. The results of this comparison are shown in Table X.1. The 1990m sample gives nearly identical Nd concentration and Nd isotopic results for both methods used. For the 3890m sample there is a significant difference in the Nd concentration determined from the two methods, but the Nd isotopic compositions are identical within the analytical uncertainty of the measurements. There are two possible reasons for the differences in concentration between the two methods. One reason may be that the spike added to the sample separated by the Chelex-100 technique was not sufficiently equilibrated with the Nd in the sample. This would account for the lower concentration observed using the Chelex method. The second possibility is that during storage of the acidified sample REE may have been desorbed from suspended particles resulting in an increased concentration in the sample separated by the Fe coprecipitation technique. This would imply that the deeper sample had a higher particulate concentration, but there are no means of confirming this. There is a regular increase in Nd concentration with depth observed for several samples from this location in which the REE were extracted by the Chelex method (see Table A2 in the appendix) as would be expected, but further comparisons with the iron method are necessary to determine if there is a regular and understandable difference in concentrations determined from the two methods.

REFERENCES

Bruland, K. W., R. P. Franks, G. A. Knauer, J. H. Martin, Anal. Chim. Acta 105, 233, 1979.

DeBaar, H. J. W., The marine geochemistry of the rare earth elements, Ph. D. Thesis, Woods Hole Oceanographic Institution, Woods Hole, Mass., 1983.

DeBaar, H. J. W., M. P. Bacon, and P. G. Brewer, Rare-earth distributions with a positive Ce anomaly in the western North Atlantic Ocean, Nature 301, 324-327, 1983.

Thompson, L. C., Complexes of the rare earths. I. Iminodiacetic acid, Inorg. Chem. 1, 490-493, 1962.

Table X.1. Comparison of Nd concentrations and Nd isotopic compositions determined in seawater samples using the shipboard Chelex-100 and laboratory Fe co-precipitation REE extraction techniques.

Depth (m)	Method	C_{Nd} (pg/g)	$\varepsilon_{Nd}(0)$
1990	Chelex-100	2.50	-13.3 ±0.3
1990	Fe co-precip.	2.53	-13.6 ±0.4
3890	Chelex-100	3.71	-12.4 ±0.5
3890	Fe co-precip.	3.92	-12.8 ±0.6

Appendix XI: Review of REE Solution Chemistry

Introduction

The initial interest in the solution chemistry of the rare earth elements was directed towards finding efficient methods of separating the rare earths from one another. As more data became available on the stabilities of rare earth complexes in aqueous solution, interests shifted toward gaining an understanding of the physical and chemical processes which might affect these stabilities. The majority of the information on the solution chemistry of the rare earths concerns complexes formed with organic ligands in dilute solutions. Only a limited number of determinations have been made for the stability of inorganic ligand complexes with REE in aqueous solution. More recently, some effort has been made to determine the rare earth element speciation in natural waters and their stabilities. These data are very limited and mostly based on theoretical calculations. This section will review the data and interpretations for the observed stability trends of the rare earth complexes and will discuss their implications for the rare earth distributions in natural waters. A comparison between the effects expected as a result of REE complex stabilities on REE distributions in natural with actual observations will be made.

Electronic configuration and bonding of the rare earth elements

Table 1 summarizes numerical data for neutral rare earth metals and their trivalent cations. The first and second transition series elements are characterized by the filling electrons into 3d and 4d orbitals

respectively. After lanthanum, electrons are added to the 4f orbital rather than the 5d. Because of the spectroscopic stability associated with half-filled and completely filled subshells, only the ground state configurations of La ($4f^0 5d^1 6s^2$), Gd ($4f^7 5d^1 6s^2$), and Lu ($4f^{14} 5d^1 6s^2$) have electrons occupying the 5d orbital level [Yost et al., 1947]. The REE are found to give up three electrons to form trivalent cations. The high oxidation potentials shown in Table 1 for the reaction $Ln \rightleftarrows Ln^{3+} + 3e^-$ indicate that oxidation of the REE to the trivalent state is quite favorable. In this trivalent state, the rare earths differ from one another only by the number of electrons in the 4f orbitals and by their cationic radii which decrease with increasing atomic number (the "lanthanide contraction"). Thus, the rare earth elements should exhibit similar behavior throughout the series, and only effects related to the progressive changes in their electronic configuration and size should be observed during the formation of complexes in aqueous solution.

With the exception of hydrated cations, only strongly chelating ligands, especially those with highly electronegative donor atoms such as oxygen, form appreciably stable complex species [Moeller et al., 1965]. This can be understood in terms of the electronic configuration and size of the REE cations. Transition metals form highly stable compounds due in part to their relatively small ionic radii and to the participation of the d electrons in the metal-ligand bonds through the hybridization of the metal electronic orbitals and their overlap with the ligand orbitals. In the case of the rare earths, the 4f orbitals are shielded from interaction with the ligand orbitals by the electrons in the 5s and 5p orbitals. Therefore, for hybridization to occur in the rare earth series, 4f electrons must be promoted to the unoccupied higher energy 5d, 6s, and 6p orbitals. Because

this is energetically unfavorable (the energy required to promote a 4f electron to a 5d orbital is ~50,000cm^{-1}), significant cation-ligand interactions are largely electrostatic (ionic) in nature. Electrostatic attraction is essentially a function of z^2/r, where z is the charge and r is the ionic radius. Thus, for the trivalent rare earths the ionic radii will be the dominant factor controlling the electrostatic interactions with other ligands. Electrostatic attractions with a given ligand would be expected to increase with atomic number along the rare earth series as a result of the corresponding decrease in ionic radii. Consequently, the heavy rare earths would be expected to form stronger complexes than the light REE. According to Moeller et al. [1965], the ionic bonding theory is supported by observations which show that complexing groups have negligible effects on the permanent magnetic moments [Fritz et al., 1960, 1961; and others] and the sharply defined visible and ultraviolet adsorption bands [Holleck and Eckardt, 1953; and others] of the trivalent rare earths. Ground state energy levels are up by only 100 - 200cm^{-1}. This small shift in the ground state energy would not be expected if the 4f electrons were involved in the bonding. As predicted by the electrostatic theory, the general trend in REE complex stability is for increasing stability with decreasing ionic radius for REE in the trivalent state as well as an increase in stability with increasing charge of REE cations for those elements which exist in more than one oxidation state in solution [Moeller et al., 1965].

Stabilities of REE complexes in aqueous solution

Organic complexes

The most intensely studied REE complexes in aqueous solution have been

those with ethylenediaminetetraacetic acid (EDTA) and closely related compounds [Wheelwright et al., 1953; Vickery, 1952; Spedding et al., 1956; Harder and Chaberek, 1959]. With growing interest in the stabilities of REE complexes, many other compounds have been studied. Reviews by Moeller et al. [1965,1968] summarize the available stability constant data for REE complexes with over 50 organic compounds in aqueous solution. Of these, only the limited number of ligands which have been studied for all of the rare earth ions can be considered when discussing trends in their stability constants.

The general reaction for binding n ligands (L) sequentially to a metal ion (M) is

$$M \xrightarrow[K_1]{L} ML \xrightarrow[K_2]{L} ML_2 \cdots \xrightarrow[K_n]{L} ML_n \cdots \qquad (I)$$

where the stability constants (K_n) for the addition of each new ligand are determined from the concentrations (denoted below by brackets) of the complexed and uncomplexed species:

$$K_n = \frac{[ML_n]}{[ML_{n-1}][L]} \qquad (1).$$

Only the first stability constant, K_1, is considered when interpreting the results of REE complex formation in aqueous solution. This is due primarily to complications introduced by steric effects resulting from the addition of more than one ligand.

From the compilation of available data for trivalent rare earths, three general trends or groupings of the REE stability constants have emerged which differ primarily in the behavior of the heavy rare earths [Moeller et

al., 1965]. These three trends are shown in Figure 1 using representative examples to illustrate each trend. The three major trends are 1) a fairly regular increase in stability constant with atomic number for the entire series, 2) an increase to Eu or Gd followed by relatively constant values in the Gd to Lu region, and 3) an increase to a maximum around Dy, followed by a decrease to Lu. For each trend, nearly all of the ligands studied exhibit an increase in the first stability constants (K_1) of the light rare earths with decreasing ionic radius in the region from La to Eu (there are some ligands for which the Eu complex is less stable than for Sm [Moeller et al., 1965]). This trend for the light REE is in agreement with the prediction based on simple electrostatic theory discussed above. For the heavy rare earths, the trends are dependent on the ligand present and do not follow the simple electrostatic model. In general, REE complexes from all three groups exhibit a discontinuity in the stability constants at Gd generally referred to as the "gadolinium break".

No conclusive mechanisms have been determined which would account for the differences in the three trends in the stability constant data. Several mechanisms have been suggested. 1) Ligand-field effects, which would presumably result if 4f electrons were involved in bonding. Thus far, however, no evidence has been found for the involvement of 4f electrons in REE bonding. 2) A reduction in coordination number at or near Gd. Originally the REE were assumed to all be six coordinate, but higher coordination has now been demonstrated for several compounds which are stable in solution. For example, Hoard et al. [1965] and Lind et al. [1965] have demonstrated the existence of both 9- and 10-coordinate La[EDTA] complexes. A change in coordination number is considered the most likely explanation for the ubiquitous Gd break. 3) Steric hindrances may also be important. With the

decreasing ionic radii of the REE, crowding of large organic ligands may occur in the heavy REE region. It is generally believed that a combination of steric factors and a change in coordination number are responsible for the different trends. Regardless of the reasons for these differences, the important observation in these trend as it relates to the stabilities of REE complexes in natural waters is that in all cases the heavy rare earths form more stable complexes than do the light rare earths. The implications this has for natural waters are discussed below.

Inorganic complexes.

In general, coordination by inorganic anions such as halides, carbonates, nitrates, and sulfates in solution is limited to ion-pair associations. Consequently, inorganic REE complexes are generally very weak. A compilation of the available stability constant data up to 1976 for inorganic REE complexes is given by Smith and Martell [1976]. Of most importance to the study of natural waters is the hydrolysis of the REE cations and their carbonate and phosphate complexing ability. These will be discussed in detail below.

Hydrolysis. Among the most important of the inorganic REE complexes are the products of hydrolysis. This subject has been reviewed in some detail by Baes and Mesmer [1976]. The only hydrolysis products which are formed to a significant extent in natural waters are the mononuclear species of which $Ln(OH)^{2+}$ is the most abundant. The polynuclear species $Ln_2(OH)_2^{4+}$ and $Ln_3(OH)_5^{4+}$ are also known to occur for some but not all of the rare earths, however, their abundances are very low relative to the mononuclear species. The general reaction for the formation of mononuclear hydrolysis

products written in terms of a reaction with water is $Ln^{3+} + nH_2O \rightleftarrows Ln(OH)_n^{3-n} + nH^+$ and has hydrolysis constants of the form

$$ {}^*K_n = \frac{[Ln(OH)_n^{3-n}][H^+]^n}{[Ln^{3+}]} , \quad (n \geq 1) \qquad (2). $$

Values of log ${}^*K_1$ at zero ionic strength (I = 0) are reported by Baes and Mesmer [1976] to lie in the range from -8.5 for La to -7.7 for Lu indicating that significant hydrolysis does not occur below pH ≈ 7. The solubility product for the complete dissociation of the solid hydroxide according to the reaction $Ln(OH)_3(s) + 3H^+ \rightleftarrows Ln^{3+} + 3H_2O$ is given by

$$ {}^*K_{s0} = \frac{[Ln^{3+}]}{[H^+]^3} \qquad (3). $$

Baes and Mesmer [1976] report values of log ${}^*K_{s0}$ for the REE at I = 0 in the range from 20.3 for La to 14.5 for Lu indicating a fairly regular decrease in solubility with increasing atomic number. From Eq.(3), the maximum concentration of free Ln^{3+} ion in aqueous solution before precipitation of the hydroxide begins is given by $\log [Ln^{3+}]_{max} = \log {}^*K_{s0} - 3pH$. The solubility of the solid hydroxide according to the equilibrium reaction $Ln(OH)_3(s) \rightleftarrows Ln(OH)_3(aq)$ has log K_{s3} in the range -7.9 to -9.6 at $\mu = 0$, but values for all of the REE are not reported [Baes and Mesmer, 1976]. These values indicate maximum solubilities of the neutral hydroxides in the range of $10^{-8} - 10^{-9}$M in aqueous solutions. The hydrolysis is often written in terms of a reaction with OH^- ions as $Ln(OH)_n^{3-n} + OH^- \rightleftarrows Ln(OH)_{n+1}^{3-(n+1)}$ which has hydrolysis constants of the form

$$ K_{n+1} = \frac{[Ln(OH)_{n+1}^{3-(n+1)}]}{[Ln(OH)_n^{3-n}][OH^-]} , \quad (n \geq 0) \qquad (4). $$

The hydrolysis constants are dependent on the ionic strength of the solution. At I = 1M the first hydrolysis constants are reduced by approximately one log unit and results in a correspondingly similar increase in the solubility.

Carbonate complexing. Very little data on the stability of REE complexes in aqueous solutions are available in the literature. In a recent study related to actinide chemistry, Lundqvist [1982] compiled the data for REE carbonate complexes and determined new values for the stability of Eu complexes with carbonate ions and hydroxyl ions at I = 1. Eu was shown to form stable mononuclear carbonate complexes, the most important species being $Eu(CO_3)^+$ and $Eu(CO_3)_2^-$. Evidence for polynuclear species and bicarbonate complexes were not found in his experiments. The general reaction for the formation of mononuclear complexes is $Eu^{3+} + n\ CO_3^{2-} \rightleftarrows Eu(CO_3)_n^{3-2n}$ which has an overall stability constant given by

$$\beta_n = \frac{[Eu(CO_3)_n^{3-2n}]}{[Eu^{3+}][CO_3^{2-}]^n} \qquad (5).$$

At I = 1M, $\log \beta_1 = 5.93$ and $\log \beta_2 = 10.72$ for mononuclear Eu carbonate complexes. Values for the solubility product, K_{s0}, for the complete dissociation of $Ln_2(CO_3)_3(s)$ has been reported for some rare earths by Turner and Whitfield [1979]. Log K_{s0} values of -26.4 for La and -25.2 for Gd were given for I = 0.7.

Lundqvist has demonstrated graphically, that Am^{3+} carbonate complexes can dominate over hydrolysis at pH up to ~9. Using Lundqvist's values of β_1 and β_2 above and $\log {}^*K_1 = -8.1$ for $Eu(OH)^{2+}$, I have constructed a similar plot for Eu complexes shown in Figure 2 which shows the value $\log [EuL_i]/[Eu^{3+}]$ as a function of $\log [CO_3^{2-}]$, where $L_i = (OH^-)_i$ or $(CO_3^{2-})_i$.

This figure shows that for Eu, carbonate complexes will also dominate over hydrolysis for log $[CO_3^{2-}] > 10^{-5}M$ and pH < 9. As an illustration, consider a solution at pH = 8.1, $[CO_3^{2-}] = 10^{-5}M$, and $[Eu]_T = 10^{-8}M$. If only hydrolysis were involved, about 50% of the total Eu would be complexed as $Eu(OH)^{2+}$. In the presence of CO_3^{2-} however, the mass balance for Eu can be written as

$$[Eu]_T = 10^{-8}M = ([Eu^{3+}] + [Eu(CO_3)^+] + [Eu(CO_3)_2^-] + [Eu(OH)^{2+}]) \qquad (6).$$

Substituting expressions for the stability constants in (2) and (5) gives

$$= [Eu^{3+}](1 + \beta_1[CO_3^{2-}] + \beta_2[CO_3^{2-}]^2 + \frac{{}^*K_1}{[H^+]}) \qquad (7).$$

Only the first hydrolysis constant for Eu is considered because no values are reported for the second and third hydrolysis products. These complexes would be much lower in concentration than $Eu(OH)^{2+}$ and would not significantly alter the results of the calculation. Using the values for ${}^*K_1$, β_1, and β_2 given above in (7) gives the Eu^{3+} concentration from which the concentrations of the remaining species can be calculated. The resulting concentrations and relative abundances are as follows:

$$[Eu^{3+}] = 6.4 \times 10^{-10}M, \qquad 6\%$$

$$[Eu(OH)^{2+}] = 6.4 \times 10^{-10}M, \qquad 6\%$$

$$[Eu(CO_3)^+] = 5.4 \times 10^{-9}M, \qquad 54\%$$

$$[Eu(CO_3)^-] = 3.3 \times 10^{-9}M, \qquad 33\%$$

As can be seen, the carbonate complexes in this example completely dominate

over the hydrolysis of Eu. In the absence of carbonate ion, 50% of the total Eu should be complexed as $Eu(OH)^{2+}$. These results indicate that carbonate complexes in natural waters could be far more important to the solution chemistry of the REE than hydrolysis. The relative speciation in natural waters will be different, however, due to competition with other cations in solution for the available ligands. The main influence of pH on the REE carbonate complex formation will be the effect on the free carbonate ion concentration of the solution. Higher pH will increase the concentration of the carbonate ion.

Phosphate complexes. Of the inorganic ligands, it appears that only phosphate ligands form strong, ionically bonded complexes with the rare earths. The most studied complexes are those involving triphosphate $(P_3O_{10})^{5-}$ and its sodium salts [Giesbrecht and Audrieth, 1958; Giesbrecht, 1960; Kundra, 1963; Kundra et al., 1965]. Giesbrecht and Audrieth [1958] have shown that the soluble triphosphate complexes are formed when the phosphate to lanthanide ratio is greater than 2:1. Although they could not determine the exact structure, they suggested that the soluble anionic triphosphate species is represented by the general formula $[Na_xLn(P_3O_{10})_2]^{7-x}$ where $x < 7$. Kundra [1963] and Kundra et al. [1965] has found the 1:1 complex $LnHP_3O_{10}^-$ to be stable at low pH. In all of these studies, the complexes are generally found to be most stable when the pH is acidic ($\approx$ 3.5). At basic pH levels the complexes are generally insoluble. These authors have not reported any stability constants for the heavy rare earths. In the light rare earth region the stability constants exhibit the same trend as observed for organic complexes. In seawater, phosphate occurs in solution as the orthophosphate, H_3PO_4, in various states of dissociation [Spencer, 1975]. Data summarized by Smith and Martell [1976] show $LnH_2PO_4^{2+}$

complexes to be stable at low pH, but at the pH of seawater, only 1% of the total phosphate is present as $H_2PO_4^-$ and therefore these complexes should not be important in seawater. No formation constants were given for HPO_4^{2-} and PO_4^{3-} complexes which may be more important in seawater and fresh water. Turner and Whitfield [1979] reported solubility product values for two rare earths (La and Gd) for the dissociation of $LnPO_4(s)$ both of which had log $K_{s0} \approx -18.3$ for $I = 0.7$.

Implications of stability constant data for the distribution of the REE in natural waters

The data for REE complexes discussed above have several implications for the distribution of rare earths in natural waters. It is clear from the preceding discussion that the most stable REE complexes are those with organic ligands in which oxygen acts as the primary electron donor. Thus, it may be expected that organic ligands will make the most stable complexes with the REE in natural waters. The effects such complexes may have on REE distributions in natural waters will depend on whether organic ligands are in solution or associated with particulate matter, as well as the total concentration of the organic ligands relative to competing inorganic ligands. It has been postulated that most particles in seawater are coated with a thin film of organic matter [Neihof and Loeb, 1974; Loeb and Neihof, 1977; Hunter and Liss, 1979]. Modeling of adsorption of trace metals onto sinking particles indicates that the adsorption properties are indeed controlled by organic coatings as opposed to surface hydroxide groups [Balistrieri et al., 1981]. Because the heavy rare earths are found to form more stable complexes than the light rare earths, it would be expected that adsorption onto sinking organic matter or organic coated particles would

preferentially remove the heavier rare earths producing a heavy rare earth depleted abundance pattern (relative to source abundances) for REE dissolved in seawater. Furthermore, if Ce is oxidized to the +4 state in natural waters, then from electrostatic theory it should form more stable complexes than its neighbors La and Pr, resulting in a Ce depletion. Similar effects would be expected for fresh water systems if organic matter is important. If organic ligands are primarily in solution rather than being associated with particles, then the opposite effects should be observed, namely, the heavy rare earths and Ce should preferentially be held in solution. Inorganic complexes, though not as stable as organic complexes, could be more important in controlling the concentrations of the REE in natural waters, particularly if organic ligand concentrations are low. In Lundqvist's [1982] determinations of stability constants for hydrolysis and carbonate complexes, the constants were determined based on changes in the distribution coefficients for the extraction of the REE onto organic ligands as a function of the pH and carbonate ion concentrations. Thus, hydrolysis and carbonate complexing can prevent the formation of organic complexes. As long as the concentrations of the REE do not exceed the limits set by the solubility of their inorganic salts, inorganic complexes should serve to keep the REE in solution, but this should affect the abundance pattern only if the individual solubilities are exceeded. The possible exception to this is complexes involving phosphate ligands. If strong complexes with phosphate are important, then a covariation between phosphate and REE concentrations in natural waters might be expected. However, according to the observations discussed above, it is apparent that REE phosphate complexes should not be important in natural waters where the pH is generally high enough to render these complexes insoluble. These predictions will be

compared to actual observations of rare earth distributions in marine and fresh waters in the discussion below.

Distribution and speciation of REE in river and seawater

The distribution of REE in river water and seawater

River water. Only a few measurements of the concentrations of the REE series have been made for river waters [Martin et al., 1976; Keasler and Loveland, 1982; Hoyle et al., 1984]. No consistent pattern emerges from these data for the REE abundances in river waters. The chondrite normalized abundance pattern for a sample collected from the confluence of the Garonne and Dordogne Rivers in France [Martin et al., 1976] is shown in Figure 3a. For comparison, average continental REE values represented by North American Shale (NAS) [Haskin et al., 1966] are shown on the same figure (Fig. 3b). It is seen that this river sample has an abundance pattern nearly identical to NAS, reflecting a derivation of its REE from an average continental source. Filtered waters from Pacific Northwest rivers [Keasler and Loveland, 1982] and the Luce River [Hoyle et al., 1984] all exhibit a heavy rare earth enrichment relative to NAS but to varying extents. It is not clear from the available data whether the differences in the REE patterns observed between these rivers reflects differences in the mean REE abundances in the geologic terranes drained by these rivers or if they are related to REE fractionation processes active within the different rivers. A slight negative Ce anomaly is observed in the 0.7μm filtered Luce River sample [Hoyle et al., 1984] and possibly in the Pacific Northwest rivers [Keasler and Loveland, 1982] which suggests that the variations may be related to fractionation of the REE in the riverine environment.

Seawater. Concentrations of the rare earth element series in seawater have been determined by several authors [Goldberg et al., 1963; Høgdahl et al., 1968; Masuda and Ikeuchi, 1978; Elderfield and Greaves, 1982; DeBaar et al., 1983; Klinkhammer et al., 1983; Hoyle et al., 1984]. Chondrite normalized REE concentration data for two Atlantic Ocean locations at similar depths of about 3000 meters are shown in Figure 3c,d. The abundance patterns for these two samples, which are representative of typical seawater REE distributions, are similar to each other but significantly different from river water (Fig. 3a) and NAS (Fig. 3b). Seawater exhibits a distinct V-shaped chondrite normalized REE pattern with a minimum in the normalized values at Eu indicating both light and heavy rare earth enrichments. The heavy REE enrichments in seawater are generally more pronounced than in river waters (when present in the latter). In addition, there is a generally well developed negative Ce anomaly characteristic of seawater which is either absent or only poorly developed in rivers and completely absent from NAS. The only exception to this was reported by DeBaar et al. [1983] for western North Atlantic samples which exhibited a positive Ce anomaly in near surface waters. In general, there is an increase in concentration of all the REE with depth with only slight changes in the REE pattern.

Speciation of REE in fresh and seawater

Determinations of the chemical forms of the REE in natural waters have never been made by direct experimental measurements. The main reasons for this are the complex nature of natural waters (which makes it difficult to identify the possible interactions with REE cations) and the difficulty of determining the concentrations of the different complex species. The oxidation states of the REE in natural waters are fairly well known. With

the exception of Ce, the oxidation state of all the REE in fresh and seawater is +3. In seawater, Ce is known to occur primarily in the +4 oxidation state, which may account for its anomalous behavior in this reservoir. Carpenter and Grant [1967] determined from florescence data in controlled experiments that cerium should be almost completely oxidized to the +4 state at the pH of seawater. Ce may also occur in the +3 oxidation state in the marine environment, especially in anoxic waters and sediment pore fluids. Mobilization of Ce in the +3 oxidation state from anoxic sediments was the explanation for the positive Ce anomaly reported for near surface, western Atlantic waters by DeBaar et al. [1983]. In fresh water, however, Ce shows normal behavior relative to La and Pr, indicating that it probably occurs only in the +3 state in these waters. Europium is known to occur in the +2 and +3 oxidation states. Sverjensky [1984] estimated the stability of Eu^{2+} and Eu^{3+} in aqueous solution over a wide range of temperatures and pressures. His calculations demonstrate that Eu should be in the +3 oxidation state in most waters below temperatures of 250°C with the possible exception of very reducing alkaline pore waters of marine sediments. The +2 oxidation state would presumably prevail for Eu in hydrothermal solutions at temperatures greater than 250°C.

Turner et al. [1981] used an equilibrium model to estimate the speciation of trace elements in fresh and seawater. Their model is based on the assumptions that 1) published stability constants can be corrected for the difference in ionic strength between the media in which they were measured and the natural system, 2) the activity coefficients of the free metal ion, free ligand, and complex are not affected by changes in the composition in the medium at constant ionic strength, and 3) any strong interactions between the medium ions and the element or ligand of interest

have been taken into account in the original measurement of the stability constants. Their model uses the compilations of stability constants by Smith and Martell [1976] and hydrolysis constants by Baes and Mesmer [1976]. It should be noted that their speciation model does not take into account the possibility of complexes involving organic ligands, although they do discuss the possible implications for this.

The results of their calculations for the speciation of the REE in seawater (pH = 8.2) and fresh water (pH = 6 and pH = 9) are given in Tables 2, 3, and 4 respectively. From the data in Table 2, the model predicts the carbonate complex will be the most abundant REE complex species in seawater with a general trend towards increased carbonate complexing with increasing atomic number. The dominance of the carbonate complex is in agreement with the stability field for hydrolysis and carbonate complexes shown in Figure 2 discussed above. As indicated earlier, the relative abundances of the carbonate and hydroxide species calculated here for the complex natural water systems are different that calculated above for the one rare earth cation, two ligand system and presumably reflects the competition from other cations for the ligands as well as other ligands for the cations. The increase in carbonate complexing is compensated by parallel decreases in the free ion concentration, Cl, and SO_4 complexes of the REE. In freshwater at pH = 6, the REE are determined to be primarily in the free ion state with some SO_4 and CO_3 complexing. At pH = 9, freshwater REE are calculated to occur primarily as OH (heavy REE) and CO_3 (light REE) complexes. These trends generally reflect the electrostatic attractions between the REE cations and the uncomplexed ligand in addition to the competing effect of hydrolysis. It is clear from the data of Turner et al. [1981] and Baes and Mesmer [1976] that the degree of hydrolysis increases with increasing pH.

The increasingly stable hydrolysis constants along the rare earth series [Baes and Mesmer, 1976] are also consistent with electrostatic theory.

Turner et al. [1981] did not include data for organic complexes in calculating the speciation of natural waters. However, they did do species calculations for some metals which included humic acid data. They found a correlation between the stabilities of metal complexes with CO_3 and humic acids in seawater. From this they suggested that rare earths and other metals which form strong carbonate complexes are the most likely to form strong complexes with organic ligands in seawater and even more likely in freshwater due to the generally higher organic concentrations. These data further support implications for REE distributions in natural waters based on stabilities of organic REE complexes discussed above.

Discussion

It is significant to note that both river water and seawater have REE concentrations which are several orders of magnitude below the limits set by the solubility of their salts. At the pH of seawater (~8), the total solubility of Nd, based on hydrolysis products alone, should be about 10^{-4}M. The carbonate solubility may be slightly lower, based on K_{s0} values given by Turner and Whitfield [1979], but the distribution of the REE among the may different ligands available should increase the overall solubility. REE phosphates have the lowest solubilities, but at the phosphate ion concentration of seawater, the REE concentrations are still several orders of magnitude too low to precipitate. It is therefore quite clear that some sort of removal process acts to keep the concentrations in these waters so low. The REE patterns of both river water and seawater must reflect this

removal process. The relative distribution of rare earth species calculated by Turner et al. [1981] should not be affected by differences in concentrations of the REE in fresh and seawater since even the highest REE concentrations observed in natural waters are well below the solubility limits of the REE complexes which are determined to dominate the speciation.

It was suggested originally by Goldberg et al. [1963] that the REE in seawater are derived from the weathering of the continental crust, a point that has been substantiated on the basis of Nd isotopic measurements of marine sediments and waters [Piepgras et al., 1979; Piepgras and Wasserburg, 1980]. It might therefore be expected that seawater REE abundance patterns be similar to NAS or average river water. Because of the differences between seawater REE patterns and those of NAS and rivers, it is probable that the seawater pattern is developed largely as a result of REE fractionation processes within the oceans rather than reflecting the pattern in the sources of REE in the oceans. Further evidence for this comes from two studies which have attempted to determine the effects of estuarine mixing of seawater and river water on the REE transport to the oceans by rivers. Martin et al. [1976] sampled waters in the Gironde estuary (at the confluence of the Garonne and Dordogne Rivers) at various salinities from 0.1 - 28 $^{o}/_{oo}$. The dissolved load concentrations decrease with increasing salinity indicating substantial REE removal in the estuary, but the overall REE pattern is little changed during the process. The light rare earths remain relatively unchanged from the 0.1 $^{o}/_{oo}$ configuration shown in Figure 3a, and in particular, there is no Ce anomaly produced such as seen in seawater. There is some indication of a heavy rare earth enrichment relative to the 0.1 $^{o}/_{oo}$ sample, but a lack of data for many of the heavy rare earths makes it unclear whether the trends are applicable to the entire

series from Eu to Lu. A second study by Hoyle et al. [1984] involved laboratory mixing experiments designed to simulate estuarine mixing between river water and seawater at different salinities. Their results indicated that the heavy rare earths are removed from solution onto particles to a greater extent than the light rare earths. This observation suggests that a heavy rare earth depleted pattern should be produced in the estuarine zone in apparent contradiction to the results of Martin et al. [1976] from the Gironde estuary. (It should be noted that the removal pattern generated in the experiments by Hoyle et al. is in contradiction with the observed distribution of REE on particles suspended in the Luce River. Their data shows that the light rare earths are preferentially associated with particles rather than the heavy rare earths. This problem was not resolved, however). Also of significance in the experiments of Hoyle et al. is the fact that no Ce anomaly was produced. The failure to develope a Ce anomaly is consistent with the observations in the Gironde estuary and suggests that this element may under go a change in oxidation state from +3 to +4 after entering the oceans which allows its more efficient removal from seawater. It is not clear the extent to which the results from these to studies are representative of processes in major river and estuary systems, but the data suggest that fractionation processes in the open ocean may be largely responsible for producing the REE patterns observed in seawater.

It is apparent that both fresh water and seawater REE distributions are generally different from what would be expected on the basis of stability constant data for organic REE complexes. Relative to NAS (which is assumed to represent the average source pattern for REE in rivers and oceans) there is a heavy rare earth enrichment in seawater and many rivers which suggests that dissolved organics may be more strongly complexing the heavy REE and

keeping them in solution. There are two major problems with this explanation, however. First, a positive Ce anomaly rather than negative would be expected since Ce should behave similarly to the heavy rare earths from electrostatic considerations discussed earlier. There would be no reason to expect any unusual behavior for Ce if it was in the +3 state. Positive Ce anomalies have only been observed in areas where they can be attributed to enhanced Ce fluxes from anoxic sediments [DeBaar et al., 1983]. Secondly, Turner and Whitfield [1979] have shown that the REE concentrations in seawater are well below the concentration limits set by the solubilities of their salts indicating that all of the rare earths are being extensively scavenged from seawater. If the model of Balistrieri et al. [1981] which suggests that the adsorption properties of particles are controlled by organic coatings is correct, then heavy rare earth depletions relative to NAS should be observed according to predictions made on the basis of the stability constant data. Since this is not observed in seawater or fresh water, it would appear that inorganic scavenging, possibly on hydroxide surfaces, may also be important.

There is considerable evidence that inorganic phases do indeed control the rare earth abundances in seawater. Although there is no obvious correlation between rare earth abundances and phosphate in seawater [Piepgras and Wasserburg, 1983], Elderfield et al. [1981] have demonstrated a very strong positive correlation between P and REE (except Ce) concentrations in marine sediments indicating that a phosphatic component controls the concentration of the trivalent REE in sediments. In ferromanganese nodules there are positive correlations between the REE and both P and Fe concentrations [Elderfield et al., 1981; Lyle, 1978], indicating the presence of two separate carrier phases in nodules. Cerium, which is tervalent in seawater,

does not correlate at all with P but shows a very strong positive correlation with Fe [Elderfield et al., 1981]. Positive Ce anomalies in ferromanganese nodules with slow growth rates compliment the negative Ce anomaly in seawater [Piper, 1974] also indicating that iron and manganese oxides or hydroxides control the removal of Ce from seawater. (Negative Ce anomalies have been observed in rapidly growing nodules and Fe-Mn crusts in active hydrothermal areas and the Bauer Basin [Toth, 1977; Elderfield and Greaves, 1981]). Thus, it is apparent that the removal of REE from seawater is controlled primarily by inorganic processes. The heavy REE enrichment in seawater relative to presumed continental source abundance patterns may be the result of greater carbonate complexing of these REE in seawater as indicated from the data of Turner et al. [1981] shown in Table 2. The only observations which can be explained in terms of organic complexing alone are the data of Hoyle et al. [1984] for the experimental mixing of seawater and river water which show that the heavy rare earths are more extensively removed from solution than the light rare earths during the flocculation of particles.

Conclusions

The solution chemistry of the rare earth elements and their distribution in natural waters has been reviewed. Although evidence for organic complexing in natural waters has been noted, predictions for the distribution of rare earths in natural waters based on measured stabilities of organic REE complexes are generally not supported by observations of the REE in natural waters. The only exception to this is the removal pattern generated for rare earths from the experimental mixing of river and seawater

[Hoyle et al., 1984]. These experimental removal patterns indicate that there is a preferential removal of heavy REE from solution onto particulate phases dominated by organic colloids. This is consistent with the observations that the heavy rare earths form stronger complexes with organic ligands than do the lighter rare earths. It is apparent that the REE pattern in seawater requires a more complex behavior of the REE than would be expected from the patterns based on the stabilities of REE complexes. This may be related to competition for cations resulting from the presence of numerous ligands in natural waters. It is shown that carbonate speciation will dominate the REE in seawater. In slightly acidic fresh waters free ion and sulfate complexes dominate, whereas in basic fresh waters hydrolysis dominates the heavy REE and carbonate speciation dominates the light REE. The concentrations of the REE in river and seawater are shown to be well below their solubility limits indicating extensive removal in natural waters. The strong correlation between the REE and Fe and P concentrations in marine sediments and ferromanganese nodules suggests that inorganic scavenging dominates the removal of REE from seawater.

REFERENCES

Baes, C. F. and R. E. Mesmer, The Hydrolysis of Cations, J. Wiley and Sons, New York, 1976.

Balistrieri, L., P. G. Brewer, and J. W. Murray, Scavenging residence times of trace metals and surface chemistry of sinking particles in the deep ocean, Deep-Sea Res. 28, 101-121, 1981.

Carpenter, J. H. and V. E. Grant, Concentration and state of cerium in coastal waters, J. Mar. Res. 25, 228-238, 1967.

DeBaar, H. J. W., M. P. Bacon, and P. G. Brewer, Rare-earth distributions with a positive Ce anomaly in the western North Atlantic Ocean, Nature 301, 324-327, 1983.

Elderfield, H. and M. J. Greaves, Negative cerium anomalies in the rare earth element patterns of oceanic ferromanganese nodules, Earth Planet. Sci. Lett. 55, 163-170, 1981.

Elderfield, H. and M. J. Greaves, The rare earth elements in seawater, Nature 296, 214-219, 1982.

Elderfield, H., C. J. Hawkesworth, M. J. Greaves, and S. E. Calvert, Rare earth element geochemistry of oceanic ferromanganese nodules and associated sediments, Geochim. Cosmochim. Acta 45, 513-528, 1981.

Fritz, J. J., P. E. Field and I. Grenthe, The low temperature magnetic properties and magnetic energy levels of some rare earth chelates of acetylacetone and ethylene-diaminetetraacetic acid, J. Phys. Chem. 65, 2070-2074, 1961.

Fritz, J. J., I. Grenthe, P. E. Field, and W. C. Fernelius, Magnetic properties of some rare earth chelates of ethylinediaminetetraacetic acid and acetylacetone between 1.3 and 77.2°K, J. Am. Chem. Soc. 82, 6199-6200, 1960.

Giesbrecht, E., Phosphates and polyphosphates of the rare earth elements-III, J. Inorg. Nucl. Chem. 15, 265-271, 1960.

Giesbrecht, E. and L. F. Audrieth, Phosphates and polyphosphates of the rare earth elements-II, J. Inorg. Nucl. Chem. 6, 308-313, 1958.

Goldberg, E. D., M. Koide, R. A. Schmitt and R. H. Smith, Rare earth distributions in the marine environment, J. Geophys. Res. 68, 4209-4217, 1963.

Harder, R. and S. Chaberek, The interaction of rare earth ions with diethylenetriaminepentaacetic acid, J. Inorg. Nucl. Chem. 11, 197-209, 1959.

Haskin, L. A., F. A. Frey, R. A. Schmitt, and R. H. Smith, Meteoritic, solar, and terrestrial rare earth distributions, in Physics and Chemistry of the Earth, (Pergamon Press, New York) 169-321, 1966.

Hoard, J. L., B. Lee, and M. D. Lind, On the structure-dependent behavior of ethylenediaminetetraacetato complexes of the rare earth LN^{3+} ions, J. Am. Chem. Soc. 87, 1612-1613, 1965.

Høgdahl, S. Melson and V. T. Bowen, Neutron activation analysis of Lanthanide elements in seawater, Adv. Chem. Ser. 73, 308-325, 1968.

Holleck, L. and D. Eckardt, Termaufspaltung durch komplexe Bindung bei Seltenen Erden in wässriger Lösung, Naturwissenschaften 40, 409, 1953.

Hoyle, J., H. Elderfield, A. Gledhill, and M. Greaves, The behavior of the rare earth elements during mixing of river and sea water, Geochim. Cosmochim. Acta 48, (in press)

Hunter, K. A. and P. S. Liss, The surface charge of suspended particles in estuarine and coastal waters, Nature 282, 823-825, 1979.

Keasler, K. M. and W. D. Loveland, Rare earth elemental concentrations in some Pacific Northwest rivers, Earth Planet. Sci. Lett. 61, 68-72, 1982.

Klinkhammer, G., H. Elderfield, and A. Hudson, Rare earth elements in seawater near hydrothermal vents, Nature 305, 185-188, 1983.

Kundra, S. K., Complex formation of rare earths with sodium triphosphate, Indian J. Chem. 1, 362, 1963.

Kundra, S. K., P. R. Subbaraman, and J. Gupta, Complex formation of light lanthanous with sodium triphosphate, Indian J. Chem. 3, 60-62, 1965.

Lind, M. D., B. Lee, and J. L. Hoard, Structure and bonding in a ten-coordinate lanthanum (III) chelate of ethylenediamenetetraacetic acid, J. Am. Chem. Soc. 87, 1611-1612, 1965.

Loeb, G. I. and R. A. Neihof, Adsorption of an organic film at the platinum-seawater interface, J. Mar. Res. 35, 283-291, 1971.

Lundqvist, R., Hydrophilic complexes of the actinides. I. Carbonates of trivalent americium and europium, Acta Chem. Scand. A36, 741-750, 1982.

Lyle, M., The formation and growth of ferromanganese oxides on the Nazca Plate, Ph. D Thesis, Oregon State University, Corvallis, OR, 1978.

Martin, J. -M., O. Høgdahl and J. C. Philippot, Rare earth element supply to the ocean, J. Geophys. Res. 81, 3119-3124, 1976.

Masuda, A. and Y. Ikeuchi, Lanthanide tetrade effect observed in marine environment, Geochem. J. 13, 19-22, 1979.

Moeller, T. E. R. Birnbaum, J. H. Forsberg, and R. B. Gayhart, Some aspects of the coordination chemistry of the rare earth metal ions, in Progress in the Science and Technology of the Rare Earths, Vol. 3, L. Eyring ed., (Pergamon Press, Oxford) 1968.

Moeller, T., D. F. Martin, L. C. Thompson, R. Ferrus, G. R. Feistel, and W. J. Randall, The coordination chemistry of yttrium and the rare earth metal ions, Chem. Rev. 65, 1-50, 1965.

Moeller, T., L. C. Thompson, and R. Ferrus, Some aspects of the stabilities of amine polycarboxylic acid chelates of the tri-positive rare earth metal ions, in Rare Earth Research, E.V. Kleber, ed. (Macmillan Co., New York) 3-11, 1961.

Neihof, R. A. and G. Loeb, Dissolved organic matter in seawater and the electric charge of immersed surfaces, J. Mar. Res. 32, 5-12, 1974.

Piepgras, D. J. and G. J. Wasserburg, Neodymium isotopic variations in seawater, Earth Planet. Sci. Lett. 50, 128-138, 1980.

Piepgras, D. J. and G. J. Wasserburg, Influence of the Mediterranean outflow on the isotopic composition of Neodymium in waters of the North Atlantic, J. Geophys. Res. 88, 5997-6006, 1983.

Piepgras, D. J., G. J. Wasserburg and E. J. Dasch, The isotopic composition of Nd in different ocean masses, Earth Planet. Sci. Lett. 45, 223-236, 1979.

Piper, D. Z., Rare earth elements in ferromanganese nodules and other marine phases, Geochim. Cosmochim. Acta 38, 1007-1022, 1974.

Smith, R. M. and A. E. Martell, Critical Stability Constants, Vol. 4 Inorganic Complexes, Plenum Press, 1976.

Spedding, F. H., J. E. Powell, and E. J. Wheelwright, The stability of the rare earth complexes with N-hydroxyethylenediaminetriacetic acid, J. Am. Chem. Soc. 78, 34-37, 1956.

Spencer, C. P., The Micronutrient Elements, Chapter 11, in Chemical Oceanography, vol. 2, J. P. Riley and G. Skirrow, eds. (Academic Press, London) 1975.

Sverjensky, D. A., Europium redox equilibria in aqueous solution, Earth Planet. Sci. Lett. 67, 70-78, 1984

Toth, J. R., Deposition of submarine hydrothermal manganese and iron, and evidence for input of volatile elements to the ocean, M. S. Thesis, Oregon State University, Corvallis, Oregon 1977.

Turner, D. R. and M. Whitfield, Control of seawater composition, Nature 281, 468-469, 1979.

Turner, D. R., M. Whitfield, and A. G. Dickson, The equilibrium speciation of dissolved components in freshwater and seawater at 25°C and 1 atm pressure, Geochim. Cosmochim. Acta 45, 855-881, 1981.

Vickery, R. C. Lanthanon complexes with ethylenediamine - NNN'N'-tetraacetic acid. Part III., J. Chem. Soc., 1895-1898, 1952.

Wheelwright, E. J. F. H. Spedding, and G. Schwarzenbach, The stability of the rare earth complexes with ethylenediaminetetraacetic acid, J. Am. Chem. Soc. 75, 4196-4201, 1953.

Yost, D. M., H. Russell, Jr., and C. S. Garner, The Rare-Earth Elements and Their Compounds, Wiley, New York, 1947.

Table 1. Numerical data for rare earth metals and tri-valent cations (after Moeller et al., [1961]). Oxidation potentials are for the reaction $Ln \rightleftarrows Ln^{3+} + 3e^{-}$.

Symbol	Atomic Number Z	Electronic Configuration Ln	Electronic Configuration Ln^{3+}	Oxidation Potential V	Crystal Radius of Ln^{3+} Å
La	57	$4f^0\ 5d^1 6s^2$	$4f^0$	+2.52	1.04
Ce	58	$4f^2\ 6s^2$	$4f^1$	2.48	1.02
Pr	59	$4f^3\ 6s^2$	$4f^2$	2.47	1.00
Nd	60	$4f^4\ 6s^2$	$4f^3$	2.44	0.99
Pm	61	$4f^5\ 6s^2$	$4f^4$	(2.42)	(0.98)
Sm	62	$4f^6\ 6s^2$	$4f^5$	2.41	0.97
Eu	63	$4f^7\ 6s^2$	$4f^6$	2.41	0.96
Gd	64	$4f^7\ 5d^1 6s^2$	$4f^7$	2.40	0.94
Tb	65	$4f^9\ 6s^2$	$4f^8$	2.39	0.92
Dy	66	$4f^{10}\ 6s^2$	$4f^9$	2.35	0.91
Ho	67	$4f^{11}\ 6s^2$	$4f^{10}$	2.32	0.89
Er	68	$4f^{12}\ 6s^2$	$4f^{11}$	2.30	0.87
Tm	69	$4f^{13}\ 6s^2$	$4f^{12}$	2.28	0.86
Yb	70	$4f^{14}\ 6s^2$	$4f^{13}$	2.27	0.85
Lu	71	$4f^{14}\ 5d^1 6s^2$	$4f^{14}$	2.25	0.84

Table 2. Calculated speciation (in % abundance) of REE cations in model seawater at pH-8.2 (from Turner et al. [1981]).

Ln^{3+} Cation	Free	OH	F	Cl	SO_4	CO_3
La	38	5	1	18	16	22
Ce	21	5	1	12	10	51
Pr	25	8	1	12	13	41
Nd	22	9	1	10	12	46
Sm	18	10	1	8	11	52
Eu	18	13	1	10	9	50
Gd	9	5	1	4	6	74
Tb	16	11	1	8	9	50
Dy	11	8	1	5	6	68
Ho	10	8	1	5	5	70
Er	8	12	1	4	4	70
Tm	11	21	1	5	6	55
Yb	5	9	1	2	3	81
Lu	5	21	1	1	1	71

Table 3. Calculated speciation (in % abundance) of REE cations in model fresh water at pH-6 (from Turner et al. [1981]).

Ln^{3+} Cation	Free	OH	F	Cl	SO_4	CO_3
La	73	<1	1	<1	25	1
Ce	72	<1	3	<1	22	3
Pr	72	1	2	<1	23	2
Nd	70	1	3	<1	24	3
Sm	68	1	3	<1	25	4
Eu	71	1	3	<1	21	4
Gd	63	1	5	<1	22	9
Tb	67	1	6	<1	22	4
Dy	65	1	6	<1	21	7
Ho	65	1	7	<1	19	8
Er	63	1	7	<1	19	10
Tm	66	1	8	<1	20	6
Yb	58	1	7	<1	17	17
Lu	59	1	8	<1	15	17

Table 4. Calculated speciation (in % abundance) of REE cations in model seawater at pH-9 (from Turner et al. [1981]).

Ln^{3+} Cation	Free	OH	F	Cl	SO_4	CO_3
La	2	10	<1	<1	<1	88
Ce	<1	5	<1	<1	<1	95
Pr	1	9	<1	<1	<1	90
Nd	<1	9	<1	<1	<1	90
Sm	<1	14	<1	<1	<1	86
Eu	<1	18	<1	<1	<1	82
Gd	<1	14	<1	<1	<1	86
Tb	<1	32	<1	<1	<1	68
Dy	<1	46	<1	<1	<1	54
Ho	<1	48	<1	<1	<1	52
Er	<1	78	<1	<1	<1	22
Tm	<1	86	<1	<1	<1	14
Yb	<1	62	<1	<1	<1	38
Lu	<1	92	<1	<1	<1	8

Figure Captions

Figure 1. Log K vs. inverse ionic radius for representative examples of the three major trends in formation constants for rare earth complexes. Scale on left refers to groups 1 and 3. Scale on right refers to group 2. DTPA = Diethylenetriaminepentaacetic acid. Dipic = 2,6-Pyridinedicarboxylic acid. EDDA = Ethylenediaminediacetic acid. (From Moeller et al. [1965]).

Figure 2. Log $[ML_i]/[M]$ vs. log $[CO_3^{2-}]$ representing the stability field for 1:1 Eu complexes with OH^- and 1:1 and 1:2 Eu complexes with CO_3^{2-} at I = 1. The value of log $[Eu(OH)^{2+}]/[Eu^{3+}]$ is shown for pH = 7, 8, and 9. The equilibria established by Eq. (2) show that there is no carbonate ion concentration dependence for the ratio $[Eu(OH)^{2+}]/[Eu^{3+}]$, so they plot as horizontal lines on this figure. Likewise, the equilibria defined by Eq. (5) show that there is no dependency on pH for the ratio $[Eu(CO_3)_i^{3-2i}]/[Eu^{3+}]$, so the stability fields for Eu cabonates do not shift with a change of pH in the solution. For a given $[Eu]_T$, it can be seen from Eq. (6) that $[Eu^{3+}]$ will be constant for a fixed pH and carbonate ion concentration. Thus, the relative abundances of Eu hydroxide and Eu carbonate complexes formed in a solution can be determined directly from the graph.

Figure 3. Chondrite normalized rare earth abundance patterns in a) Garonne-Dordogne Rivers (solid line) [Martin et al., 1976], b) North American Shale (dashed line) [Haskin et al., 1966], c) Western North Atlantic seawater (solid line) [DeBaar et al., 1983], and d) Eastern North Atlantic seawater (dashed line) [Elderfield and Greaves, 1982]. The left-hand scale refers to water samples (a, c, and d) and the right-hand scale refers to North American Shale (b).

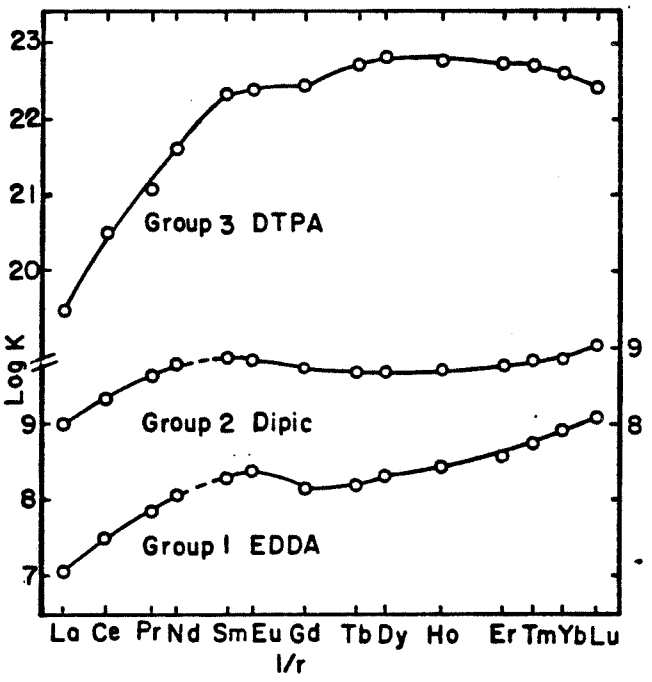
23
22
21
20
Log K
9
8
7
Group 3 DTPA
Group 2 Dipic
Group 1 EDDA
9
8
La Ce Pr Nd Sm Eu Gd Tb Dy Ho Er Tm Yb Lu
I/r

Figure 1

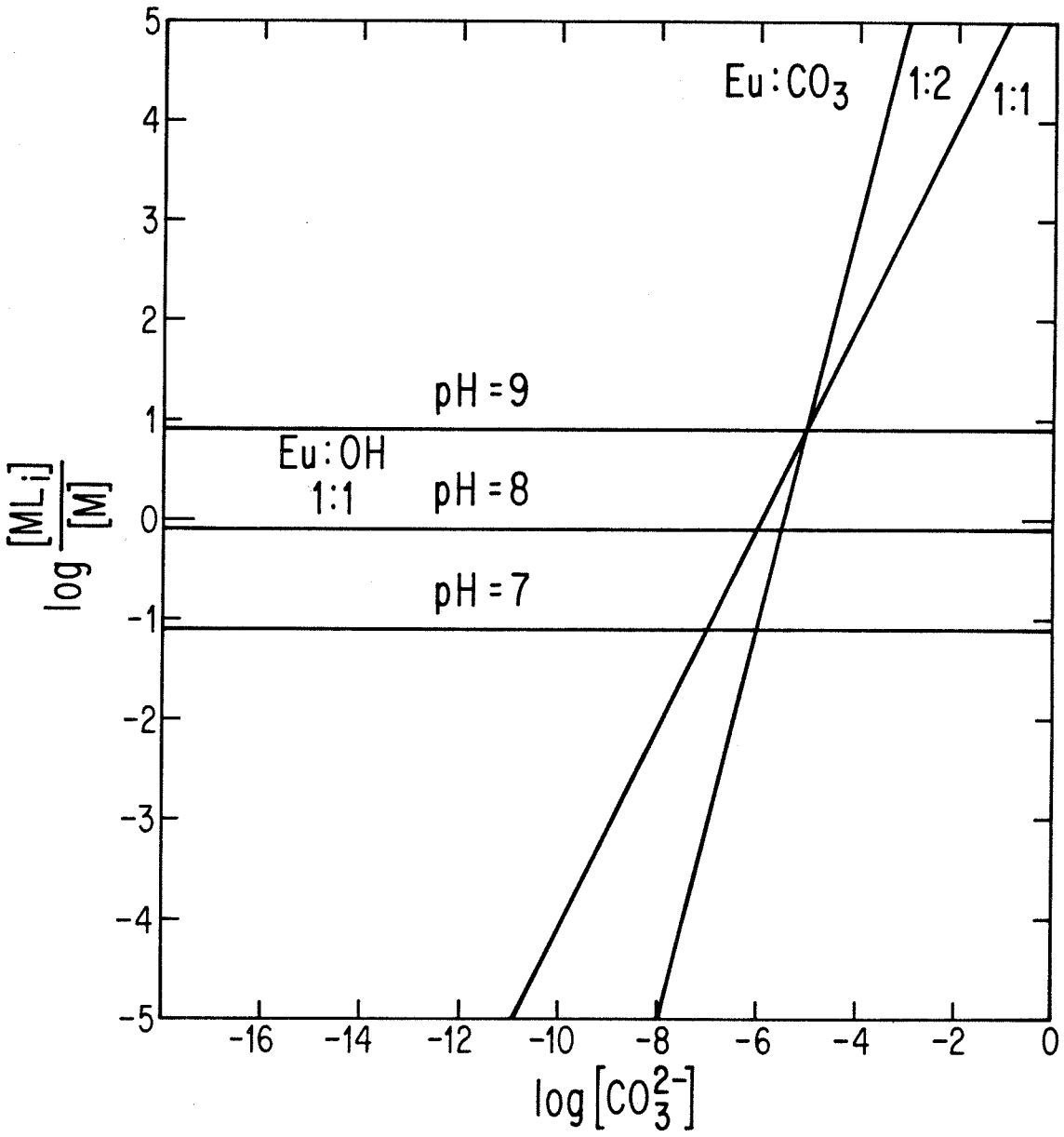
Eu:CO3
1:2
1:1
pH=9
Eu:OH
1:1
pH=8
pH=7
log [ML_i]/[M]
log [CO3 2-]
5
4
3
2
1
0
-1
-2
-3
-4
-5
-16
-14
-12
-10
-8
-6
-4
-2
0

Figure 2

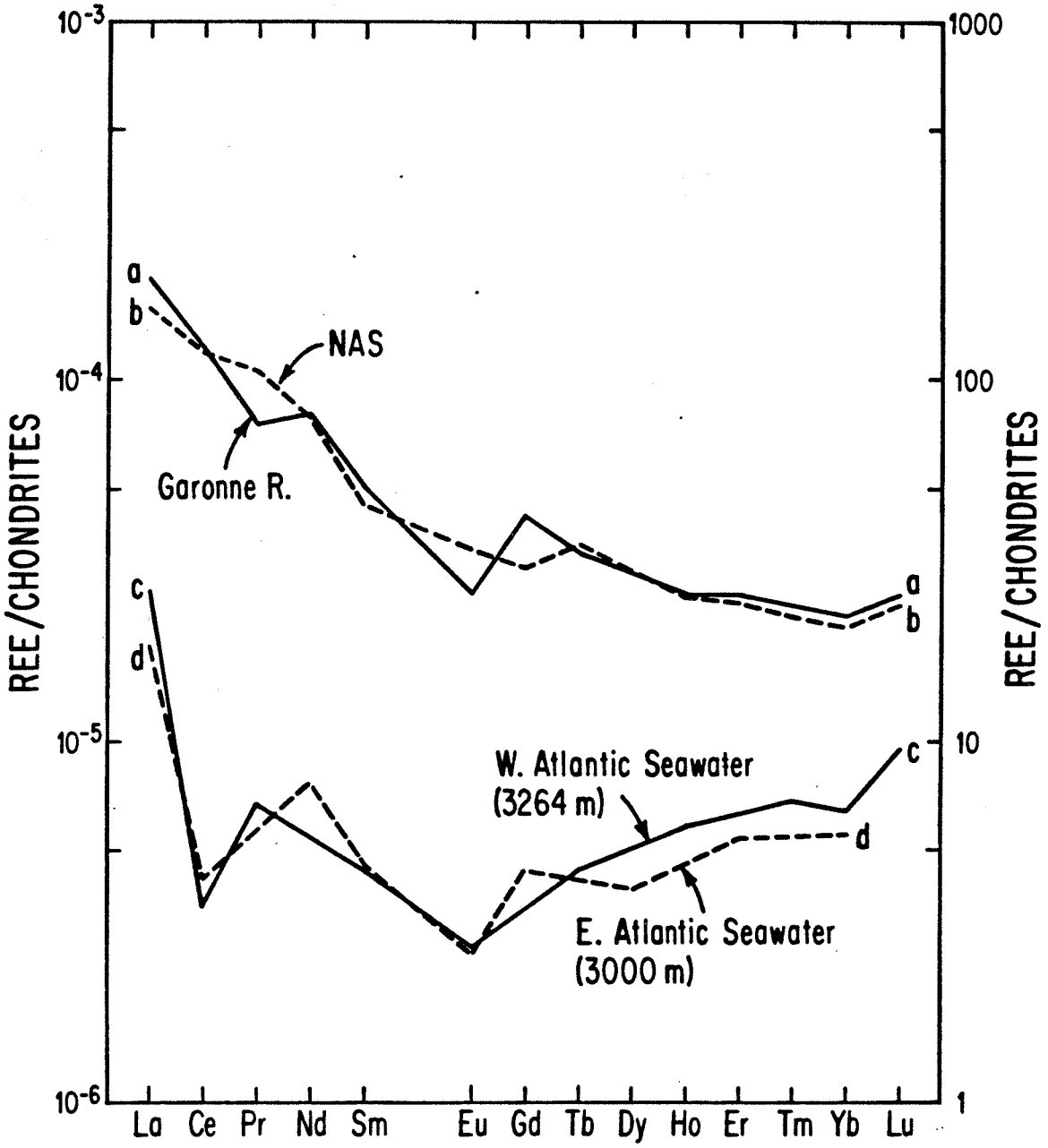
10-3
10-4
10-5
10-6
1000
100
10
1
REE/CHONDRITES
REE/CHONDRITES
a
b
NAS
Garonne R.
c
d
W. Atlantic Seawater
(3264 m)
E. Atlantic Seawater
(3000 m)
La Ce Pr Nd Sm Eu Gd Tb Dy Ho Er Tm Yb Lu

Figure 3

APPENDIX XII

Data Tables

Table A1. Results of Sm, Nd, and Sr analyses of ferromanganese sediments.

Sample	Location	Sediment type	C_{Nd} (ppm)	C_{Sm} (ppm)	$\frac{^{147}Sm}{^{144}Nd}$	$\frac{^{143}Nd}{^{144}Nd}$[b]	$\varepsilon_{Nd}(0)$	$\frac{^{87}Sr}{^{86}Sr}$[d]	$\varepsilon_{Sr}(0)$
I. PACIFIC OCEAN									
OC73-3-12P	20°22'12"S 112°19'12"W	MS	20.7	5.01	0.146	0.511791 ±20	-1.1 ±0.4	-	-
duplicate	"	MS	-	-	-	0.511839 ±18	-0.2 ±0.3	0.708971 ±30	+63.5 ±0.6
OC73-3-12MG3	20°43'12"S 112°27'00"W	MS	15.7	3.60	0.137	0.511644 ±28	-4.0 ±0.6	0.790040 ±37	+64.4 ±0.7
duplicate	"	MS	16.5	3.56	0.130	0.511670[c] ±25	-3.5 ±0.5	-	-
52DR5	00°36'N 86°06'W	HC	2.05	0.39	0.115	0.511779 ±26	-1.4 ±0.5	-	-
MD1-1-1 Top	31°N 155°W	MN	196	50.0	0.153	0.511629 ±15	-4.3 ±0.3	-	-
MD1-1-1 Bottom	"	MN	129	33.1	0.155	0.511631 ±28	-4.2 ±0.5	-	-
DWHD-47	41°59'S 102°01'W	MN	175	42.5	0.146	0.511622 ±22	-4-4 ±0.4	0.709015 ±40	+64.1 ±0.8
Antp-58D	18°57'N 135°48'E	MN	225	51.4	0.138	0.511576 ±37	-4.3 ±0.7	-	-

Table A1. (continued)

Sample	Location	Sediment type	C_{Nd} (ppm)	C_{Sm} (ppm)	$\frac{^{147}Sm}{^{144}Nd}$	$\frac{^{143}Nd}{^{144}Nd}$[b]	$\varepsilon_{Nd}(0)$	$\frac{^{87}Sr}{^{86}Sr}$[d]	$\varepsilon_{Sr}(0)$
SCAN-35D	20°55'N 142°22'E	MN	143	32.7	0.138	0.511667 ±25	-3.5 ±0.5	-	-
MN-139 0-1mm		MN	-	-	-	0.511662 ±20	-3.6 ±0.4	-	-
MN-139 36-37mm		MN	-	-	-	0.511608 ±24	-4.6 ±0.5	-	-
II. ATLANTIC OCEAN									
V27-58 195m	75°32'22"N 02°39'47"E	MN	117	30.0	0.155	0.511334 ±22	-10.0 ±0.4	-	-
CYP74-12	36°56'N 33°04'W	HC	4.45	1.01	0.136	0.511256 ±32	-11.5 ±0.6	-	-
KNR42-166	35°36'18"N 58°41'24"W	MN	280	-	-	0.511267 ±18	-11.4 ±0.3	-	-
S-M	33°57'N 65°47'W	MN	179	45.1	0.152	0.511234 ±21	-12.0 ±0.4	-	-
BP-2381	31°04'12"N 78°08'30"W	MN	107	23.1	0.129	0.511284 ±22	-11.0 ±0.4	0.709030 ±40	+64.3 ±0.8
BP-2382	31°01'36"N 78°18'48"W	MN	59.4	14.2	0.145	0.511323 ±42	-10.2 ±0.8	-	-

Table A1. (continued)

Sample	Location	Sediment type	C_{Nd} (ppm)	C_{Sm} (ppm)	$\frac{^{147}Sm}{^{144}Nd}$	$\frac{^{143}Nd}{^{144}Nd}$[b]	$\varepsilon_{Nd}(0)$	$\frac{^{87}Sr}{^{86}Sr}$[d]	$\varepsilon_{Sr}(0)$
VEMA F.Z.	10°53'42"N 45°17'48"W	MN	155	38.5	0.149	0.511304 ±18	-10.6 ±0.4	-	-
CIRCE-244D	08°22'S 13°13'W	MN	233	59.6	0.154	0.511227 ±18	-12.1 ±0.4	0.709068 ±37	+64.8 ±0.8
CHN-115 Sta. 146	30°12'48"S 39°21'30"W	MN	250	56.2	0.135	0.511129 ±38	-14.0 ±0.7	-	-
duplicate	"	MN	-	-	-	0.511128 ±22	-14.0 ±0.4	-	-
III. INDIAN OCEAN									
DODO-127D	06°40'01"S 51°54'00"E	MN	199	44.0	0.133	0.511443 ±26	-7.8 ±0.5	-	-
Antp-109D	29°58'23"S 60°47'49"E	MN	169	38.7	0.138	0.511415 ±31	-8.5 ±0.6	-	-
DODO-232D	05°22'59"S 97°28'59"E	MN	262	68.6	0.158	0.511476 ±29	-7.3 ±0.6	-	-
DODO-62D	16°18'00"S 104°16'01"E	MN	90.3	22.5	0.150	0.511472 ±24	-7.3 ±0.5	0.709090 ±60	+65.2 ±1.2
DODO-62D sed.	"	RC	33.0	8.31	0.152	0.511361 ±25	-9.5 ±0.5	-	-

Table A1. (continued)

Sample	Location	Sediment type	C_{Nd} (ppm)	C_{Sm} (ppm)	$\frac{^{147}Sm}{^{144}Nd}$	$\frac{^{143}Nd}{^{144}Nd}$[b]	$\varepsilon_{Nd}(0)$	$\frac{^{87}Sr}{^{86}Sr}$[d]	$\varepsilon_{Sr}(0)$
PCE55-31	36°27'07"S 110°02'24"E	MN	134	30.3	0.136	0.511292 ±46	-10.8 ±0.9	-	-
IV. ANTARCTIC OCEAN									
BT-14-3	56°13'S 164°20'W	MN	67.2	17.4	0.156	0.511511 ±30	-6.6 ±0.6	-	-
V. SCOTIA SEA									
E28-5	57°54'S 57°00'W	MN	63.0	14.2	0.136	0.511578 ±28	-5.3 ±0.5	-	-
VI. LAKE ONEIDA, N.Y.--LACUSTRINE									
Lake Oneida	43°10'N 75°45'W	MN	34.0	9.19	0.163	0.511292 ±29	-10.9 ±0.6	-	-

[a] MN = manganese nodule, MS = metalliferous sediment, HC = hydrothermal crust, RC = red clay.

[b] Data normalized to $^{150}Nd/^{142}Nd=0.2096$. Reported errors are 2σ of the mean.

[c] Spiked with ^{150}Nd and normalized to $^{146}Nd/^{142}Nd=0.636155$.

[d] Data normalized to $^{86}Sr/^{88}Sr = 0.1194$. Errors are 2σ of the mean.

Table A2. Results of Sm and Nd analyses for seawater samples. The $^{143}Nd/^{144}Nd$ ratios were determined in samples spiked with ^{150}Nd and normalized to $^{144}Nd/^{142}Nd = 0.878499$. Reported errors are two standard deviations from the mean. 2σ errors for concentration measurements are ~ 0.1%.

Depth (m)	C_{Nd} ($\times 10^{-12}$ g/g)	C_{Sm} ($\times 10^{-12}$ g/g)	$\frac{^{147}Sm}{^{144}Nd}$	$\frac{^{143}Nd}{^{144}Nd}$	$\varepsilon_{Nd}(0)$
I. ATLANTIC OCEAN					
OCE 63, Cast 1 (29°53'00"N, 76°14'12"W).					
300	2.00	0.462	0.140	0.511287 ±30	-10.9 ±0.6
OCE 63, Cast 2 (27°57'14"N, 70°23'25"W).					
1000	-	-	-	0.511174 ±22	-13.1 ±0.4
2200	2.57	0.516	0.121	0.511161 ±33	-13.4 ±0.6
3400	3.19	0.623	0.118	0.511156 ±27	-13.5 ±0.5
OCE 63, Cast 3 (27°01'42"N, 74°20'00"W).					
50	-	-	-	0.511357 ±47	-9.6 ±0.9
OCE 63, Cast 4 (27°06'30"N, 74°21'00"W).					
4100	-	-	-	0.511146 ±37	-13.7 ±0.7
A-II 109-1, Station 30 (36°15'38"N, 61°58'27"W).					
5	2.08	0.474	0.138	0.511361 ±23	-9.5 ±0.4
200	1.96	-	-	0.511365 ±20	-9.4 ±0.4
400	2.11	-	-	0.511303 ±21	-10.6 ±0.4
600	2.11	-	-	0.511318 ±27	-10.3 ±0.5
800	2.20	-	-	0.511288 ±27	-10.9 ±0.5

Table A2 (cont.)

Depth (m)	C_{Nd} ($\times 10^{-12}$ g/g)	C_{Sm} ($\times 10^{-12}$ g/g)	$\frac{^{147}Sm}{^{144}Nd}$	$\frac{^{143}Nd}{^{144}Nd}$	$\varepsilon_{Nd}(0)$
1100	2.60	0.525	0.122	0.511128 ±21	-14.0 ±0.4
1800	2.66	-	-	0.511157 ±22	-13.5 ±0.4
3000	2.72	0.546	0.121	0.511180 ±13	-13.0 ±0.3
4000	3.80	-	-	0.511161 ±23	-13.4 ±0.4
4850	9.01	-		0.511153 ±16	-13.6 ±0.3
A-II 109-1, Station 39 (36°13'00"N, 52°07'12"W)					
5	1.14	-	-	0.511342 ±27	-9.9 ±0.5
A-II 109-1, Station 79 (36°15'49"N, 19°57'27"W)					
5	1.34	-	-	0.511310 ±20	-10.5 ±0.4
A-II 109-1, Station 95 (36°17'41"N, 10°02'27"W)					
Surface	1.80	0.376	0.126	0.511264 ±33	-11.4 ±0.7
200	2.01	0.417	0.125	0.511208 ±19	-12.5 ±0.4
500	2.26	0.473	0.126	0.511240 ±30	-11.9 ±0.6
800	2.48	0.528	0.128	0.511304 ±28	-10.6 ±0.5
1000	2.34	0.519	0.134	0.511348 ±29	-9.8 ±0.6
"	2.35	---	---	0.511334 ±20	-10.0 ±0.4
1150	2.61	0.532	0.127	0.511251 ±28	-11.7 ±0.5

Table A2 (cont.)

Depth (m)	C_{Nd} ($\times 10^{-12}$ g/g)	C_{Sm} ($\times 10^{-12}$ g/g)	$\frac{^{147}Sm}{^{144}Nd}$	$\frac{^{143}Nd}{^{144}Nd}$	$\varepsilon_{Nd}(0)$
1300	2.49	0.533	0.129	0.511253 ±26	-11.6 ±0.5
2000	2.46	0.498	0.122	0.511221 ±20	-12.2 ±0.4
3000	2.84	0.556	0.118	0.511208 ±25	-12.5 ±0.5
4000	3.33	0.644	0.117	0.511245 ±22	-11.8 ±0.4
A-II 109-1, Station 101 (36°45'15"N, 08°36'20"W).					
650	5.16			0.511340 ±20	-9.9 ±0.4
TTO/TAS Station 63 (7°44'00"N, 40°42'30"W).					
790	2.29			0.511240 ±18	-11.9 ±0.4
1990	2.50			0.511164 ±16	-13.3 ±0.3
2910	2.65			0.511203 ±20	-12.6 ±0.4
3890	3.71			0.511210 ±26	-12.4 ±0.5
4280	3.82			0.511231 ±22	-12.0 ±0.4
4810	4.34			0.511243 ±16	-11.8 ±0.3
TTO/NAS, Station 142 (61°21'N, 8°01'W).					
750	3.08	0.618	0.121	0.511455 ±29	-7.7 ±0.6
TTO/NAS, Station 144 (67°40'N, 3°17'W)					
65	2.06	0.393	0.115	0.511321 ±25	-10.3 ±0.5

Table A2 (cont.)

Depth (m)	C_{Nd} ($\times 10^{-12}$ g/g)	C_{Sm} ($\times 10^{-12}$ g/g)	$\frac{^{147}Sm}{^{144}Nd}$	$\frac{^{143}Nd}{^{144}Nd}$	$\varepsilon_{Nd}(0)$
3750	2.35	0.441	0.113	0.511359 ±24	-9.5 ±0.5
TTO/NAS, Station 149 (76°53'N, 1°02'E)					
2800	2.42	0.466	0.116	0.511299 ±18	-10.7 ±0.4
TTO/NAS, Station 167 (64°03'N, 33°20'W)					
840	2.38	0.424	0.108	0.511124 ±20	-14.1 ±0.4
2310	2.97	0.581	0.118	0.511408 ±24	-8.6 ±0.5
II. PACIFIC OCEAN					
CEROP II (36°47'N, 122°48'W)					
1000	3.23	0.630	0.118	0.511652 ±36	-3.8 ±0.7
duplicate	-	-	-	0.511729 ±25	-2.3 ±0.5
CEROP II (36°50'N, 122°50'W).					
2400	-	-	-	0.511723 ±25	-2.4 ±0.5
GS-7901-139 (0°47'20"N, 86°07'21"W).					
2500	2.24	0.416	0.112	0.511717 ±34	-2.5 ±0.7
duplicate	-	-	-	0.511742 ±28	-2.1 ±0.5
Marine Chemistry 80, Station 17 (14°41'N, 160°01'W).					
2000	-	-	-	0.511848 ±24	0.0 ±0.5

Table A2 (cont.)

Depth (m)	C_{Nd} ($\times 10^{-12}$ g/g)	C_{Sm} ($\times 10^{-12}$ g/g)	$\frac{^{147}Sm}{^{144}Nd}$	$\frac{^{143}Nd}{^{144}Nd}$	$\varepsilon_{Nd}(0)$
Marine Chemistry 80, Station 31 (20°00'S, 159°59'W).					
30	0.411	-	-	0.511861 ±39	+0.3 ±0.8
2800	2.57	-	-	0.511617 ±36	-4.5 ±0.7
4500	3.68	-	-	0.511435 ±29	-8.1 ±0.6
A-II 107-11, Station 261 (47°47'33"S, 83°16'31"W).					
3900	3.69	0.683	0.112	0.511444 ±26	-7.9 ±0.5
III. DRAKE PASSAGE & SOUTHERN OCEAN					
A-II 107-11, Station 292 (60°54'02"S, 89°24'23"W).					
5050	4.09	-	-	0.511430 ±28	-8.2 ±0.6
A-II 107-11, Station 315 (61°01'10"S, 62°15'21"W).					
50	1.85	0.347	0.109	0.511381 ±50	-9.1 ±1.0
800	2.30	0.432	0.113	0.511388 ±39	-9.0 ±0.7
2000	3.25	0.610	0.113	0.511418 ±38	-8.4 ±0.7
3600	4.21	0.800	0.115	0.511389 ±21	-8.9 ±0.4
A-II 107-11, Station 327 (56°27'55"S, 66°33'01"W).					
50	1.19	-	-	-	-
650	1.31	-	-	0.511375 ±40	-9.2 ±0.8
1900	1.93	-	-	0.511429 ±33	-8.2 ±0.6

Table A3. Hydrographic data for seawater samples

Depth (m)	Salinity (°/₀₀)	O_2 (µMol/kg)	PO_4^{3-} (µMol/kg)	NO_3^- (µMol/kg)	SiO_3 (µMol/kg)
A-II 109-1 Station 30.					
5	36.319	221	0.00	0.03	0.69
200	36.523	224	0.11	3.06	1.59
400	35.404	208	0.21	4.90	2.08
600	35.864	174	0.72	13.24	5.81
800	35.351	166	1.27	21.37	12.39
1100	35.063	218	1.08	19.69	13.39
1800	34.977	264	0.98	17.39	12.76
3000	34.958	269	1.14	17.89	20.85
4000	34.901	267	1.17	18.09	28.94
4850	34.896	263	1.24	18.97	34.59
A-II 109-1 Station 95					
Surface	36.545	230	0.01	0.20	1.34
200	35.891	222	0.33	5.82	2.74
500	35.651	198	0.81	13.97	6.56
800	36.019	184	0.85	14.33	8.76
1000	35.961	184	0.98	16.24	10.97
1150	36.057	186	0.96	16.04	11.46
1300	36.020	193	0.96	15.90	11.74
2000	35.210	238	1.18	18.44	19.48
3000	35.063	238	1.33	20.29	33.35
4000	34.903	240	1.44	21.55	44.90
A-II 109-1 Station 101					
650	36.587				

Table A3 (continued)

Depth (m)	Salinity (°/₀₀)	O_2 (µMol/kg)	PO_4^{3-} (µMol/kg)	NO_3^- (µMol/kg)	SiO_3 (µMol/kg)
TTO/TAS Station 63					
0	36.099	-	0.06	0.1	1.8
200	35.006	116	1.74	27.3	13.2
390	34.755	110	2.09	32.9	18.7
590	34.617	132	2.22	34.4	24.0
790	34.610	135	2.31	35.4	29.0
980	34.704	150	2.20	33.1	29.1
1990	34.930	-	1.35	20.4	19.8
2910	34.938	260	1.37	20.2	28.9
3890	34.889	260	1.43	20.9	40.7
4280	34.811	-	1.62	23.7	52.3
4810	34.815	242	1.76	25.7	72.2